The Role of Unsaturated Soil Property Functions in the Practice of Unsaturated Soil Mechanics

A Thesis Submitted to the College of Graduate Studies and Research

In Partial Fulfillment of the Requirements

For the Degree of Ph.D.

In the Department of Civil Engineering

University of Saskatchewan

Saskatoon, Saskatchewan, Canada

By

Murray D. Fredlund

December, 1999

PERMISSION TO USE

In presenting this thesis in partial fulfillment of the requirements for a postgraduate degree from the University of Saskatchewan, the author agrees that the libraries of this University may make it freely available for inspection. The author further agrees that permission for copying this thesis in any manner, in whole or in part, for scholarly purposes may be granted by the Head of the Department or the Dean of the College in which the thesis was done. It is understood that any copying or publication or use of this thesis or parts thereof for financial gain shall not be allowed without written permission. It is also understood that due recognition shall be given to the author and to the University of Saskatchewan in any scholarly use which may be made of any material in this thesis.

Request for permission to copy or to make other use of material in this thesis in whole or in part should be addressed to:

Head, Department of Civil Engineering
University of Saskatchewan
57 Campus Drive
Saskatoon, Saskatchewan, Canada
S7N 5A9

ABSTRACT

The implementation of unsaturated soil mechanics into engineering practice is dependent, to a large degree, upon an ability to predict nonlinear, unsaturated soil property functions. Such unsaturated soil property functions as the soil-water characteristic curve, the shrinkage curve, the permeability curve, and the shear strength curve have been shown to vary depending on water content levels. These unsaturated soil property functions have been defined for the classical soil mechanics areas of seepage and shear strength. Much information has been accumulated on the volume change behavior of unsaturated soils; however, to-date the role of unsaturated soil, volume change functions has not been defined; nor have the prediction procedures been formulated.

The primary objective of this thesis is to provide methods of determining the constitutive relationships for an unsaturated soil. Experimental laboratory techniques, theoretical and statistical methods will be examined to provide the basis for the constitutive surfaces. Soil property functions will also be represented mathematically to facilitate a continuous and smooth representation of soil behavior. The resulting constitutive surfaces will provide the practicing engineer with mathematical relationships that form the basis for modeling seepage and volume change (or any coupled combination) in unsaturated or saturated soil.

ACKNOWLEDGEMENTS

It's hard to summarize all that has happened in the previous 3½ years. There were many times when I wondered if I would ever complete my degree. I feel a considerable amount of relief in knowing it is finally completed.

I would firstly like to thank my wife Barb for helping to support my endeavors by working 6 days a week at 2 different jobs for the past 3½ years. In spite of her two jobs, she still managed to surprise her husband with dates and outings to make sure engineering did not monopolize his time. Thank you Barb and I love you!

I must mention my mother and father who provided endless help, guidance, and granola to get me through my program. Without my father's patience in explaining some of the more difficult concepts of unsaturated soil mechanics on the back of a napkin from Burger King, this thesis would have taken much longer. I must also make mention of my parents-in-law who have worked hard to keep my wife and I happy with home upgrades and Flapper pie.

I would also like to recognize my supervisor Prof. Wilson and his family for taking my wife and I into their lives. I could not imagine having a better supervisor during my graduate program. I have found that Prof. Wilson has challenged my character as well as my intellect during the course of my program. I must also say that if it wasn't for the thick skin I received from his wife Carmen, I don't think I could have made it through the defense...

I would like to acknowledge my friends (and their respective wives) Mark Vanstone, Gord Hundaby, Kerwin Besler, Grant Romancia, Carl Spivak, Grady Janzen, Cam Lewis, Rob Donahue, and Larry Peters for making sure that my studies included squash, weight lifting, coffee, hot-tubbing and surround-sound movie reviews.

I have been fortunate to have a close family to provide their support and friendship over the past 3½ years. I would like to thank my siblings Jocelyn, Kenton (and his wife Kelli), and Brendon as well as my "extended-city" family consisting of my grandparents and relatives from Saskatoon, Lanigan, Calgary, and Winnipeg for the investment each of them has made in my life.

Special thanks goes to my committee members Dr. Gary Kachanowski, Dr. Curt Berthalot, Dr. Dennis Pufahl, Dr. Devorali Wulfsohn, and Dr. Bruce Sparling for their recommendations and guidance that helped shape my program. I would also like to thank NSERC for providing the funding for this research for the first two years of the thesis.

The acknowledgements would not be complete without thanking Jesus Christ for the countless prayers that have been answered over the past 3½ years.

"For I know the thoughts that I think toward you, says the Lord,
thoughts of peace and not of evil, to give you a future and a hope.
Then you will call upon Me, and go and pray to Me, and I will Listen to you.
And you will seek Me and find Me, when you search for Me with all your heart."

Jeremiah 29:11-13

CONTENTS

List of Figures

List of Tables

CHAPTER 1.0 Unsaturated Soil Property Functions for the Practice of Unsaturated Soil Mechanics

1.1 Introduction

The implementation of unsaturated soil mechanics into engineering practice comes at a time when the geotechnical engineer is accepting a new paradigm for soil mechanics. Computers and numerical modeling play a dominant role in responding to practical applications and sensitivity studies for addressing the 'What if --- ?' concerns in geotechnical engineering problems. For many problems involving unsaturated soils, it is necessary to determine unsaturated soil property functions for solving numerical models. These functions can be approximated from either a knowledge of the soil-water characteristic curve or the grain size distribution of the soils involved. This implementation procedure deviates somewhat from historical classical soil mechanics procedures but will provide an acceptable procedure for engineering practice.

The application of soil mechanics in engineering practice has evolved since the framework was laid out by Terzaghi (1923). Engineers have been familiar with mechanical soil property constants and soil property functions such as the grain-size distribution and the compression curve for several decades. More recently, the soil-water characteristic curve has emerged as a key function in predicting important physical relationships for unsaturated soils. Large amounts of experimental data have been gathered to substantiate the many possible variations for these relationships. Examples of reference type soils used in saturated soil mechanics includeLondon Clay, Boston Blue Clay and Ottawa sand. The properties of such soils often form a basis for comparison among experimental results.

In general, however, development and implementation of soil mechanics to routine engineering practice has been limited to problems where the soils are saturated. Theoretical developments and laboratory testing procedures for the application of soil mechanics to unsaturated soils have

emerged during the past 30 years. Implementation of this new technology into engineering practice has been restricted by two critical factors. In the first case, advanced numerical computing techniques are required to solve complex, highly nonlinear equations. In the second case, a procedure for describing the constitutive surfaces of unsaturated soils is not available. Both of these shortcomings are interrelated and the development of both technologies must be concurrent. While considerable progress has been made with respect to numerical solutions and computing, the application of unsaturated soil technology has been stalled by an inability to mathematically describe the constitutive surfaces for unsaturated soils.

The numerical modeling of the movement of water and contaminants through soils is an area of application of the research presented in this thesis. It is now common in geotechnical engineering practice to model seepage in soils. Finite element and finite difference software solutions are available to solve the mathematics behind the seepage and contaminant transport partial differential equations. An example of this is seepage through a slope consisting of two soil types (Figure 1-1). The problem may be evaluated to correctly determine infiltration and flow rates as well as the location of the phreatic surface. The accuracy of the solution of this problem is dependent on the correct representation of the soil-water characteristic curve and the permeability curve of both soil materials.

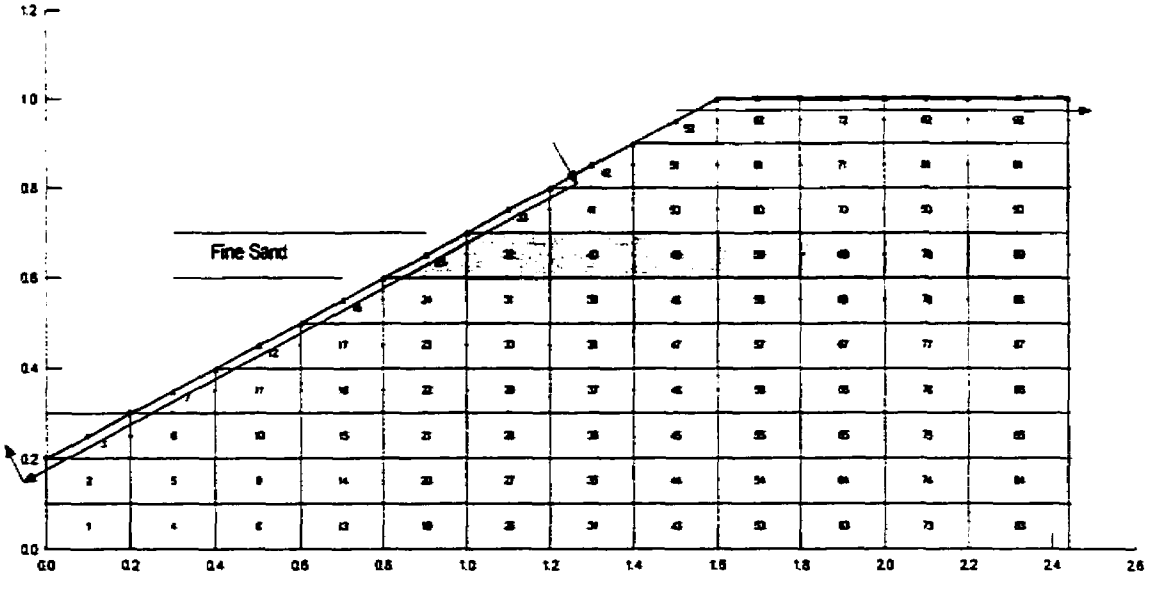

Figure 1-1 Typical example of transient seepage involving infiltration

The volume change behavior of soils may also be modeled using the methods outlined in this thesis. Volume change of clay soils has often been modeled as a process separate from seepage in soils when, in fact, the processes represent a coupled solution of seepage (continuity) and volume change (equilibrium). An example of this is the consolidation and subsequent desaturation of mine tailings at the Jeb Pit located near McClean Lake in northern Saskatchewan. Mine tailings are spigoted out as a slurry and allowed to consolidate under their own self weight. The effective stress in the soil will therefore increase. As the deposition of tailings slows, the tailings may undergo drying as a result of evaporative fluxes and the soil suction stress state will increase. This stress path may be seen in Figure 1-2. This process is difficult to model without a mathematical representation of the constitutive surface of a soil. This thesis provides methods for the development of such constitutive surfaces.

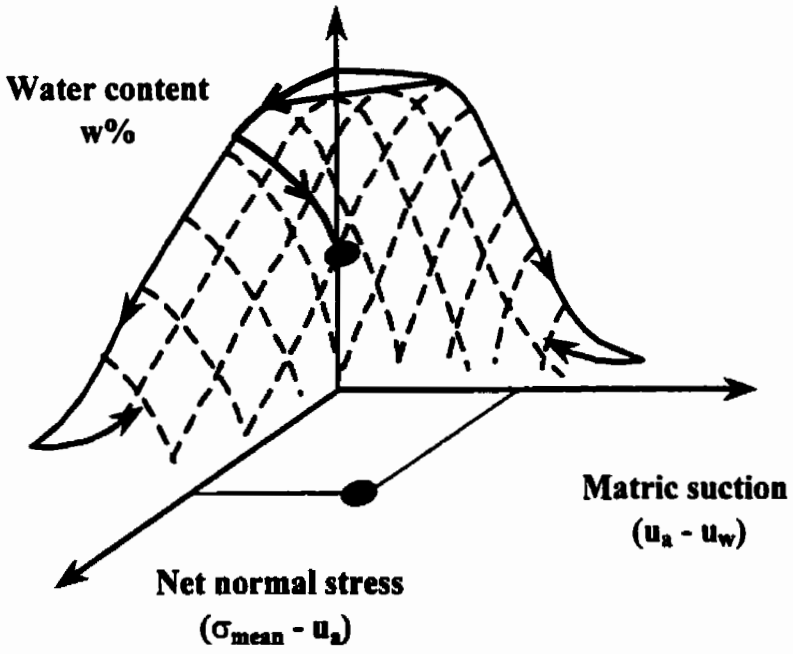

Figure 1-2 Example of stress page followed by mine tailings

This thesis provides a new integrated procedure for describing the necessary soil property functions and constitutive surfaces for solving volume change problems in unsaturated soil mechanics.

1.2 Overview

Terzaghi's (1923) theory did not specify a method for analyzing unsaturated soils. The need for unsaturated soil mechanics has grown steadily in recent years. Practicing engineers have determined that saturated soil mechanics has not been adequate to solve many problems for soils above the water table. Soil properties, such as permeability, compression index, Young's Modulus, etc., which were previously assumed to be constant in saturated soil mechanics, have been found to vary substantially depending upon the degree of saturation of the soil. It has become necessary to define a number of soil property functions to implement the practice of unsaturated soil mechanics. These functions are shown below.

Table 1-1 Soil property functions required for various geotechnical problems

Function	*Soil Property*	*Dependent Variable*	*Application*
Soil-water characteristic curve	Gravimetric water content, w	Soil suction	Unsaturated seepage modeling
Permeability	Hydraulic conductivity, k	Soil suction	Unsaturated seepage modeling
Water storage	m^2_w	Soil suction	Unsaturated seepage modeling
Shrinkage	Void ratio	Gravimetric water content, w	Volume change/deformation modeling
Swell	Void ratio	Gravimetric water content, w	Volume change/deformation modeling
Shear strength	Shear strength	Soil suction	Volume change/deformation modeling
Thermoconductivity	Thermoconductivity	Soil suction	Evapotranspiration modeling
Specific heat	Specific heat	Soil suction	Evapotranspiration modeling
Unfrozen water content	Unfrozen volumetric water content	Degrees below freezing	Evapotranspiration modeling
Diffusion	Diffusion	Soil suction	Contaminant transport modeling
Adsorption	Adsorption	Soil suction	Contaminant transport modeling

The successful application of unsaturated soil mechanics to current engineering practice is dependent upon the relatively easy methods of representing and determining the unsaturated soil property functions described above.

The largest obstacle in applying unsaturated soil mechanics to engineering practice has been the complexity and expense of obtaining unsaturated soil property functions. A typical seepage problem involving only two soil types may cost $2000 to $5000 in laboratory fees to obtain the two soil-water characteristic curves and permeability functions. This thesis focusas on two methods for simplifying the determination of unsaturated soil property functions.

Firstly, methods of fitting mathematical equations to unsaturated soil property functions are developed to provide a means of quantifying unsaturated soil properties. This will allow practicing engineers to manage large amounts of unsaturated soils data with relative ease. Secondly, theoretical methods for the estimation of soil property functions from limited data (also called pedo-transfer functions) are developed for the estimation of unsaturated soil property functions from simple data such as the grain-size distribution or Atterberg limits. These pedo-transfer functions allow for a low-cost method of implementing unsaturated soil mechanics in engineering practice. The limitation of these pedo-transfer function comes with the risk involved in the accuracy of the individual pedo-transfer function.

Five soil property functions for application to unsaturated soils are analyzed in this thesis. These functions are shown in Table 1-2.

Table 1-2 Soil-property functions examined in this thesis

Function	*Soil Property*	*Dependent Variable*	*Application*
Grain-size distribution	Percent passing	Particle diameter	Laboratory analysis
Soil-water characteristic curve	Gravimetric water content, w	Soil suction	Unsaturated seepage modeling
Water storage	m^2_w	Soil suction	Unsaturated seepage modeling

Shrinkage	Void ratio	Gravimetric water content, w	Volume change/deformation modeling
Compression (consolidation) curve	Void ratio	Net normal stress	Volume change/deformation modeling

The grain-size distribution soil property function is considered first because of the close relation to the soil-water characteristic curve. The compression soil property function will be examined since it is required for the calculation of unsaturated soil constitutive surfaces.

Equations have been previously presented for the fitting of soil property functions. The most common equations have been used to represent the soil-water characteristic curve are Brooks and Corey,(1964); van Genuchten,(1981); and Fredlund and Xing, (1993). Theoretical methods for the estimation of soil property functions from limited data (also called pedo-transfer functions) have also been presented in the research literature (Rawls, 1983; Arya and Paris, 1981). The most commonly presented pedo-transfer functions are for the estimation of the soil-water characteristic curve and the coefficient of permeability relationship. Some of these equations and pedo-transfer functions have proven successful for specific application. However, a generalized approach for application to unsaturated soil mechanics is required.

Considerable research has focused on the application of computer models for analyzed problems in soil mechanics. Seepage, contaminant transport, stress and volume change are some of the areas that have received attention. Finite element models have permitted more realistic simulations to be carried out for difficult problems. In general, these finite element models make use of the latest numerical methods to assist in numerical convergence for highly non-linear problems such as those encountered in unsaturated soils. At the same time, the models depend on the reasonableness of the soil property functions used as input.

This thesis shows that it is timely to adopt a philosophy in soil mechanics that uses soil property functions (i.e., in particular, unsaturated soil property functions), to represent complex saturated/unsaturated soils conditions. A common difficulty associated with this type of approach has been the lack of mathematical functions that represent soil properties as smooth functions. For example, mathematical functions are required to provide a continuous

description of the soil property functions for the finite element method. The soil property functions must provide superior representation of the soil properties such that non-linear formulations and non-linear solutions for complex problems in unsaturated soils can be optimized.

The convergence of finite element solutions can be improved by using soil property functions that are both smooth and physically realistic. Typical soil property functions, such as the compression function, are often represented by a straight line function on an arithmetic or semi-logarithm plot. Attempts to increase the accuracy of the compression curve have led to the splicing together of two straight line portions. Difficulty in applying this representation to a numerical model can be encountered. For example, the difficulties related to the distinct break in slope at the intersection of the two straight line portions may be encountered. A smooth mathematical representation of the soil property function should provide a superior form for numerical modeling.

Spline functions have frequently been used to provide a continuous representation of soil property functions. While the spline provides a continuous representation, it may not be physically realistic, particularly for regions between the designated data points. The problem becomes further accentuated when a derivative of the spline function must be taken (e.g., computing the water storage modulus).

Laboratory testing provides the data for the assessment of soil property functions. However, only a limited number of data points can realistically be measured in the laboratory and it is necessary to obtain a mathematical representation of the entire soil property function. The mathematical representation provides both an interpolation technique together with the parameters that must be quantified. In other words, the use of information technology systems, along with the concept of continuous soil property functions, form the philosophical basis to enhance the numerical modeling of saturated/unsaturated soil systems.

1.3 Research Application Summary

The mathematical methods presented in this thesis are valuable to the engineering community in that they form the basis for modeling soil problems. Engineering practice now accepts the validity of finite element or finite difference methods and such calculations are not commonplace. What has received significantly less attention is the formulation of appropriate mathematical relations to represent the soil properties used as input to these numerical models. This thesis attempts to develop mathematical methods for the estimation and representation of soil property functions used as input to numerical modeling programs. In particular, emphasis is placed on the soil property functions for unsaturated soils.

The processes common to geotechnical engineering practice today are: seepage, consolidation, heat flow, evapotranspiration, stress/deformation, contaminant transport, and slope stability. There exists for each of these problems finite element or finite difference software solutions. The validity of the output of these programs is to a large extent, dependant on the validity of the soil properties input to the model. There is often much money invested in the model but very little money invested to ensure that the soil properties used are representative of those in the field across the spectrum of field state conditions.

The soil properties required for each type of typical engineering problem may be seen in Table 1-3. Table 1-3 summarizes the soil property functions which are needed to perform a saturated/unsaturated analysis of the problem.

Table 1-3 Summary of soil properties required for each type of model.

Model	Soil Properties
Seepage	Permeability 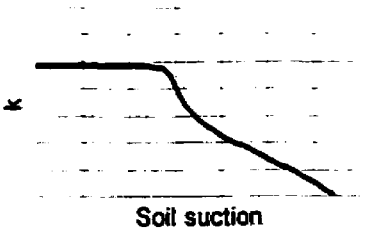

	Soil-water characteristic curve 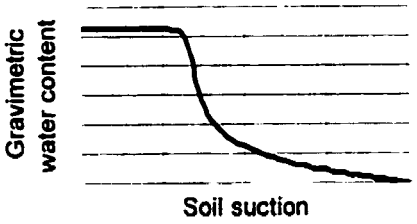
Slope Stability	Shear strength 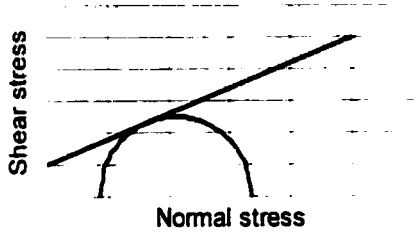
Consolidation	Compression 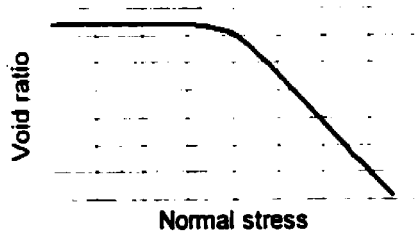 Permeability 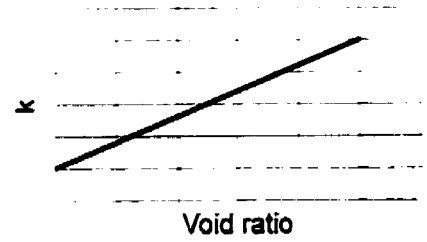
Stress/Deformation	Compression

<table>
<tr>
<td></td>
<td>
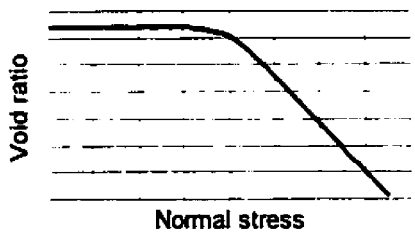

Shear strength
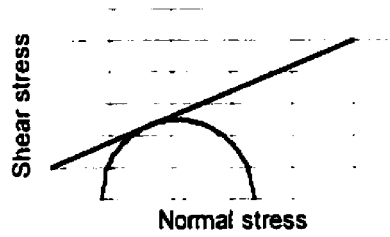

Shrinkage
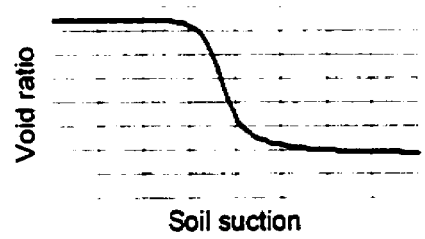

</td>
</tr>
<tr>
<td>Contaminant Transport</td>
<td>Diffusion
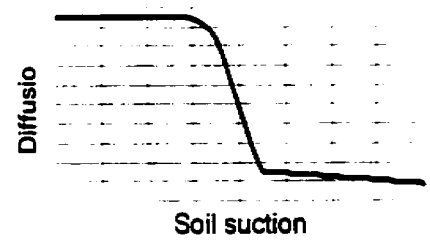

</td>
</tr>
<tr>
<td>Heat Flow</td>
<td>Specific heat
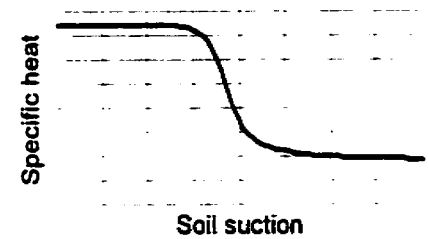

</td>
</tr>
</table>

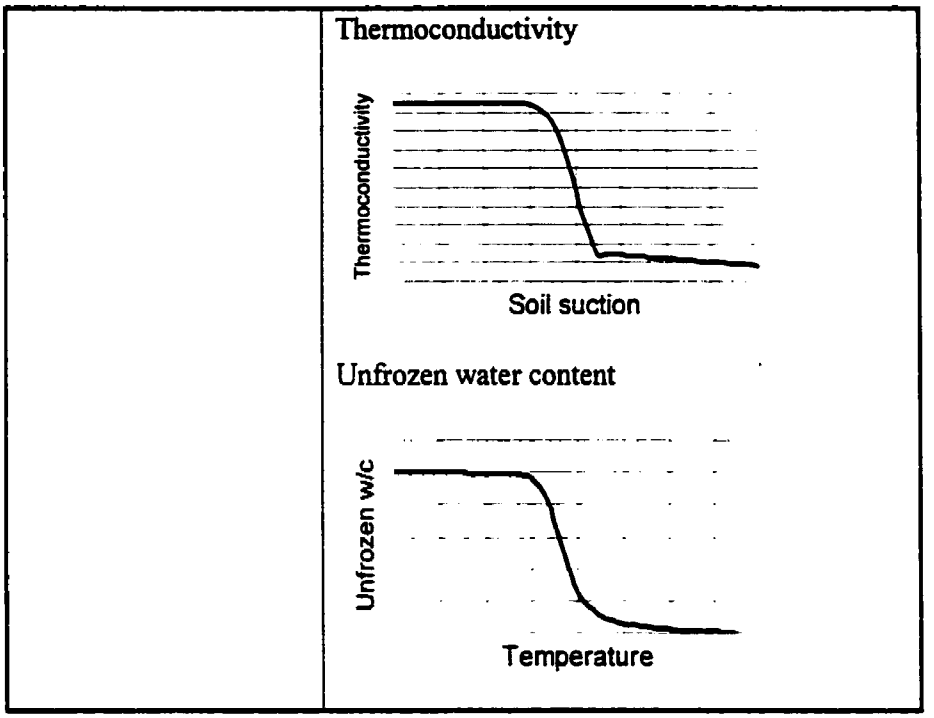

The finite element and finite difference methods are mathematical techniques. The ideal input to these programs is therefore mathematical functions that accurately and realistically represent soil properties. Mathematical representation of the grain-size distribution, the soil-water characteristic curve, the compression curve, and the shrinkage curve as well as the mathematical representation of the constitutive surfaces are examined in this thesis.

Many of these soil properties are not measured properly because of the costs associated with the laboratory procedures. This thesis will also examine methods to estimate soil property functions from simple laboratory data. The estimation of the soil-water characteristic curve and the shrinkage curve are examined in this thesis.

1.4 Objective and Scope

This thesis presents a new technique and general procedure for developing the soil property functions required to solve problems in unsaturated soils. The emphasis is directed at the estimation of the soil-water characteristic curve together with volume change functions (and water content functions) for unsaturated soil. In order to achieve the broad objectives outlined

above, it is necessary to develop a numerical procedure to represent the grain-size distribution curve. Mathematical representation of the grain-size distribution curve is a fundamental step within the general procedure as the basis for the description of the associated soil property functions for unsaturated soils.

A number of soil property functions are being studied. New mathematical representation has been developed for the following functions.

1. Unimodal equation for the fit of the grain-size distribution,
2. Bimodal equation for the fit of the grain-size distribution,
3. Bimodal equation for the fit of the soil-water characteristic curve,
4. Three-parameter equation for the fit of the compression curve,
5. Four-parameter equation for the fit of the compression curve,
6. Equation for the fit of the shrinkage curve.

The objectives of the thesis are to develop procedures for the estimation of several pedo-transfer functions for unsaturated soils. The specific pedo-transfer functions studied are:

1. Unimodal estimation of the soil-water characteristic curve from the grain size distribution function,
2. Bimodal estimation of the soil-water characteristic curve from the grain size distribution function,
3. Estimation procedure for the shrinkage curve
4. Estimation function for the volume change constitutive surface based on the compression curve, the shrinkage curve and the soil-water characteristic curve,
5. Estimation function for the water content constitutive surface based on the compression curve, the shrinkage curve and the soil-water characteristic curve.

The scope of this thesis involves the development of comprehensive mathematical procedures for representing unsaturated soil property functions. The procedure to represent soil property functions is primarily restricted to the behavior of unsaturated soils during drying, along with the accompanying volume changes. Limited attention will be given to the wetting curves associated with volume change. There are other unsaturated soil property functions that could

be further studied such as permeability, thermal properties and contaminant transport functions. However, these are considered to be outside the scope of this thesis. This thesis is directed at the study of volume change and water content change, as well as the necessary functions leading up to the unsaturated soil property functions.

1.5 Outline of the Thesis

This thesis develops a series of soil property functions, starting with the grain size distribution and leading up to the volume change functions for an unsaturated soil. There is a natural progression to the order in which the soil property functions are proposed.

Chapter 1 summarizes the contributions of this thesis to research of saturated and unsaturated soil mechanics. The objective and the scope of the research program is presented. A summary of the concepts of soil-property functions is also provided along with a statement defining the philosophical approach being advocated for modeling saturated/unsaturated soil systems. Chapter 2 provides a background summary of the current development in unsaturated soil mechanics. Future direction of research and the application of the technology presented in this thesis will also be presented. Chapter 3 introduces and analyzes several new equations for the representation of the grain-size distribution. Calculations based on the grain size distribution data are also presented for illustration and verification purposes. A new method for the estimation of the soil-water characteristic curve from grain size distribution data is presented in Chapter 4. A wide range of grain size data sets are analyzed and the predicted soil-water characteristic curves are compared to measured values for verification. Chapter 5 presents a theoretical representation of the compression curve from experimental data measured in an oedometer, as well as data measured in an isotropic triaxial test. These functions are for a saturated soil and forms the reference or basic soil characteristic for volume change. Chapter 6 introduces an equation capable of fitting the shrinkage curve. In this chapter, a method of estimating the shrinkage curve is proposed and verified using data from the research literature. Chapter 7 summarizes the application of individual soil-property functions to the development of three-dimensional constitutive surfaces for volume change and water content change in unsaturated soils.

CHAPTER 2.0 Overview of the Integrated Procedure for Describing Soil Property Functions

2.1 Introduction

Application of the general procedure presented in this thesis will provide contributions for two areas of saturated/unsaturated soils technology. Firstly, the fitting equations presented form the foundation for a standardized representation of soil property functions. Standardized representation of soil property functions is conducive to the development of constitutive relations for unsaturated soils. Furthermore, a standardized approach allows principles of information technology to be applied for the convenient management of large amounts of soils data.

The second area of application for the research presented in this thesis relates to the area of numerical modeling. The equations and methods presented herein form the basis for describing input parameters for describing soil behavior in finite element modeling. Benefits from the mathematical representation will give increased accuracy in the description of soil properties as well as alleviation of difficult convergence problems frequently encountered while solving problems in unsaturated soils. A general mathematical procedure to model many soil property functions is presented in this thesis. This procedure allows for the complete mathematical description of the constitutive behavior for saturated or unsaturated soils.

2.2 Significance of the Soil-Water Characteristic Curve

The soil-water characteristic curve (SWCC) has become the central relationship in describing the behavior of unsaturated soils (Fredlund, 1993). It has been shown that the soil-water characteristic curve may be used as the basis for the estimation of many other unsaturated soil property functions (Fredlund, 1997). Proper mathematical representation of this curve is therefore important. Equations for the representation of the soil-water characteristic curve as well as a theoretical method for the estimation of the same curve are presented in this thesis.

Numerous equations have been proposed to model the soil-water characteristic curve (Sillers, 1997). The equations vary in a number of different ways. The historical development of the equations show that each researcher has attempted to enhance the work of previous researchers in an attempt to improve and account for different characteristics of the curve (Barbour, 1999). Each improvement has provides a representation of the soil-water relationship that more closely resembles the natural curve. The soil-water characteristic curve is typically plotted as the volumetric water content versus soil suction in the soil. The relationship is typically S-shaped on a semi-log scale and yields different curves based on the type of soil described. The curve has become the standard relationship used for determining the water storage function, in saturated/unsaturated finite element seepage problems. The curve is also used in the estimation of a permeability function for unsaturated soils.

The soil-water characteristic curve can be used as a foundation for calculating other related soil property functions such as permeability, shear strength and volume change. It forms a partial basis for describing the engineering behavior of an unsaturated soil and provides a means of relating the fundamental soil properties to one another. The soil-water characteristic curve becomes particularly important when modeling more than one aspect of soil behavior in a single analysis. Furthermore, important information for the pore size distribution and the amount of water contained in the pores at a given suction is provided. The soil-water characteristic curve has three stages that describe the process of desaturation of a soil as shown in Figure 1 (i.e., for increasing suction). These are outlined below starting with saturation conditions in the soil.

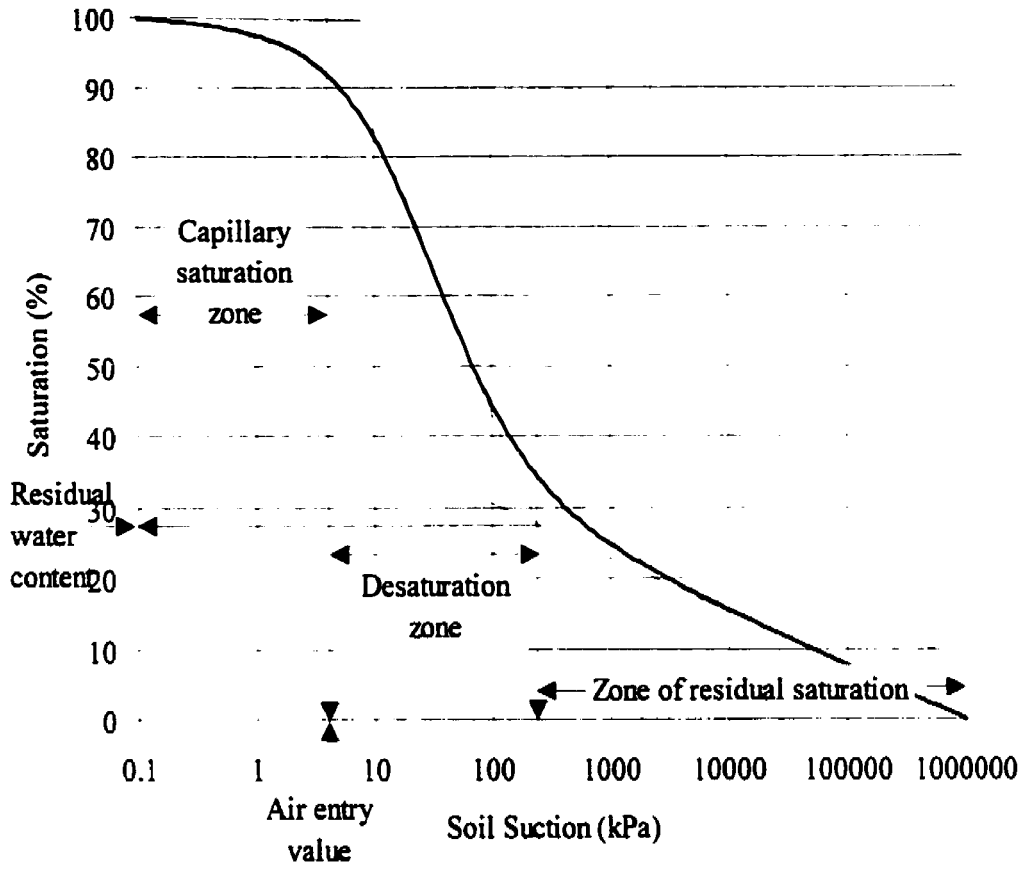

Figure 2-1 Soil-water characteristic curve illustrating the components (Sillers, 1997)

1. The *Capillary Saturation Zone* where the pore-water is in tension but the soil remains saturated. This stage ends at the air entry value, ψ_b, where the applied suction overcomes the capillary water forces in the largest pore in the soil.

2. The *Desaturation Zone* is where water is displaced by air within the pores. Liquid water drains from the pores and is displaced by air. This stage ends at the residual water content, θ_r, where the pore-water becomes discontinuous and the coefficient of permeability is greatly reduced.

3. The *Residual Saturation Zone* where the water is tightly adsorbed onto the soil particles and flow occurs in the form of vapor. This stage is terminated at oven dryness. When the soil is heated to 105° C, the soil is defined to have zero water content and the soil suction is

approximately 1 x 10^6 kPa (Fredlund and Rahardjo, 1994). This point forms a benchmark for all soils and any water not driven off at this point is considered chemically bonded to the soil. It does not appear to be important with respect to the engineering behavior of the soil.

Laboratory studies have shown that there is a relationship between the soil-water characteristic curve and unsaturated soil properties (Fredlund and Rahardjo, 1993b). The soil-water characteristic curve is a measured soil property that is used to derive other soil functions and provides a common reference to the stress-state. In other words, it ensures that each soil property is referenced to the same stress-state.

There is a high degree of variability in the type of soil-water characteristic curves that can be measured. However, all curves appear to have a number of distinguishing features. The distinguishing characteristics that have been defined are the air-entry value of the curve, residual water content, and residual suction of the curve, as well as the common point of zero water content corresponding to a soil suction of 1,000,000 kPa. These features can be seen in Figure 2-2. A detailed description of the construction technique used to define these characteristics can be found in Vanapalli, Sillers, and Fredlund (1998).

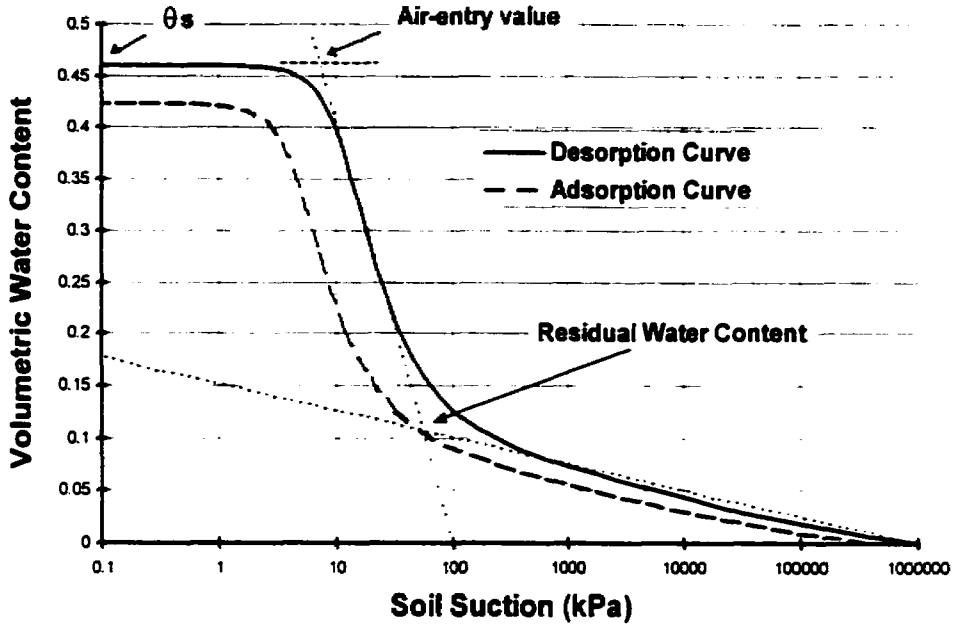

Figure 2-2 Definition of variables associated with the soil-water characteristic curve.

2.3 Equations for the Soil-Water Characteristic Curve

Several equations have been presented as models for defining soil-water characteristic curves (Sillers, 1997). Five of the most common methods are the Brooks and Corey equation (1964), the Gardner equation (1974), the van Genuchten and Burdine equation (1953), the van Genuchten and Mualem equation (1976), the van Genuchten equation (1980), and the Fredlund and Xing (1994) equation. A summary of these equations are presented in the following paragraphs.

The following soil-water characteristic equations are presented in terms of gravimetric rather than volumetric water content. Representation of the soil-water characteristic curve in terms of gravimetric water content disallows experimental errors associated with volume change of the soil during drying.

2.3.1 The Brooks and Corey Equation

A power-law relationship was proposed by Brooks and Corey (1964). This model represented the first attempt to use an equation to describe the soil-water characteristic curve. The equation is as follows.

$$w(\psi) = w_r + (w_s - w_r)\left[\frac{a_c}{\psi}\right]^{n_c}$$

Equation 2-1

where:

a_c = bubbling pressure (kPa),

n_c = pore size index,

w_s = saturated gravimetric water content,

w_r = residual gravimetric water content, and

ψ = soil suction (kPa).

2.3.2 The Gardner Equation

Gardner (1964) presented a continuous equation for the first coefficient of permeability function. The form of the equation has subsequently been the basis for the soil-water characteristic curve as well as many other equations proposed in subsequent literature. Gardner's equation for the soil-water characteristic curve is given as follows.

$$w(\psi) = w_{rg} + (w_s - w_{rg})\left[\frac{1}{\left[1 + a_g \psi^{n_g}\right]}\right]$$

Equation 2-2

where:

a_g = soil parameter that is primarily a function of the air entry value of the soil in kPa,

n_g = soil parameter that is primarily a function of the rate of water extraction from the soil, once the air entry value has been exceeded,

w_s = saturated gravimetric water content,

w_{rg} = residual gravimetric water content, and

ψ = soil suction (kPa).

2.3.3 The van Genuchten Equation

van Genuchten (1980) presented a three parameter equation with the flexibility to fit a wide range of soils. The parameters of the equation were typically found using a least-squares algorithm.

$$w(\psi) = w_{rvg} + (w_s - w_{rvg}) \left[\frac{1}{\left[1 + (a_{vg}\psi)^{n_{vg}} \right]^{m_{vg}}} \right]$$

Equation 2-3

where:

a_{vg} = soil parameter that is primarily a function of the air entry value of the soil in kPa,

n_{vg} = soil parameter that is primarily a function of the rate of water extraction from the soil, once the air entry value has been exceeded,

m_{vg} = soil parameter that is related to the residual water content of the soil. Typical range (0.9-1.1),

w_s = saturated gravimetric water content,

w_{rvg} = residual gravimetric water content, and

ψ = soil suction (kPa).

2.3.4 The van Genuchten and Mualem/Burdine Equations

Two separate simplifications to the van Genuchten equation have been proposed. Relations between the *m* and *n* parameters of the van Genuchten equation were prescribed to reduce the

number of fitting parameters from three to two. The simplifications proposed by Mualem (1976) and Burdine (1953) can be seen below. The Maulem (1976) equation is as follows:

$$w(\psi) = w_{rm} + (w_s - w_{rm}) \left[\frac{1}{\left[1 + (a_m \psi)^{n_m} \right]^{\left(1 - \frac{1}{n_m}\right)}} \right]$$

Equation 2-4

where:

a_m = soil parameter that is primarily a function of the air entry value of the soil in kPa,

n_m = soil parameter that is primarily a function of the rate of water extraction from the soil, once the air entry value has been exceeded,

w_s = saturated gravimetric water content,

w_{rm} = residual gravimetric water content, and

ψ = soil suction (kPa).

The Burdine (1953) equation is as follows:

$$w(\psi) = w_{rb} + (w_s - w_{rb}) \left[\frac{1}{\left[1 + (a_b \psi)^{n_b} \right]^{\left(1 - \frac{2}{n_b}\right)}} \right]$$

Equation 2-5

where:

a_b = soil parameter that is primarily a function of the air entry value of the soil in kPa,

n_b = soil parameter that controls the slope at the inflection point in the soil-water characteristic curve with a typical range of 1 to 2,

w_s = saturated gravimetric water content,

w_{rb} = residual gravimetric water content, and

ψ = soil suction (kPa).

2.3.5 Fredlund and Xing Equation

Fredlund and Xing (1993) presented a three-parameter equation with the flexibility to fit a wide range of soils. The equation also provides increased accuracy in the high suction range. The parameters of the equation were typically found using a least-squares algorithm.

$$w(\psi) = w_s \left[1 - \frac{\ln\left(1+\frac{\psi}{h_r}\right)}{\ln\left(1+\frac{10^6}{h_r}\right)} \right] \left[\frac{1}{\left[\ln\left[\exp(1) + \left(\frac{\psi}{a_f}\right)^{n_f} \right] \right]^{m_f}} \right]$$

Equation 2-6

where:

w_s = saturated gravimetric water content,

a_f = fitting parameter related to the air entry value for the soil,

n_f = fitting parameter related to the maximum slope of the curve,

m_f = fitting parameter related to the curvature of the slope, and

h_r = typically represents the soil suction related to residual water content (kPa),

ψ = soil suction (kPa).

The equations presented above have all been used to model the soil-water characteristic curve. While the Brooks & Corey (1964) equation was the first popularized equation used to represent the soil-water characteristic curve, it's primary drawback was the lack of continuous representation. The representation of water content at suctions less than the bubbling pressure or air-entry value (AEV) is typically ignored. Gardner (1964) then proposed a continuous

equation originally used to represent soil-water permeability as a function of soil suction. The equation was later used extensively to represent the soil-water characteristic curve. van Genuchten (1980) presented a three-parameter equation which could be used to mathematically represent the soil-water characteristic curve. Simplifications to the van Genuchten (1980) equation were later proposed by Mualem (1976) and Burdine (1953) to reduce the number of parameters. Fredlund & Xing (1993) presented a four-parameter equation capable of providing an improved fit of the soil-water characteristic curve at higher suctions. The representation of the soil-water characteristic curve by the Fredlund & Xing (1993) equation allowed the soil-water state to be represented from completely dry to saturated conditions.

2.4 Use of Saturated Soil Properties and the Soil-water Characteristic Curve

Theory governing the behavior of unsaturated soils has been available for several years and has shown that the soil-water characteristic curve (SWCC) is the central relationship describing how a soil behaves as it desaturates. Research has shown that empirical relationships can be used to describe unsaturated property functions related to the soil-water characteristic curve. These empirical relationships can then be used to predict the permeability, shear strength, thermal, and diffusion properties as a soil desaturates. The process for predicting the behavior of an unsaturated soil is then greatly simplified.

Classical soil mechanics has emphasized specific types of soils (e.g., saturated sands, silts, and clays and dry sands). Many textbooks cover the theories related to these types of soils in a completely dry or a completely saturated condition. Recently, it has been shown that attention must be given to soils that do not fall into these common categories. Many of these soils can be classified as unsaturated soils. Engineering related to unsaturated soils has typically remained empirical due to the complexity of their behavior.

An unsaturated soil consists of more than two phases and therefore the natural laws governing its behavior are changed. Central to the behavior of an unsaturated soil is the relationship between the relative amounts of water and air as the soil desaturates. This relationship is

described by the soil-water characteristic curve. Laboratory studies have shown that there is a relationship between the soil-water characteristic curve and unsaturated soil properties (Fredlund and Rahardjo, 1993b). Properties such as hydraulic conductivity, shear strength, water storage, unfrozen water content, specific heat, thermal conductivity, and diffusion can all be related to the soil-water characteristic curve.

2.5 Examples of Unsaturated Soil Property Functions

A theoretical framework for unsaturated soil mechanics has been firmly established over the past couple of decades. The constitutive equations for volume change, shear strength and flow for unsaturated soil have become generally accepted in geotechnical engineering (Fredlund and Rahardjo, 1993a). The measurement of soil parameters for the unsaturated soil constitutive models, however, remains a demanding laboratory process.

The following sections present typical soil property functions. These functions have been used by geotechnical engineers in the solution of a wide variety of problems. Accurate representation of these functions greatly enhances their application in engineering practice. A listing of unsaturated soil property functions may be seen in the following table.

Table 2-1 Typical soil property functions

Function	*Soil Property*	*Dependent Variable*	*Application*
Soil-water characteristic curve	Gravimetric water content, w	Soil suction	Unsaturated seepage modeling
Permeability	Hydraulic conductivity, k	Soil suction	Unsaturated seepage modeling
Water storage	m^2_w	Soil suction	Unsaturated seepage modeling
Shrinkage	Void ratio	Gravimetric water content, w	Volume change/deformation modeling
Swell	Void ratio	Gravimetric water content, w	Volume change/deformation modeling
Shear strength	Shear strength	Soil suction	Volume change/deformation modeling

Thermoconductivity	Thermoconductivity	Soil suction	Evapotranspiration modeling
Specific heat	Specific heat	Soil suction	Evapotranspiration modeling
Unfrozen water content	Unfrozen volumetric water content	Degrees below freezing	Evapotranspiration modeling
Diffusion	Diffusion	Soil suction	Contaminant transport modeling
Adsorption	Adsorption	Soil suction	Contaminant transport modeling

2.5.1 Coefficient of Permeability Functions

The difference between the coefficients of permeability of a clay and a gravel can be greater than 10 orders of magnitude. Obtaining an accurate assessment of this parameter often becomes a major obstacle in analyzing the amount of seepage through a soil. Knowing the coefficient of permeability (or hydraulic conductivity) of a soil is vital for field management of resources and maintenance of environmental quality.

Much effort has been expended to develop computer models capable of analyzing seepage through soils. The problem is further complicated by the fact that seepage through an unsaturated soil varies according to the degree of saturation of the soil. Many measurements must be made at various degrees of saturation to provide confidence in the hydraulic properties. It is, therefore, of value to utilize simplified theoretical methods for the prediction of the hydraulic conductivity of soils.

Models that can be used to predict the coefficient of permeability of soils can be divided into three categories. The model either predict: (1) the saturated coefficient of permeability of a soil (Ahuja, 1989; Russo, 1980; Brakensiek, 1992; Rawls, 1993; Sperry, 1994), or, (2) the curve describing the variation in the coefficient of permeability as a soil desaturates (Fredlund, 1994), or, (3) both the saturated coefficient of permeability and the curve showing the variation of the coefficient of permeability as a soil desaturates (i.e., Durner, 1994).

Once the saturated coefficient of permeability of a soil is known, it can be assumed to be a relatively unique function of the water content (Fredlund, Xing, and Huang, 1994). The

function appears to be essentially unique as long as the volume change of the soil structure is negligible or reversible. A function that relates the soil-water characteristic curve and the coefficient of permeability was presented by Campbell (1974). These models allow the complete coefficient of permeability function to be estimated from a saturated coefficient of permeability and a soil-water characteristic curve.

2.5.2 Water Storage Functions

The water storage function provides the change in volumetric water content versus soil suction. This function is useful in modeling seepage through an unsaturated soil as it indicates the rate of change in the water storage of a soil at a given soil suction.

In mathematical terms, the water storage curve is the derivative or slope of the soil-water characteristic curve equation when the soil-water characteristic curve is represented in terms of volumetric water content. The soil-water characteristic curve is typically measured in terms of gravimetric water content and must therefore be converted to volumetric water content. The soil-water characteristic curve represented in terms of gravimetric water content may be scaled directly to volumetric water if the effects of volume change are assumed to be negligible. The Fredlund & Xing (1994) equation (represented in terms of volumetric water content) and its derivative are as follows:

$$\theta_w(\psi) = \left[1 - \frac{\ln\left(1 - \frac{\psi}{\psi_r}\right)}{\ln\left(1 - \frac{1000000}{\psi_r}\right)}\right] \cdot \frac{1}{\ln\left[\exp(1) - \left(\frac{\psi}{a}\right)^n\right]^m} \cdot \theta$$

Equation 2-7

The derivative of Equation 2-7 provides a water storage function as follows:

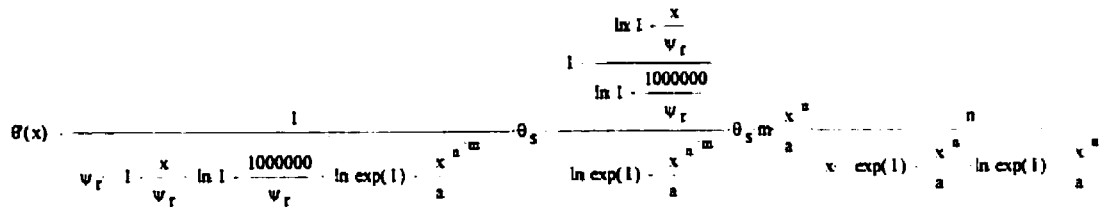

Equation 2-8

where: x = soil suction.

The water storage function provided above is used in solving transient unsaturated seepage and flux boundary models such as the SoilCover model (USG, 1997).

2.5.3 Volume Change Functions

Most changes in the stress-state of a soil produce a volume change. The amount of volume change and the time interval over which this volume change occurs is significant for a number of problems. Heave, shrinkage and consolidation problems rely on a description of the volume change of a soil.

The aim of this thesis is to provide a procedure to describe volume change functions. This global objective requires mathematical descriptions for the shrinkage curve function, the soil-water characteristic curve, and the compression curve.

2.5.3.1 Shrinkage Curve Function

The shrinkage curve has historically been used as a means to obtain the shrinkage limit as a classification property. More recently, the shrinkage curve has been used to represent the relationship between volume change and water content change. The shrinkage curve for soils can be measured and used as the basis for finite element simulations where both volume change and water content change need to be predicted.

Typical research emphasis involves the application of the shrinkage curve to a particular problem. Other research involves proper techniques involved in the measurement of the

shrinkage curve. Further theoretical development for describing the shrinkage curve and its relationship to other unsaturated soil functions using a mathematical relationship are presented in this thesis. Calculations to extend the soil-water characteristic curve to compute the volume change function are also presented.

2.5.3.2 Compression Curve Function

The compression curve is a central soil property function to a wide variety of soil problems. Classic formulations for the solution to settlement, heave, and consolidation analysis depend on the laboratory measurement of the compression curve. The accuracy with which the compression soil-property function is represented will determine the accuracy of the final solution. Typical straight-line approximations of the compression curve cause a break in the compression curve when moving between the recompression and virgin compression branches. These 'breaks' are physically unrealistic and can lead to numerical instability in finite element programs. A continuous equation to provide a smooth transition between soil states and improve convergence in numerical models is presented in this thesis.

The primary contribution of this thesis will be the development of procedures to integrate the soil property functions to describe volume change with respect to the two independent stress states for matric suction and total stress.

2.6 General Procedure for the Integration of Unsaturated Soil Property Functions

Several approaches can be taken towards the determination of unsaturated soil property functions (Fig. 3). The term, **unsaturated soil property functions,** refers to such relationships as: 1.) coefficient of permeability versus soil suction, 2.) water storage variable versus soil suction, and 3.) shear strength versus soil suction and (4) the volume change function.

Laboratory tests can be used as a direct measure of the required unsaturated soil property. For example, a (modified) direct shear test can be used to measure the relationship between matric suction and shear strength (Fredlund et al., 1997). These tests are costly and time consuming

and the necessary equipment may not be available. Therefore, it may be necessary to revert to an indirect laboratory test involving the measurement of the soil-water characteristic curve for the soil.

The soil-water characteristic curve can be used in conjunction with the saturated shear strength properties of the soil, to predict the relationship between shear strength and matric suction. Some accuracy will likely be lost in reverting to this approach; however, the trade-off between accuracy and cost may be acceptable for many engineering projects.

The approach outlined above is an example for a procedure to predict soil behavior on the basis of integrating soil properties that can be readily measured. The procedure provided in this thesis begins with the grain-size analysis of the soil. A classification test such as a grain size analysis is used to estimate the soil-water characteristic curve which in turn is used to determine the unsaturated soil property function. A theoretical curve could be fitted through the data from a grain size analysis. The theoretical grain size curve can then be used to predict the soil-water characteristic curve.

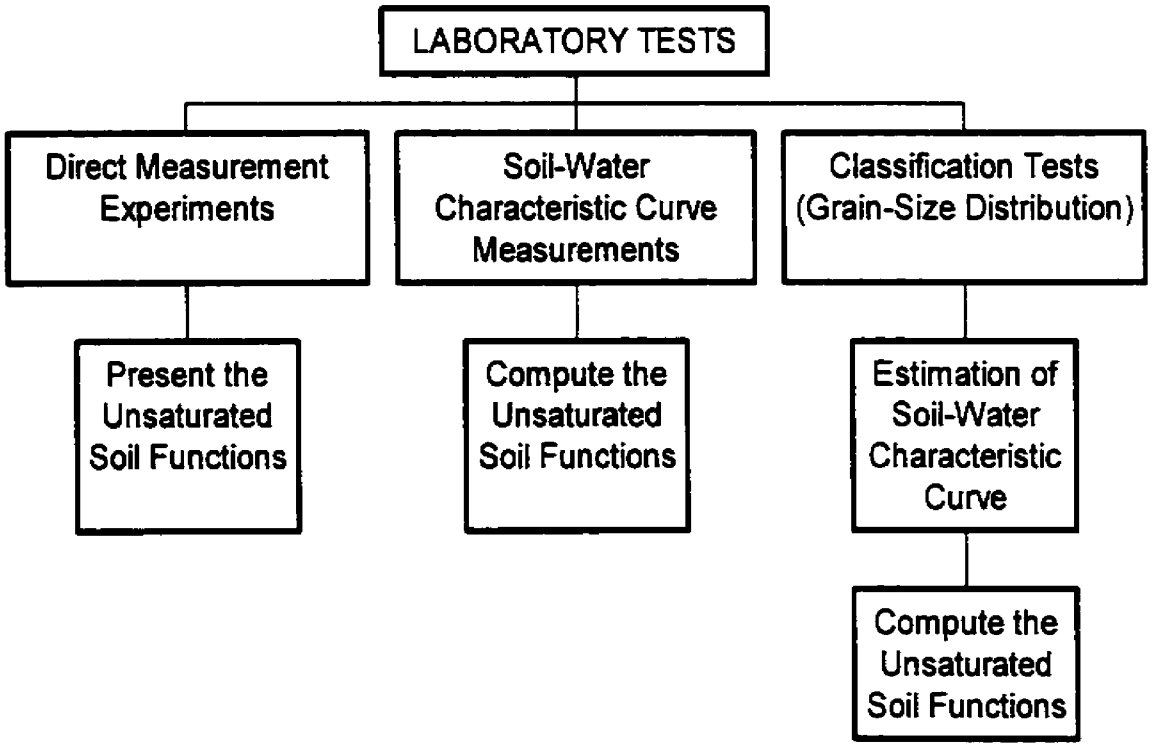

Figure 2-3 Approaches that can be used in the laboratory to determine the unsaturated soil properties.

2.6.1 Soil property function representation

There are several methods of representation of soil property functions. The pros and cons of each of these different representation methods will be outlined in the following points.

1. Digital points:

The simplest representation of a soil property function is given by a series of points along the function. Representing a curve with a series of points is simple and commonly used. In fact, it has been used for decades by geotechnical engineers in hand drawn plots for presentation of consolidation test results. However, this simple approach does not to provide any indication of the type of function which generated the points. Furthermore, the series of points do not provide continuous representation of function. Typically, linear interpolation is used to determine values between generated points.

2. Fit, closed-form equation:

Fitting an equation to a set of laboratory or experimental points provides acceptable method of interpretation that is both smooth and continuous. Fitting is typically performed by a nonlinear, least squares algorithm. Equation parameters are adjusted to accommodate the variability in soils. Finite element programs such as PDFlex™ allow direct input of equations.

3. Complex equation:

Certain soil property functions may be represented by complex equations. These equations typically involve integration. An example of this is the Fredlund and Xing (1994) equation for the estimation of hydraulic conductivity. Closed form solutions are not available for these complex equations. Their evaluation at certain points involves algorithms that must perform the integration.

4. Algorithm (Pedo-Transfer Function):

Estimation of the soil-water characteristic curve has received significant attention in the field of soil science. Bunze (1987) was the first to describe such estimation techniques as 'pedo-transfer

functions'. Bunze (1987) used the term to describe algorithms which estimate soil property functions from limited or simple data. The term 'pedo-transfer functions' is broad enough to include estimations of other soil property functions such as permeability or shear strength. Pedo-transfer functions may provide output in digital or equation form.

2.7 General Categories Defining the History of the Soil

There are three primary categories of soil behavior that must be independently analyzed. The categories are as follows:

1.) slurried or soils that are initially remolded at a high water content,

2.) compacted soils, and

3.) undisturbed soils.

Data can generally be found in the research literature for each of the above categories. Usually the easiest data to analyze is that obtained from initially slurried soils. This highly remolded condition may not bear much resemblance to natural soils but the data often proves to be of great value in the establishment of constitutive forms for fundamental behavior of the soil. This data can be considered of value to determine the form for unsaturated soil property functions for tailings impoundment and hydraulicaly placed soil.

Compacted soils have an induced stress history and the testing of these soils in the laboratory produces results that can differ considerably from those of initially slurried specimens.

The third class involves the test results obtained from undisturbed samples tested in the laboratory. Once again, the test results may have distinctive features from those of the above categories.

The proposed soil property functions should be applicable for all types of soil stress histories. It is generally preferable to start with the results from initially slurried specimens but eventually, it is necessary to be able to simulate the results of undisturbed and compacted specimens. The above three categories of soil history will be given consideration for each of the soil property functions studied in the present work.

2.8 Summary

Research to-date in the area of saturated and unsaturated soils has provided the mathematical basis for representation of certain soil property functions, namely, the soil-water characteristic curve and the grain-size distribution. Mathematical representation of volume change functions such as the compression curve and shrinkage curve was found to be inadequate for the finite element modeling of volume change. This thesis enhances current mathematical representation of the grain-size distribution, shows how these new grain-size equations may be used to estimate the soil-water characteristic curve, and provides mathematical representation of the compression and shrinkage soil property functions. The mathematical foundation provided by these functions then allows for mathematical representation of the two constitutive surface for an unsaturated soil. These mathematical constitutive surfaces may then be used to model coupled seepage and volume change problems in saturated or unsaturated soils.

2.9 References

Arya, L.M., and Paris J.F., (1981), A physicoempirical model to predict the soil moisture characteristic from particle-size distribution and bulk density data, Soil Science Society of America Journal, Vol. 45, pp. 1023-1030.

Brooks R.H. and A.T. Corey, (1964), Hydraulic Properties of Porous Media, Colorado State Univ. Hydrol. Paper, No. 3, 27, pp. March 1964.

Burdine, N.T., (1953), Relative permeability calculations from pore size distribution data, Journal of Petroleum Technology, Vol. 5, No. 3, pp. 71-78

Campbell, G.S., (1985), Soil Physics with Basic, Elsevier, New York

Fredlund, D. G. and H. Rahardjo. 1993. Soil mechanics for unsaturated soils. John Wiley & Sons, Inc., New York.

Fredlund, D.G., and Xing, A., (1994), Equations for the soil-water characteristic curve, Canadian Geotechnical Journal, Vol. 31, No. 3, pp. 521-532.

Fredlund, M.D., D.G. Fredlund, and G.W. Wilson, (1997), Prediction of the Soil-Water Characteristic Curve from Grain-Size Distribution and Volume-Mass Properties, 3rd Brazilian Symposium on Unsaturated Soils, Rio de Janeiro, April 22-25

Fredlund, M.D., Fredlund, D.G. and Wilson, G.W., (1999), An Equation to Represent Grain-Size Distribution, Canadian Geotechnical Journal, (In Review).

Fredlund, M. D., Fredlund, D. G., and Wilson, G. W., (1998), Application of Knowledge-Based Systems in Estimating Unsaturated Soil Property Functions for Numerical Modelling, Proceedings of the Second International Conference on Unsaturated Soils, UNSAT2, Beijing, China, August 27 – 30, pp. 479-484.

Fredlund, M. D., Fredlund, D. G., and Wilson, G. W., (1997), Estimation of Unsaturated Soil Properties Using a Knowledge-Based System, Proc. of the Fourth Congress on Computing in Civil Engineering, ASCE, Philadelphia, PA., June 16 – 18, pp. 501-510.

Fredlund, M. D., Wilson, G. W., and Fredlund, D. G., (1997), Indirect Procedures to Determine Unsaturated Soil Property Functions, Proceedings of the 50th Canadian Geotechnical Conference, Golden Jubilee, Ottawa, Canada, October 20 – 22, 1997, pp. 407-414.

Fredlund, M.D., Wilson, G.W., and Fredlund, D.G. (1997) Prediction of Soil-Water Characteristic Curve from Grain-size Distribution, Proc. of the 3rd Brazilian Symposium on Unsaturated Soils, NSAT'97, Rio de Janeiro, Brazil, April 21-25, Vol. 1, pp. 13 - 24.

Fredlund, D.G., Xing, A., Fredlund, M.D., and Barbour, S.L. (1996) The Relationship of the Unsaturated Shear Strength to the Soil-Water Characteristic Curve, Canadian Geotechnical Journal, Vol. 33, No. 3, pp. 440-448.

Siller, W. S., (1997), The Mathematical Representation of the Soil-Water Characteristic Curve, M.Sc. Thesis, University of Saskatchewan, Saskatoon, 241p.

Vanapalli, S., Sillers, S., and Fredlund, M.D., (1998). The Meaning and Relevance of Residual State to Unsaturated Soils, Proceedings of the 51st Canadian Geotechnical Conference, Edmonton, Alberta, Vol. 1, pp. 101-112.

CHAPTER 3.0 An Equation to Represent Grain-Size Distribution

3.1 Introduction

The grain-size distribution is a simple, yet informative test routinely performed in soil mechanics. Valuable information regarding the amount of each particle size can be determined in the laboratory with a series of sieves. The finer particle sizes are usually determined through the use of a hydrometer analysis; thereby extending the particle size range down to the clay size fraction. Recent research has made use of the grain-size distribution as the basis for the estimation of other soil properties such as the soil-water characteristic curve (Gupta and Larson, 1979; Arya and Paris, 1981; Haverkamp and Parlange, 1986). It is of value to be able to mathematically represent the grain-size distribution curve as a continuous function that will allow further analysis to be performed. The specific objective of this chapter is to develop a mathematical description for the grain-size distribution of any given soil. This forms the foundation step for the general procedure to determine the related soil property functions and constitutive relations.

Mathematically representing the grain-size distribution provides several benefits to soil mechanics. Firstly, the soil can be classified using the best-fit parameters. Secondly, the mathematical equation can be used as the basis for further soil analysis and description. An example is the estimation of the soil-water characteristic curve from the grain-size distribution. Thirdly, a mathematical equation can provide a method of representing the entire curve between measured data points.

ASTM D422-54T provides a basic testing and reporting method whereby the results of a sieve and hydrometer analysis are plotted on a semilog graph. An interpretation method for the series of plotted points is specified in the procedure. Manual interpretation methods such as sketching in a complete curve, have often been used to provide a complete grain-size distribution curve. Gardner (1956) proposed a two-parameter log-normal distribution to provide a description of

grain-size distribution data. While the above methods are feasible, both methods have limitations that will be discussed later in this chapter.

Two new models to fit grain-size data are proposed in this chapter. These models consist of a unimodal and a bimodal mathematical function. The two new equations provide greater flexibility for fitting a wide variety of soils.

3.2 Definition of variables

The grain-size distribution for a soil is defined as the relationship between percent passing (by mass) and the particle size. It has also been called the mass-based aggregate size distribution or the ASD. The particle size represents the size of particles that can pass a particular sieve mesh. The percent passing represents the mass percentage of particles passing a particular sieve size.

A number of variables are used to describe the physical attributes of the soil. The main variables are as follows: % clay, % silt, % sand, % coarse, d_{10}, d_{20}, d_{30}, d_{50}, C_u, and C_c. These variables are defined as follows:

d = particle diameter, mm,

% clay = percentage of clay-sized particles present in the soil (USCS definition is d > 0.005 mm),

% silt = percentage of silt-sized particles present in the soil (USCS definition is 0.005 < d < 0.075 mm),

% sand = percentage of sand-sized particles present in the soil (USCS definition is 0.075 < d < 4.75 mm),

d_{10} = diameter at which 10% of the soil particles pass,

d_{20} = diameter at which 20% of the soil particles pass,

d_{30} = diameter at which 30% of the soil particles pass,

d_{50} = diameter at which 50% of the soil particles pass,

d_{60} = diameter at which 60% of the soil particles pass,

C_u = Coefficient of uniformity, d_{60}/d_{10}, and

C_c = Coefficient of curvature, $d_{30}^2/(d_{10} \times d_{60})$.

The magnitude of the values for the above variables may vary slightly depending on the method used to represent the grain-size distribution. The reason for the variation is that the parameters must be interpolated from the grain-size distribution curve.

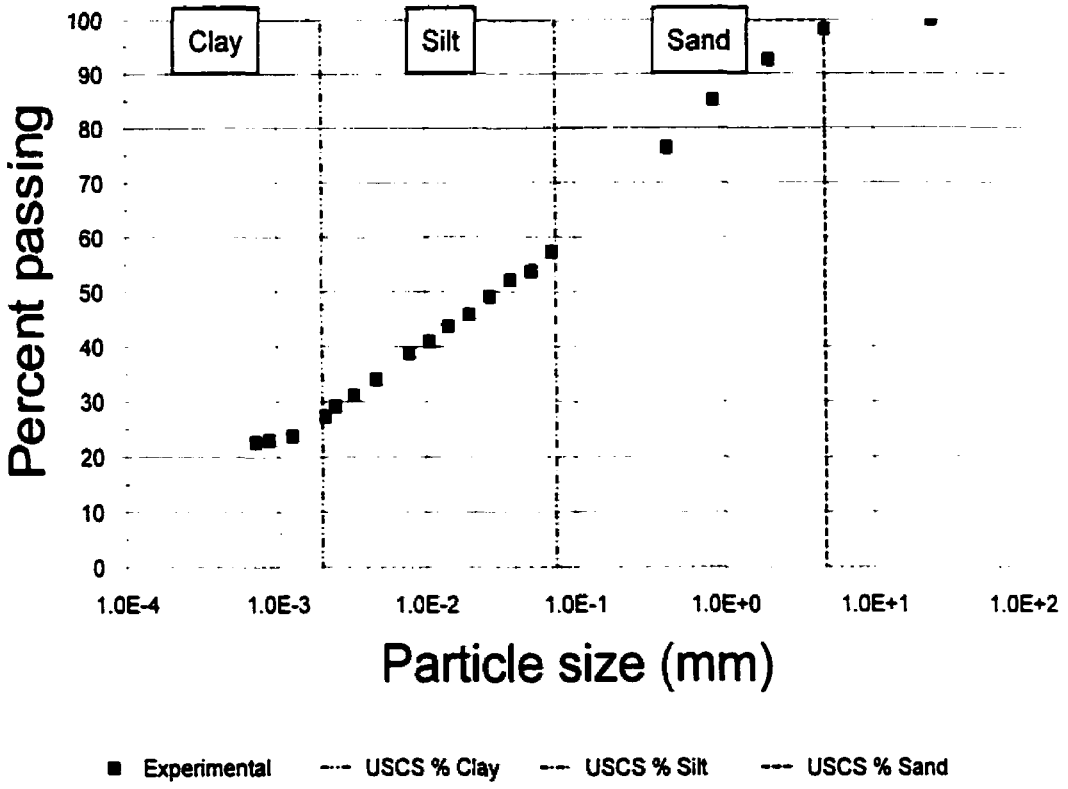

Figure 3-1 Experimental points on grain-size distribution for a well-graded residual waste rock from the University of Saskatchewan (11579)

Experimental data for a typical grain-size distribution curve are illustrated in Figure 3-1. A sieve analysis and a hydrometer analysis is used to measure points on the grain-size distribution curve in accordance with ASTM D422-54T. The finest sieve size used is the #200 sieve which allows particles finer than 0.075 mm to pass. Particles finer than 0.075 mm are classified as silt and clay size particles and a hydrometer analysis (ASTM D422) is used to determine points on the grain-size distribution finer than the #200 sieve. The results provide an indication of the amount of silt and clay size particles in the soil.

3.3 Background

Heywood (1947) referred to sieving as the "Cinderella" of the sizing processes: "it does most of the hard work yet is greatly neglected with regards to research" (Harr, 1977). Sieving has become one of the most common and easy to perform tests in soil mechanics; yet its value has often been ignored. Statistical representation methods are easily applied to the results of the sieve test (Harr, 1977). Because of the correlation between specific surface and particle size, the percentage distribution of the various sizes of individual particles within a soil has served as an important soil characteristic (Bauer, 1972). It remains to this day as one of the most common methods of physical analysis. Harr (1977) described the sieve test as follows:

> *A representative sample of the material is placed at the top of a nest of sieves of successively smaller openings and the system is shaken so that particles able to do so may pass through the openings large enough to permit their passage. Determinations are made of the weight fractions (usually as a percentage of the total weight) which have passed one sieve and are retained upon the next smaller size.*

The ASTM sieve sizes used in the test can be found in Lambe (1951). Various errors that may be encountered in the sieve test are discussed by Herdan (1960).

Numerous methods for particle-size analysis in the laboratory and field have been developed over the years. These include the elutriation method, the test-tube-shaking method, the Wiegner sedimentation cylinder, the photoelectric method, the pipette method, and the hydrometer method. Of these methods, only the latter two have found general acceptance (Kohnke, 1968).

ASTM D422-54T (1958) presented a standard for testing of the grain-size distribution. The method summarized the work of research already performed. Standard sieve sizes, reporting methods, and methods for performing a hydrometer analysis were presented. The sieve analysis allowed points on the grain-size distribution to be determined for particle sizes greater than the #200 sieve or 0.074 mm. The hydrometer analysis was presented by ASTM to standardize a method for determining the grain-size distribution for particles smaller than the #200 sieve. The

hydrometer analysis allowed for separation of particle sizes based on Stoke's law. ASTM did not present a method for interpreting the points on the grain-size distribution curve. Interpretation of the grain-size distribution was typically carried out manually.

Gardner (1956) used a two-parameter, log-normal distribution to fit grain-size distribution data. Kempil and Chepil (1965) further confirmed the work of Gardner (loc cit.). The two-parameter fit of the grain-size distribution was performed using a geometric mean parameter, x_g, and a geometric standard deviation, σ_g. The method of fitting log-normal equations to the grain-size distribution was not recommended for general use. However, the reason given for not using the log-normal method was the lack of computing power necessary to fit the equation to data. Hagen et al (1987) presented a computerized, iterative procedure that required only two sieves to determine the parameters for a standard, two-parameter log-normal distribution. Unfortunately, the log-normal distribution often failed to provide a close fit of the grain-size distribution at the extremes of the curve (Gardner, 1956; Hagen et al, 1987). Wagner (1993) later improved upon the log-normal equation by presenting three and four parameter log-normal equations.

Campbell (1985) presented a classification diagram based on the assumption that the particle-size distribution is approximately log-normal. This assumption led to the particle-size distribution being approximated with a Gaussian distribution function. With this assumption, any combination of sand, silt, and clay can be represented by a geometric (or log) mean particle diameter and a geometric standard deviation. Values were summarized in a modified USDA textural classification chart by Shirizi (1984).

The first limitation associated with using a log-normal type of equation is the assumption that the grain-size distribution is symmetric. In reality, the grain-size distribution is often non-symmetric and can be better fit by a different type of equation. Secondly, a method for fitting soils that are bimodal or gap-graded is often of value and the four-parameter log-normal equations have not been found to be satisfactory for fitting gap-graded grain-size distributions.

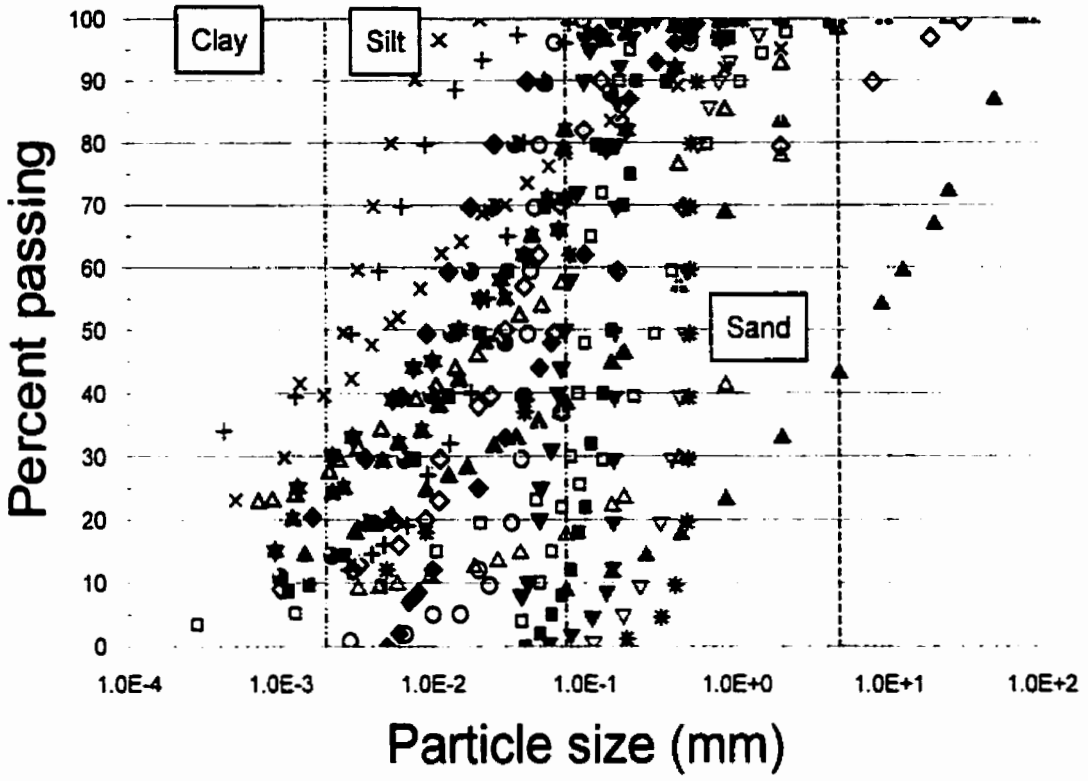

Figure 3-2 Typical grain-size distribution data collected from literature

Typical grain-size distribution curves for several soils are shown in Figure 3-2. The data illustrates that the variance between different soils can be significant.

There are three general categories of grain-size distributions. These three types of distributions are known as *well-graded* soils, *uniform* soils, and *gap-graded* soils. Figure 3-3 illustrates each type of grain-size distribution. This chapter focuses on these three categories of grain-size distributions and provides equations to fit the experimental data for each category. The well-graded soils and the uniform soils are examined and a unimodal method of fitting an equation is developed and then a mathematical method of representing a gap-graded soil is subsequently presented.

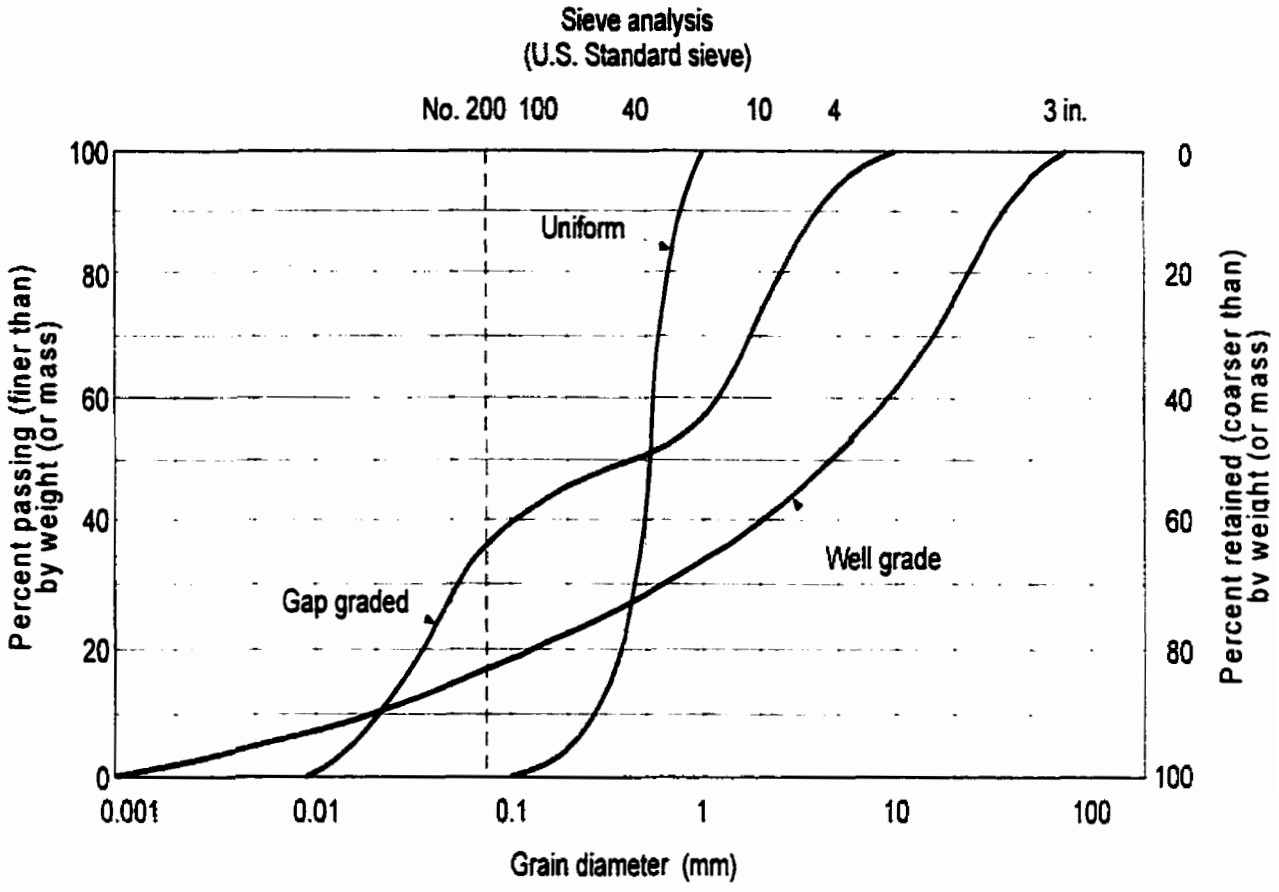

Figure 3-3 Three primary types of grain-size distribution curves (Holtz & Kovacs, 1981)

3.4 Unimodal Equation for the Grain-size Distribution

The selection of an appropriate, mathematical equation involves a review of a variety of equations that could be used to fit soils data. It has been observed that the soil-water characteristic curve possesses a shape similar to that of the grain-size distribution. This is to be expected since the soil-water characteristic curve describes the void distribution in a soil while the grain size curve provides information on the distribution of the solid phase of the soil. Since the solids plus the voids add up to the total soil volume, it is to be expected that the distribution of the solids phase (i.e., grain-size distribution) would tend to bear an inverse relationship to the distribution of voids (i.e., soil-water characteristic curve), and vice versa.

A summary of several of the equations used to fit the soil-water characteristic curve is shown in Table 3-1. Examples of equations that have been presented are those by Brooks and Corey, 1964; Gardner, 1974; van Genuchten, 1980; Burdine, 1953; Mualem, 1976; Fredlund and Xing, 1994.

Table 3-1 Equations that have been used to represent the soil-water characteristic curve.

Authors of equations	Equation	Definition of variables
Fredlund & Xing (1994)	$w_w = w_s \left[1 - \frac{\ln\left(1+\frac{\psi}{h_r}\right)}{\ln\left(1+\frac{10^6}{h_r}\right)} \right] \left[\frac{1}{\left[\ln\left[\exp(1) + \left(\frac{\psi}{a_f}\right)^{n_f} \right] \right]^{m_f}} \right]$	w_s = Saturated gravimetric water content, a_f = Fitting parameter closely related to the air entry value for the soil, n_f = Fitting parameter related to the maximum slope of the curve, m_f = Fitting parameter related to the curvature of the slope, h_r = Constant parameter used to adjust lower portion of curve, ψ = soil suction.
Van Genuchten (1980)	$w_w = w_{rvg} + (w_s - w_{rvg}) \left[\frac{1}{\left[1 + (a_{vg}\psi)^{n_{vg}} \right]^{m_{vg}}} \right]$	w_s = Saturated gravimetric water content, w_{rvg} = Residual gravimetric water content of the soil, a_{vg} = Fitting parameter, n_{vg} = Fitting parameter, m_{vg} = Fitting parameter.
Van Genuchten & Mualem (1976)	$w_w = w_{rm} + (w_s - w_{rm}) \left[\frac{1}{\left[1 + (a_m\psi)^{n_m} \right]^{\left(1-\frac{1}{n_m}\right)}} \right]$	w_s = Saturated gravimetric water content, w_{rm} = Residual gravimetric water content of the soil, a_m = Fitting parameter, n_m = Fitting parameter.
Van Genuchten & Burdine (1953)	$w_w = w_{rb} + (w_s - w_{rb}) \left[\frac{1}{\left[1 + (a_b\psi)^{n_b} \right]^{\left(1-\frac{2}{n_b}\right)}} \right]$	w_s = Saturated gravimetric water content, w_{rb} = Residual gravimetric water content of the soil, a_b = Fitting parameter, n_b = Fitting parameter.
Gardner (1958)	$w_w = w_{rg} + (w_s - w_{rg}) \left[\frac{1}{\left[1 + a_g\psi^{n_g} \right]} \right]$	w_s = Saturated gravimetric water content, w_{rg} = Residual gravimetric water content of the soil, a_g = Fitting parameter, n_g = Fitting parameter.

Brooks and Corey (1964)	$w_w = w_r + (w_s - w_r)\left[\frac{a_c}{\psi}\right]^{n_c}$	a_c = Bubbling pressure (kPa), n_c = Pore size index, t_r = Residual volumetric water content, ψ = Suction (kPa).

Brooks and Corey (1964) and Gardner (1974) presented three parameter equations while van Genuchten (1953) and Fredlund and Xing (1994) presented four parameter equations. It would appear that a similar form of equation to those shown in Table 1 could be used to represent the grain-size distribution.

An accurate representation of the clay fraction of the grain-size distribution was considered necessary in order to complete the mathematical function. Since the Fredlund and Xing (1994) equation allows independent control over the lower end of the curve (i.e., the fine particle size range), it was selected as the basis for the development of a grain-size distribution equation. The reversed scale of the grain-size distribution as well as characteristics unique to the grain-size distribution, required that the original Fredlund and Xing (1994) equation to be modified to the form shown below:

$$P_p(d) = \frac{1}{\ln\left[\exp(1) + \left(\frac{a_{gr}}{d}\right)^{n_{gr}}\right]^{m_{gr}}} \left[1 - \frac{\ln\left(1 + \frac{h_{rgr}}{d}\right)}{\ln\left(1 + \frac{h_{rgr}}{d_m}\right)}\right]^7$$

Equation 3-1

where: a_{gr} = parameter related to the initial breaking point of the curve,
n_{gr} = parameter related to the steepest slope of the curve,
m_{gr} = parameter related to the shape of the curve,
hr_{gr} = parameter related to the amount of fines in a soil,
d = diameter of any particle size under consideration, and
d_m = diameter of the minimum allowable size particle.

Equation 3-1 is referred to as the unimodal equation and was presented in Fredlund (1997). The unimodal equation can be used to fit a wide variety of soils as shown in Figure 3-4, Figure 3-5, and Figure 3-6. A quasi-Newton least squares regression algorithm was used to adjust three of the five parameters to fit the equation to each soil. The algorithm works by progressively minimizing the squared differences between the equation and experimental data. The best-fit particle size distribution function can be plotted over of the grain-size distribution data, typically on a logarithmic scale.

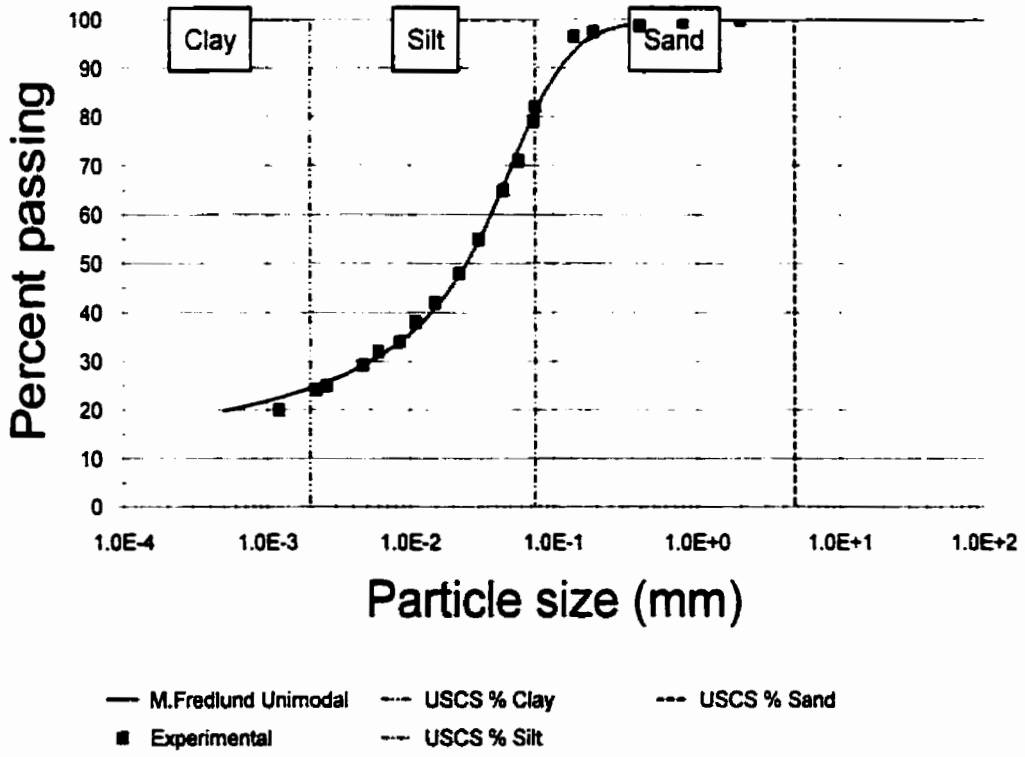

(a)

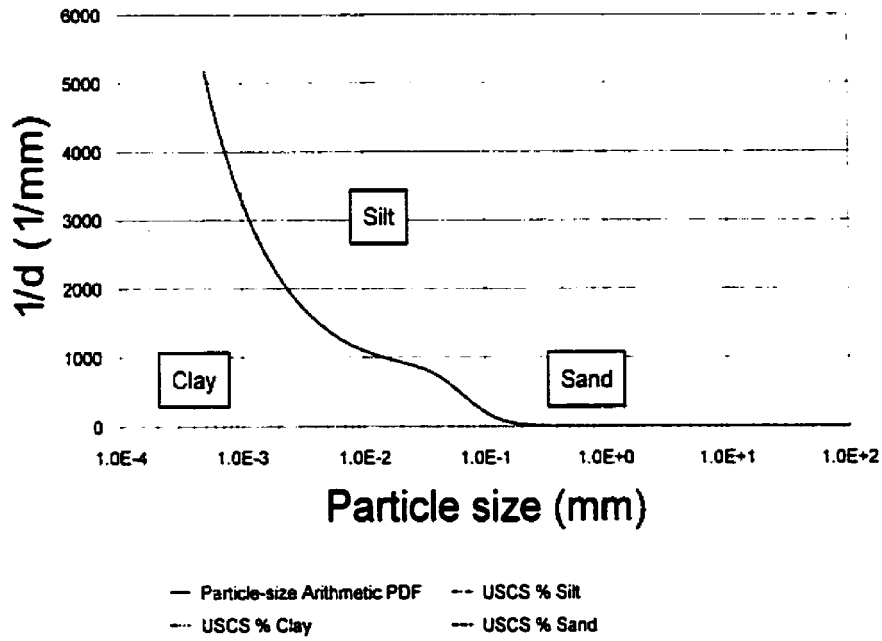

(b)

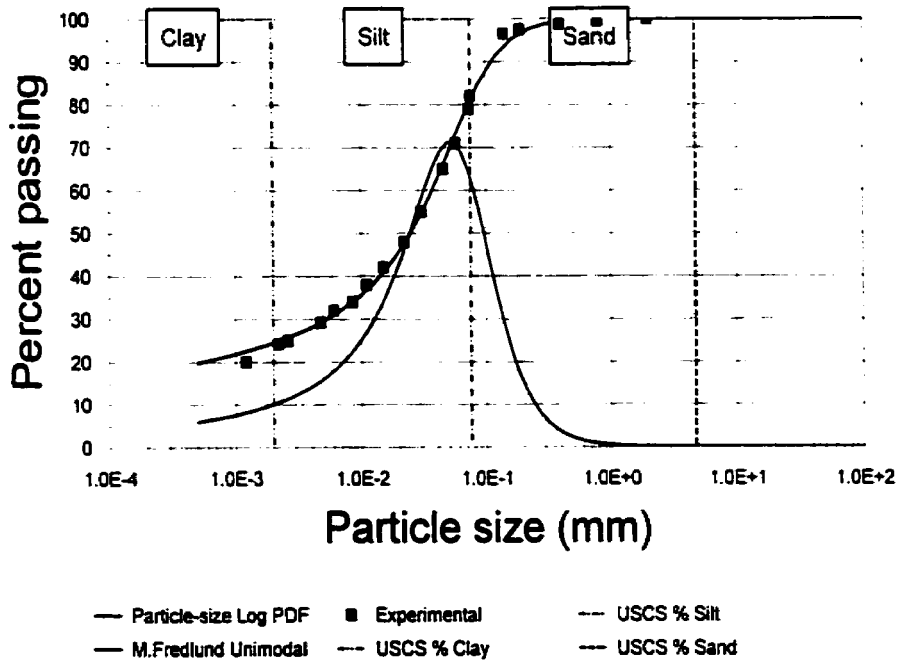

(c)

Figure 3-4 Uniform silt from the Pilot Butte area of Saskatchewan (optimum compression) from Y.F. Ho (1988) fit with unimodal equation (a) fit curve, R^2=0.998 (b) arithmetic probability density function (c) logarithmic probability density function (10030)

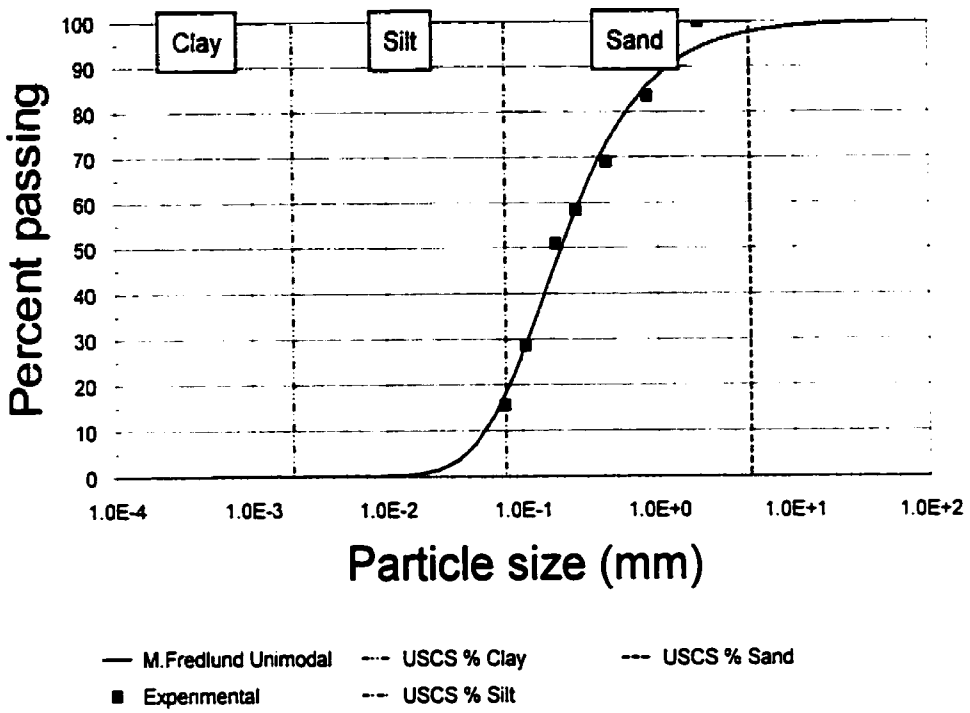
Clay
Silt
Sand
Percent passing
100
90
80
70
60
50
40
30
20
10
0
1.0E-4
1.0E-3
1.0E-2
1.0E-1
1.0E+0
1.0E+1
1.0E+2
Particle size (mm)
M.Fredlund Unimodal
Experimental
USCS % Clay
USCS % Silt
USCS % Sand

(a)

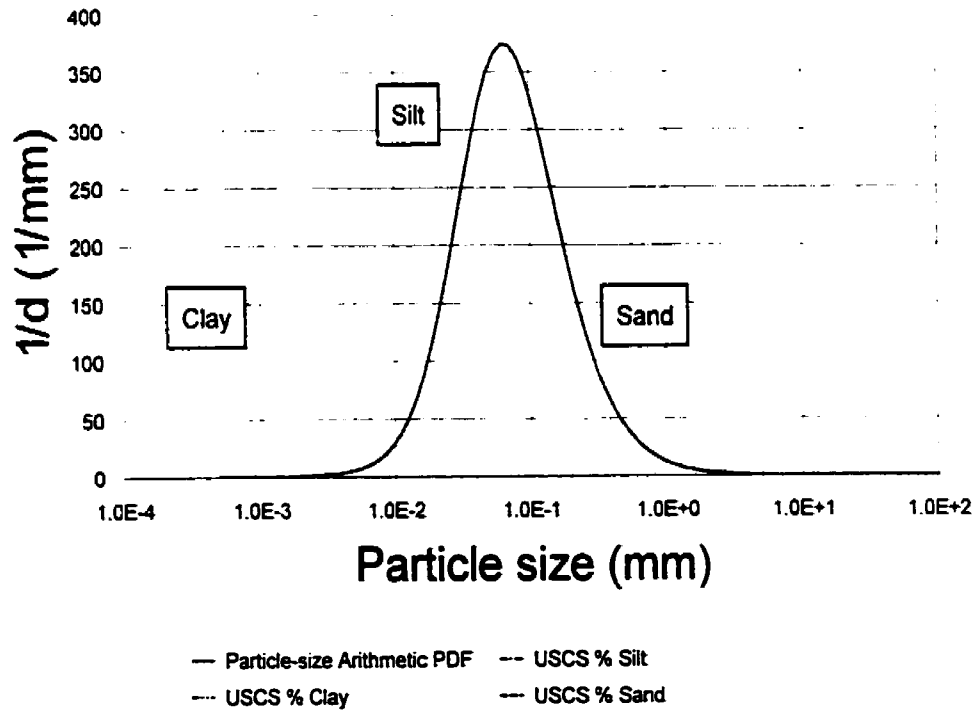
Silt
Clay
Sand
1/d (1/mm)
400
350
300
250
200
150
100
50
0
1.0E-4
1.0E-3
1.0E-2
1.0E-1
1.0E+0
1.0E+1
1.0E+2
Particle size (mm)
Particle-size Arithmetic PDF
USCS % Clay
USCS % Silt
USCS % Sand

(b)

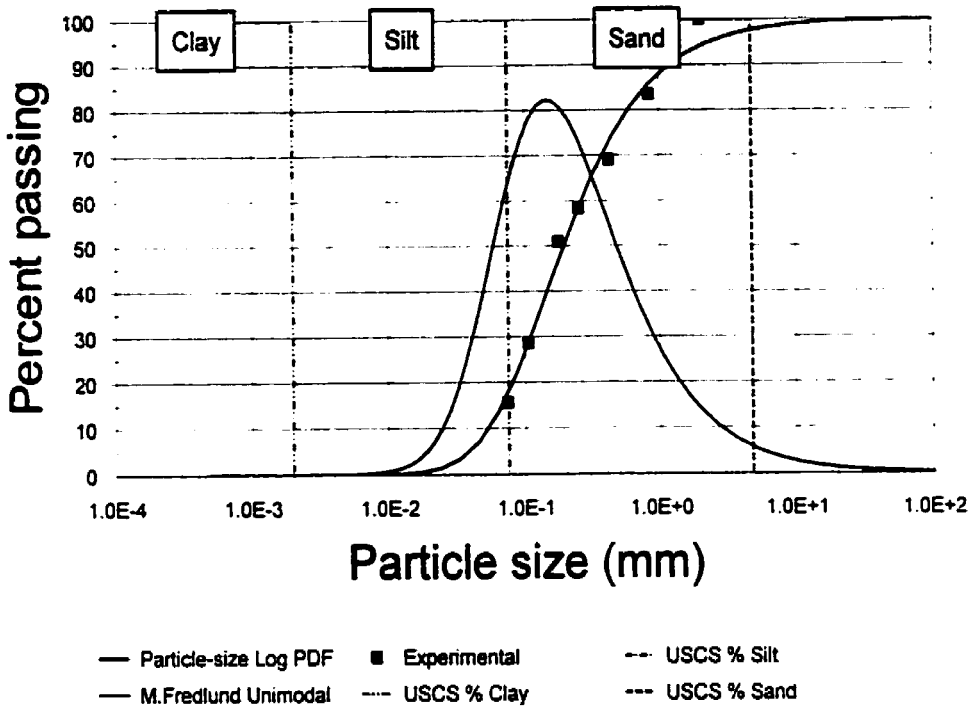

(c)

Figure 3-5 Rubicon Sandy Loam from Topp,G. C. (1969) fit with unimodal equation (a) fit curve, R^2=0.985 (b) arithmetic probability density function (c) logarithmic probability density function (63)

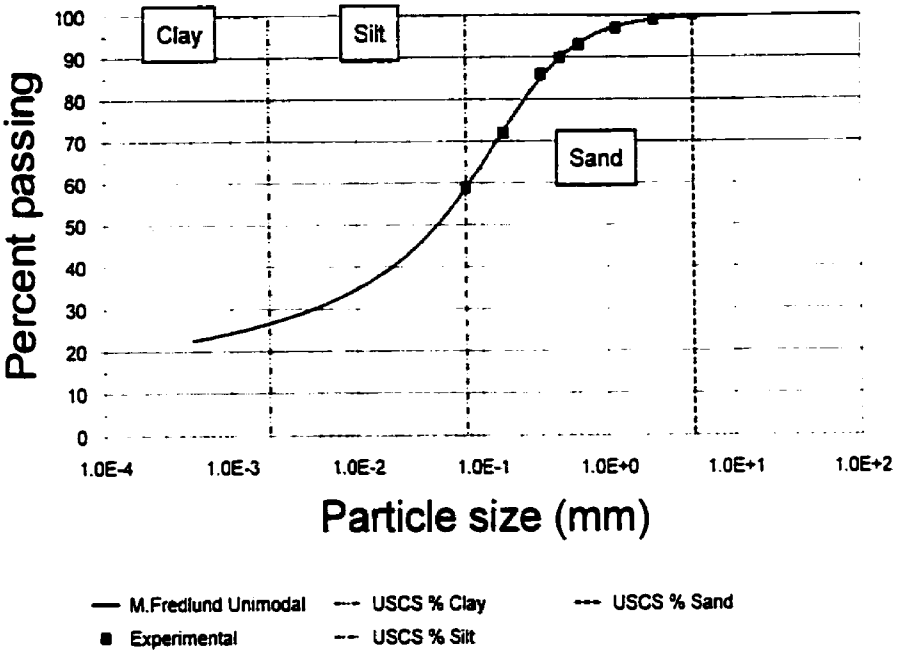
Clay
Silt
Sand
Percent passing
100
90
80
70
60
50
40
30
20
10
0
1.0E-4
1.0E-3
1.0E-2
1.0E-1
1.0E+0
1.0E+1
1.0E+2
Particle size (mm)
M.Fredlund Unimodal
Experimental
USCS % Clay
USCS % Silt
USCS % Sand

(a)

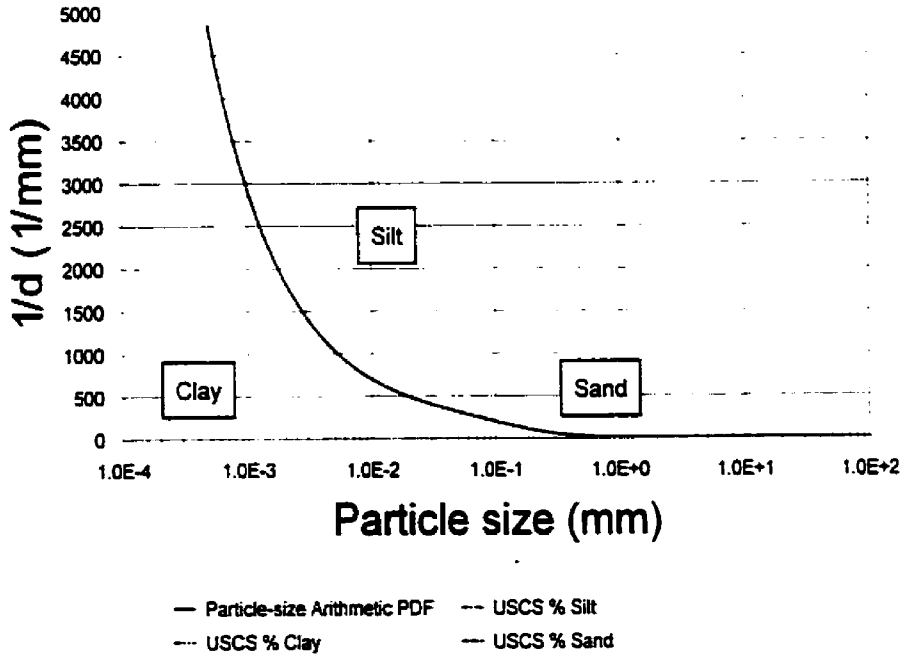
1/d (1/mm)
5000
4500
4000
3500
3000
2500
2000
1500
1000
500
0
Silt
Clay
Sand
1.0E-4
1.0E-3
1.0E-2
1.0E-1
1.0E+0
1.0E+1
1.0E+2
Particle size (mm)
Particle-size Arithmetic PDF
USCS % Clay
USCS % Silt
USCS % Sand

(b)

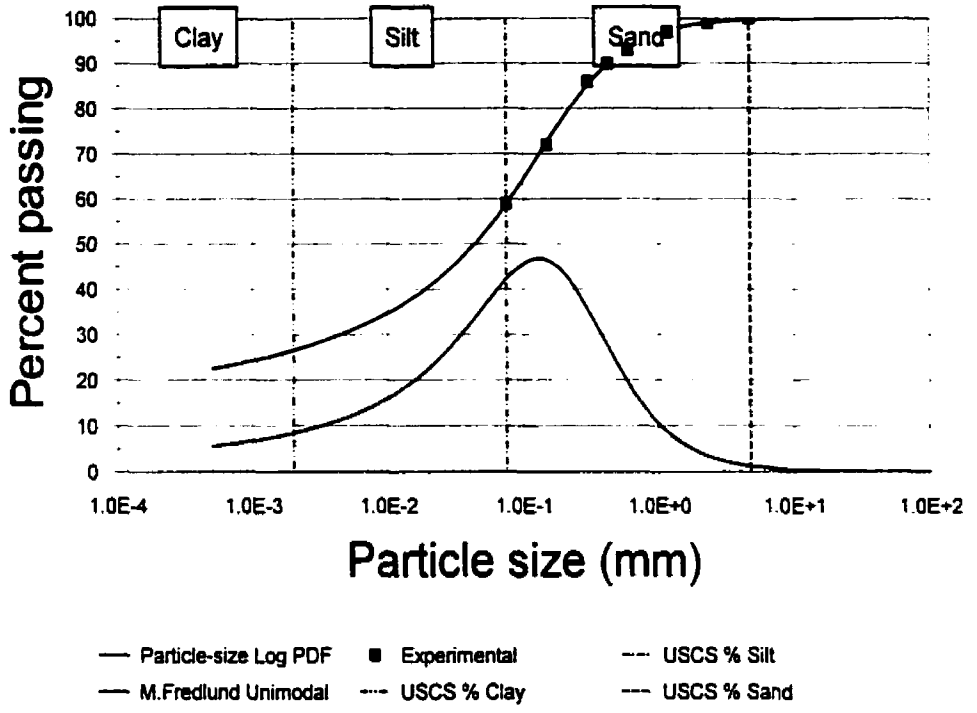

(c)

Figure 3-6 Sandy Silt of medium plasticity from University of Saskatchewan fit with unimodal equation (a) fit curve, R^2=0.999 (b) arithmetic probability density function (c) logarithmic probability density function (11648)

The unimodal equation provided significant improvements in the fit of grain-size data over previous mathematical representations (i.e. normal distribution). The variation of R^2 versus percent clay may be seen in Figure 3-7. The R^2 value was plotted versus percent clay because the representation of fines by the new equation was considered important. This is to be expected due to the increase in the number of parameters used to represent the grain-size distribution. The complexity of the proposed unimodal equation due to the added parameters is considered to be insignificant due to the amount of available curve-fitting software currently available.

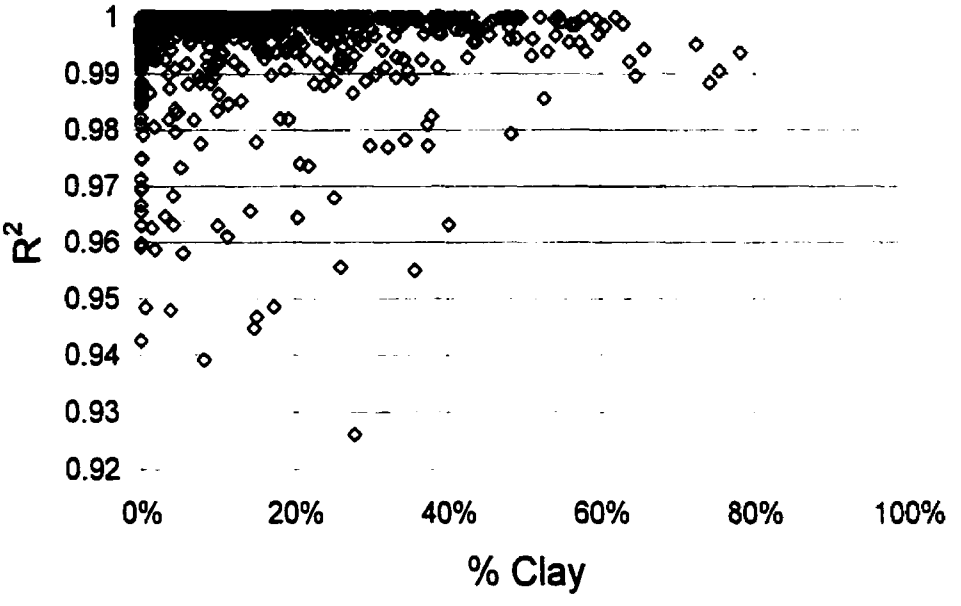

Figure 3-7 Variation of the R^2 error as a function of clay content represented in a soil increases.

The particle size distribution provides information on the amount and dominant sizes of particles present in a soil. However, another form can also be used to visualize the distribution of particle sizes by differentiating the particle size distribution curve. The differentiation produces a particle-size probability density function (PDF). The differentiated form of the unimodal grain-size equation can be seen in Equation 3-2. The parameters presented in the particle-size PDF are the same as defined in Equation 3-1.

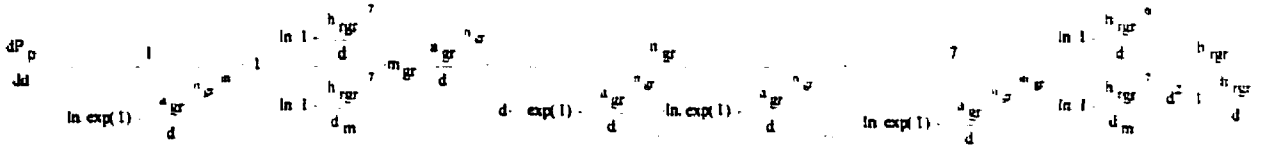

Equation 3-2

The particle size distributions presented in this chapter are calculated using Equation 3-2. The highest point on the PDF plot is the mode or the most frequent particle size. Since Equation 3-2 is a PDF, the natural laws of probability hold such that the area under the differentiated curve must equal 1 as shown below.

$$\int_{-\infty}^{+\infty} \frac{dP_p}{dd} dx = 1$$

Equation 3-3

where: x = particle-size diameter.

Equation 3-2 can also be used to calculate probabilities. Equation 3-4 shows how to calculate the probability that a soil particle diameter will fall in a certain range. In Equation 3-4, Equation 3-2 is arithmetically integrated between the specified particle diameter sizes. The probability is determined by the following relationship.

$$\text{probability}(d_1 < d < d_2) = \int_{x=d_1}^{x=d_2} p(x)dx$$

Equation 3-4

It is convenient to represent the PDF function in a different manner when plotted on a logarithmic scale. The arithmetic PDF function will often appear distorted when plotted on a logarithmic scale. The peak of Equation 3-4 will not represent the most frequent particle size because of the logarithmic distribution of the particle-size scale. To overcome this limitation, the PDF function is often represented as presented in Equation 3-5. Taking the log of particle size and differentiating the grain-size equation produces a PDF which appears more physically realistic. The peak of Equation 3-5 will represent the most frequent particle size.

$$p_l(d) = \frac{dP_p}{d\log(d)} = \frac{dP_p}{dd} \ln(10) \cdot d$$

Equation 3-5

where: $p_l(d)$ = logarithmic probability density function.

It must be noted that the probability of the logarithmic PDF must be calculated according to Equation 3-6.

$$\text{probability}(d_1 < d < d_2) = \int_{x=\log(d_1)}^{x=\log(d_2)} p_1(x)dx$$

Equation 3-6

The probability density function for various grain-size curves as calculated from Equation 3-5 may be seen in Figure 3-4, Figure 3-5, and Figure 3-6.

3.5 Parametric Study of the Proposed Grain-size Distribution Equation

A parametric study of the proposed unimodal equation shows behavior similar to that of the original Fredlund and Xing (1994) equation. The a_{gr} parameter is related to the initial break of the equation and its effect on the grain-size distribution curve can be seen in Figure 3-8 where a_{gr} is varied and the other equation parameters are held constant. The a_{gr} parameter provides an indication of the largest particle sizes.

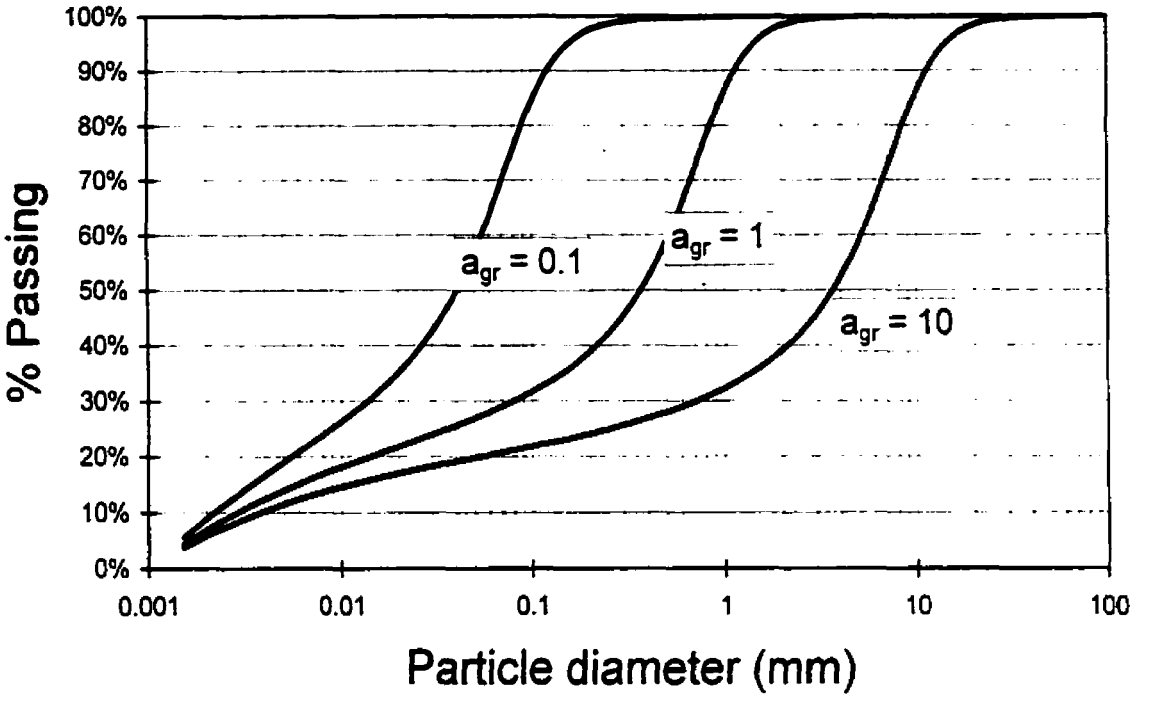

Figure 3-8 Effect of varying the a_{gr} parameter while n_{gr}=4.0, m_{gr}=0.5, hr_{gr}=1000, and d_m=0.001

Figure 3-9 shows how the parameter n_{gr} influences the slope of the grain-size distribution. The point of maximum slope of the grain-size distribution indicates the dominant particle size (i.e., on a logarithm scale) present in the soil as seen in Figure 3-5. The parameter m_g controls the break onto the finer particle size of the sample. The effect of the m_g parameter can be seen in Figure 3-10. The parameter, h_{rgr}, affects the shape of this fine particle size of the curve. However, the amount of variation produced on the curve is quite minimal as shown in Figure 3-11. In some cases the h_{rgr} can be modified to improve the fit of the overall equation. With the best fit analysis shown, h_{rgr} was adjusted manually to facilitate the best fit. It was found that a value of 0.001 for h_{rgr} provided a reasonable fit in most cases.

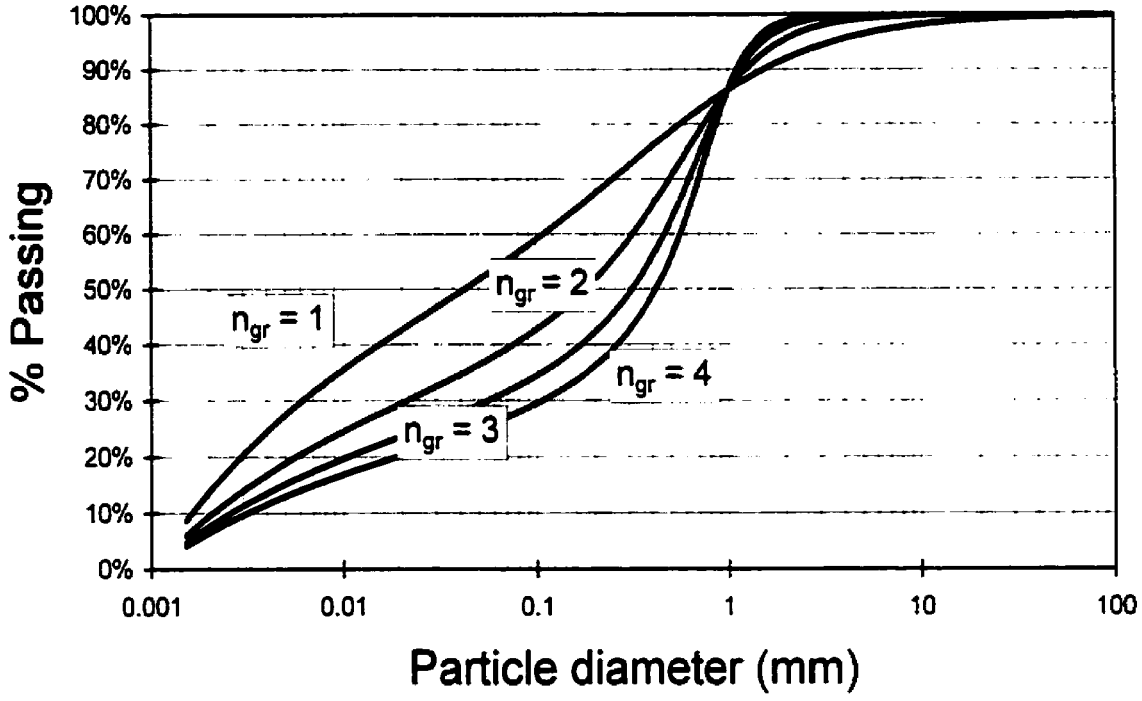

Figure 3-9 Effect of varying the n_{gr} parameter while a_{gr}=1.0, m_{gr}=0.5, hr_{gr}=1000, and d_m=0.001

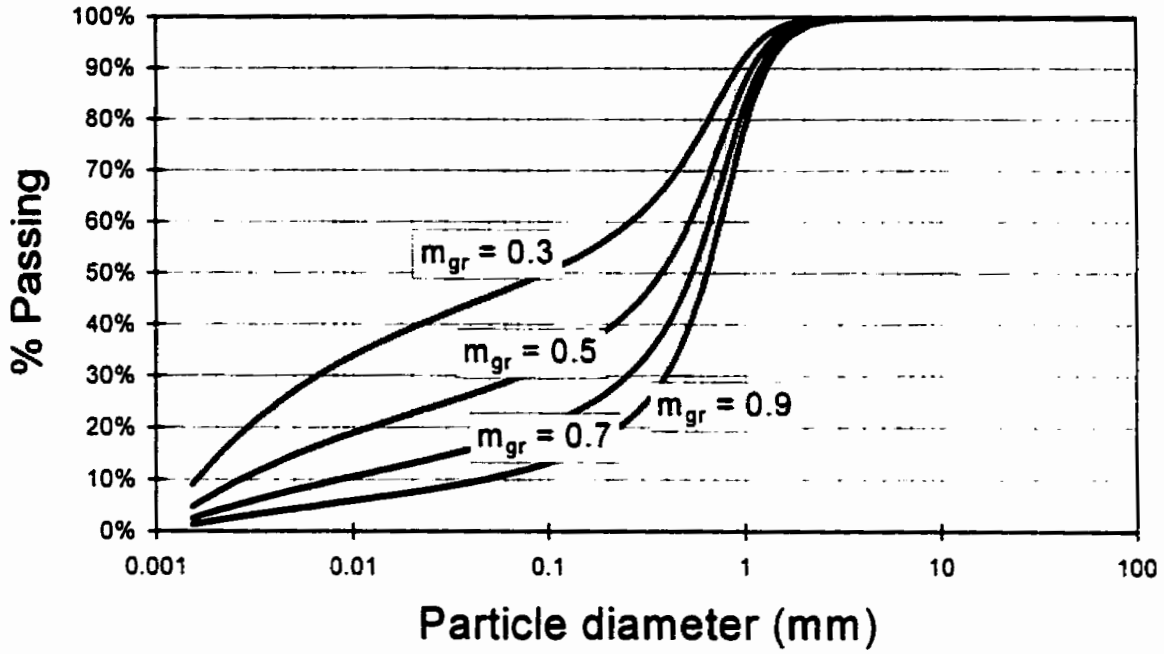

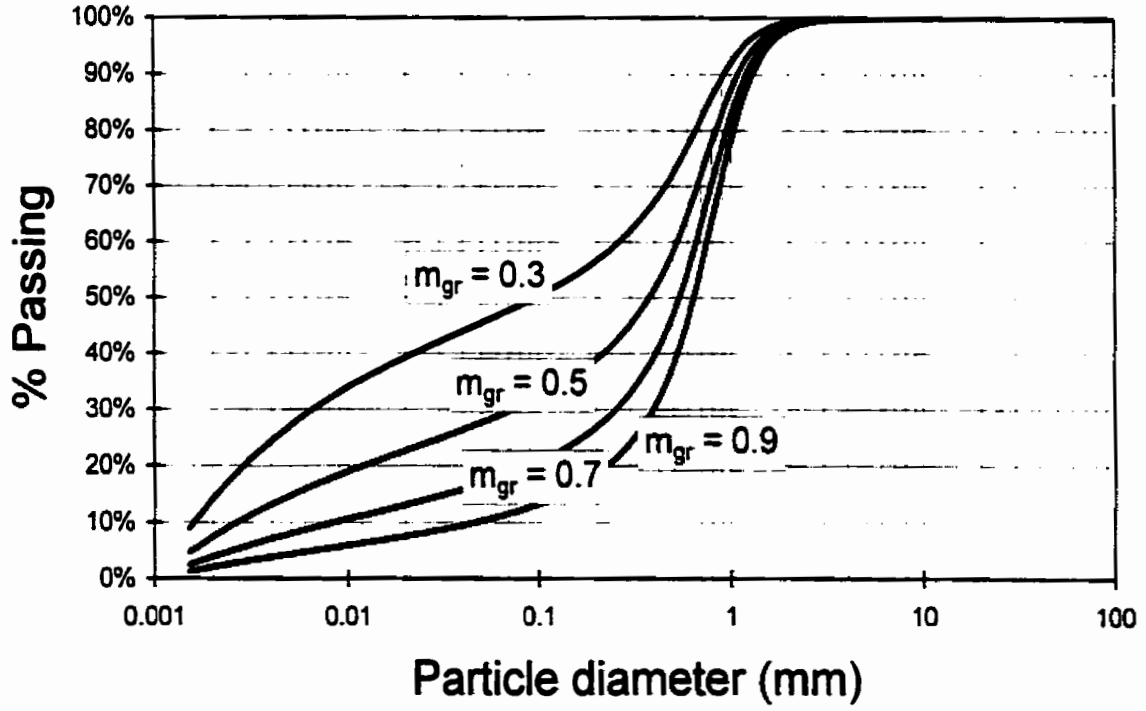

Figure 3-10 Effect of varying the m_{gr} parameter while a_{gr}=1.0, n_{gr}=4.0, hr_{gr}=1000, and d_m=0.001

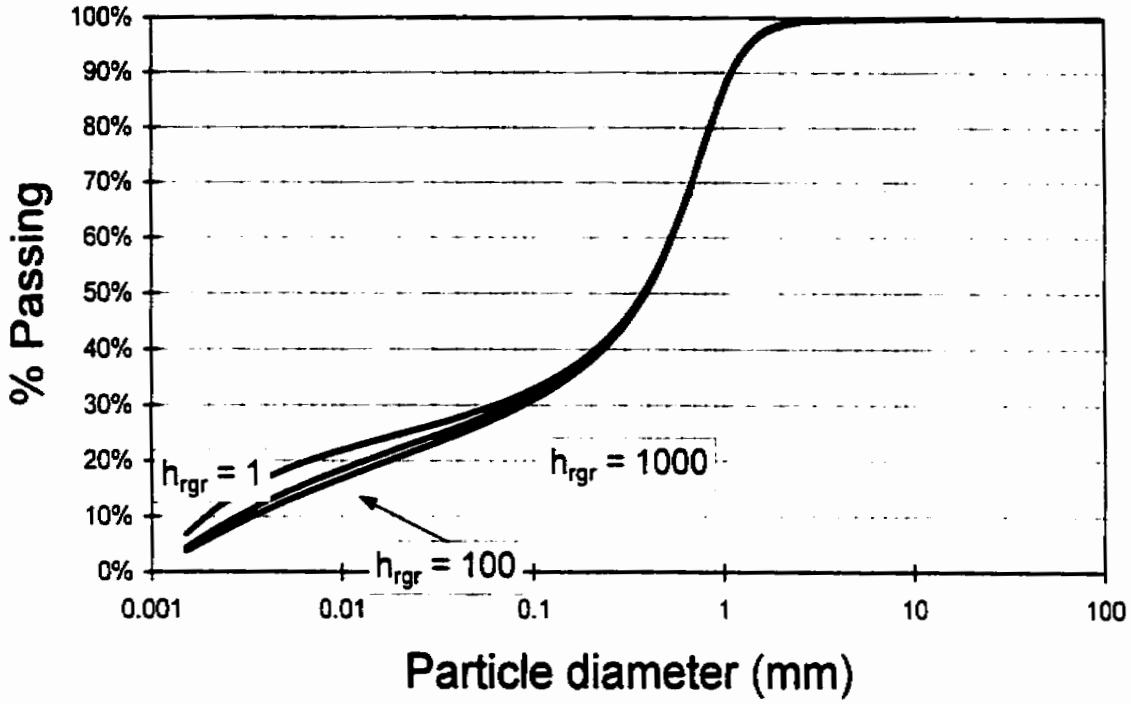

Figure 3-11 Effect of varying the h_{rgr} parameter while a_{gr}=1.0, n_{gr}=4.0, m_{gr}=0.5, and d_m=0.001

The unimodal equation (Equation 3-1) provides a good representation of the experimental data presented in Figure 3-2. This mathematical equation appears to have versatility in handling a wide variety of soil types.

3.6 Bimodal Equation for the Grain-size Distribution Curve

There is a limitation in using the unimodal equation (i.e., Equation 3-1) when the soils are gap-graded as shown in Figure 3-12. In this case, it is necessary to consider the use of a bimodal, best-fit. Soils frequently have particle size distributions that are not consistent with a unimodal

distribution and as a result, attempts to fit the unimodal equation to certain data sets can often lead to unsatisfactory results.

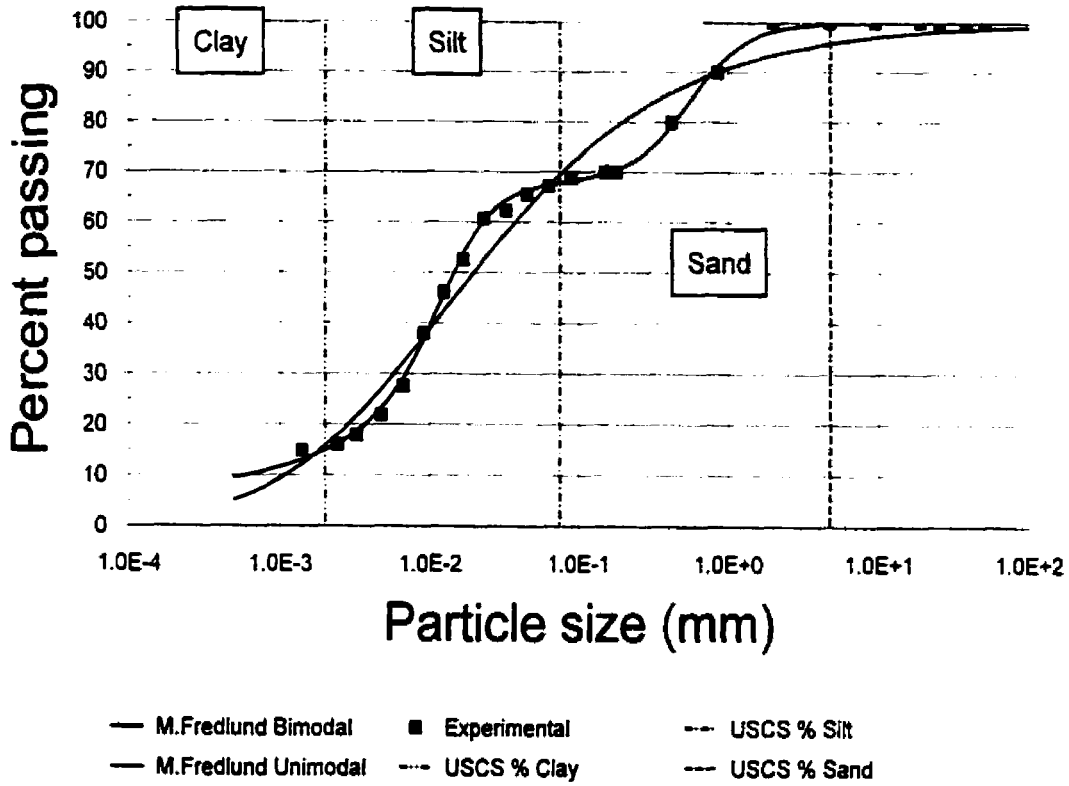

Figure 3-12 Example of fit of gap-graded Saprolitic Soil from the University of Saskatchewan with unimodal equation, R2=0.978, and the bimodal equation, R^2=0.999 (11491)

The characteristic shape of a bimodal or gap graded soil is the double "hump" seen in the experimental data. These anomolies indicate that the particles are concentrated around two separate particle size ranges. From a mathematical standpoint, a gap-graded soil can be viewed as a combination of two or more separate soils (Durner, 1994). This allows for the "stacking" of more than one unimodal equation.

$$P_p(d) = \left[\sum_{i=1}^{k} w_i \left[\frac{1}{\ln\left[\exp(1) + \left(\frac{a_{gr}}{d} \right)^{n_{gr}} \right]^{m_{gr}}} \right] \right] \left[1 - \left[\frac{\ln\left(1 + \frac{d_r}{d}\right)}{\ln\left(1 + \frac{d_r}{d_m}\right)} \right]^7 \right]$$

Equation 3-7

where: k = the number of "subsystems" that for the total particle-size distribution,

w_i = the weighting factors for the subcurves, subject to $0 < w_i < 1$ and $\Sigma w_i = 1$.

For a bimodal curve, k would be equal to 2 and the number of parameters to be determined would be 4 x k + (k-1). The unimodal equation is used as the basis for the bimodal equation. The final equation for a bimodal curve is shown below in its extended form.

$$P_p(d) = \left\{ w \left[\frac{1}{\ln\left(\exp(1) + \left(\frac{a_{bi}}{d} \right)^{n_{bi}} \right)^{m_{bi}}} \right] + (1-w) \left[\frac{1}{\ln\left(\exp(1) + \left(\frac{j_{bi}}{d} \right)^{k_{bi}} \right)^{l_{bi}}} \right] \right\} \left[1 - \left(\frac{\ln\left(1 + \frac{hr_{bi}}{d}\right)}{\ln\left(1 + \frac{hr_{bi}}{d_m}\right)} \right)^7 \right]$$

Equation 3-8

where:

a_{bi} = parameter related to the initial breaking point of the curve,

n_{bi} = parameter related to the steepest slope of the curve,

m_{bi} = parameter related to the shape of the curve,

j_{bi} = parameter related to the second breaking point of the curve,

k_{bi} = parameter related to the second steep slope of the curve,

l_{bi} = parameter related to the second shape of the curve,

hr_{bi} = parameter related to the amount of fines in a soil,

d = diameter of any particle size under consideration, and

d_m = diameter of the minimum allowable size particle.

The bimodal data sets can be closely fit using the bimodal best-fit. However, the bimodal fit provided only an adequate fit of unimodal data sets. In other words, unimodal data sets were better fit using the unimodal equation. . Figure 3-17 represents the R^2 value of the bimodal fit as the amount of fines in a soil increases. The results of fitting the bimodal curve to several different soils can be seen in Figure 3-13 to Figure 3-16

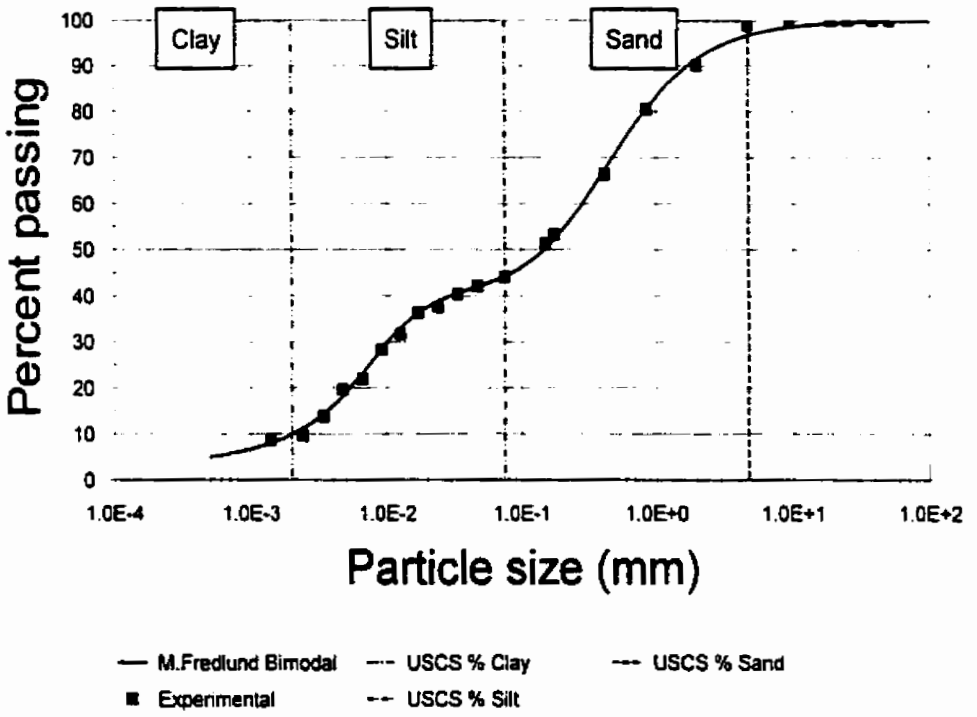

(a)

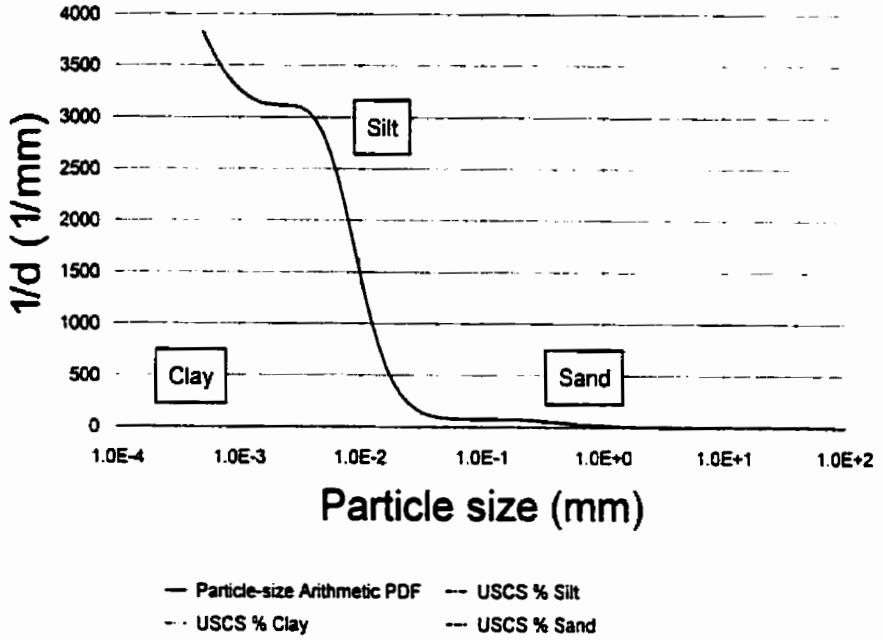

(b)

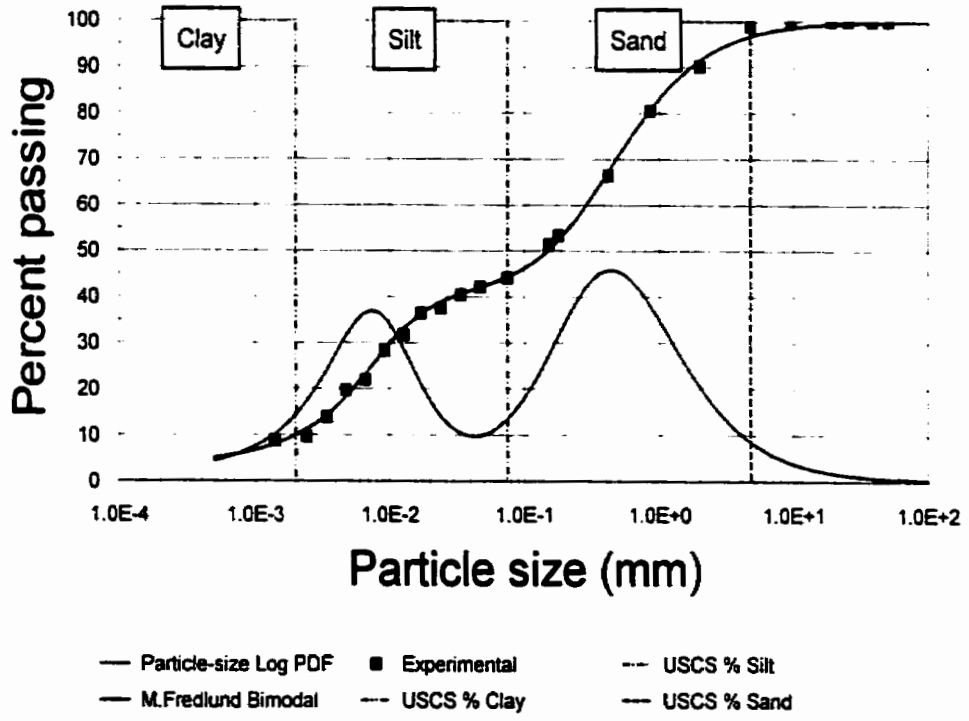

(c)

Figure 3-13 Example of fit of gap-graded Saprolitic Soil from the University of Saskatchewan with bimodal equation (a) fit curve, R^2=0.999 (b) arithmetic probability density function (c) logarithmic probability density function (11492)

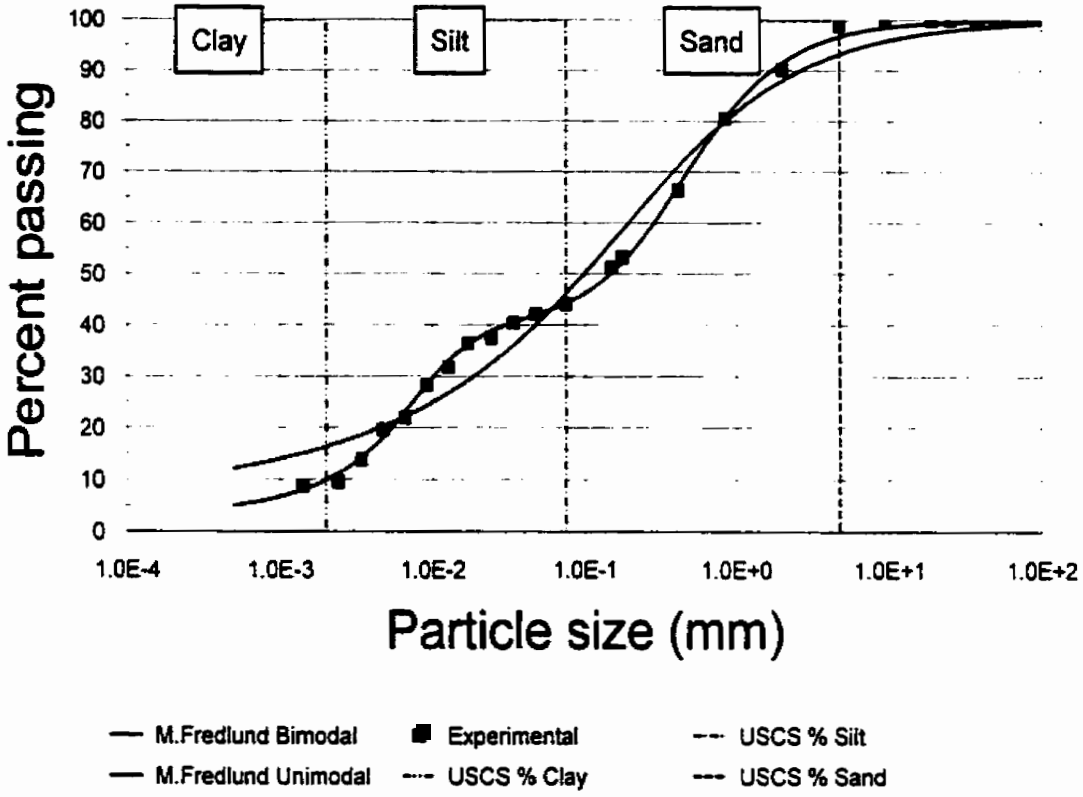

Figure 3-14 Example of fit of gap-graded Saprolitic Soil from the University of Saskatchewan with bimodal equation, R^2=0.999 (11492)

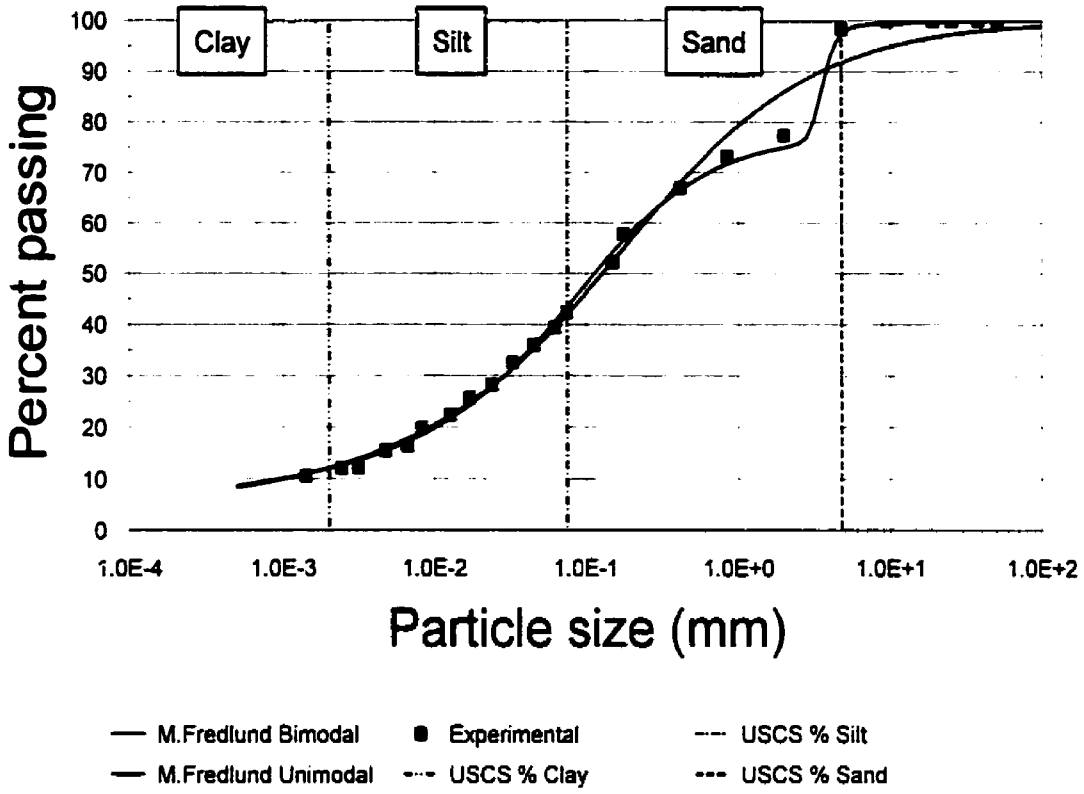

Figure 3-15 Example of fit of gap-graded Saprolitic Soil from University of Saskatchewan with bimodal equation, R^2=0.999 (11493)

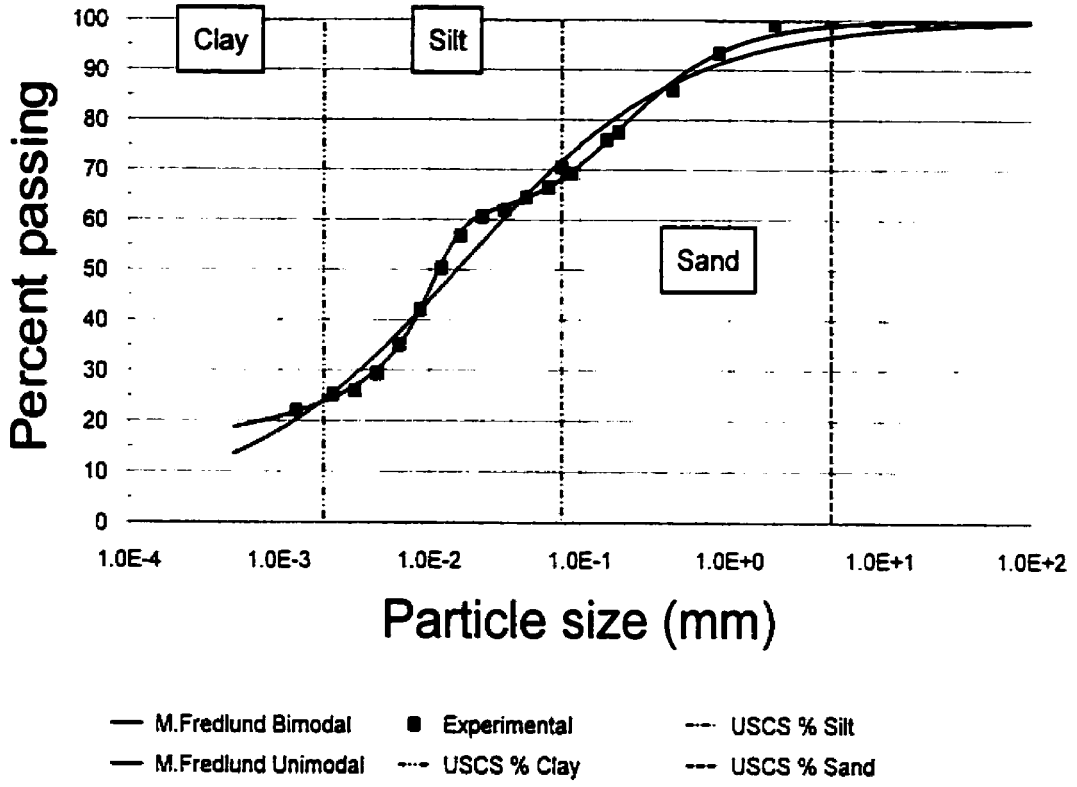

Figure 3-16 Example of fit of gap-graded Saprolitic Soil from University of Saskatchewan with bimodal equation, R^2=0.999 (11498)

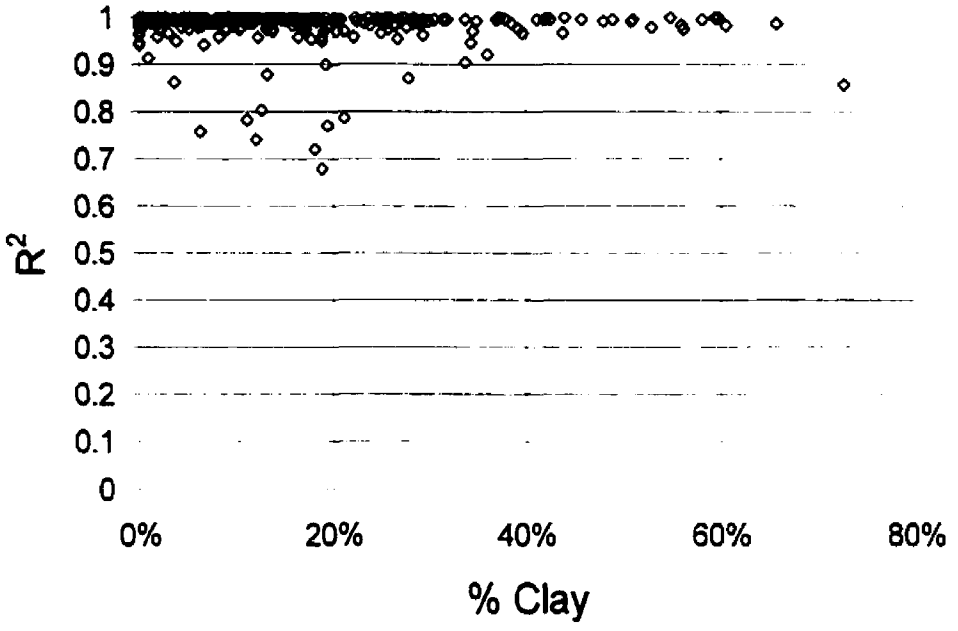

Figure 3-17 Variation or R^2 versus percent clay for the bimodal fit of the grain-size distribution.

3.7 Application of the Mathematical Function for the Grain-size Distribution

The grain size distribution has been used extensively for the classification of soils. The application of the mathematical equations in this chapter can be applied to geotechnical engineering practice. The use of equations to fit the grain-size distribution provides several advantages. Firstly, the sieve or hydrometer analysis data does not provide a continuous grain-size distribution for a soil. The equations presented in this chapter provide a method for estimating a continuous function. Secondly, quantification of soils based on their grain size distribution is possible when equations are fit to datasets of soils information. Thirdly, equations provide a consistent method for determining physical indices such as percent clay, percent sand, percent silt, and particle diameter variables such as d_{10}, d_{20}, d_{30}, d_{50}, and d_{60}.

It has also been found that the grain size distribution is central to most methods of estimating the soil-water characteristic curve (Gupta and Larson, 1979; Arya and Paris, 1981; Haverkamp

and Parlange, 1986, Ranjitkar, 1989). An accurate representation of the soil particle sizes is essential when the grain-size distribution curve is used as the basis for the estimation of the soil-water characteristic curve. The equations presented in this chapter appear to provide an excellent basis for the estimation of the soil-water characteristic curve (Fredlund et. al, 1997).

3.7.1 Parameters of the grain-size distribution equations

The unimodal fit of the grain-size distribution has been fit to many experimentally measured grain-size data sets extracted from research papers. The unimodal fit performed well with the exception of soils exhibiting bimodal behavior. The parameters of the unimodal equation vary in a manner similar to the parameters in the Fredlund and Xing (1994) soil-water characteristic curve equation.

Histograms showing the frequency distribution of particles when using the equation can be seen in Figure 3-18, Figure 3-19, and Figure 3-20. One aspect of this study was to determine whether equation parameters could be grouped according to soil textural classifications. For example, is there a range of the n_{gr} parameter typical for silty sands? The results of this research indicate that general parameter groups can be identified but specific parameter groupings cannot be identified. The influence of equation parameters on each other does not allow for specific groupings. It was found that grouping soils is more successful when parameters with physical significance are selected. Successful groupings soil properties was achieved by grouping soils according to physical parameters such as percent clay, percent silt, and percent sand for variables such as d_{10}, d_{20}, d_{30}, d_{50}, and d_{60}.

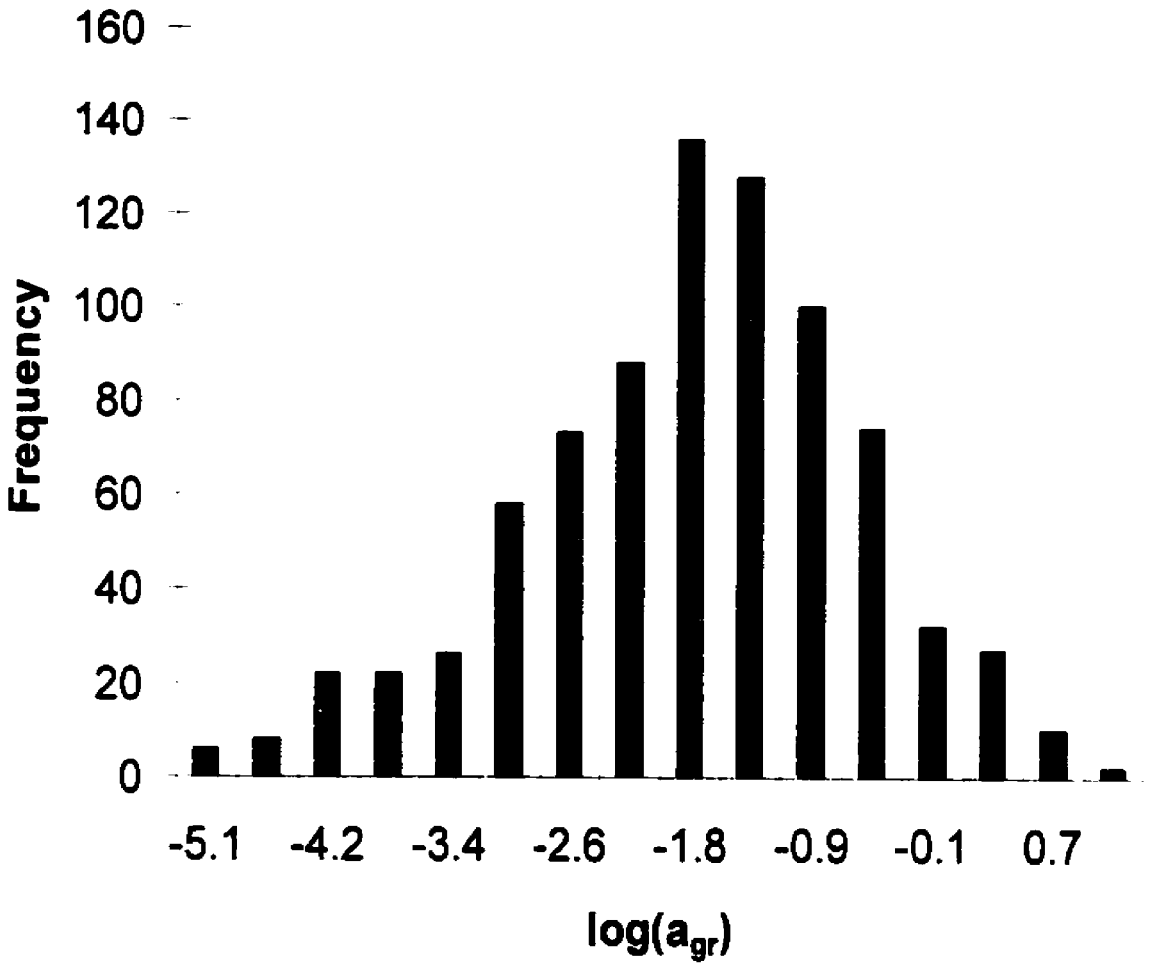

Figure 3-18 Frequency distribution of the natural logarithm of a_{gr} parameter when using the unimodal equation

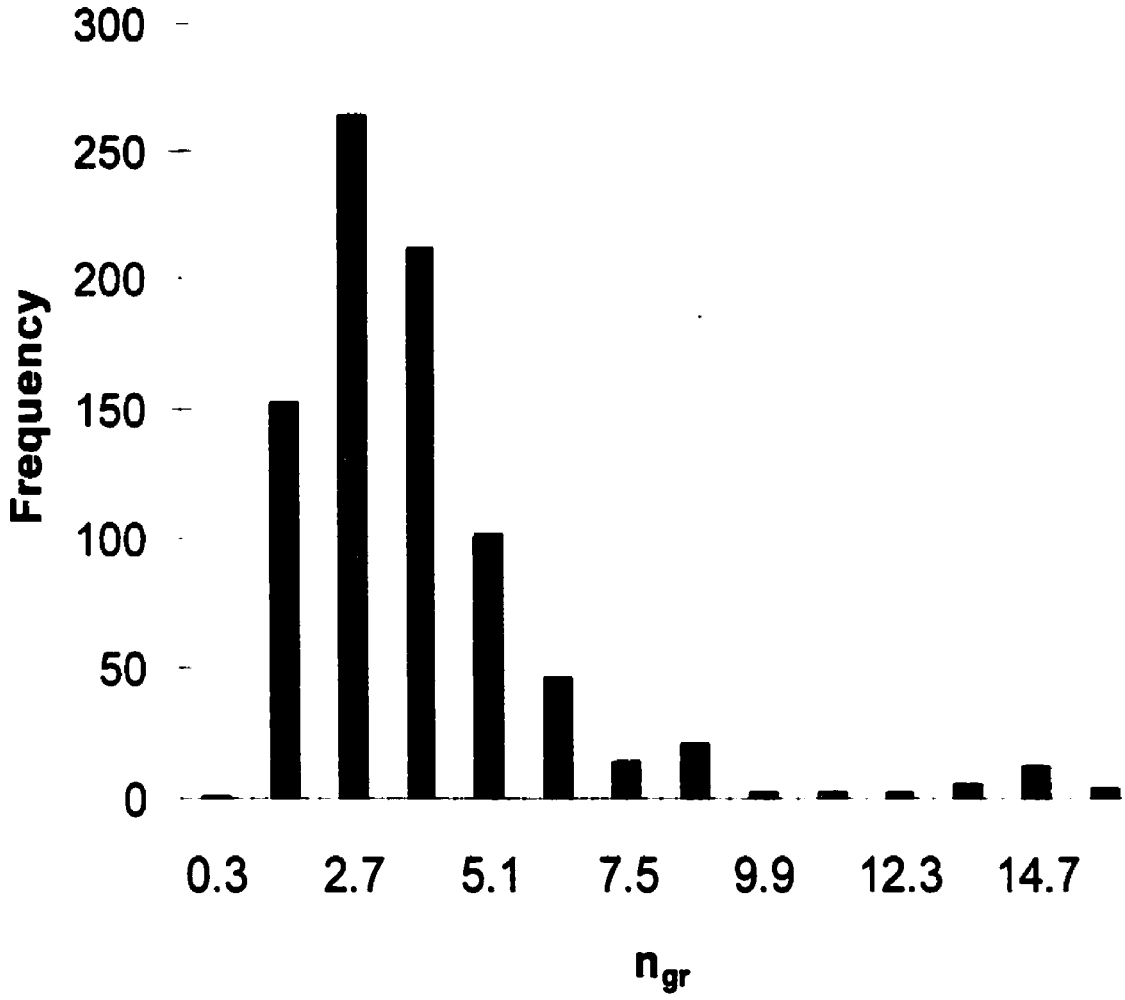

Figure 3-19 Frequency distribution of the n_{gr} parameter when using the unimodal equation

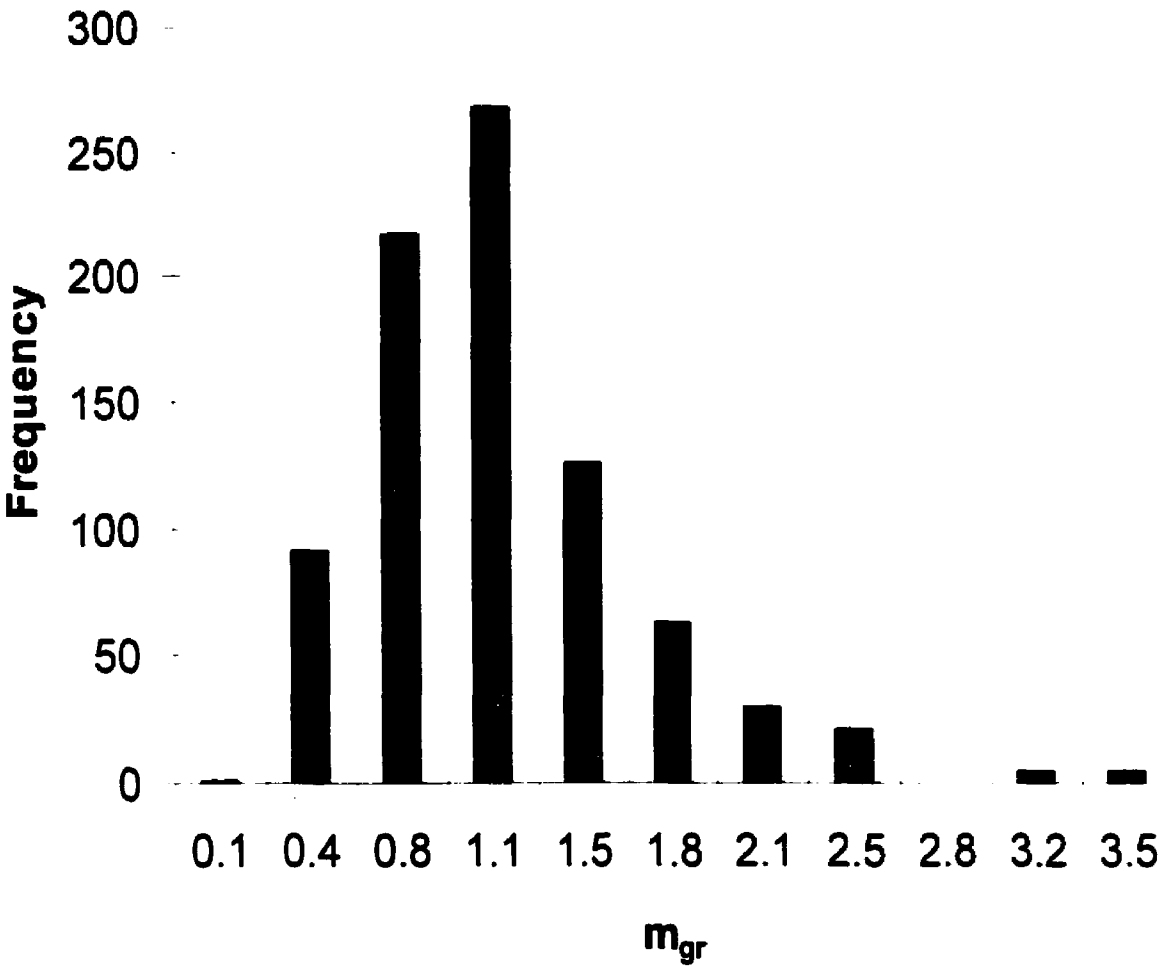

Figure 3-20 Frequency distribution of the m_{gr} parameter when using the unimodal equation

3.7.2 Determining physical parameters from the grain-size distribution equation

One of the benefits of the two grain-size equations presented in this chapter is that conventional physical variables can be computed from the curves. The most commonly used variables are percent clay, percent sand, and percent silt. Also used are diameter variables such d_{10}, d_{20}, d_{30}, d_{50}, and d_{60}. The equations presented are of the form, $P_p(d)$ where d is particle diameter (mm). The percent clay, percent silt, and percent sand may therefore be a read off of the curve by substituting in the appropriate diameters. The diameters used depend upon the criteria associated with the various classification methods. For example, the USDA classification

boundaries are 0.002, 0.05, and 2.0 for percent clay, percent silt, and percent sand, respectively. The USCS classification uses boundaries of 0.002, 0.075, and 4.75 for percent clay, percent silt, and percent sand, respectively. The divisions can be determined for any classification method by substituting into the equations the appropriate diameters as shown in Figure 3-21.

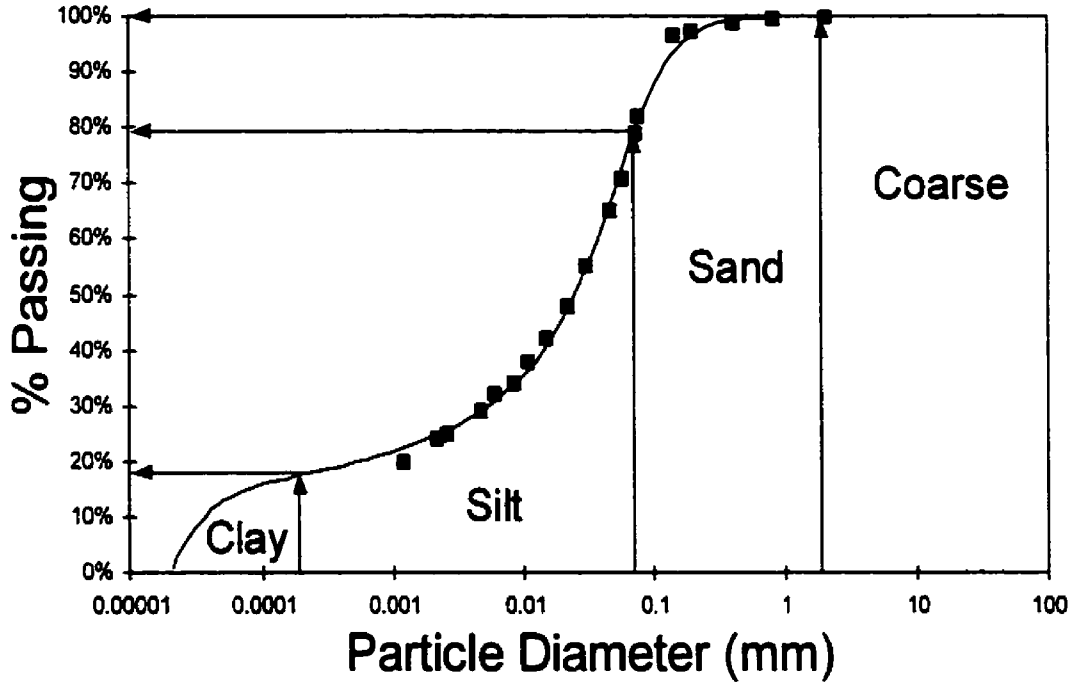

Figure 3-21 Determination of the soil fractions (i.e., % clay, % silt, and % sand) when using the unimodal equation

The diameter variables must be read off of the curve in an inverse manner. The particle size diameter answers to the question,"What particle diameter has 10 percent of the total mass smaller than this size?". Taking the inverse of either the unimodal or bimodal equation is difficult. A half-length algorithm was therefore used to read diameters off the grain size curve. An initial guess diameter was selected and the correction distance was progressively halved until the iteration process yielded a minimal error. The results of this process can be seen in Figure 3-22.

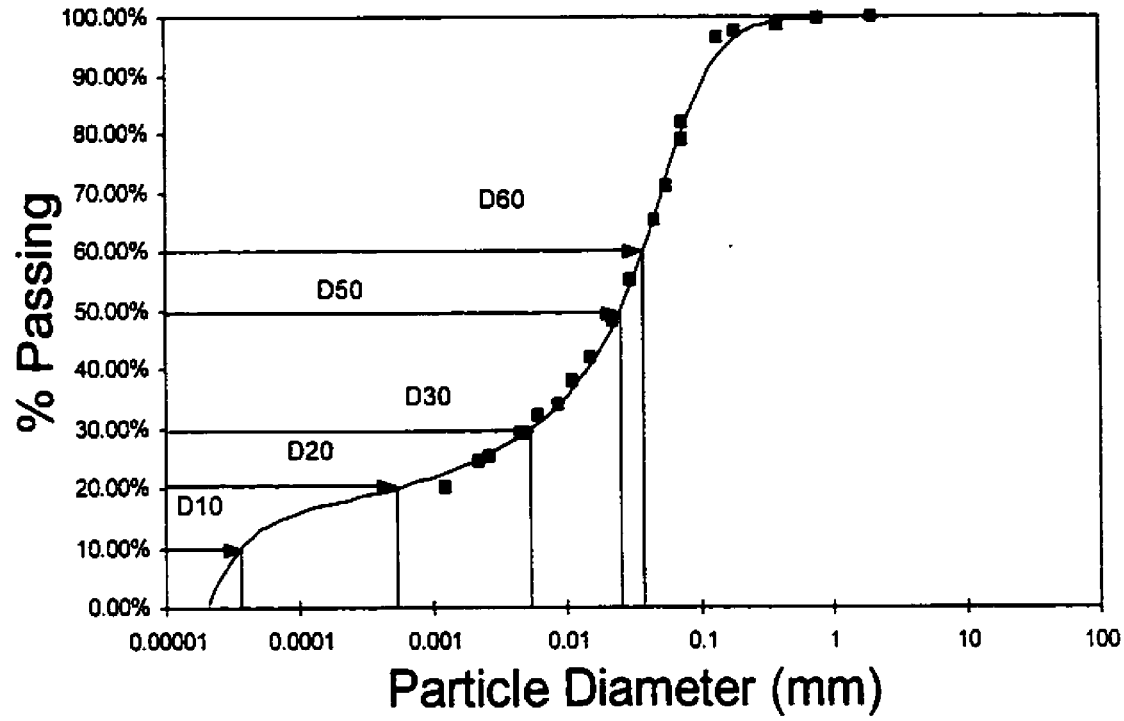

Figure 3-22 Determination of the percent passing for any particle size, *d*, for a unimodal grain-size distribution

3.7.3 Application to the estimation of the soil-water characteristic curve

Many current estimation methods use the grain size distribution as the basis of prediction for the soil-water characteristic curve (Arya and Paris, 1981; Haverkamp and Parlange, 1986). A primary use of the grain-size equations is to provide a basis for the estimation of the soil-water characteristic. The soil-water characteristic curve has found to be sensitive to grain-size distribution (Fredlund, 1995). Methods of estimating the soil-water characteristic curve have been limited by the lack of a continuous grain-size distribution function. Current models often require grain size information to be estimated from the grain-size curve.

The grain-size distribution is theoretically a continuous curve representing the amount of various particle sizes present in soil. The soil-water characteristic curve is primarily a

representation of the pore-sizes present in the soil. A method for translating the particle-size distribution into a pore-size distribution is central to most methods of estimating the soil-water characteristic curve. An analysis of the soil can be performed by differentiating the grain size equation as shown by Equation 3-2. The differentiated equation will produce a particle-size probability density function that can be used as the basis for further analysis of the soil. The particle-size distributions, calculated according to Equation 3-1, can vary over several orders of magnitude. The particle-size probability density functions for several types of soils were shown in Figure 3-4, Figure 3-5, and Figure 3-6.

3.8 Conclusions

Fitting of the grain-size distribution has historically been a manual process or has involved the use of lognormal distributions of one, two, or three parameters. Unimodal and bimodal equations are presented in this chapter to fit essentially any grain-size distribution dataset. The unimodal equation was found to provide a good fit of a variety of soils. The extremes of the grain-size distribution were also well-fit by the equation.

Gap-graded soils can be fit using a bimodal equation. The bimodal equation allowed mathematical representation of any grain-size distribution where the sample contains two distinctly different, but dominant particle size groups.

Mathematical representation of the grain-size distribution provides numerous benefits. Curves can be identified and categorized. Likewise, the grain-size curves can be located in a data base using searching techniquies. Grain-size variables (i.e., % clay, d_{10}, d_{60}, etc.) can be mathematically determined from the equation. The unimodal and bimodal equations provide a method for fitting the three major soil categories of well-graded soils, uniform soils, and gap-graded soils.

The proposed continuous mathematical function for the grain-size curve sets the stage for further analysis to estimate the soil-water characteristic curve of a soil.

3.9 References

Arya, L.M., and Paris J.F., 1981, A physicoempirical model to predict the soil moisture characteristic from particle-size distribution and bulk density data, Soil Science Society of America Journal, Vol. 45, pp. 1023-1030.

Bauer, L.D., Walter H. Gardner, Wilford R. Gardiner, 1972, Soil Physics, John Wiley & Sons, Inc., New York

Brooks R.H. and A.T. Corey,, 1964, Hydraulic Properties of Porous Media, Colorado State Univ. Hydrol. Paper, No. 3,, 27, pp. March 1964.

Burdine, N.T., 1953, Relative permeability calculations from pore size distribution data, Journal of Petroleum Technology, Vol. 5, No. 3, pp. 71-78

Campbell, G.S., 1985, Soil Physics with Basic, Elsevier, New York

Fredlund, D.G., and Xing, A., 1994, Equations for the soil-water characteristic curve, Canadian Geotechnical Journal, Vol. 31, No. 3, pp. 521-532.

Fredlund, M.D., D.G. Fredlund, and G.W. Wilson, 1997, Prediction of the Soil-Water Characteristic Curve from Grain-Size Distribution and Volume-Mass Properties, 3rd Brazilian Symposium on Unsaturated Soils, Rio de Janeiro, April 22-25

Gardner, W.R., 1974, The permeability problem, Soil Science, 117, 243-249

Gupta, S.C., and Larson, W.E., 1979, Estimating soil-water retention characteristics from particle size distribution, organic matter percent, and bulk density, Water Resources Research Journal, Vol. 15, No. 6, pp. 1633-1635

Gupta, S.C., and W.E. Larson, 1979, A model for predicting packing density of soils using particle-size distribution, Soil Science Society of America Journal, Vol. 43, 758-764

Hagen, L.J., E.L. Skidmore and D.W. Fryrear, 1987, Using two sieves to characterize dry soil aggregate size distribution, Transactions of the ASAE, 30(1), 162-165

Harr, M.E., 1977, Mechanics of particulate media, McGraw - Hill International Book Company, New York, 27-33

Haverkamp, R., and Parlange, J.Y., (1986)., Predicting the water-retention curve from a particle-size distribution: 1. Sandy soils without organic matter., Soil Science,, Vol. 142, No. 6,, pp. 325-339.

Holtz, Robert D. and Kovacs, William D., 1981, An introduction to geotechnical engineering, Prentice-Hall, Inc., Englewood Cliffs, New Jersey

Kohnke, Helmut, 1968, Soil Physics, McGraw-Hill Book Company, New York

Lambe, William T., 1951, Soil Testing, John Wiley & Sons, Inc., New York

Mualem, Y., 1976, A new model for predicting the hydraulic conductivity of unsaturated porous media., Water Resources Res., 12, 513-522

Ranjitkar Shyam, and Sunder B, 1989, Prediction of hydraulic properties of unsaturated granular soils based on grain size data, Ph.D Thesis, University of Massachusetts, 75-131

Shirizi MA, Boersma L., 1984, A unifying quantitative analysis of soil texture, Soil Science Society of America Journal, 48, 142-147

van Genuchten, M.T., 1980, A closed form equation for predicting the hydraulic conductivity of unsaturated soils, Soil Science Society America Journal, pp. 892-890.

Wagner, L.E., and Ding, D., 1994, Representing aggregate size distributions as modified lognormal distributions, American Society of Agricultural Engineers, Vol. 37, No. 3, pp. 815-821

CHAPTER 4.0 Estimation of the Soil-Water Characteristic Curve from the Grain-size Distribution and Volume-Mass Properties

4.1 Introduction

This chapter presents a model for the estimation of the soil-water characteristic curve (SWCC) based on the grain-size distribution, dry density, void ratio, and specific gravity of a soil. The primary information on the grain-size distribution model is the M.Fredlund (1997) fit of the grain-size distribution (Figure 4-1). The grain-size distribution curve can be viewed as incremental particle sizes from the smallest to the largest assembled to build a soil-water characteristic curve. Small increments of uniform-sized particles are transposed to a soil-water characteristic curve representing the average particle size. Once the entire grain-size distribution curve is incrementally analyzed, the individual soil-water characteristic curves are superimposed to give the soil-water characteristic curve for the entire soil.

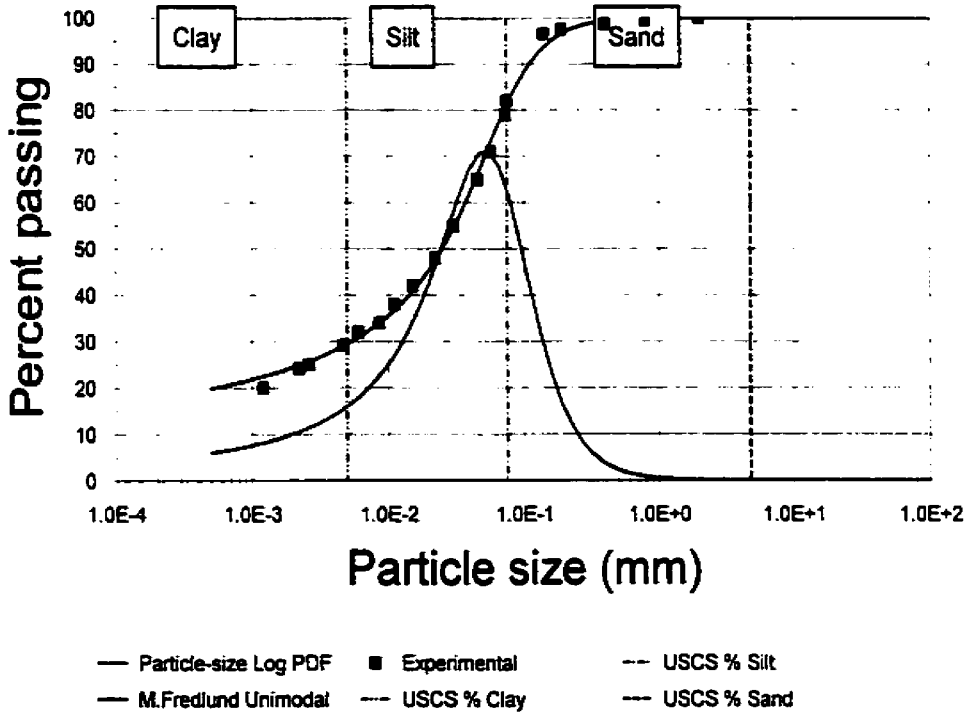

Figure 4-1 Fit of grain-size curve for Uniform Silt from Ho (1988) with M. Fredlund (1997) grain-size equation

In order to build the general soil-water characteristic curve, it must be assumed that the soil-water characteristic curve for each uniform particle size is relatively unique. Typical soil-water characteristic curves for a mixture of sand, silt, and clay were obtained from literature and fitted with the Fredlund and Xing (1994) equation. This provided approximations for the curve fitting parameters for the Fredlund and Xing (1994) equation classified according to effective grain diameter. Trial and error calibrations of the model were performed for 15 mid-range uniform soil types.

The shape of the estimated soil-water characteristic curve is primarily controlled by the grain-size distribution and secondarily influenced by the density of the soil. A mathematical equation is required to represent the grain-size distribution. The M.Fredlund (1997) unimodal and bimodal fits of the grain-size distribution curve were used as the basis for the estimation of the soil-water characteristic curve. The use of the unimodal and bimodal grain-size distribution equations provided an accurate representation of the grain-size distribution that could be used in the estimation of the soil-water characteristic curve.

4.2 Literature Review

The soil-water relationship has been the focus of attention for several reasons. This relationship can be used to provide the shear strength of a soil, estimating groundwater pollution, predicting erosion, and calculating evaporation and infiltration of the soil/air interface. Classical saturated soil mechanics is not adequate for the description of many problems such as those mentioned above. The soil hydraulic properties of an unsaturated soil must be known in order to model the processes mentioned above.

A wealth of basic soils information is available in various data sets. This information typically includes porosity, dry density, water content, and a grain-size distribution. Soil transport

models, however, require a description of the soil–water characteristic curve. Experimental descriptions of the soil-water characteristic curve can be costly and time consuming.

A number of methods exist for the estimation of the soil-water characteristic curve. The methods vary in details but can be grouped into four general categories.

The six different estimation functions tested in this chapter represent the last two of the three following general categories. The three broad categories for estimation techniques can be described as those which: i) Statistically estimate the water content at various soil suctions or those that, ii) estimate parameters of an algebraic retention function (Rawls and Brakensiek, 1985; Vereecken et al, 1989, Scheinost, 1996), or iii) a physio-empirical model approach (Fredlund and Wilson, 1997; Arya and Paris, 1981, Tyler and Wheatcraft, 1989).

This chapter presents a new approach to the physio-empirical model presented by Arya and Paris (1981). The physio-empirical model can be improved through knowledge gathered from parametric studies performed on soil-water characteristic curves. The combination of the physio-empirical model and the parametric study provides for significant increase in the accuracy of the estimation technique.

4.3 Definitions

The following definitions are useful to properly identify conceptual models used in the estimation process.

A soil property function is a relationship between a soil variable and either the soil suction or the stress state of a soil.

A pedo-transfer function (Bouma, 1989) is a function that has as its arguments basic data describing the soil such as grain-size distribution, dry density, and porosity, and yields as a result a soil property function.

A soil-water characteristic curve is either: (i) a monotonic, single-valued function that yields water content (m^3/m^3) for a given scale of matric potentials expressed as suction (kPa) or (ii) a hydrostatic relation consisting of two functions of the first type, including a drying and a wetting branch (Tietje, 1993).

4.4 Representation of the gain-size distribution

The Pedo-Transfer Function, (PTF) presented in this chapter uses the M.Fredlund (1997) unimodel and bimodel equations to represent the grain-size distribution. The equations are presented in Chapter 3 of this thesis. The unimodal equation is as follows.

$$P_p(d) = \left[\frac{1}{\ln\left(\exp(1) + \left(\frac{a_{gr}}{d} \right)^{n_{gr}} \right)^{m_{gr}}} \right] \left[1 - \left(\frac{\ln\left(1 + \frac{d_r}{d} \right)}{\ln\left(1 + \frac{d_r}{d_m} \right)} \right)^7 \right]$$

Equation 4-1

where: a_{gr} = parameter related to the initial breaking point of the curve,
n_{gr} = parameter related to the steepest slope of the curve,
m_{gr} = parameter related to the shape of the curve,
d_r = parameter related to the amount of fines in a soil,
d = diameter of any particle size under consideration, and
d_m = diameter of the minimum allowable size particle.

The bimodal equation used to fit the grain-size distribution is presented below.

$$P_p(d) = \left\{ w \left[\frac{1}{\ln\left(\exp(1) + \left(\frac{a_{bi}}{d} \right)^{n_{bi}} \right)^{m_{bi}}} \right] + (1-w) \left[\frac{1}{\ln\left(\exp(1) + \left(\frac{j_{bi}}{d} \right)^{k_{bi}} \right)^{l_{bi}}} \right] \right\} \left[1 - \left(\frac{\ln\left(1 + \frac{d_{rbi}}{d} \right)}{\ln\left(1 + \frac{d_{rbi}}{d_m} \right)} \right)^7 \right]$$

Equation 4-2

where: a_{bi} = parameter related to the initial breaking point of the curve,
n_{bi} = parameter related to the steepest slope of the curve,

m_{bi} = parameter related to the shape of the curve,

j_{bi} = parameter related to the second breaking point of the curve,

k_{bi} = parameter related to the second steep slope of the curve,

l_{bi} = parameter related to the second shape of the curve,

d_{rbi} = parameter related to the amount of fines in a soil,

d = diameter of any particle size under consideration, and

d_m = diameter of the minimum allowable size particle.

Most PTFs use grain-size information in some form as the basis for the estimation method. Of the three broad categories of estimations listed above, category ii) involved the estimation of parameters of a soil-water characteristic curve. The most commonly used soil-water characteristic curve functions are described in the following sections.

4.5 Representation of the soil-water characteristic curve

Although many different equations have been proposed to represent the soil-water characteristic curve (Sillers, 1996), three equations will be utilized by the PTFs presented in this chapter. The three equations are summarized below.

The Brooks and Corey (1964) equation (Equation 4-3)was the first equation used to represent the soil-water characteristic curve.

$$w_w = w_r + (w_s - w_r)\left[\frac{a_c}{\psi}\right]^{n_c}$$

Equation 4-3

where:

a_c = bubbling pressure (kPa),

n_c = pore size index,

w_r = residual gravimetric water content,

ψ = soil suction (kPa).

The van Genuchten equation (1980) shown below presented a three-parameter equation flexible enough to fit a variety of soils.

$$w_w = w_{rvg} + (w_s - w_{rvg}) \left[\frac{1}{\left[1 + (a_{vg}\psi)^{n_{vg}} \right]^{m_{vg}}} \right]$$

Equation 4-4

where:

w_s = saturated gravimetric water content,

w_r = residual gravimetric water content of the soil,

a_{vg} = fitting parameter,

n_{vg} = fitting parameter, and

m_{vg} = fitting parameter.

The Fredlund and Xing (1994) equation was presented as a flexible, continuous equation that can represent a water content of zero at a suction of 1,000,000 kPa.

$$w_w = w_s \left[1 - \frac{\ln\left(1 + \frac{\psi}{h_r}\right)}{\ln\left(1 + \frac{10^6}{h_r}\right)} \right] \left[\frac{1}{\left[\ln\left[\exp(1) + \left(\frac{\psi}{a_f} \right)^{n_f} \right] \right]^{m_f}} \right]$$

Equation 4-5

where:

w_s = saturated gravimetric water content,

a_f = fitting parameter corresponding to the soil suction at the inflection point and is closely related to the air entry value for the soil,

n_f = fitting parameter related to the maximum slope of the curve,

m_f = fitting parameter related to the curvature of the slope, and

h_r = constant parameter used to adjust the lower portion of curve.

4.6 Description of Pedo-Transfer Functions

The estimation of the soil-water characteristic curve has previously been performed based on one of the three methods presented below. The new method presented in this chapter is based on a physical model method. The new method is compared to previously presented results to provide a reference for this study.

4.6.1 Point Regression Method

Some of the methods proposed utilizing the point regression method are Husz (1967), Renger (1971), Gupta and Larson (1979), Rawls et al. (1982), and Puckett et al. (1985). A method utilizing this method of estimation was not evaluated in this study.

4.6.2 Functional Parameter Regression Method

This method assumes that functional parameters of the final equation can be correlated to basic physical properties of the soil. An example of this method is the correlation between the air entry parameter of a soil-water characteristic curve equation and basic soil properties such as percent sand or porosity. Paclepsky et al. (1982), Cosby et al. (1984), Rawls and Brakensiek (1989), Nicolaeva et al (1986), and Vereecken et al (1989) are a few of the researchers that used the functional parameter regression method.

For this study, the Rawls and Brakensiek (1985) and the Vereecken et al. (1989) methods are used for comparison to the proposed new method. Rawls and Brakensiek (1985) presented regression equations for estimating the parameters of the Brooks and Corey (1964) equations. The regression equations estimated the bubbling pressure, φ_b, the pore size index, λ, and the residual water content, θ_r, for the Brooks and Corey (1964) equation shown in Equation 4-3.

The Vereecken et al (1984) method involved fitting a dataset of forty Belgian soil series with the van Genuchten (1980) equation. A one-dimensional sensitivity analysis was then performed on the optimized parameters of the soil-water characteristic curve to check their relative importance and stability. A principle factoral analysis was then used to reveal the

structure in the data and to examine the relationship between the soil-water characteristic curve and the basic measured soil properties. Regression equations were then established. Vereecken et al (1984) concluded that the soil-water characteristic curve could be estimated at a reasonable level of accuracy using soil properties such as grain-size distribution, dry density, and carbon content.

4.6.3 Physical Model Method

Arya and Paris (1981) presented the first physio-empirical method to estimate the soil-water characteristic curve. The model made use of basic soil information such as the grain-size distribution. The volumetric water coefficient was then calculated based on the pore sizes and the pore radii were converted to equivalent soil suctions through the use of the capillary theory. The estimation method used an α empirical constant to account for uncertainty in the estimation. The formulations for the pore radius were based on spherical particles and cylindrical pores.

Arya and Paris (1981) assumed the pore-size distributions and the grain-size distributions of soils to be approximately congruent. That is, larger particles produce larger interparticle voids than smaller particles and vice versa. The grain-size distribution was divided into M size fractions. The mass of solid in the ith particle class is equated to the mass of N_i spherical particles with a radius R_i. The volume was given by:

$$V_n = \frac{4}{3} N_i \pi R_i^3$$

Equation 4-6

The volume of voids was subsequently represented by a single capillary tube of radius r_i.

$$V_{ns} = \pi r_i^2 h_i$$

Equation 4-7

where h_i is the capillary tube length. Arya and Paris (1981) also assume that the particles are not spherical and represent the true capillary pore length of an R_i class as:

$$h_i = 2R_i N_i^{\alpha}$$

Equation 4-8

where α is an empirical constant between 1 and 2.

Various models have been proposed to estimate the random packing nature of spherical particles in an attempt to properly estimate the pore-size distribution of a heterogeneous system (Iwata et al, 1988).

The Arya and Paris (1981) model was later modified by Havercamp and Parlange (1986), who applied the concept of shape similarity between the soil-water characteristic curve and the cumulative grain-size distribution for sandy soils without organic matter. Bupta and Ewing (1992) applied the Arya-Paris model in two ways: i) to the grain-size distribution in order to model intraaggregate pores and ii) to the aggregate-size distribution to model the interaggregate pores. Nimmo (1997) presented a method of accounting for the influence of structure through the use of aggregate-size distributions.

Some criticism was presented (Havercamp and Parlange 1982, 1986; Arya and Paris, 1982) regarding the empirical nature of the α parameter presented in the Arya and Paris (1981) estimation. Tyler and Wheatcraft (1989) presented an analysis correlating the fitting parameter α to physical properties of the soil using fractal mathematics. It was hypothesized that α is equal to the fractal dimension of the pore trace and expresses a measure of the tortuosity of the pore trace . The fractal dimension of the pore traces ranged from 1.011 to 1.485 for all but one soil tested.

4.6.4 Description of the New Proposed Model

The physio-empirical method was selected for a new model because of its fundamental and theoretical basis. It was hypothesized that the grain-size distribution provides a physical description that should be used as the basis for any estimation. However, the grain-size distribution is limited in that it does not give an indication of the *insitu* density of the soil. The

porosity of the soil is then used as an attempt to account for the packing arrangements of the various individual grain-sizes.

Previous models involved the translation of the grain-size distribution to equivalent water contents. The pore-size values are then used to calculate corresponding volumetric water contents and capillary pressures. The proposed method presented in this chapter first divides the grain-size distribution into small groups of relatively uniform particles. It is hypothesized by this study that for each uniform group of particles there exists a relatively unique soil-water characteristic curve.

4.7 Theory of Proposed New Model for Predicting the Soil-Water Characteristic Curve

The M.Fredlund (1997) unimodal and bimodal equations were used for fitting of grain-size curves (See Equation 4-1 and Equation 4-2). The M.Fredlund (1997) grain-size equations allowed for a continuous fit and proper definition of the extremes of the curve. The mathematical fit of the grain-size distribution data led to the development of a new algorithm capable of predicting the soil-water characteristic curve. The new model uses a combination of the capillary model and a knowledge of the variation of the soil-water characteristic curve in the estimation. The volume-mass properties and the grain-size distribution form the basic information needed for the estimation of the soil-water characteristic curve.

The theory of the new approach is based on several theorems (or principles). These theorems are outlined below.

Theorem 1 - A soil composed entirely of a uniform, homogeneous particle size would have a unique drying soil-water characteristic curve.

Theorem 2 – The capillary model is best suited for the estimation of the air entry value of each collection of uniform, homogeneous particle sizes.

Theorem 3 – The soil-water characteristic curve for soil composed of more than one particle size is the sum of the soil-water characteristic curves for each individual particle size.

The theorems presented above allowed for the formulation of the new method based on the capillary model and the soil-water characteristic curve information intrinsic to each uniform particle size.

A model was required that describes the soil-water characteristic curve for each individual particle size. The Fredlund and Xing (1994) equation was selected to model the soil-water characteristic curve because of its ability to fit the entire range of soil suctions. A description of the Fredlund and Xing (1994) equation parameters for each collection of uniformly-sized particles is required.

The a_f parameter in the Fredlund and Xing (1994) model has been shown to be loosely related to the air entry value of the soil. Figure 4-2 shows the relationship between the air entry value of the soil and the a_f fitting parameter of the Fredlund and Xing (1994) equation for the dataset used to train the proposed new pedo-transfer function. It can be seen that the af parameter is typically higher than the actual air entry value. It was found that this is predominantly the case when the n_f and m_f parameters revert to extremes. The a_f parameters is a relatively good approximation for typical soil-water characteristic curves. The difference between the a_f parameter and the air entry value as calculated by Vanapalli and Fredlund (1998) can be further reduced if the n_f and m_f parameters vary in a related manner. The variation in the Fredlund and Xing (1994) equation using a range of n_f and m_f parameters used in the estimation and keeping the a_f parameter constant at 100 kPa can be seen in Figure 4-3. Once the pore radii of the soil particles is known, the equivalent air-entry value (i.e., soil suction) can be calculated based on the capillary model shown in Equation 4-9. This soil suction will be the air entry value for a soil with uniform particles.

$$\psi = 2\gamma \frac{\cos\Theta}{\rho_w g r}$$

Equation 4-9

where: γ = surface tension of water,

Θ = contact angle,

ρ_w = the density of water,

g = acceleration of gravity,

r = pore radius,

ψ = soil suction.

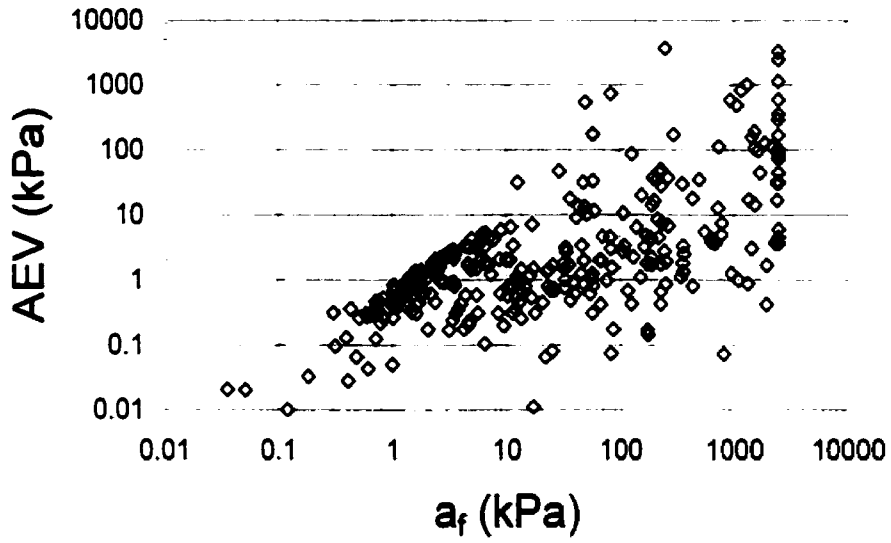

Figure 4-2 Relationship between the air entry value from the Fredlund (1998) construction and the a_f parameter of the Fredlund and Xing (1994) equation for 311 soils from the training dataset

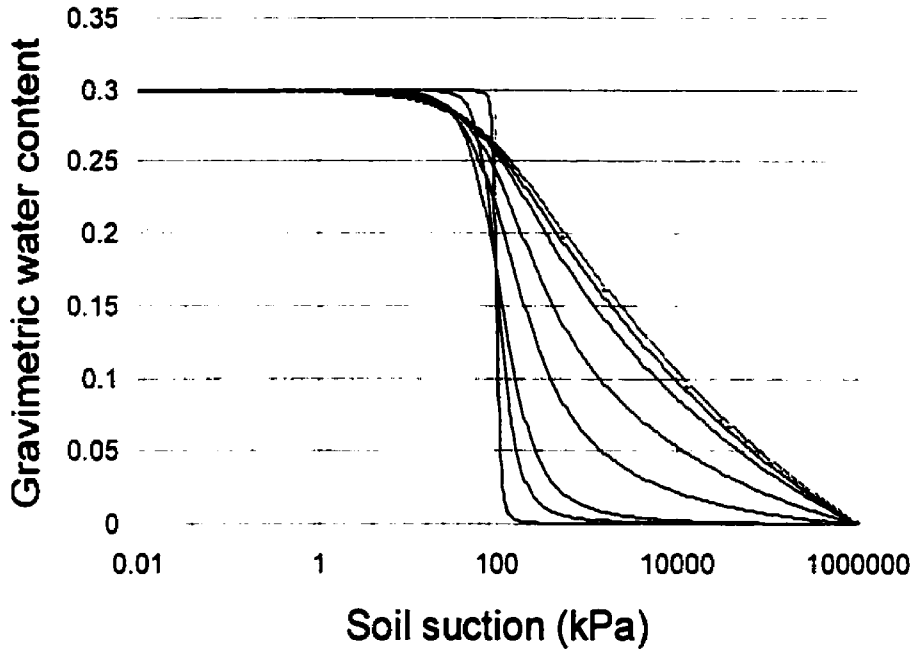

Figure 4-3 Illustration of variation of n_f and m_f parameters according to grain-diameter while holding a_f constand at 100 kPa

An approximate shape for the soil-water characteristic curve can be calculated for each uniform collection of particles. Estimating the shape for a pure coarse sand or a pure clay can be done with reasonable certainty. The experimentally measured soil-water characteristic curve for a collection of glass beads was used as a benchmark. It was assumed that the shape for the glass beads was representative of a soil-water characteristic curve for uniform coarse particles. The soil-water characteristic curve for glass beads can be seen in Figure 4-4. The soil-water characteristic curve for a pure clay was estimated by plotting the results of a group of soils from research literature with a high clay content. The group of clay soils can be seen in Figure 4-5. The glass beads and the clay soils provide limiting values for groups of soils consisting of uniformly-sized particles. The limiting values were then used as the basis for the estimation and can be seen in Figure 4-6.

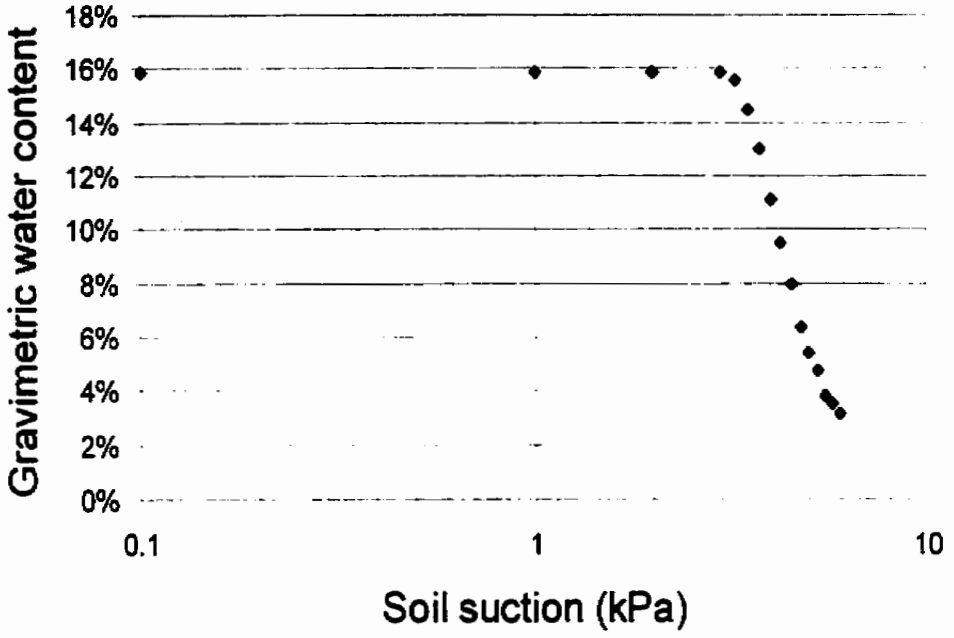

Figure 4-4 Soil-water characteristic curve for uniform glass beads, diameter=0.181mm ±10% from Nimmo et al., 1996 (119)

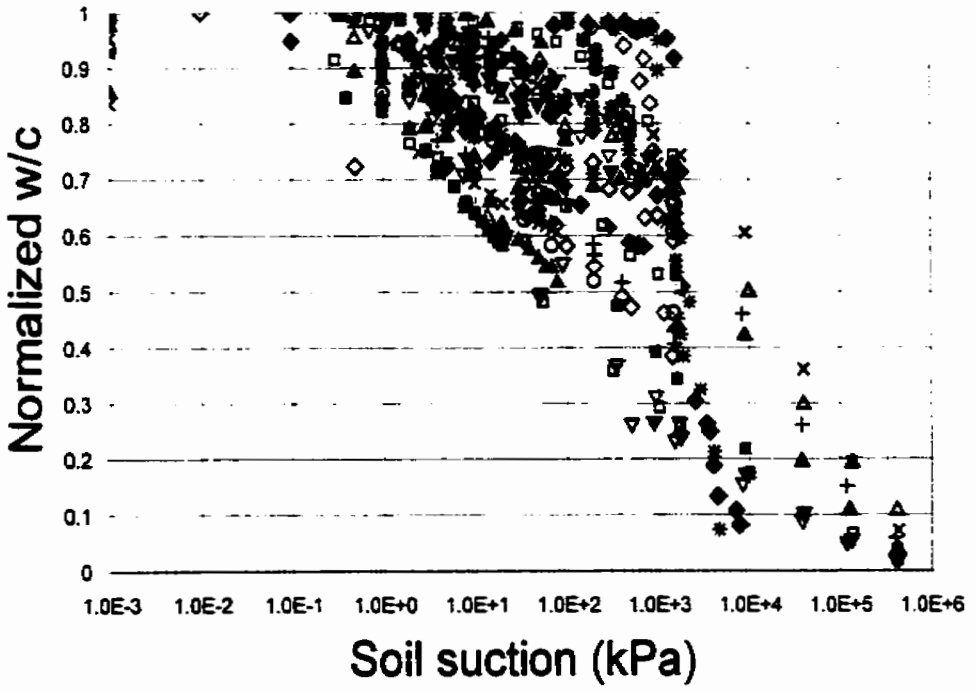

Figure 4-5 Selection of typical soil-water characteristic curves for relatively pure clay soils

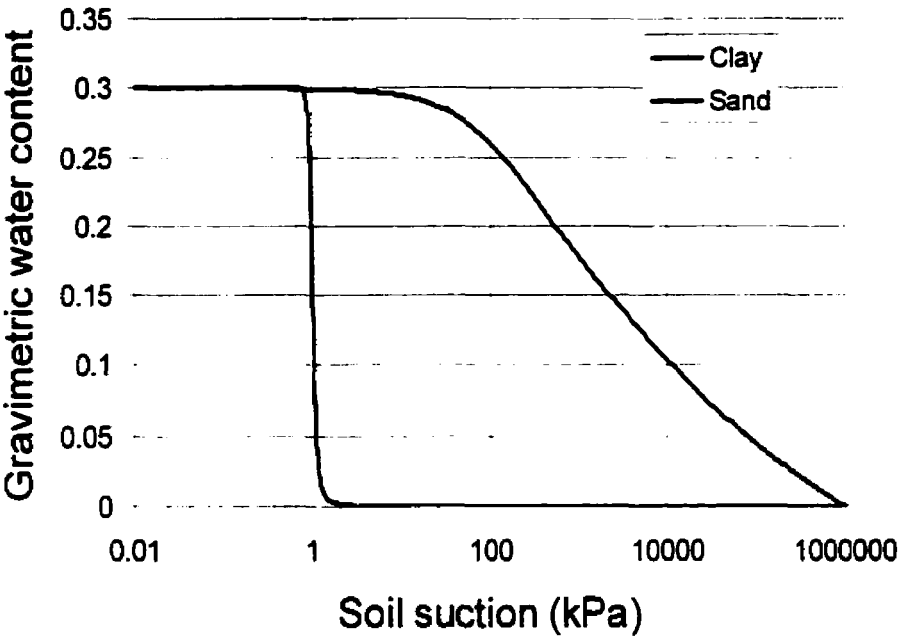

Figure 4-6 Assumed boundary soil-water characteristic curves for groupings of uniform coarse and fine particles sizes; Sand: $a_f = 1$, $n_f = 20$, $m_f = 2$, $h_r = 3000$, Clay: $a_f = 100$, $n_f = 1$, $m_f = 0.5$, $h_r = 3000$

A representative soil-water characteristic curve has now been established for a pure sand and a pure clay. It is also necessary to estimate a typical soil-water characteristic curve for uniform grain-sizes between coarse sand-sized particles and clay-sized particles. Representation of typical soil-water characteristic curves for coarse soils, fine soils, as well as incremental soils was achieved by altering the parameters of the Fredlund and Xing (1994) equation. This allows for a smooth transition in representation of the soil-water characteristic curve when moving from coarse-sized particles to fine-sized particles.

The boundary soil-water characteristic curves as well as the air-entry value for each group of uniform soil particles can now be estimated. A description of the shape of the soil-water characteristic curve at intermediate grain-sizes is required.

The n_f and m_f shape parameters for the Fredlund and Xing (1994) equation are required for each uniform collection of particles. The shape, and resulting n_f and m_f parameters, of the soil-water

characteristic curves for pure sands, pure silts and pure clays is estimated as shown above. A dataset combining soils from Rawls et al. (1985), Sillers, (1997), and the CECIL soil survey was then used for determination of approximate trends in the n_f and m_f parameters. An effective grain-size diameter was calculated for each grain-size curve based on Equation 4-10 (Vukovic et al., 1992). The effective grain-size diameter was then plotted opposite the n_f and m_f parameters. The n_f and m_f parameters were determined for each soil by fitting experimental data with a least-squares regression algorithm. The resulting variation of the n and m parameters can be seen in Figure 4-7 and Figure 4-8 respectively.

$$\frac{1}{d_e} = \frac{3}{2}\frac{\Delta g_l}{d_l} + \sum_{i=2}^{i=n} \frac{\Delta g_i}{d_i}$$

Equation 4-10

where: d_l = largest diameter of the last fraction of the material,

Δg_l = weight of the material of the last, finest fraction, in parts of total weight, and

d_e = effective grain diameter.

The end result of the above analysis is the establishment of representative plots for n_f and m_f. These plots describe reasonable variations in the two parameters with grain-size. It is now possible for n_f and m_f parameters to be estimated for any soil composed of uniform diameter particles.

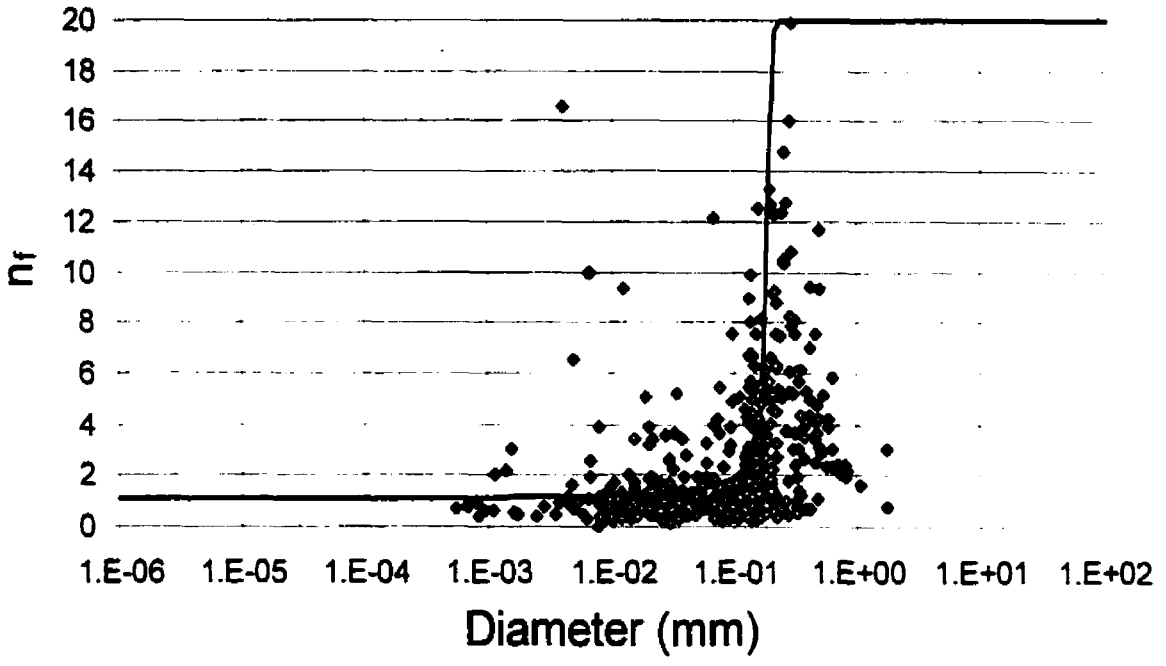

Figure 4-7 Plot showing the variation of the n_f parameter with effective grain diameter for the Fredlund and Xing (1994) equation used to fit the soil-water characteristic curve.

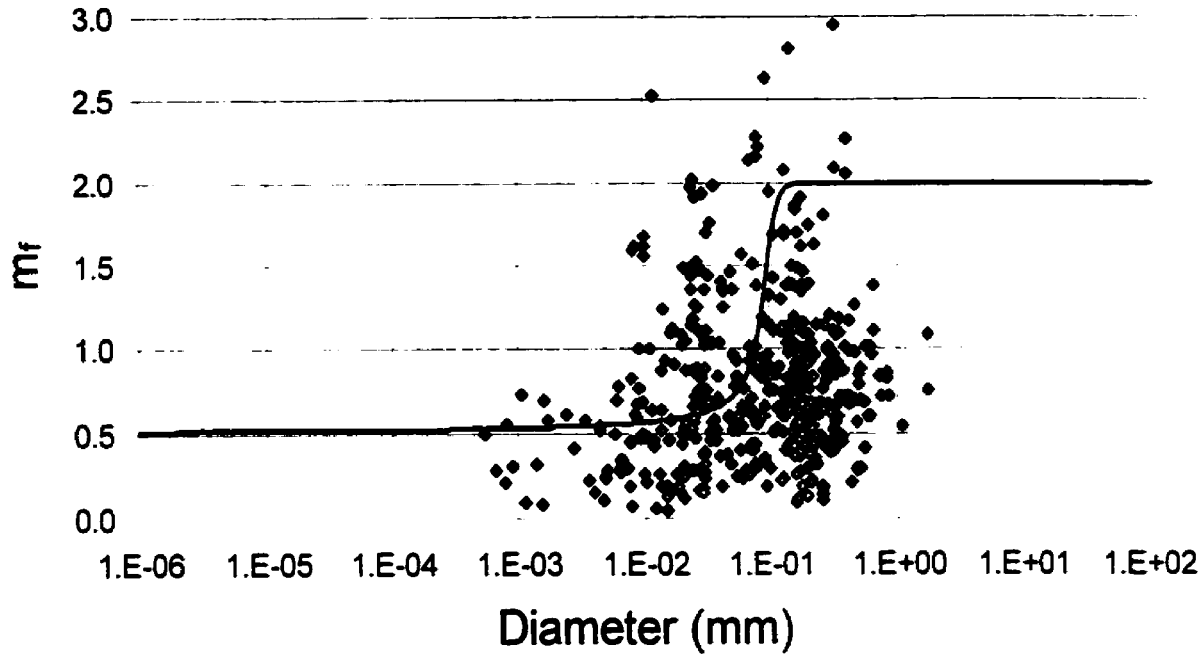

Figure 4-8 Variation of the m_f parameter with effective grain diameter for use with the Fredlund and Xing equation (1994) used to fit the soil-water characteristic curve.

An equation with a form similar to the van Genuchten (1980) equation was then fit through the experimental data to provide an estimate of the n_f and m_f Fredlund and Xing (1994) parameters based on grain-size diameter. This resulted in Equation 4-11.

$$p(\phi) = p_1 \left[\frac{1}{\ln\left(\exp(1) + \left[\frac{10^{-\log(\phi)-1}}{p_2} \right]^{p_3} \right)} \right]^{p_4} + p_5$$

Equation 4-11

where: p_1, p_2, p_3, p_4, p_5 = curve parameters,

ϕ = grain diameter, and

$p(\phi)$ = parameter value.

Equation 4-11 can be used to represent either the n_f or the m_f parameter variance with grain-size diameter. The optimal equation parameters for representing the variation of n_f are $p_1 = 19$, $p_2 = 50$, $p_3 = 30$, $p_4 = 1$, $p_5 = 1$. The optimal equation parameters for representing the variation of m_f are $p_1 = 1.5$, $p_2 = 100$, $p_3 = 10$, $p_4 = 1$, $p_5 = 0.5$. The fit of equations representing the variation of n_f and m_f are shown in Figure 4-7 and Figure 4-8, respectively.

The grain-size distribution curve was then divided into small divisions of uniform soil particles. Starting at the smallest diameter size, a packing porosity, n_p, was then estimated (Harr, 1977) for each division and a soil-water characteristic curve generated. This is illustrated in Figure 4-9. The divisional soil-water characteristic curves were then summed starting with the smallest particle size and continuing until the volume of pore space equaled that of the entire heterogeneous soil structure. The result is a predicted soil-water characteristic curve.

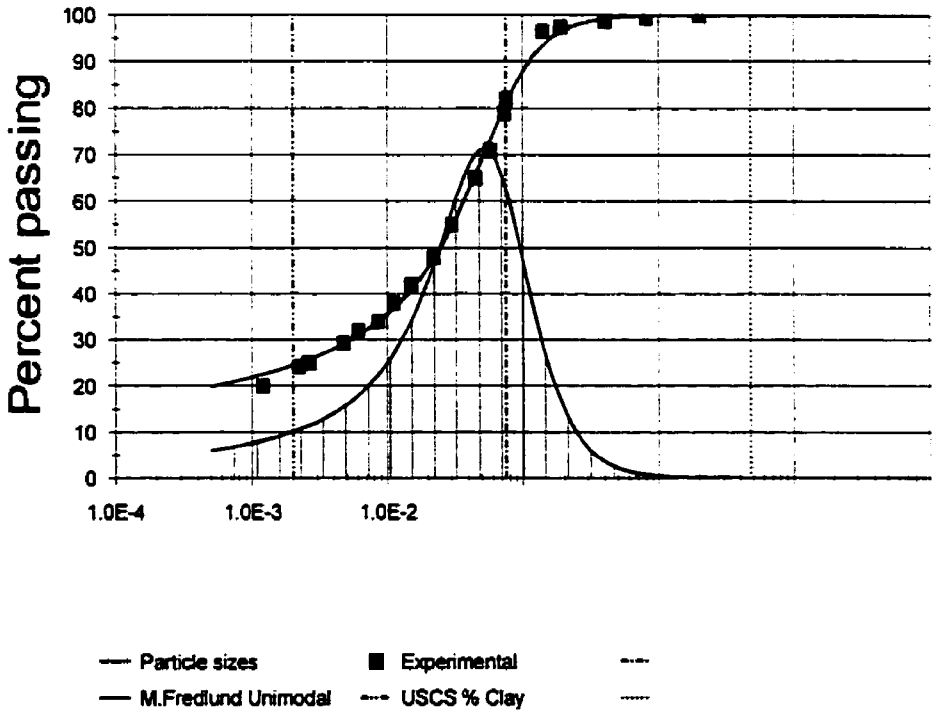

Figure 4-9 Small divisions of particle size used to build complete soil-water characteristic curve

4.7.1 Pore Volume

The grain-size distribution curve can be divided into *n* fractions of uniformly-sized particles. Each fraction contains its own packing arrangement and porosity. It is assumed that the summation of the individual fraction porosities will be greater than the natural, *insitu* porosity of the soil. In the assemblage of soil particles, the voids created between larger particles will be filled with smaller particles. This, in essence, reduces the influence of the larger particles on the soil-water characteristic curve. Experimental results have shown this to be the case. The porosities of the individual fractions are summed until the measured porosity of the *insitu* soil is reached. The remaining particle fractions are ignored.

The assumed "packing" structure of each uniformly-sized fraction is of importance. Characteristics of different "packings" were calculated by Smith (1929) and are summarized in Table 4-1. It is important to note that i) the porosity is independent of particle size, and ii) the porosity varies between 25.95% and 47.64%. These packing porosities are determined for idealized spherical particles. Soil particles are commonly angular and, as such, a greater range of porosity variation is expected.

Table 4-1 Some characteristics of ideal packings (Smith, 1929)

Packing	Volume of unit cell	Porosity (%)
Cubic	d^3	47.64
Orthorhombic	$0.87d^3$	39.54
Tetragonal-spheroidal	$0.75d^3$	30.19
Rhombohedral	$0.71d^3$	25.95

The assumed packing porosity, n_p, of each grain-size fraction needs to be approximated. In this research study, it is assumed that the n_p variable is the same for each successive particle fraction. It is the authors opinion that n_p be determined as a function of particle diameter.

It is first assumed that the grain-size distribution represents a percent by weight distribution. A unit volume of soil ($1m^3$) is analyzed. The weight of soil can be calculated relative to the total unit weight of the soil. Individual weight fractions can then be calculated as follows.

$$W_i = (g_{i+1} - g_i)\rho_i$$

where: W_i = weight of individual fraction (kg),

g = function representing percent passing versus particle diameter,

i = counter from 1, 2,..., n,

n = number of fractions into which grain-size distribution is divided,

ρ_t = total density of the soil sample (kg/m^3).

The average diameter for each weight fraction can also be calculated by taking the logarithmic average of the *i*th and *i+1*th particle size divisions. Average diameters in this analysis were calculated arithmetically.

The pore volume associated with each fraction is computed as being proportional to the total pore volume of the sample. The n_p provides us with an assumed porosity for the *i*th fraction. Calculation of the pore volume is possible once the porosity is known.

$$V_{v_i} = \frac{W_i}{G_s \rho_w} \frac{n_p}{(1-n_p)}$$

where: V_{vi} = volume of voids (m^3),

G_s = specific gravity of the soil,

ρ_w = density of water (kg/m^3),

n_p = assumed packing porosity.

The contribution of the *i*th grain-size fraction to the total soil sample can now be computed. Since the volume of voids of each fraction, V_{vi}, is known along with the total volume of the sample, (1m^3), the contribution of each fraction to the whole is equal to V_{vi}. The sum of all the voids can then be calculated as follows.

$$V_v = \sum_{i=1}^{i=n} V_{v_i}$$

One of the results of using this technique is that V_v can be greater than or less than the actual volume of voids, V_{vt}, in the *insitu* soil. Methods are presented in this chapter for analyzing situations where the actual volume of voids is not equal to the analytically computed volume of voids. If the computed volume of voids, V_v, is greater than V_{vt}, the analytical effect of the voids

greater than V_{vt} on the soil-water characteristic curve is ignored. This truncation results in the elimination of the effect of coarse-sized particles on the soil-water characteristic curve since the grain-size curve is evaluated from fine to coarse-sized particles. This seems reasonable since the effect of coarse-sized particles can be negligible if the voids are filled with finer-sized particles.

If the sum of voids, V_v, is less than the actual volume of voids, V_{vt}, the resulting soil-water characteristic curve will not reach saturated conditions. A suitable way of analyzing this imbalance has not as of yet been determined. Additional research is required to determine a proper solution for this problem.

4.8 Description of the Dataset to be Analyzed in Verifying the Proposed Model

A sample dataset of 188 soils was selected from data presented in literature. The soils included data from Sillers (1997), Rawls (1985), and Williams (1992). All soils selected had an experimentally measured grain-size distributions and experimentally measured soil-water characteristic curve. In addition, the measured soil parameters necessary for the estimation of all six pedo-transfer functions presented in this chapter were also a requirement. Figure 4-10 summarizes the variance of grain-size parameters in the selected dataset. The selected dataset provides a wide distribution of soils from a number of different sources. The objective was to provide a random selection of soils not biased by one particular group of investigators. The presence of an experimentally measured soil-water characteristic curve also allowed for verification of the results obtained when using different estimation techniques.

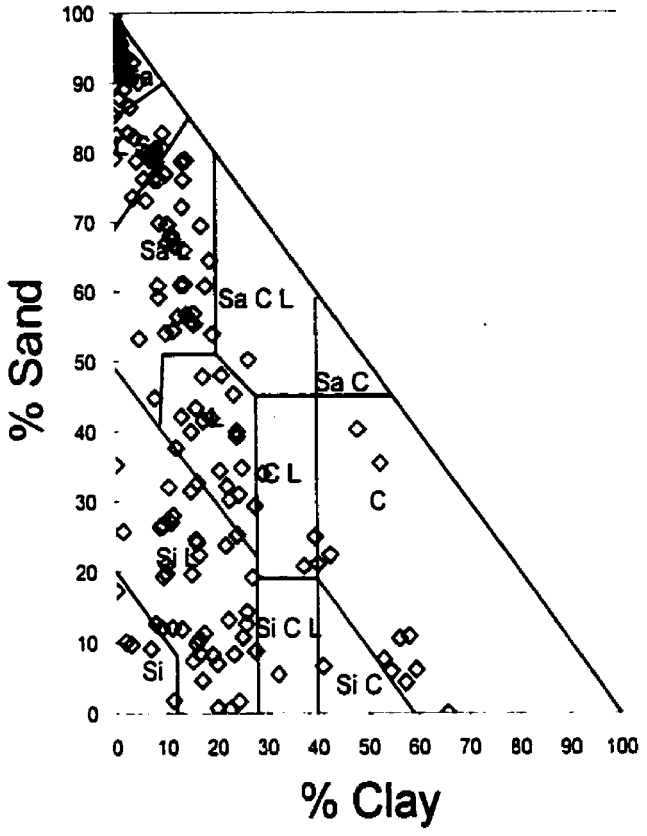

Figure 4-10 USDA classification for 188 soils used in the evaluation of pedo-transfer functions.

The reliability of the new pedo-transfer function was evaluated by cross-validation. With cross-validation (Hjorth, 1994), the reliability of a pedo-transfer function is assessed by (1) drawing a random subsample from the data set, (2) developing a pedo-transfer function for the subsample, and (3) testing the accuracy of the pedo-transfer function against the data left after subsampling. Data was first selected based on the availablility of data containing a grain-size distribution and enough volume-mass properties (i.e., void ratio, dry density, and specific gravity) to perform the estimation.

The database was then split into soils with an even index number and soils with an odd index number. The even soils were used to train the proposed new pedo-transfer function. Soils which contained an odd index were used to test the new pedo-transfer function. This dataset was

further reduced by selecting only the soils that contained sufficient data for the estimation of all six pedo-transfer functions evaluated in this study.

4.9 Analysis of Results of Estimation by New Model

The results of comparisons between experimental and predicted data can be seen in Figure 4-11, to Figure 4-18. Ten optimal estimations of the soil-water characteristic curve by the new proposed method can be seen in Figure 4-19.

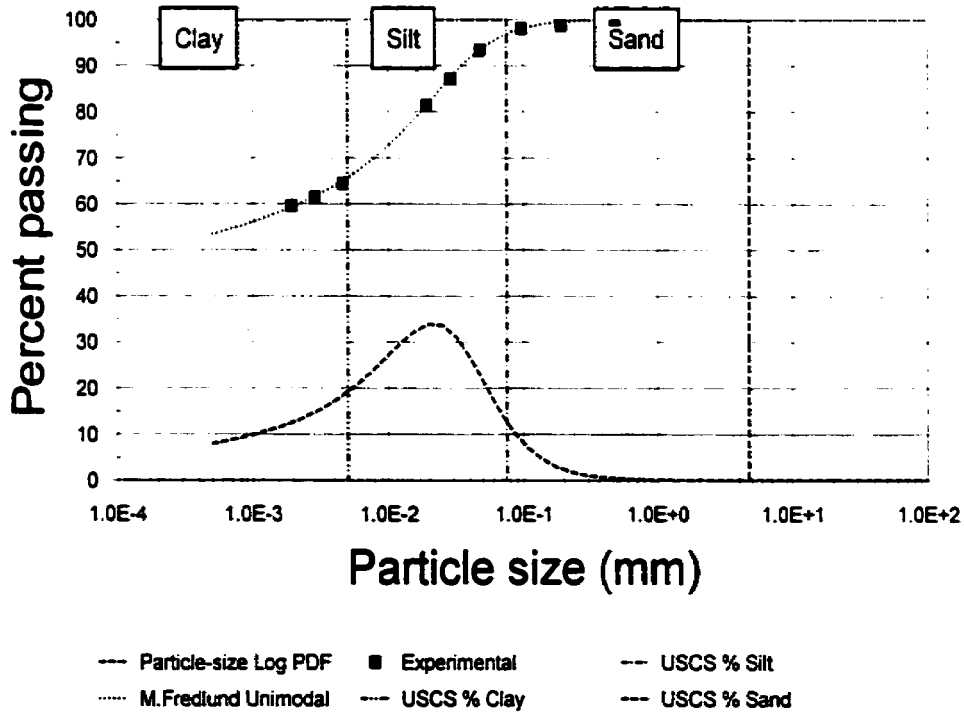

Figure 4-11 Grain-size distribution fit for a Clay published by Russam, 1958, $R^2 = 0.999$ (12429)

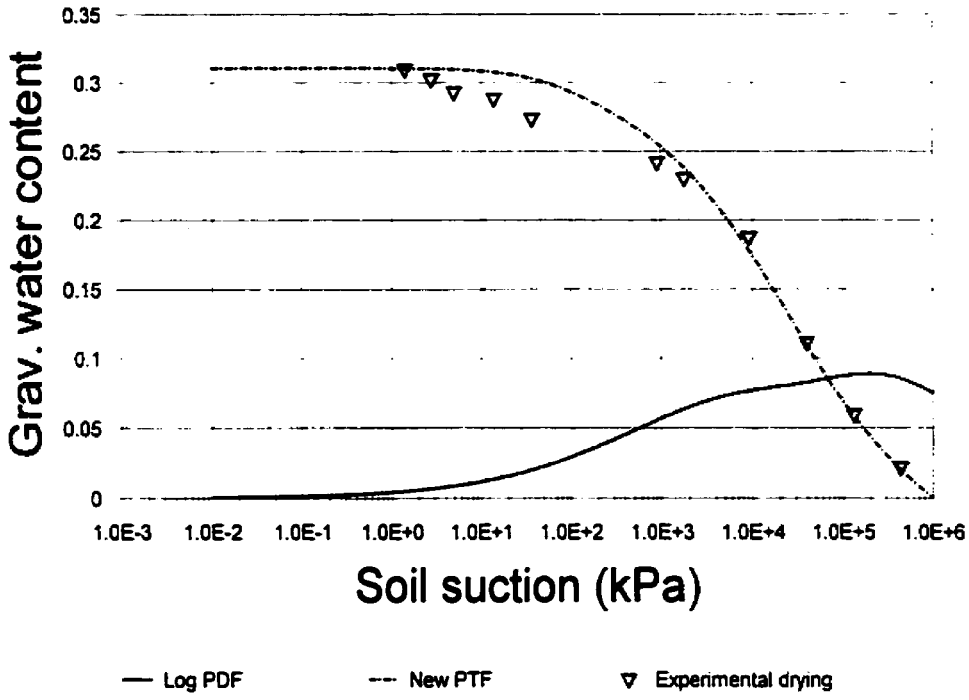

Figure 4-12 Comparison of experimental, predicted, and logarithmic probability density curves for a Clay published by Russam, 1958, $R^2 = 0.982$ (12429)

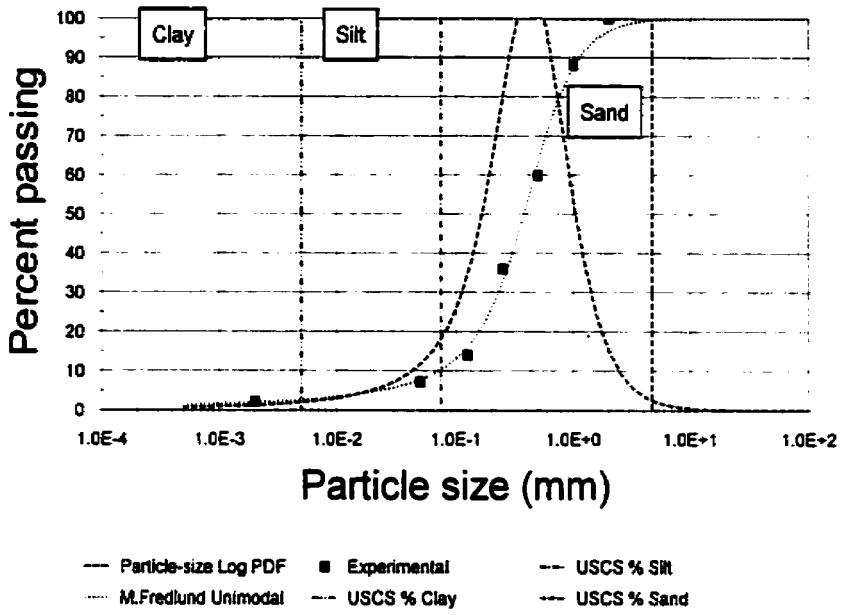

Figure 4-13 Grain-size distribution fit for a Sand originally published by Dane et al., 1983, $R^2 = 0.996$ (10727)

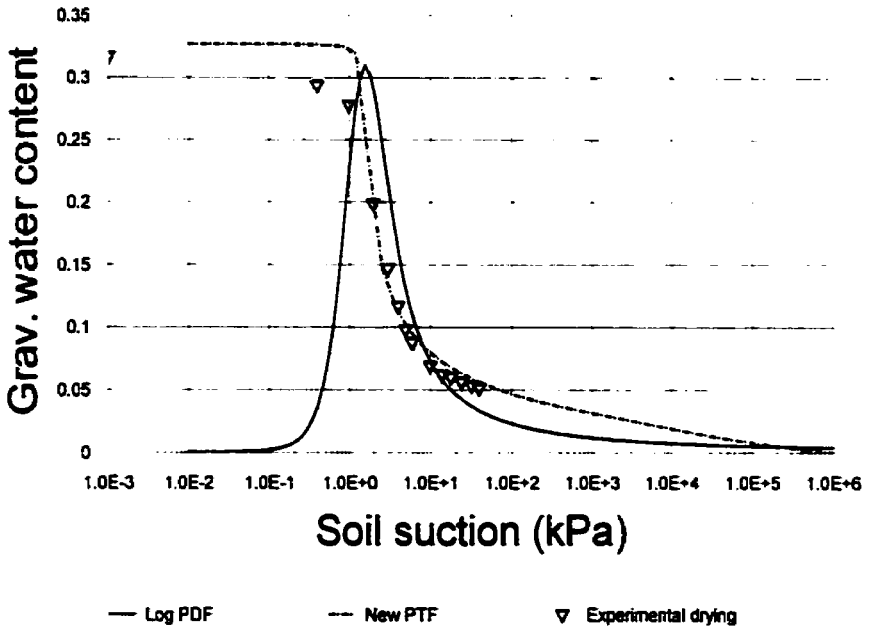

Figure 4-14 Comparison of experimental, predicted, and logarithmic probability density curves for a Sand originally published by Dane et al., 1983, $R^2 = 0.969$ (10727)

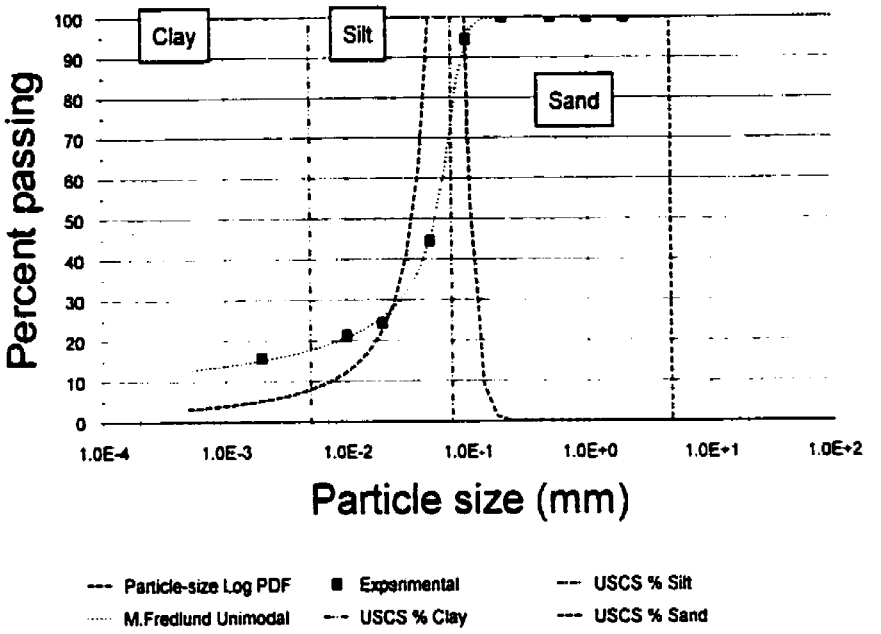

Figure 4-15 Grain-size distribution for a Silt Loam originally published by Vereecken, 1986, $R^2 = 0.999$ (11305)

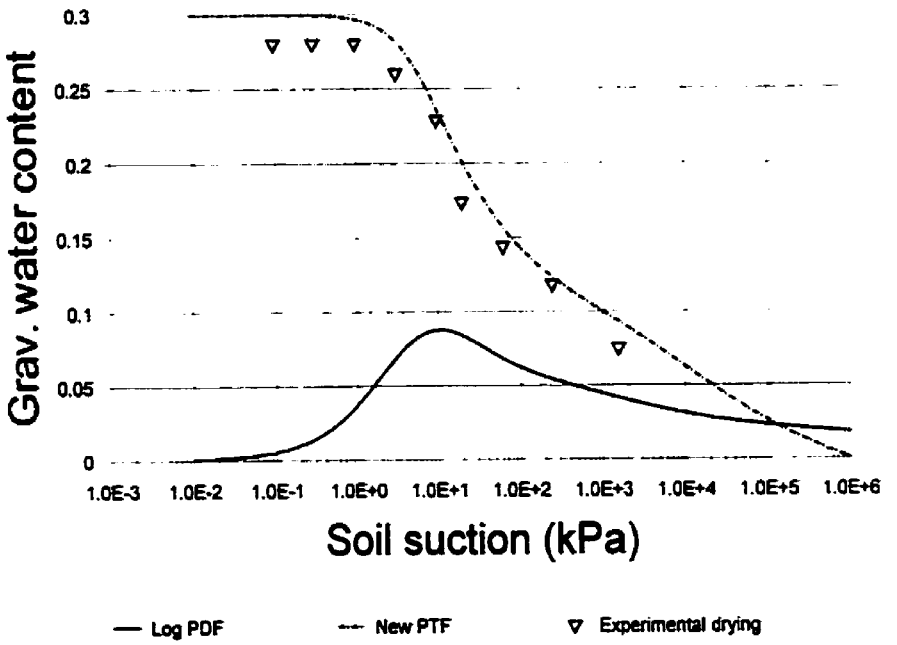

Figure 4-16 Comparison of experimental, predicted, and logarithmic probability density curves for a Silt Loam originally published by Vereecken, 1986, $R^2 = 0.944$ (11305)

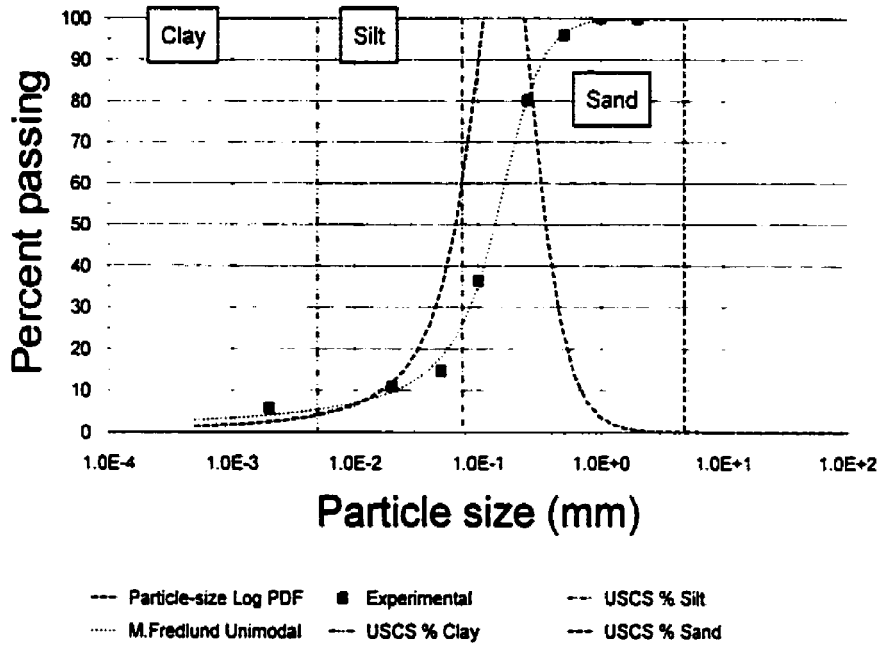

Figure 4-17 Grain-size distribution for a for a Sandy Loam originally published by Schuh et al., 1991, R^2 = 0.999 (11177)

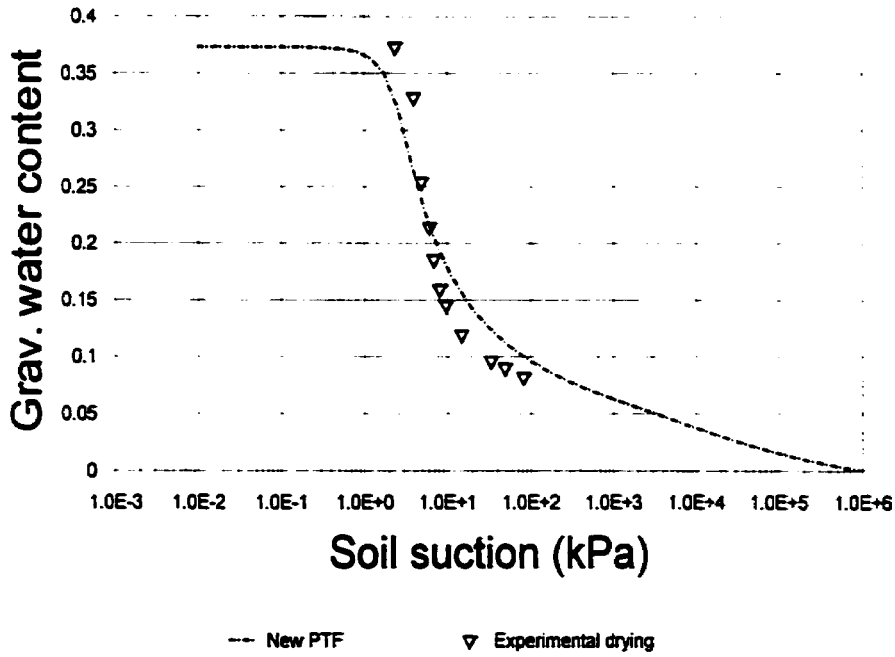

Figure 4-18 Comparison of experimental, and predicted data for a Sandy Loam originally published by Schuh et al., 1991, R^2 = 0.869 (11177)

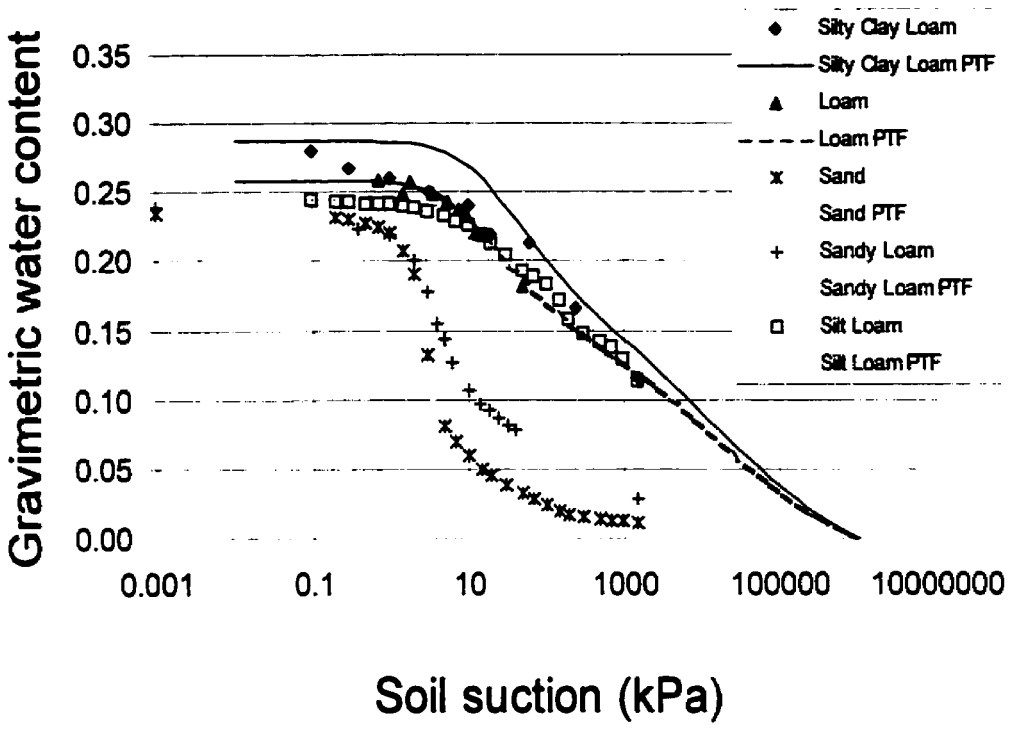

Figure 4-19 Best estimation for each of five textures of the soil-water characteristic curve using the proposed new pedo-transfer function. Silty Clay Loam R^2=0.80; Loam R^2=0.98; Sand R^2=0.99; Sandy Loam R^2=0.97; Silt Loam R^2=0.99.

The estimation of a soil-water characteristic curve from grain-size distribution has been attempted for all soil types. Clays, tills and loams appear to be more difficult to predict than silts and sands, although the accuracy of the estimation algorithm still seems reasonable. Results tended to be sensitive to the packing porosity, n_p. More research is required in order to fully understand the influence of the packing porosity.

The proposed new pedo-transfer function was found to successfully estimate the soil-water characteristic curve for a wide range of textural classes. Using pre-defined soil-water characteristic curves for each individual grain-size class allowed an increased stability when estimating the soil-water characteristic curve of all textural classes.

Several groups of soils have typically caused difficulties when estimating the soil-water characteristic curve. These general categories of soils include: (i) soils that have a high amount of clay-sized particles, (ii) soils that contain large amounts of coarse-size particles mixed with

fines, (iii) soils that exhibit bimodal behavior such as sand-bentonite mixtures, and (iv) special soils such as mine tailings and waste rock. The theory associated with the proposed new pedo-transfer function allows increased accuracy when estimating the soil-water characteristic curve for the aforementioned soils. Each of these categories of soils are discussed below.

4.9.1 Clay Dominated Soils

The validity of applying the capillary model to clay-sized particles is a matter of debate. The proposed new pedo-transfer function uses the capillary model merely to obtain the air-entry value for each group of uniform-size clay particles. The shape of the soil-water characteristic curve is then estimated in a natural manner from the n_f and m_f Fredlund and Xing (1994) curve parameters. This method was found to promote stability in the new proposed pedo-transfer function when performing calculations on clay-dominated soils. It also provided the advantage of viewing realistic effects of the clay-sized particles on the entire estimated soil-water characteristic curve.

The new pedo-transfer function was found to be sensitive to the clay-sized particles present in the grain-size curve. It therefore follows that the accuracy of the estimation could be improved by performing a hydrometer analysis on soils containing greater than 10% clay-sized particles. The ability of the M.Fredlund (1997) equation to fit the grain-size distribution in the silt and clay regions of the curve was also a factor. It was found that the accuracy of the estimation could be improved by varying the minimum particle diameter, d_m, or by using the bimodal fit of the grain-size distribution as the basis for the pedo-transfer function.

Significant deterioration in the reliability of the estimation was found as the amount of fines increased. The results of the comparison between the estimated error and the percent clay show a decrease in the accuracy in the estimation as the clay content of the soil increased. The relationship between percent clay and estimated error for values between 0.0 and 1.0 can be seen in Figure 4-20.

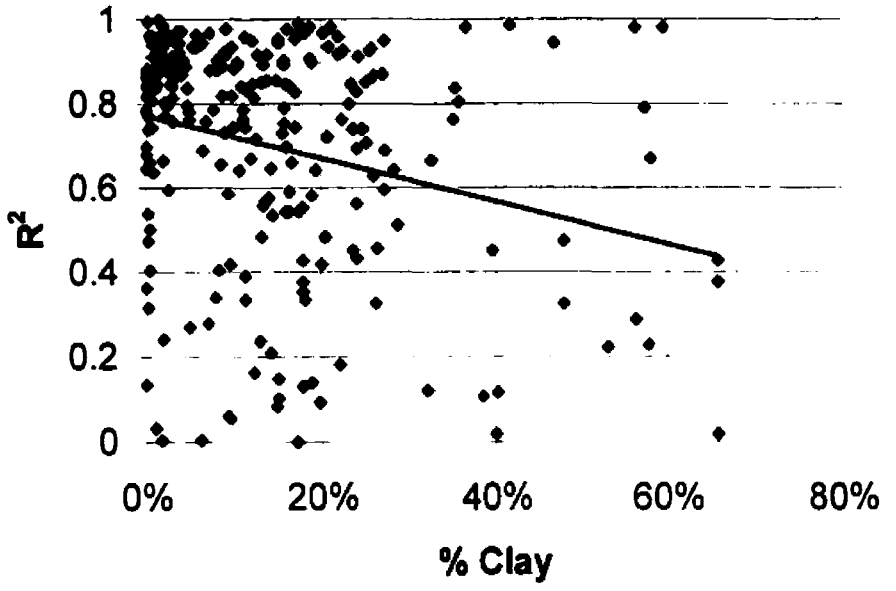

Figure 4-20 Linear interpolation relationship between the percentage of fines in a soil and the accuracy of the new pedo-transfer function for R^2 values between 0.0 and 1.0

4.9.2 Coarse and Fine Mixture Soils

A typical problem when estimating the soil-water characteristic curve from grain-size data is the difficulty in estimating the air-entry value for soils with a large amount of medium to fine-sized particles as well as coarse-sized particles. If the influence of all particle-sizes are weighted the same, the air-entry value is assumed to be controlled by the coarse-sized particles. Due to mixing, however, the effect of the coarse-sized particles is often negligible because the fines fill the voids between the coarse-sized particles.

The new pedo-transfer function alleviates this problem by building the soil-water characteristic curve beginning with the finest-sized particles. Based on the packing porosity, n_p, the effect of the coarse-sized particles is often ignored. This behavior has been confirmed by experimental testing. The accuracy of the new pedo-transfer function is therefore greatly improved for the aforementioned soils.

4.9.3 Bimodal Soils

The estimation of the soil-water characteristic curve for a gap-graded soil has not previously been possible. The bimodal representation of the grain-size distribution presented in Chapter 3 allows gap-graded soils to be represented mathematically. This mathematical representation can be used as the basis for the new pedo-transfer function.

An example of a typical soil exhibiting bimodal behavior is a sand-clay bentonite mixture. Such soils are commonly used in engineering practice and modeling seepage characteristics of such soils is often required. It is, therefore, useful to be able to accurately estimate the soil-water characteristics of such soils.

The estimation of the soil-water characteristic curve for a gap-graded soil is used as an example of a bimodal soil. A Saprolitic soil was studied at the University of Saskatchewan (Pavier, 1999). The soil had an initial void ratio of 0.85, a dry density of 1434 kg/m^3, and a specific gravity of 2.65. A sieve and hydrometer analysis were performed and the results are shown in Figure 4-21. Three different Tempe Cell tests were performed using 1 bar, 3 bar, and 5 bar high air entry disks. The experimental results are plotted alongside the estimation results in Figure 4-22. The results show that the new pedo-transfer function can be used to estimate the resulting bimodal soil-water characteristic curve for gap-graded soils.

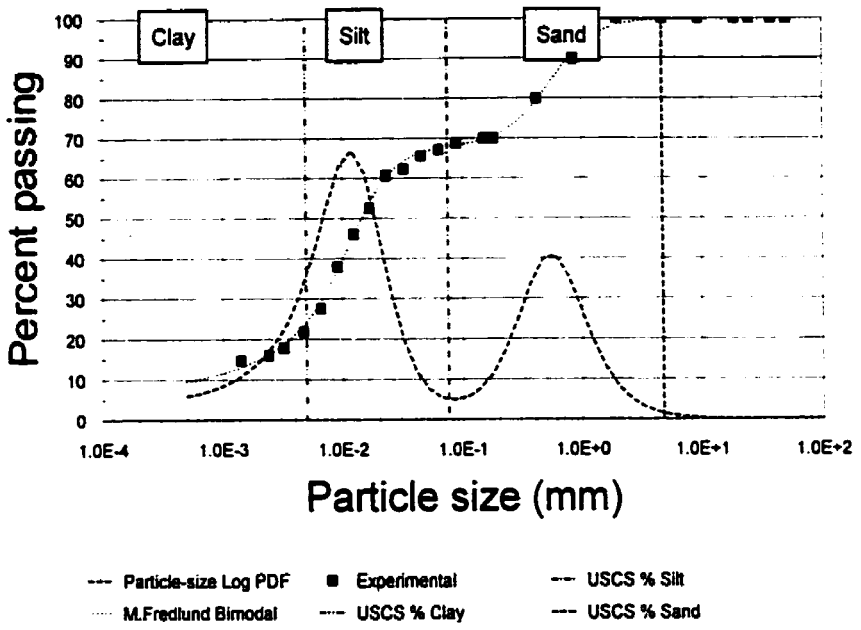

Figure 4-21 Grain-size distribution resulting from hydrometer and sieve analysis of a Saprolitic soils, Unsaturated Soil Group, University of Saskatchewan, 1998,, R^2=0.999 (11491)

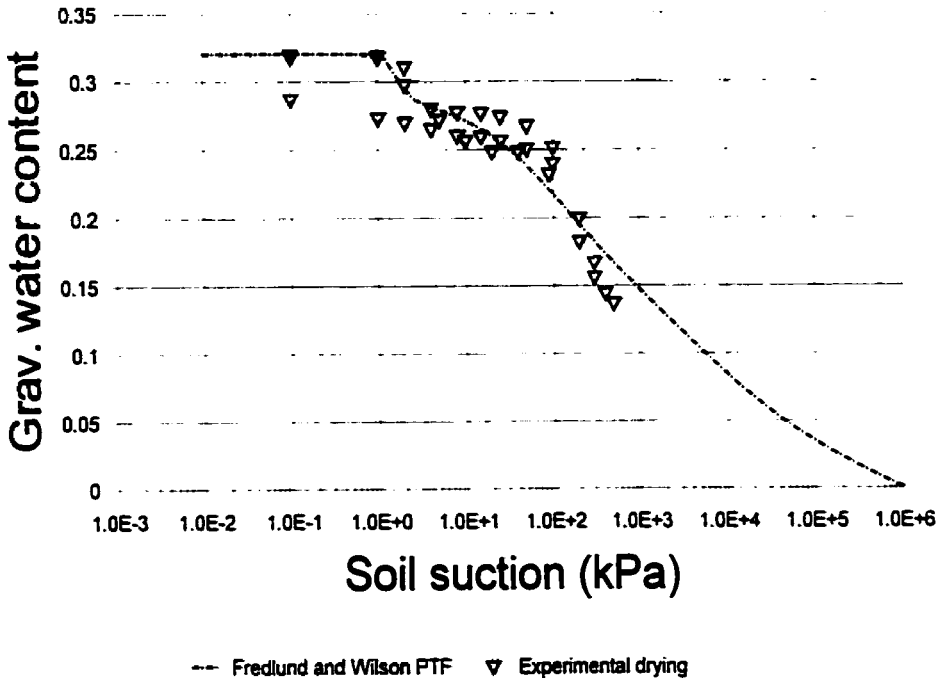

Figure 4-22 Results of 1 bar, 3 bar, and 5 bar tempe cell tests compared to bimodal estimation, Unsaturated Soil Group, University of Saskatchewan, 1998, R^2=0.858 (11491)

4.9.4 Packing Porosity

The packing porosity, n_p, is the primary variable used to control the estimation of the soil-water characteristic curve. The estimation of a reasonable packing porosity is crucial for the estimation of the soil-water characteristic curve. The two methods that were found to be reasonable for providing an estimation of the packing porosity involved: (i) statistical methods, and (ii) the use of a neural net. Statistical methods involve finding the normal distribution of the packing porosity for the textural category for which a packing porosity is desired. It is then possible to calculate a mean and variance of the packing porosity. This has the advantage that it is possible to obtain confidence limits on possible packing porosity values.

An improvement on the statistical method was to allow the packing porosity to be estimated through the use of a neural net. A neural net is an artificial intelligence technique by which an algorithm can be trained to respond to various input stimuli.

The neural net presented in this chapter was trained with soils from the training dataset. The packing porosity of each soil was first adjusted to provide an optimal estimation. These adjusted packing porosities were then used in conjunction with the inputs of the USDA classification of % clay, % silt, % sand, % coarse, d_{10}, d_{20}, d_{30}, d_{50}, d_{60}, porosity, water content, dry density, and specific gravity. The neural net was then trained (Goh, 1999) and yielded R^2 equal to 0.830 for the training set. The neural net was then used to estimate packing porosities for the testing dataset.

It is often desireable to know the effect of packing porosity on an estimation. Unfortunately, the packing porosity does not always influence the estimation in the same manner. The effect of the packing porosity is illustrated in Figure 4-23 and Figure 4-24 for a sand and a silty loam.

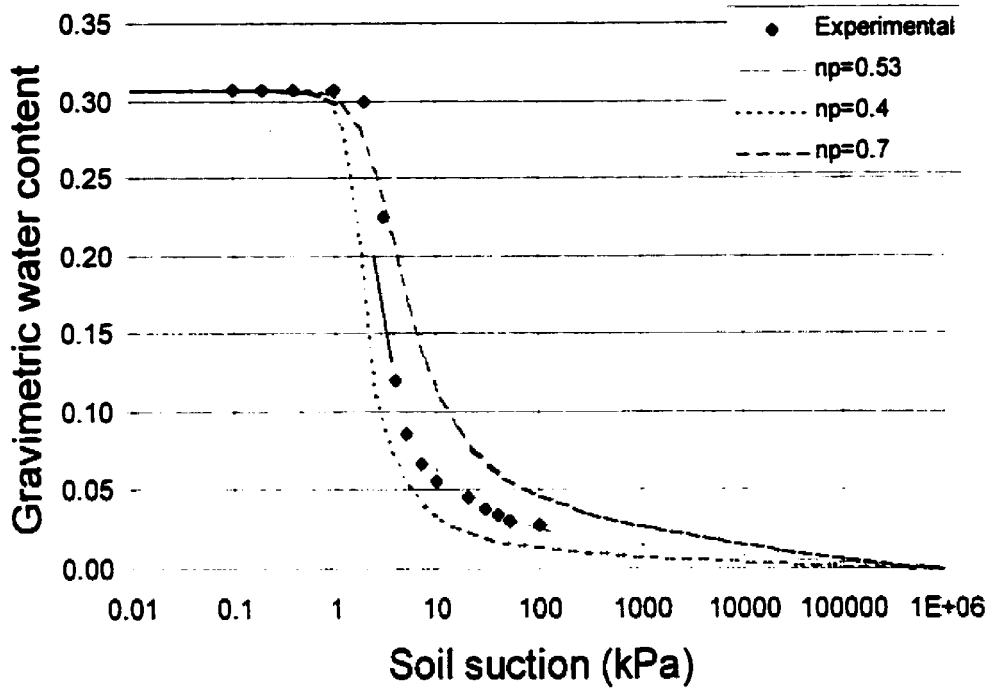

Figure 4-23 Effect of varying packing porosity, n_p, for a Sand originally published by Mualem, 1984 (112)

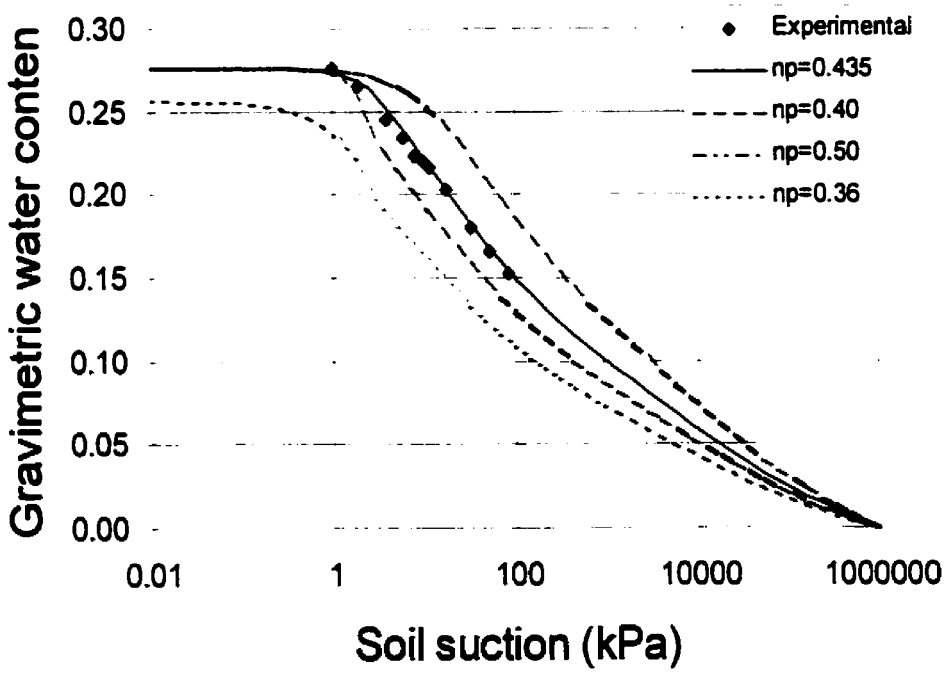

Figure 4-24 Illustration of the effect of varying packing porosity, n_p, for a Loam originally published by Schuh et al., 1991 (11194)

It should be noted that the resulting estimation does not reach 100% saturation as shown in Figure 4-24 with n_p equal to 0.36. This condition will occur if the packing porosity falls too far below the actual porosity of a soil.

4.9.5 Waste Rock

The packing porosity neural net was trained on a dataset that did not contain specialty soils such as waste rock. There has been an increased interest in modeling the seepage properties of waste rock due to the design of covers (Wilson, 1999). It has been shown that the packing porosity, n_p, can be adjusted to yield a good estimate of the soil-water characteristic curve of waste rock (Swanson, 1998). It has generally been found that the packing porosity must be adjusted higher when estimating soil-water properties of waste rock. An analysis of waste rock soils indicated that, on average, the packing porosity must be increased by an average of 27.9% when dealing with waste rock. This analysis was based on five soils obtained from a mine site in Montana, United States. The results of one adjustment of the estimation can be seen in Figure 4-25.

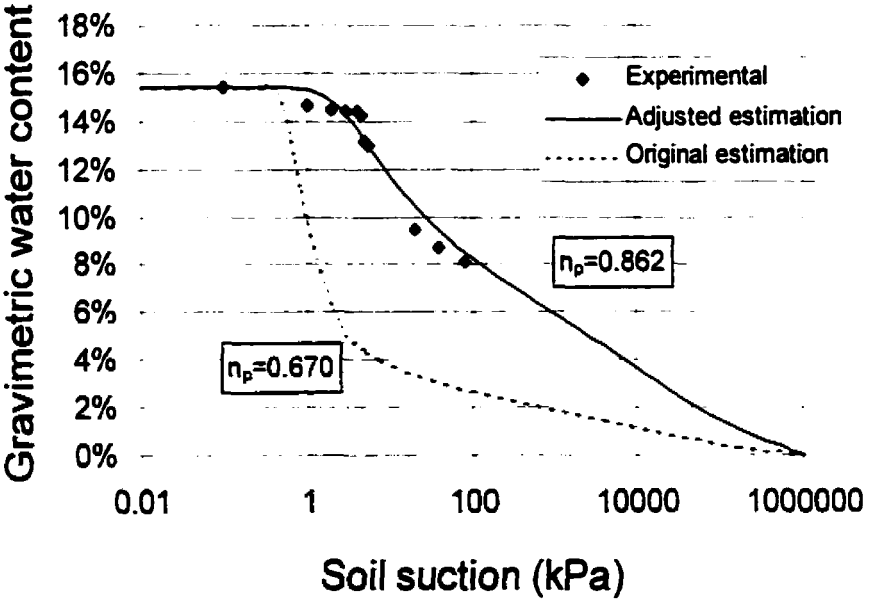

Figure 4-25 Example of adjustment of the proposed new pedo-transfer function for the estimation of the soil-water characteristic curve of a waste rock originally published by Herasymuik, 1996 (11552)

4.9.6 Adjustment of the Pedo-Transfer Function According to Stress History

It has been shown in research literature that the soil-water characteristic curve of a soil is dependent upon the stress history of a soil. For example, if two samples are taken from the same soil and one sample is compacted wet of optimum to a specified density, ρ_t, and the other sample is compacted dry of optimum to the same density, ρ_t, the resulting soil-water characteristic curves will be different. Vanapalli (1994) showed experimentally the changes to the soil compacted both dry of optimum and wet of optimum as well as at optimum. It has also been shown experimentally that the soil-water characteristic curve of a soil will change when the overburden pressure on the soil is changed. The purpose of this section is to illustrate how the pedo-transfer function presented in this chapter might be modified to account for various stress histories.

The soils used for the calibration of the pedo-transfer function represent soils with a minimal effects of stress history. The pedo-transfer function is also calibrated for the estimation of drying, rather than wetting, soil-water characteristic curves. A method of adjusting the proposed new pedo-transfer function to account for stress history changes will be presented in the following sections.

The *compaction* of a soil results in the rearrangement of the structure of clay particles. It is this rearrangement of the structure of a soil that yields differences in the soil-water characteristic curve. It was considered to be outside the scope of this thesis to examine the effects of structure on the soil-water characteristic curve. A method of modifying the soil-water characteristic pedo-transfer function to account for the effects of structure was not studied in detail.

A study undertaken by Vanapalli (1994) allowed the effects of *compression* on the soil-water characteristic curve to be quantified. A method of implementing these findings into the pedo-transfer function is presented in the following sections. The correction to the pedo-transfer function is presented as a modification to the Fredlund and Xing (1994) fit of the soil-water characteristic curve. The correction must therefore be provided with a fit of the pedo-transfer function obtained using the Fredlund and Xing (1994) equation.

A correction is introduced to the soil-water characteristic curve allows the air entry value in the Fredlund and Xing (1994) equation to increase as compression increases. The effect of various compression levels on the air entry value has been examined by Vanapalli (1994) for a sandy clay till. Vanapalli (1994) summarized that the air entry value of a soil followed a line drawn through the steepest slope of the soil-water characteristic curve for soils compacted at optimum and dry of optimum. A straight line with a slightly different slope was followed for soils compacted wet of optimum. A modification to the Fredlund and Xing (1994) equation is therefore presented to account for changes in the air entry value as the level of compression increases. As a first approximation, the air entry value is assumed to increase linearly on a semilog plot at a rate corresponding to the steepest point of the soil-water characteristic curve.

Modification of the air entry value for the Fredlund and Xing (1994) equation is achieved by making the a_f parameter a function of net normal stress. The a_f parameter has been shown to be related to the air entry value therefore this technique is considered a reasonable assumption. First, a straight line is drawn through the steepest point on the soil-water characteristic curve. The line is then shifted such that the soil-water characteristic curve is unmodified when the net normal stress is at a minimum. The construction is shown in Figure 4-26. The final equation for the modified Fredlund and Xing (1994) equation is shown as Equation 4-14.

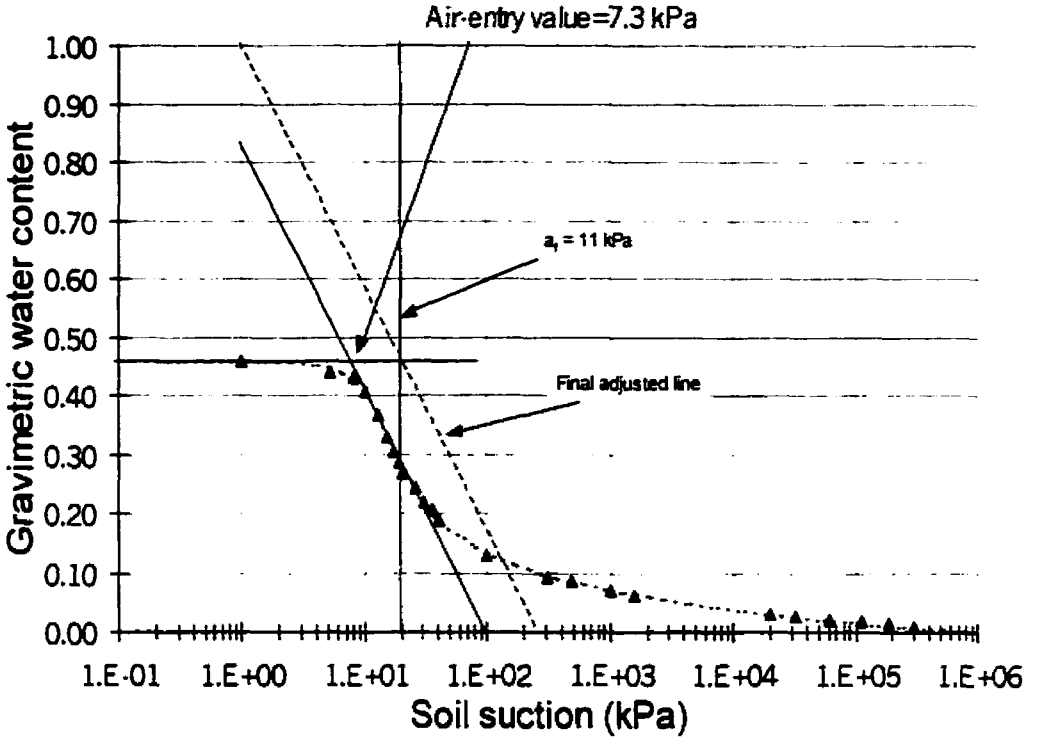

Figure 4-26 Calculation of modification for air-entry value for a Loam using the Fredlund and Xing (1994) equation, a_f=11.1, n_f=3.56, m_f=0.54, h_r=48.4 (91)

The straight line on a semilog plot can be represented by Equation 4-12.

$$w = m \log(a_f) - b$$

Equation 4-12

where: a_f = Fredlund and Xing (1994) parameter related to the air entry value of the soil,

w = initial water content of the soil specimen,

m = slope of the line on a semilog plot,

b = y-axis intercept at a value of 1.0.

Calculation of the a_f parameter requires that Equation 4-12 be solved in terms of a_f.

$$a_f = 10^{\frac{(b-w)}{m}}$$

Equation 4-13

Substituted Equation 4-13 into the Fredlund and Xing (1994) equation results in the following equation:

$$w_w(\psi) = w_s\left[1 - \frac{\ln\left(1+\frac{\psi}{h_r}\right)}{\ln\left(1+\frac{10^6}{h_r}\right)}\right]\left[\frac{1}{\left[\ln\left[\exp(1)+\left(\frac{\psi}{10^{\frac{(b-w_s)}{m}}}\right)^{n_f}\right]\right]^{m_f}}\right]$$

Equation 4-14

Equation 4-14 represents the soil-water characteristic curve in terms of soil suction and initial water content. The correction can be adjusted to account for various loading conditions by adjusting the slope, *m*. The result of the correction when applied to various compression levels can be seen in Figure 4-27.

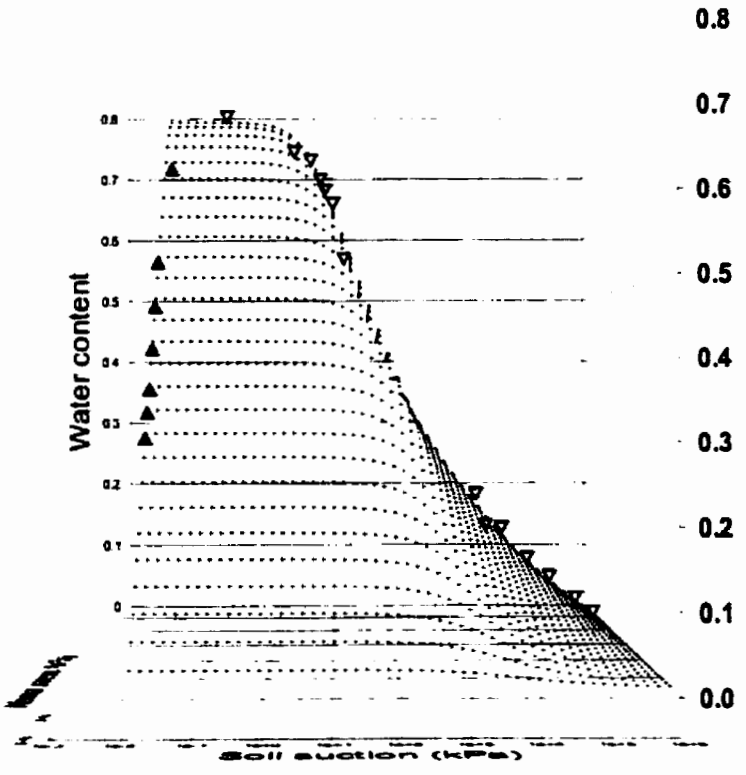

Figure 4-27 Adjustment of the soil-water characteristic curve according to stress history for a oligocenic clay originally published by Nascimento, 1961 (12436)

4.10 Comparison of Results to Other Pedo-Transfer Functions

Numerous studies on the estimation of the soil-water characteristic curve have been presented in research. A comparison of the proposed new estimation technique to existing models is necessary to verify the advantages of the new model. The following new estimation models were selected for comparison.

Arya and Paris (1981)
Scheinost (1996)
Rawls et al. (1985)
Vereecken et al. (1989)
Tyler and Wheatcraft (1989)

The aforementioned pedo-transfer functions were selected based on either the frequency of references to the method or the success of the method (Tietje et al. 1993). It was the intent of the author to compare the new proposed pedo-transfer function to currently published pedo-transfer functions that showed the greatest potential level of success in estimating the soil-water characteristic curve.

The pedo-transfer functions were evaluated based on the set of data used to test the new proposed method. A set of data was selected which contained a wide range of textural classifications. The dataset was also selected to ensure that enough data was present for each soil to allow all pedo-transfer functions to produce an estimation.

4.10.1 Arya and Paris (1981)

The Arya and Paris (1981) pedo-transfer function was the first method to use the physio-empirical method to estimate the soil-water characteristic curve. It was developed for a small database and the extrapolation to a larger databases is generally possible with a reasonable

decrease in accuracy. A value of α equal to 1.38 is generally accepted as a reasonable estimate. Later investigation by Arya et al. (1982) showed that the average α varied among textural classes and ranged in value from 1.1 for finer textures to 2.5 for coarse-textured soils. The α value was estimated from Table 4-2 where possible for the analysis presented in this chapter. The method requires a reasonably defined grain-size distribution. Estimations performed with the Arya and Paris (1981) pedo-transfer function as shown in Figure 4-28, Figure 4-29, Figure 4-30, and Figure 4-31. Arya et al. (1999) presented a method of estimating α based on the number of spherical particles and the pore length. The estimation of α presented by Arya et al. (1999) is not included in this analysis.

Table 4-2 Values of alpha, α, proposed by Arya et al. (1982)

USDA Texture	Alpha
Sand	1.285
Sandy Loam	1.459
Loam	1.375
Silt Loam	1.15
Clay	1.16

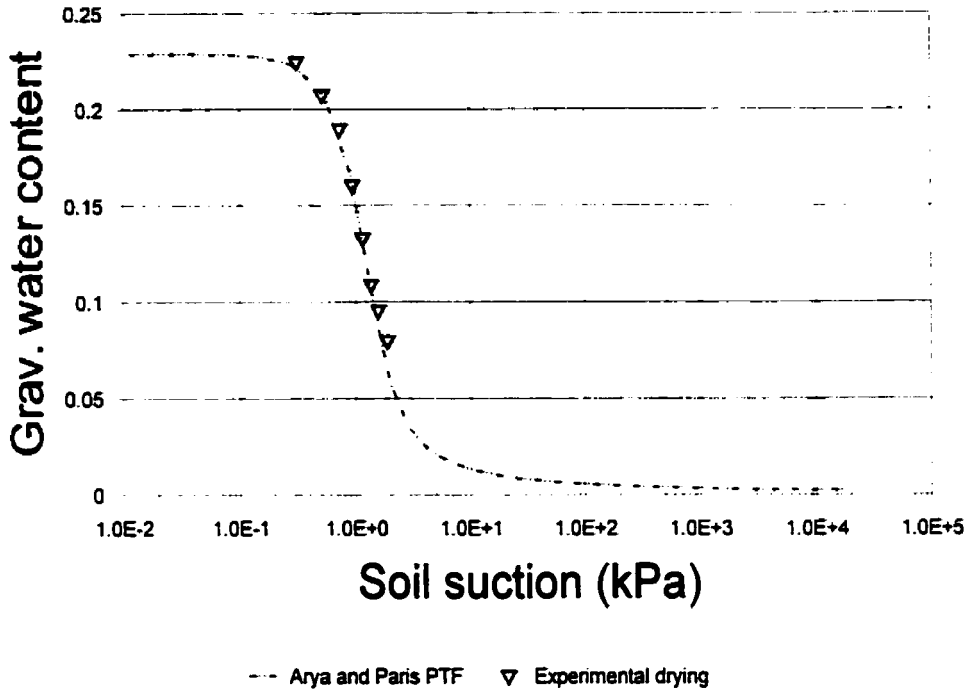

Figure 4-28 Estimation of the soil-water characteristic curve for a Virginia Mixed Sand by the Arya and Paris (1980) pedo-transfer function, R^2=0.981 (10921)

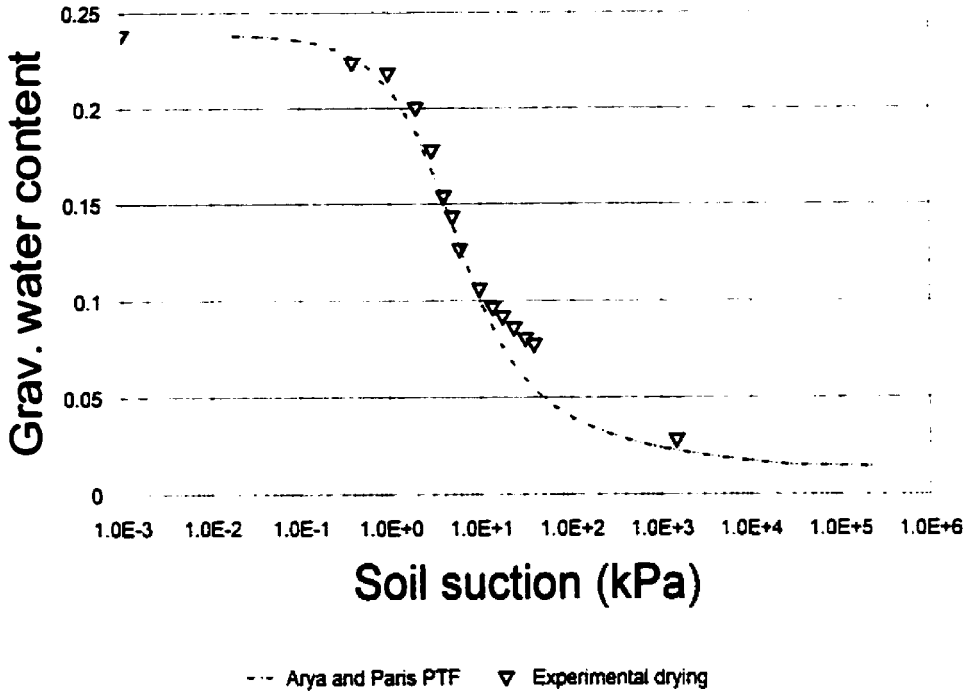

Figure 4-29 Estimation of the soil-water characteristic curve for a Sandy Loam by the Arya and Paris (1980) pedo-transfer function, R^2=0.960 (10741)

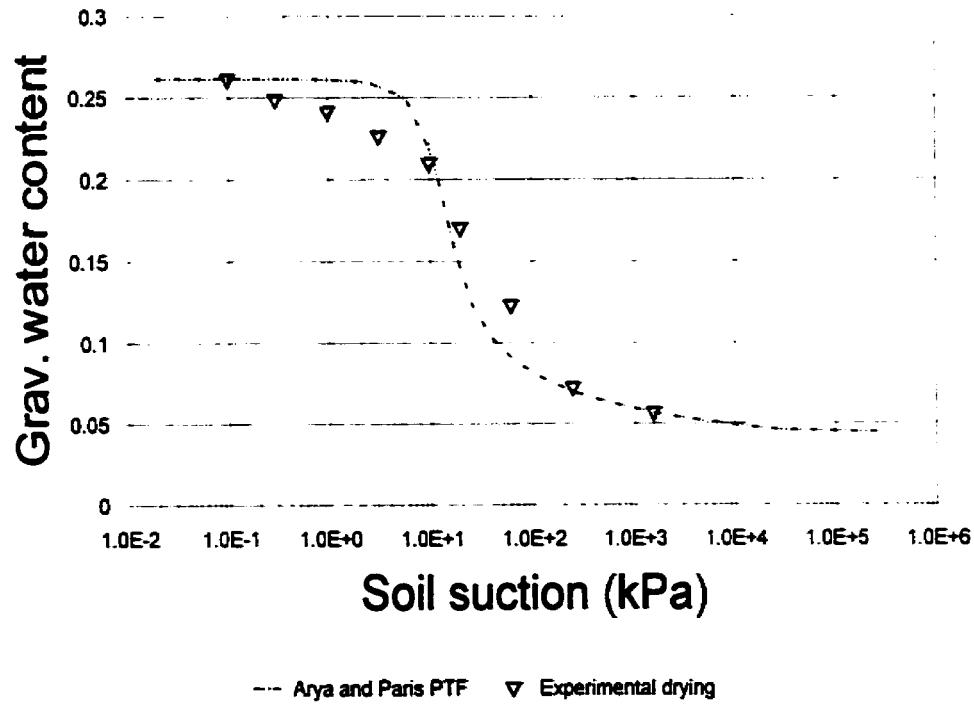

Figure 4-30 Estimation of the soil-water characteristic curve for a Sandy Clay Loam by the Arya and Paris (1980) pedo-transfer function, R^2=0.934 (11322)

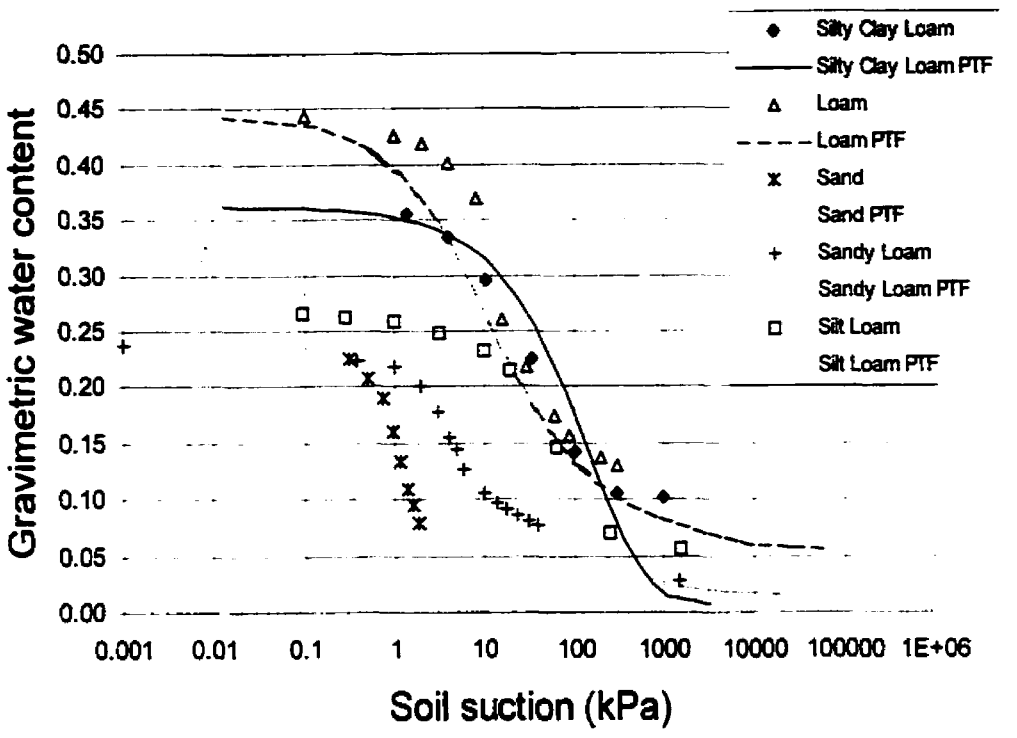

Figure 4-31 Best estimation for each of five textures of the soil-water characteristic curve using the Arya and Paris (1981) pedo-transfer function. Silty Clay Loam R^2=0.85; Loam R^2=0.87; Sand R^2=0.98; Sandy Loam R^2=0.96; Silt Loam R^2=0.91.

4.10.2 Scheinost (1996)

The Scheinost (1996) pedo-transfer function used linear regression to estimate the parameters of a van Genuchten-type equation. It was developed to account for extreme variation between soil parameters; texture varying between gravel and clay, organic content up to 81 g/kg, and bulk density from 0.80 to 1.85 mg/m^3. The pedo-transfer function was trained on a soils dataset located near Munich, Germany.

The Scheinost (1996) pedo-transfer function was able to estimate the desaturation rate of most soils with reasonable accuracy. Five estimations performed using the Scheinost (1996) method are shown in Figure 4-32.

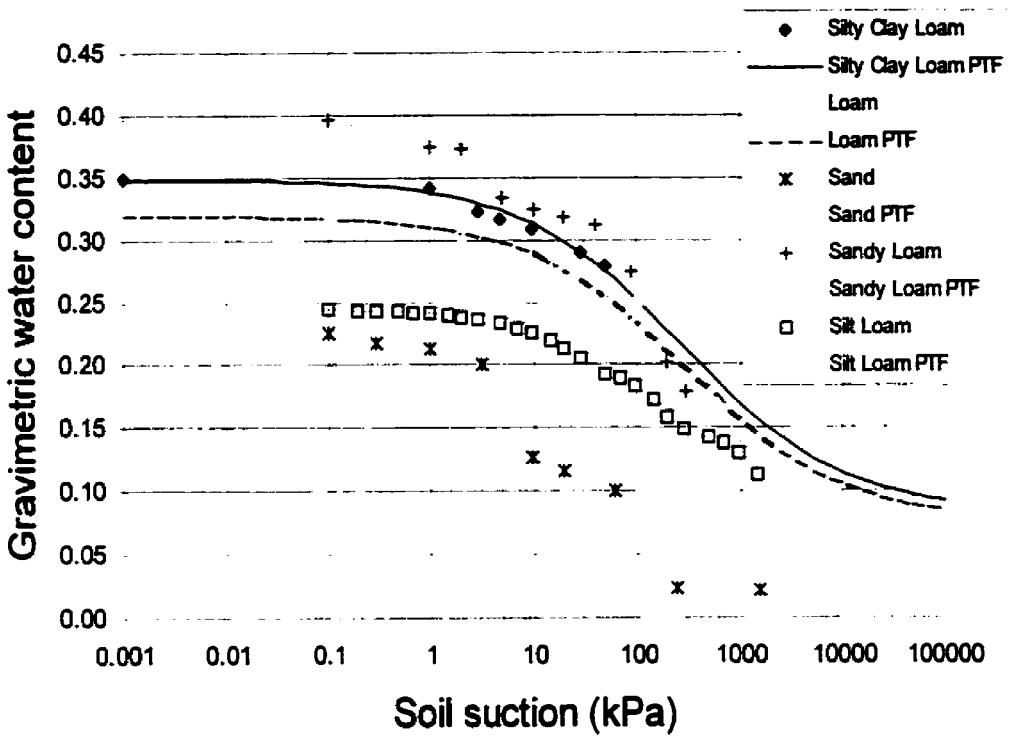

Figure 4-32 Best estimation for each of five textures of the soil-water characteristic curve using the Scheinost (1996) pedo-transfer function. Silty Clay Loam R^2=0.96; Loam R^2=0.76; Sand R^2=0.64; Sandy Loam R^2=0.95; Silt Loam R^2=0.91.

4.10.3 Rawls et al. (1985)

The Rawls et al. (1985) pedo-transfer function is based on a regression that estimates the parameters of the Brooks and Corey (1964) equation. While the estimation of the air-entry value, AEV, for most soils was quite reasonable, the desaturation rate was overestimated for most soils. This is most likely due to the sharp initial slope inherent in the Brooks and Corey (1964) equation. Results of various estimations can be seen in Figure 4-33.

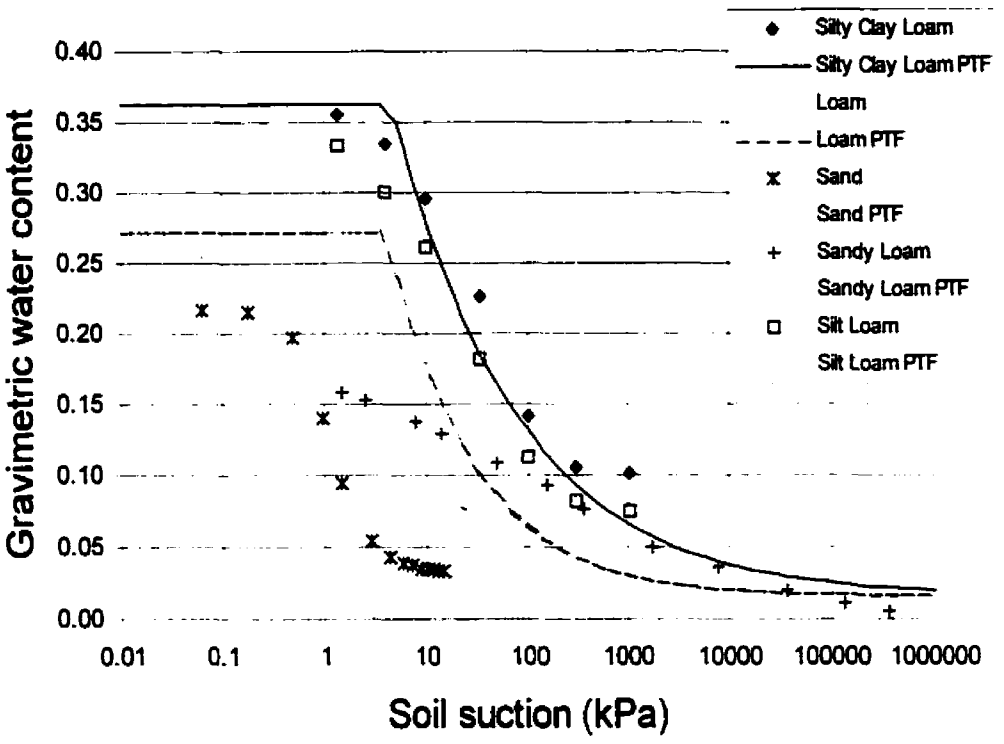

Figure 4-33 Best estimation for each of five textures of the soil-water characteristic curve using the Rawls and Brakensiek (1985) pedo-transfer function. Silty Clay Loam R^2=0.94; Loam R^2=0.58; Sand R^2=0.50; Sandy Loam R^2=-0.29; Silt Loam R^2=0.93.

4.10.4 Vereecken et al. (1989)

The Vereecken et al. (1989) pedo-transfer function uses statistical regression to estimate the parameters of the van Genuchten (1980) equation. The Vereecken et al. (1989) pedo-transfer function is considered to work for a wide range of soils due to its ability to account for high organic matter contents. In general, the method performed well for the estimation of desaturation rates. Examples of estimations performed with the Vereecken (1989) method can be seen in Figure 4-34.

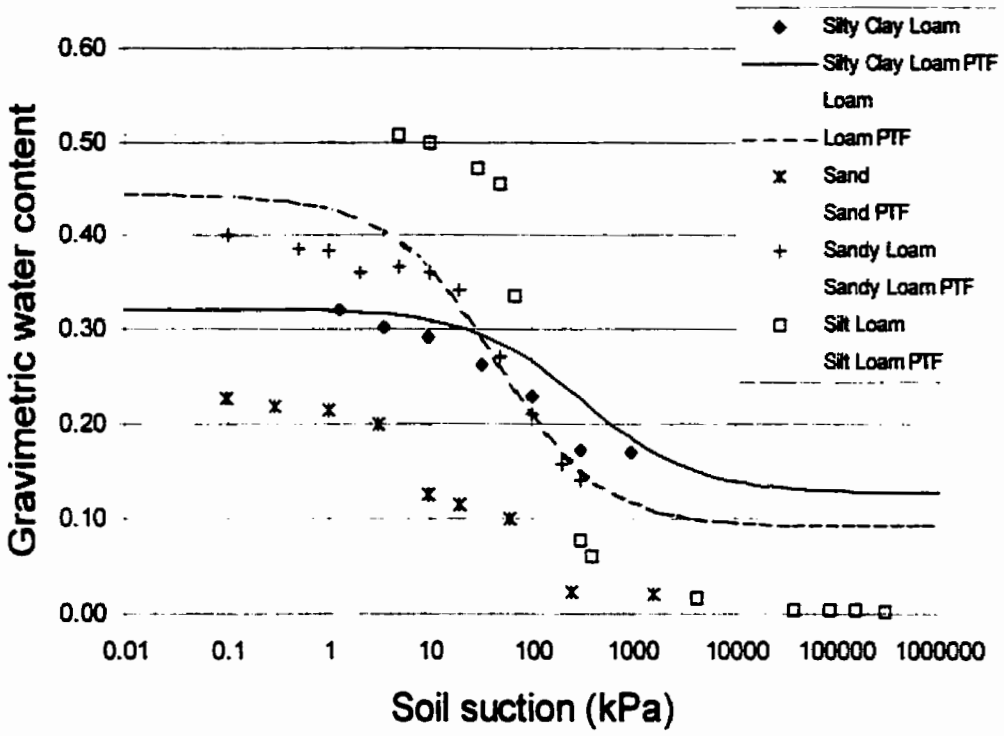

Figure 4-34 Best estimation for each of five textures of the soil-water characteristic curve using the Vereecken et al. (1989) pedo-transfer function. Silty Clay Loam R^2=0.74; Loam R^2=0.87; Sand R^2=0.73; Sandy Loam R^2=0.92; Silt Loam R^2=0.91.

4.10.5 Tyler and Wheatcraft (1989)

Tyler and Wheatcraft (1989) use a fractal dimension to estimate the Arya and Paris (1981) alpha, α, input parameter. The fractal dimension is calculated via linear regression over the number of particles in the grain-size fractions. It failed, however, to improve on the performance of the Arya and Paris (1981) estimation. Estimations performed with the Tyler and Wheatcraft (1989) estimation canbe seen in Figure 4-35, Figure 4-36, and Figure 4-37.

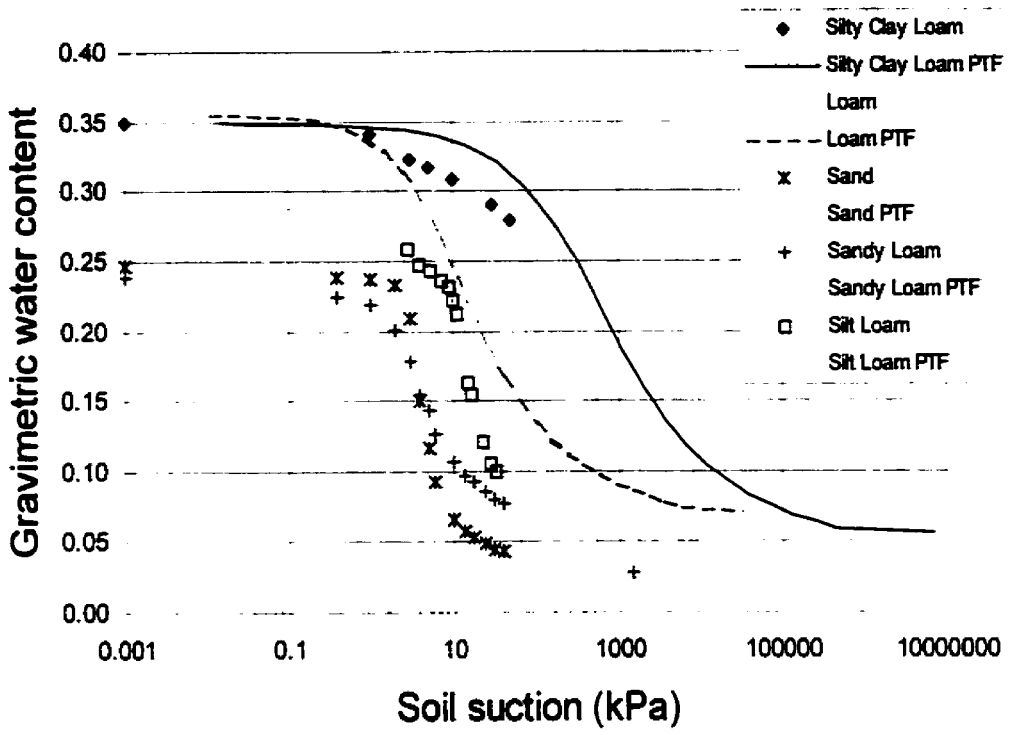

Figure 4-35 Best estimation for each of five textures of the soil-water characteristic curve using the Tyler and Wheatcraft (1989) pedo-transfer function. Silty Clay Loam R^2=-0.01; Loam R^2=0.89; Sand R^2=0.86; Sandy Loam R^2=-0.98; Silt Loam R^2=0.77.

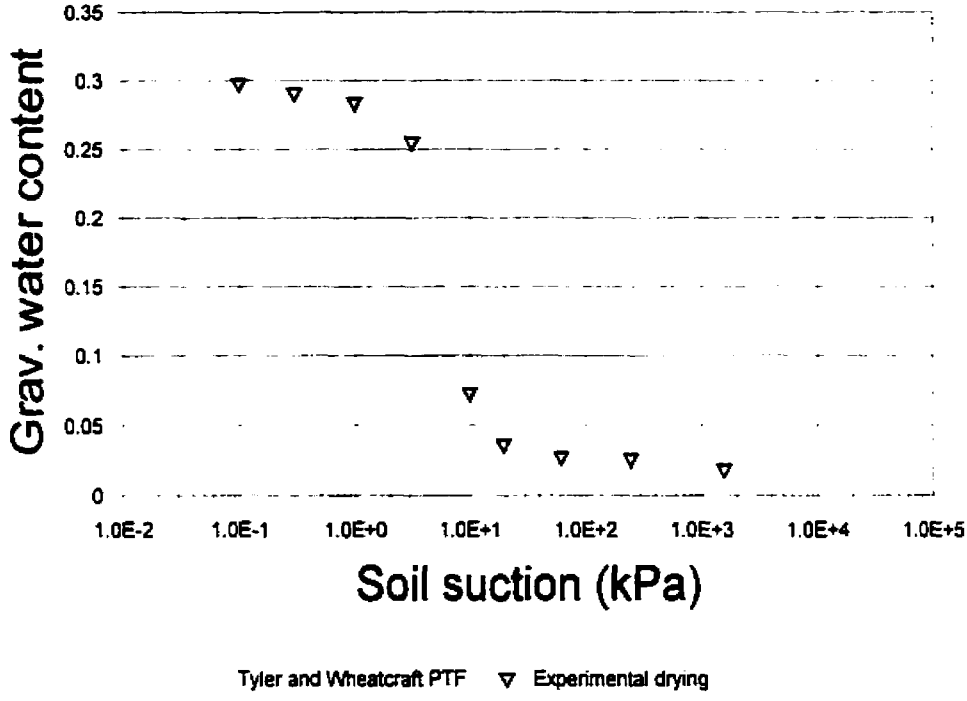

Figure 4-36 Estimation of the soil-water characteristic curve for a Loamy Sand by the Tyler and Wheatcraft (1989) pedo-transfer function, R^2=0.981 (11287)

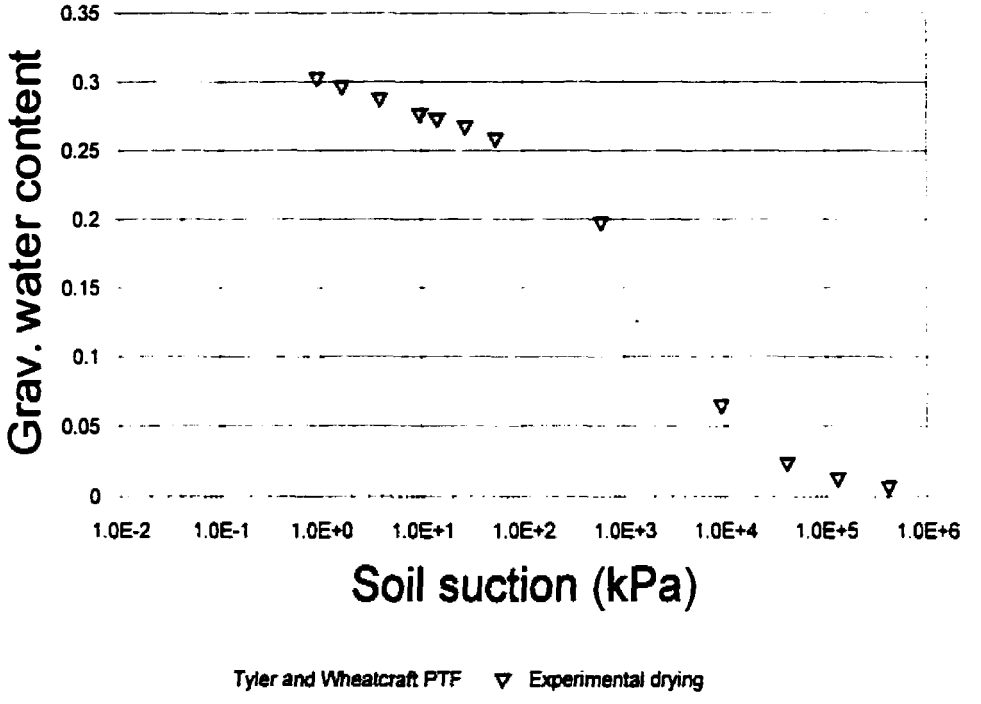

Figure 4-37 Estimation of the soil-water characteristic curve for a Clay Loam by the Tyler and Wheatcraft (1989) pedo-transfer function, R^2=0.962 (12425)

4.10.6 Methods of Evaluation

The six pedo-transfer functions were evaluated in the following way: (i) the R^2 values produced through the use of each pedo-transfer function are compared, (ii) the difference between measured and estimated air-entry values is compared, and (iii) the difference between measured and estimated maximum slopes is compared.

4.10.6.1 Comparison of R^2 results

Typical methods of comparison between experimental and estimated results include mean difference, MD, root mean squared difference, RMSD, sum-of-squares, or R^2. The R^2 method was used to compare the results of the six pedo-transfer functions presented in this chapter. The R^2 value gives an indication of the success of each pedo-transfer function in estimating water content. Mathematically, R^2 is calculated in the following way:

$$R^2 = 1.0 - \frac{SS_{ptf}}{SS_{tot}}$$

Equation 4-15

where: SS_{ptf} = the sum-of-squares of the experimental points from the pedo-transfer function, and

SS_{tot} = the sum-of-squares of the distances of the points from a horizontal line where Y equals the mean of all the data points.

Soils in the test dataset were selected where the R^2 value is between 0.0 and 1.0 with a value of 1.0 representing a perfect fit. A value of 0.0 indicates the fit is the same as a horizontal line through the average of the y-coordinates. The frequency distribution was then plotted to give an indication of the results of the pedo-transfer function. The results of the R^2 analysis will be presented in the following sections.

4.10.6.2 Comparison of Air-Entry Values

It is important in geotechnical engineering to know the soil suction at which a soil begins to rapidly desaturate. The six pedo-transfer functions were, therefore, evaluated based on their ability to correctly estimate the air-entry value (AEV) for a soil. The air entry value for the experimental data was calculated by first fitting the data with the Fredlund and Xing (1994) equation. A construction was then performed according to the procedure published by Vanapalli and Fredlund (1998) which allowed the air-entry value to be calculated based on the fit of the experimental data. The air-entry value for each pedo-transfer function was calculated by performing the construction on the estimated points. The air-entry value calculated from the fit of experimental data was then taken to be the correct value and compared to the estimated air-entry value using the following equation.

$$SD = \frac{1}{n}\sum_{i=1}^{n}\left[\log(AEV_{ptf}) - \log(AEV_e)\right]^2$$

Equation 4-16

where: AEV_{ptf} = air-entry value of pedo-transfer function,

AEV_e = air-entry value of experimental data,

n = number of data points,

SD = average squared difference.

4.10.6.3 Comparison of Maximum Slope

The rate at which a soil desaturates is also important in the engineering practice. The six pedo-transfer functions were, therefore, evaluated on their success at estimating the rate at which a soil desaturates. A complication arises because the rate at which a soil desaturates is not commonly constant. The best representation of rate was, therefore, taken as the maximum slope of the soil-water characteristic curve. For experimental data, this maximum slope was calculated by fitting experimental data with the Fredlund and Xing (1994) equation, and then determining the point of maximum slope from the fit curve.

The maximum slope is a unitless measure and is calculated as a change in the ordinate, Δy, on the normalized soil-water characteristic curve divided by the change in the log of soil suction or $\log(\psi_f/\psi_i)$. Each pedo-transfer function was evaluated by calculating a maximum slope from the estimated points on the soil-water characteristic curve. The squared difference between experimental and estimated results was then calculated according to the following equation:

$$SD = \frac{1}{n}\sum_{i=1}^{n}\left[MS_{ptf} - MS_{e}\right]^{2}$$

Equation 4-17

where: MS_{ptf} = maximum slope of pedo-transfer function,

MS_e = maximum slope of experimental data,

n = number of data points,

SD = average squared difference.

4.10.7 Results and Discussion of the Fit Between Prediction and Experimental Data

The results of the statistical analysis showed that the proposed new pedo-transfer function performed well. Comparison of the proposed new pedo-transfer function to previously proposed pedo-transfer functions indicates significantly improved performance in most areas.

Each pedo-transfer function was evaluated based on the R^2 value, the air-entry value (AEV), and the maximum slope. A summary of the distributions of R^2 can be seen in Figure 4-45. The proposed new pedo-transfer function showed an improved accuracy in the error distribution.

The proposed new pedo-transfer function showed reasonable accuracy when compared to the maximum slope of experimental data. The purpose of this comparison was to obtain an indication of the accuracy of the maximum desaturation rate for the six pedo-transfer functions. Representation of the comparison between estimated and measured results can be seen in Figure 4-38. Table 4-3 indicates reasonable performance by the proposed new pedo-transfer function. The best performance was obtained using the Vereecken (1989) method. The performance of the Rawls (1985) method indicates some uncertainty as to whether the method was properly implemented in the calculations for this chapter.

Results of the comparisons between the measured and estimated air-entry values, AEV, indicated significant improvements of the new pedo-transfer function over existing methods. A plot of the comparison between air-entry values can be seen in Figure 4-39 to Figure 4-44. The average of the logarithm of squared differences between experimental and measured results for the test dataset is shown in Table 4-4. The new pedo-transfer function and the Arya and Paris (1981) methods showed the highest level of confidence in correctly estimating the air-entry value of a soil.

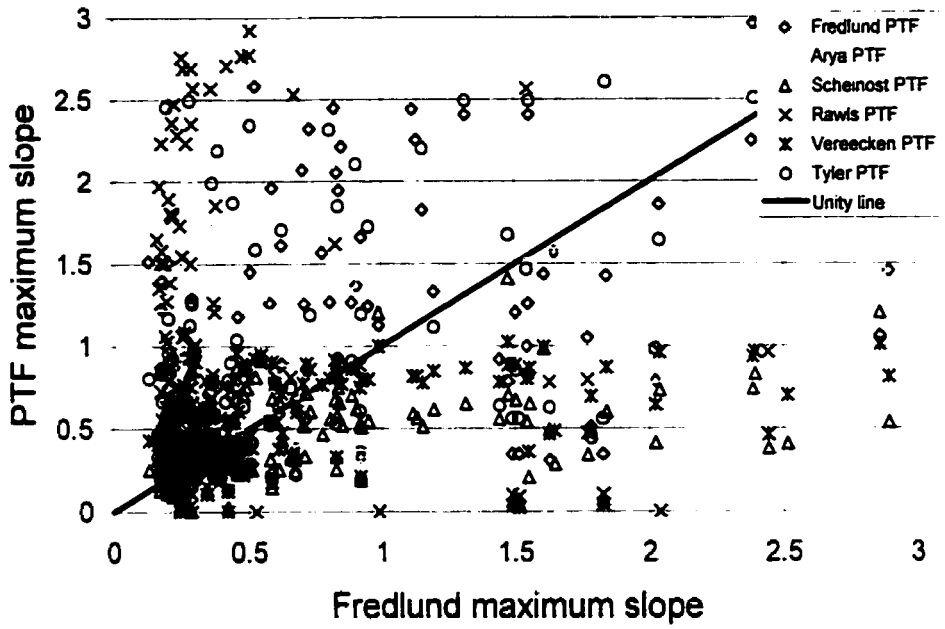

Figure 4-38 Difference between measured and estimated maximum slope of all six pedo-transfer functions

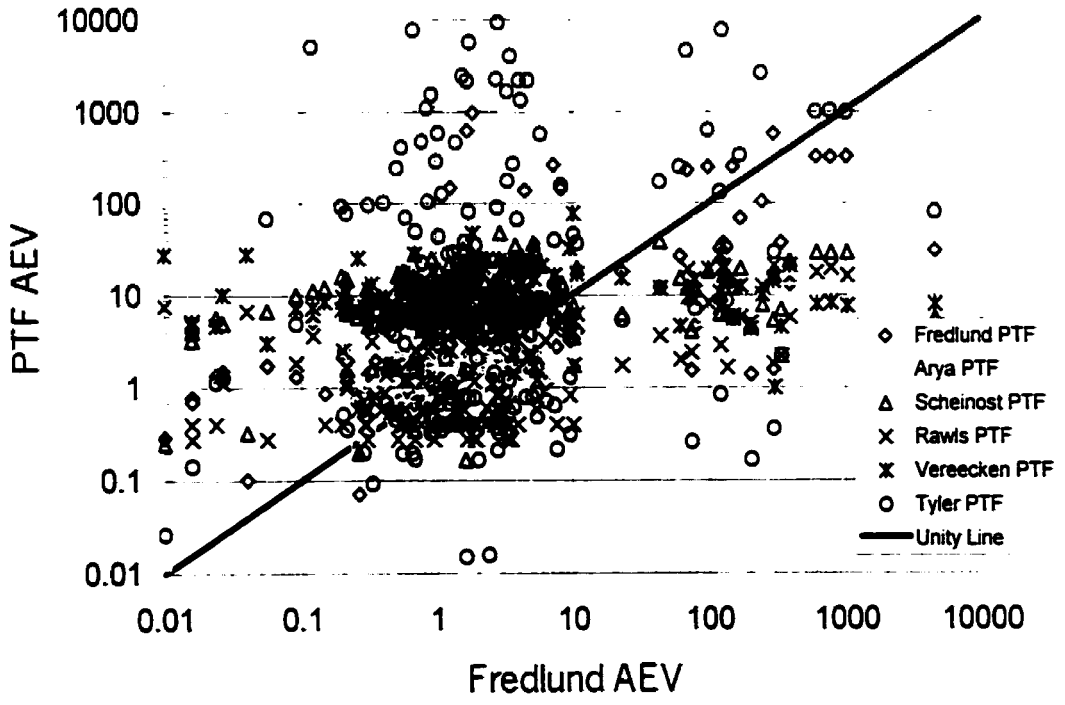

Figure 4-39 Difference between measured and estimated air-entry value (AEV) for all six pedo-transfer functions

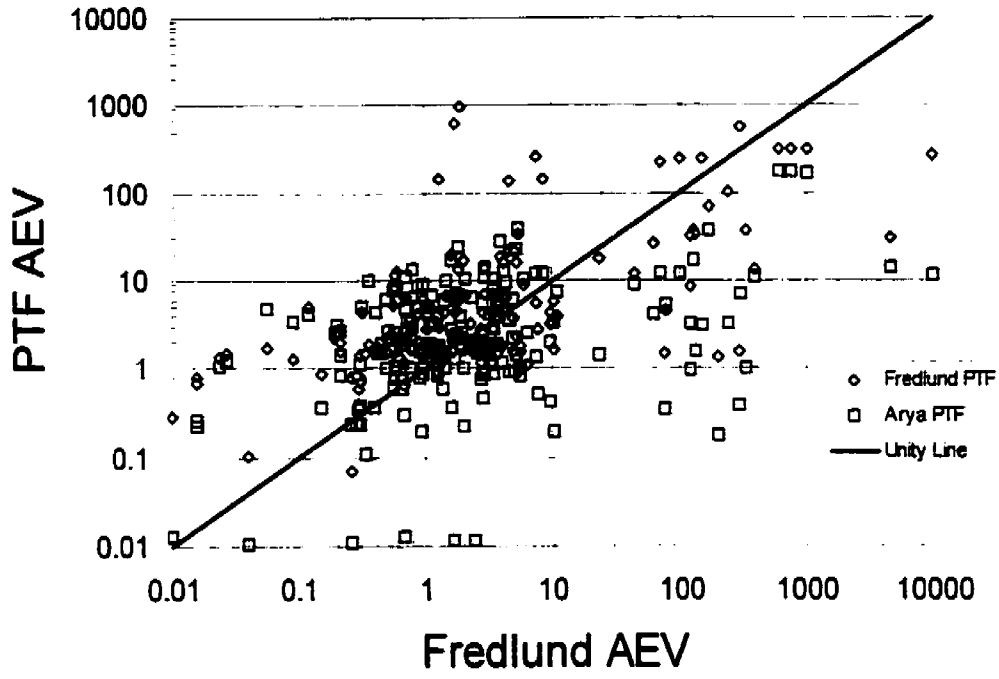

Figure 4-40 Difference between measured and estimated air-entry value (AEV) for the Fredlund and Arya pedo-transfer functions

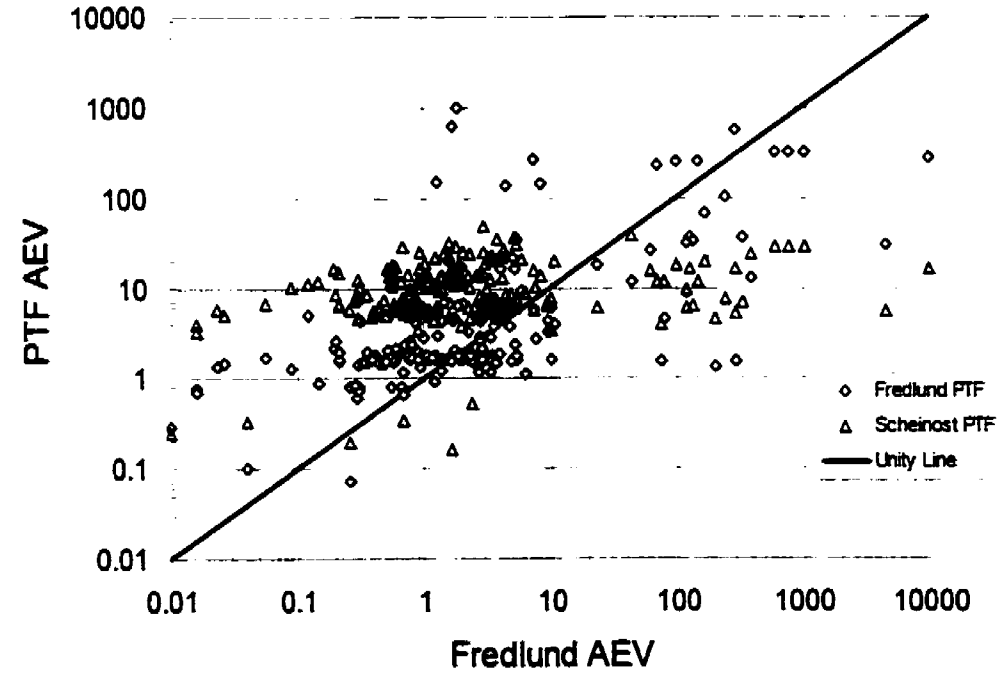

Figure 4-41 Difference between measured and estimated air-entry value (AEV) for the Fredlund and Scheinost pedo-transfer functions

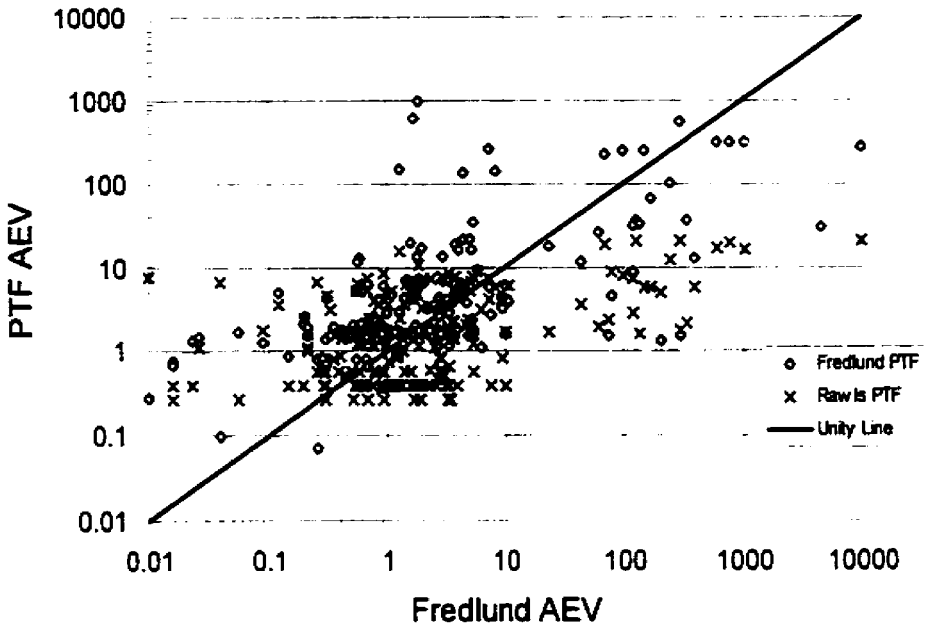

Figure 4-42 Difference between measured and estimated air-entry value (AEV) for the Fredlund and Rawls pedo-transfer functions

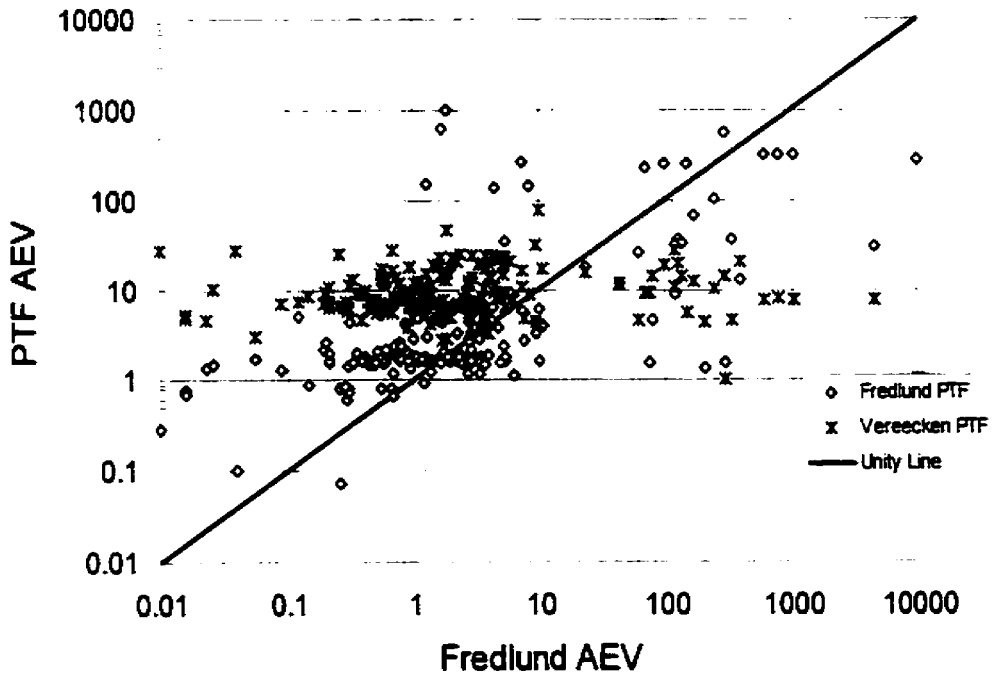

Figure 4-43 Difference between measured and estimated air-entry value (AEV) for the Fredlund and Vereecken pedo-transfer functions

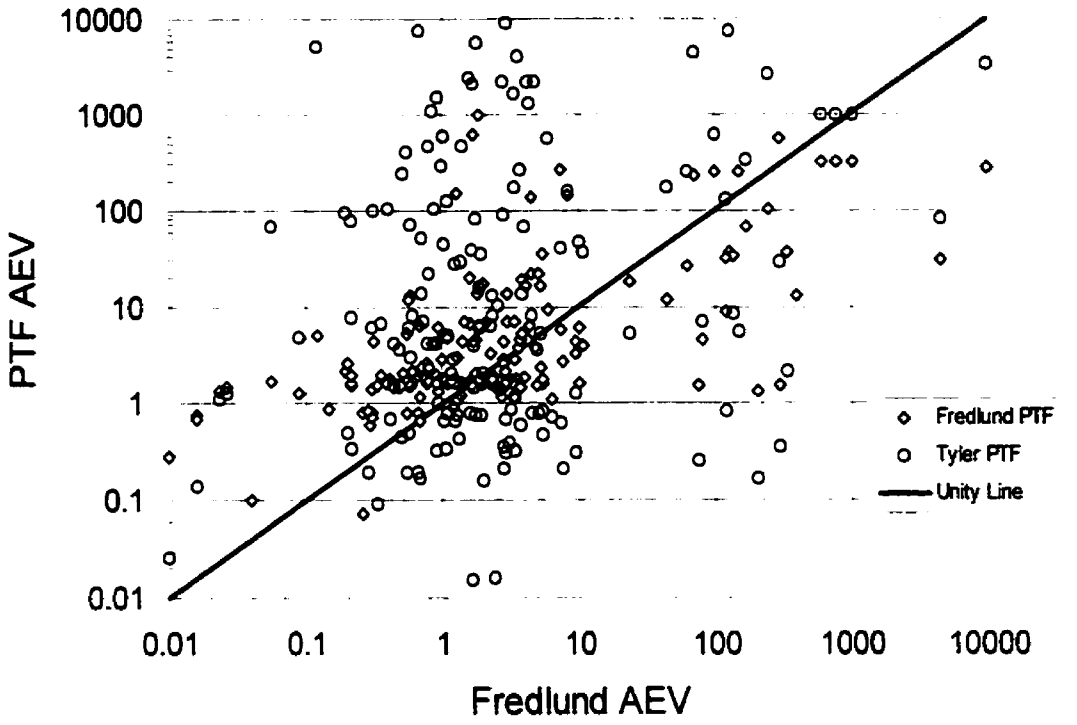

Figure 4-44 Difference between measured and estimated air-entry value (AEV) for the Fredlund and Tyler pedo-transfer functions

Table 4-3 Squared difference between estimated and measured maximum slopes for all six pedo-transfer functions

Pedo-Transfer Function	Squared Difference
Fredlund PTF Max Slope	0.487
Arya Max Slope	0.586
Scheinost Max Slope	0.476
Rawls Max Slope	7.850
Vereecken Max Slope	0.462
Tyler Max Slope	0.988

Table 4-4 Squared log difference between estimated and measured air-entry values for all six pedo-transfer functions

Pedo-Transfer Function	Squared Difference
Fredlund PTF AEV	0.585
Arya AEV	0.862
Scheinost AEV	1.1911
Rawls AEV	0.787
Vereecken AEV	1.3281
Tyler AEV	3.438

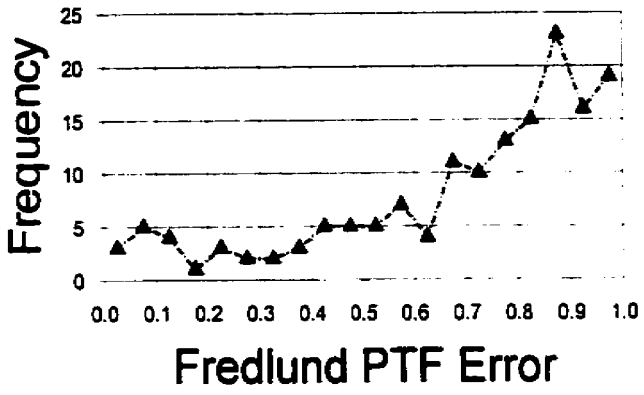
Frequency
25
20
15
10
5
0
0.0 0.1 0.2 0.3 0.4 0.5 0.6 0.7 0.8 0.9 1.0
Fredlund PTF Error

(a)

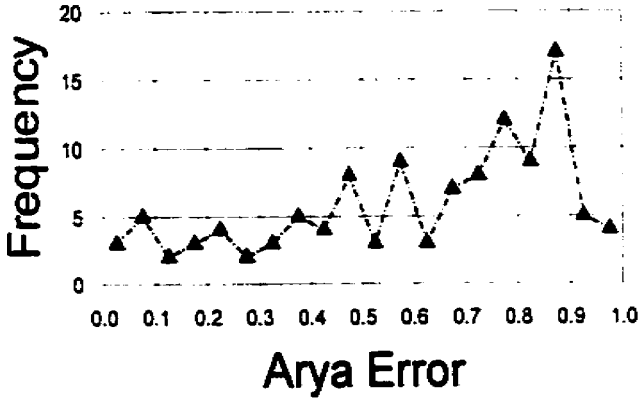
Frequency
20
15
10
5
0
0.0 0.1 0.2 0.3 0.4 0.5 0.6 0.7 0.8 0.9 1.0
Arya Error

(b)

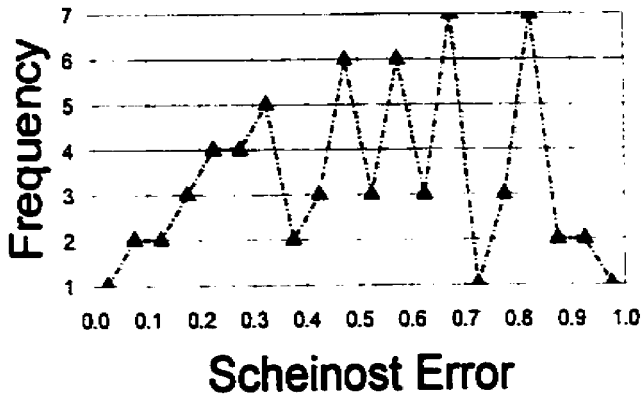
Frequency
7
6
5
4
3
2
1
0.0 0.1 0.2 0.3 0.4 0.5 0.6 0.7 0.8 0.9 1.0
Scheinost Error

(c)

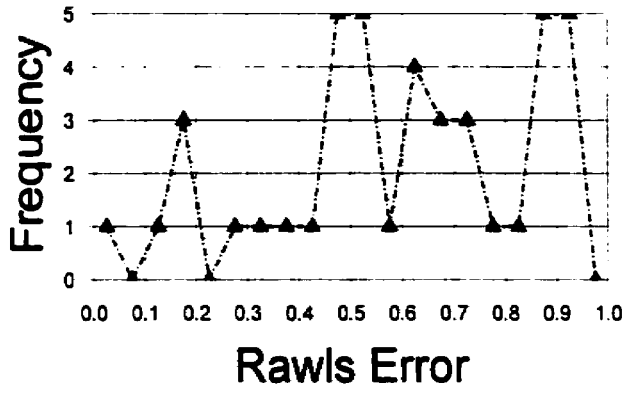
Frequency
0
1
2
3
4
5
0.0 0.1 0.2 0.3 0.4 0.5 0.6 0.7 0.8 0.9 1.0
Rawls Error

(d)

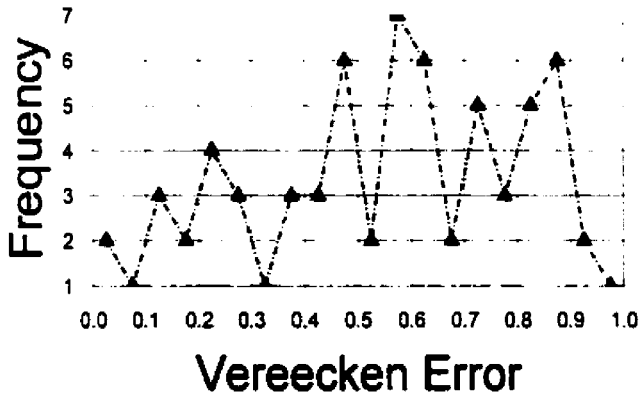
Frequency
1
2
3
4
5
6
7
0.0 0.1 0.2 0.3 0.4 0.5 0.6 0.7 0.8 0.9 1.0
Vereecken Error

(e)

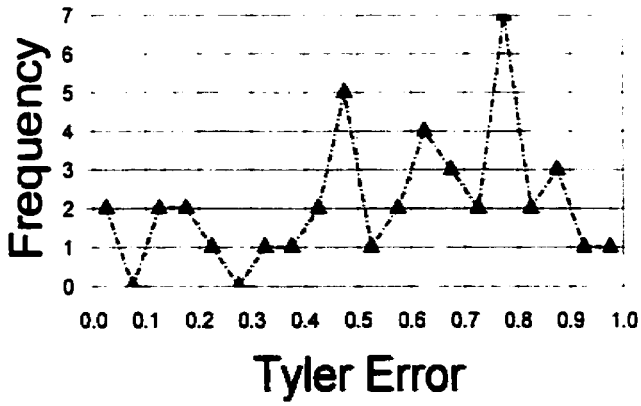
Frequency
0
1
2
3
4
5
6
7
0.0 0.1 0.2 0.3 0.4 0.5 0.6 0.7 0.8 0.9 1.0
Tyler Error

(f)

Figure 4-45 Comparison of frequency distribution of R^2 for values between 0.0 and 1.0 for all six pedo-transfer functions

4.11 Conclusions

The minimum particle size was found to have direct influence upon the success of the soil-water characteristic curve estimation. If the minimum particle size variable was set too low, there would be an overabundance of clay size particle that would dominate the estimation. If the minimum particle size was set too high, this would cause an absence of smaller particles to result in the soil drying out prematurely.

The estimation of soil-water characteristic curve from grain-size distribution was found to be accurate for sands, and reasonably accurate for silts. Clays, tills and loams were more difficult to predict although the accuracy of the estimation algorithm was still reasonable. Results tended to be sensitive to the packing porosity, n_p, and more research will be needed to fully analyze this value.

The proposed new pedo-transfer function was also compared to five other pedo-transfer functions. The success of each pedo-transfer function was evaluated based on R^2, air-entry value, and maximum slope. The proposed new pedo-transfer function showed an improved accuracy in the R^2 error distribution.

The proposed new pedo-transfer function showed reasonable accuracy when compared to the maximum slope of experimental data. The best performance was obtained using the Vereecken (1989) method. The performance of the Rawls (1985) method indicates some uncertainty as to whether the method was properly implemented in the calculations for this chapter.

Results of the comparisons between the measured and estimated air-entry values, AEV, indicated significant improvements of the new pedo-transfer function over existing methods. The new pedo-transfer function and the Arya and Paris (1981) methods showed the highest level of confidence in correctly estimating the air-entry value of a soil.

4.12 References

Aberg, B., 1996, Void sizes in granular soils, Journal of Geotechnical Engineering, Vol. 122, No. 3, pp. 236-239

Ahuja, L.R., Naney, J.W., and Williams, R.D., 1985, Estimating soil-water characteristics from simpler properties or limited data, Soil Sci. Soc. Am. Journal., Vol. 49, pp. 1100-1105.

Arya L.M., Richter J.C., and Davidson S.A., 1982, A comparison of soil moisture characteristic predicted by the Arya-Paris model with laboratory-measured data, AgRISTARS Tech. Rep. SM-L1-04247, JSC-17820, NASA-Johnson Space Center, Houston, TX.

Arya Lalit M., Leij Feike J., van Genuchten Martinus Th., Shouse Peter J., 1999, Scaling Parameter to Predict the Soil Water Characteristic from Particle-Size Distribution Data, Soil Science Society of America Journal, Vol. 63, pp. 510-519

Arya, L.M., and Paris J.F., 1981, A physicoempirical model to predict the soil moisture characteristic from particle-size distribution and bulk density data, Soil Science Society of America Journal, Vol. 45, pp. 1023-1030.

Bouma, J., 1989, Using soil survey data for quantitative land evaluation, Adv. Soil Sci., Vol. 9, pp. 177-213

Brooks R.H. and A.T. Corey,, 1964, Hydraulic Properties of Porous Media, Colorado State Univ. Hydrol. Paper, No. 3,, 27, pp. March 1964.

Cosby, B.J., Hornberger, G.M., Clapp, R.B., and Ginn, T.R., 1984, A statistical exploration of the relationship of soil moisture characteristics to the physical properties of soils, Water Resour. Res., Vol. 20, pp. 682-690

Dane, J.H. and Hruska, S., 1983, In-situ determination of soil hydraulic properties during drainage., Soil Science Society of America,, Vol. 47, No. 4,

Fredlund, D.G., and Xing, A., 1994, Equations for the soil-water characteristic curve, Canadian Geotechnical Journal, Vol. 31, No. 3, pp. 521-532.

Fredlund, M.D., D.G. Fredlund, and G.W. Wilson, 1997, Prediction of the Soil-Water Characteristic Curve from Grain-Size Distribution and Volume-Mass Properties, 3rd Brazilian Symposium on Unsaturated Soils, Rio de Janeiro, April 22-25

Fredlund, M.D., Sillers, W.S., Fredlund, D.G., Wilson, G.W., 1996, Design of a knowledge-based system for unsaturated soil properties, Third Canadian Conference on Computing in Civil and Building Engineering, pp. 659-677

Ghosh, R.K., 1980, Estimation of soil-moisture characteristics from mechanical properties of soils, Soil Science Journal, Vol. 130, No. 2, pp. 60-63

Gupta, S.C., and Larson, W.E., 1979, Estimating soil-water retention characteristics from particle size distribution, organic matter percent, and bulk density, Water Resources Research Journal, Vol. 15, No. 6, pp. 1633-1635

Harr, M.E., 1977, Mechanics of particulate media, McGraw - Hill International Book Company, New York, 27-33

Haverkamp, R., and Parlange, J.Y., 1986, Predicting the water-retention curve from particle-size distribution: 1. Sandy soils without organic matter, Soil Sci., Vol. 142, pp. 325-339

Hjorth, J.S.U., 1994, Computer intensive statistical method, validation, model selection and bootstrap, Chapman and Hall, London

Husz, G., 1967, The determination of pF-curves from texture using multiple regressions., Z. Pflanzenernahr. Dung. Bodenkd., Vol. 116((2), pp. 23-29

Nicolaeva, S.A., Pachepsky, Y.A., Shcherbakov, R.A., and Shcheglov, A.I., 1986, Modelling of moisture regime for ordinary Chernozems, Pochvovedenie, Vol. 6, pp. 52-59

Nimmo, John R., 1997, Modeling structural influences on soil water retention, Soil Science Society of America Journal, 61, 712-719

Pachepsky, Y., Shcherbakov, R.A., Varallyay, G., Rajkai, K., 1982, Statistical analysis of water retention relations with other physical properties of soils, Pochvovedenie, Vol. 2, pp. 42-52

Puckett, W. E.; Dane, J. H.; Hajek, B. F., 1985, Physical and Minerological Data to Determine Soil Hydraulic Properties, Soil Science Society of America Journal, 49, 831-836

Rawls W.J. and D.L. Brakensiek, 1985, Prediction of soil water properties for hydrologic modelling, In E.B. Jones and T.J. Ward (Eds.). Watershed Management in the Eighties., Proc. of Symp. sponsored by Comm. on Watershed Management, I & D Division, ASCE, ASCE Convention, Denver, CO, April 30-May 1, pp. 293-299

Rawls W.J. D.L. Brakensiek, 1989, Estimation of Soil Water Retention and Hydraulic Properties, H.J. Morel-Seytoux (ed.), Unsaturated Flow in Hydrologic Modeling Theory and Practice, Kluwer Academic Publishers, Beltsville, MD, 275-300

Rawls W.J. D.L. Brakensiek, and B. Soni, 1983, Agricultural Management Effects on Soil Water Processes Part I: Soil Water Retention and Green and Ampt Infiltraion Parameters, Soil and Water Division of ASAE, 82-2589

Rawls, W.J., Brakensiek, D.L., and Saxton, K.E., 1982, Estimation of soil water properties., Trans. ASAE, Vol. 108, pp. 1316-1320

Renger, M., 1971, The estimation of pore size distribution from texture, organic matter content and bulk density, Z. Kluturtech. Flurbereinig., Vol. 130, pp. 53-67

Russam , K., 1958, An Investigation into the Soil Moisture Conditions Under Roads in Trinidad, B.W.I., Geotechnique, Vol. 8, pp. 57-71.

Scheinost, A.C., W. Sinowski, K. Auerswald, 1997, Regionalization of soil water retention curves in a highly variable soilscape, I. Developing a new pedotransfer function, Geoderma, 78, 129-143

Schuh et al., 1991, Water Resource Inv. No.18, NDSWC

Sillers, W. S., 1996, Mathematical representation of the soil-water characteristic curve, M.Sc. Thesis, Department of Civil Engineering, University of Saskatchewan, Saskatoon

Smith, W.O., 1929, Packing of homogeneous spheres, Physics Review, Vol. 34, pp. 1271, 1929

Tietje, O., and M. Tapkenhinrichs, 1993, Evaluation of pedo-transfer functions, Soil Science Society of America Journal, 57, 1088-1095

Tyler, Scott W., and Stephen W. Weatcraft, 1989, Application of fractal mathematics to soil water retention estimation, Soil Science Society of America Journal, Vol. 53, No. 4, 987-996

van Genuchten, M.T., 1980, A closed form equation for predicting the hydraulic conductivity of unsaturated soils, Soil Science Society America Journal, pp. 892-890.

Vereecken, H., J. Maes, J. Feyen, and P. Darius, 1989, Estimating the soil moisture retention characteristic from texture, bulk density, and carbon content, Soil Science, Vol. 148, No. 6, 389-403

Vukovic, Milan, and Soro, Andjelko, 1992, Determination of hydraulic conductivity of porous media from grain-size composition, Water Resources Publications, Littleton, CO

Wagner, L.E., and Ding, D., 1994, Representing aggregate size distributions as modified lognormal distributions, American Society of Agricultural Engineers, Vol. 37, No. 3, pp. 815-821

Williams, R.D., Ahuja, L.R., and Naney, J.W., 1992, Comparison of methods to estimate soil water characteristics from texture, bulk density, and limited data., Soil Science,, Vol. 153,, pp. 172-184.

CHAPTER 5.0 Equations To Represent The Compressibility of a Soil

5.1 Introduction

Considerable research has focused on the application of computer models to soil mechanics problems during the past three decades. Seepage, contaminant transport, and volume change are some of the areas that have received attention. Finite element models have allowed for easy modeling of difficult problems. These finite element models make use of the latest numerical methods to allow convergence of highly nonlinear problems. However, the dependence on establishing the correct soil property functions as input remains the most critical aspect for accuracy.

Central to the modeling of volume change processes is the measurement of the compression curve. Computer software performing modeling of volume change typically requires a description of the elastic properties of a soil. The majority of software models make use of linear or nonlinear elastic parameters to represent the elastic behaviour of a soil. This representation appears remote from the conventional compressibility measurements for a soil and is limited at best. The purpose of this chapter is to present continuous equations capable of representing the compression soil property function.

The compression soil property function is central to a wide variety of soil problems. Classic formulations for the solution to settlement, heave, and consolidation depend on the laboratory measurement of the compression curve. The accuracy with which the compression soil property function is represented will influence the accuracy of the final solution. Typical straight-line approximations of the compression curve were reasonable for a one-dimensional settlement analysis but are not satisfactory for two and three-dimensional analysis using finite element modeling. Typically, the compressibility of a soil is broken into independent sections representing moving between the recompression and virgin compression branches. These 'breaks' are physically unrealistic and can lead to numerical instability in finite element

analysis. The use of continuous equations provide a smooth transition between stress states and thereby improve convergence for numerical modeling.

The compression curve also forms the basic representation for the volume-mass unsaturated soil-property functions. Other unsaturated soil-property functions (e.g., permeability and shear strength) have been approximated in terms of the properties of the saturated soil and the soil-water characteristic curve (Fredlund, 1993, Fredlund, 1996, Vanapalli, 1995).

Likewise, the volume-mass properties, in terms of stress state, can be defined with reference to the saturated soil, compression curve and other information such as the soil-water characteristic curve. The compression properties of a saturated soil have not been defined in a flexible manner that lends itself to a continuous mathematical function. Therefore, defining suitable mathematical functions for the compression characteristics of a saturated soil becomes the first step towards mathematically defining the overall constitutive surface to represent the volume-mass properties.

A general formulation for the three-dimensional constitutive surfaces of an unsaturated soil has been defined by Fredlund (1993). A typical constitutive surface defined in terms of the void ratio of a soil can be seen in Figure 5-1. Figure 5-1 shows that the compression curve forms the saturated limiting condition for the definition of the three-dimensional surface. As such, the compression curve becomes one reference curve in defining the overall constitutive behavior of an unsaturated soil.

Defining the overall volume-mass constitutive behavior of an unsaturated soil requires that a second constitutive surface be defined. Figure 5-2 shows the water content constitutive surface. The limiting water content compression curve with respect to $(\sigma-u_a)$, is related to the void ratio compression curve with respect to $(\sigma-u_a)$, by the specific gravity of the soil, Gs (or ρ_s/ρ_w where ρ_s=density of solids and ρ_w=density of water). The other limiting curve in Figure 5-1 (i.e., with respect to (u_a-u_w)), is the soil-water characteristic curve that plays a dominant role in modeling the complete constitutive surfaces.

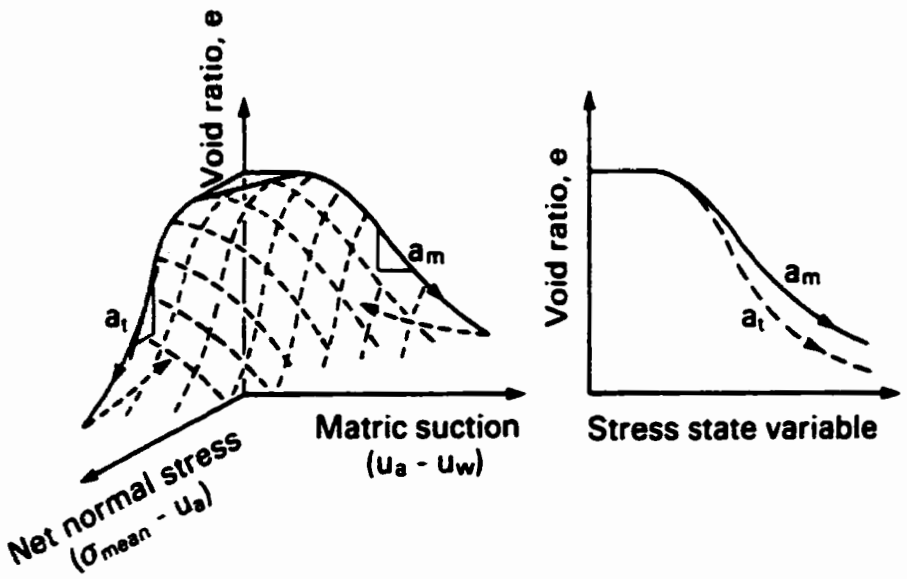

Figure 5-1 Void ratio constitutive surfaces for an unsaturated soil expressed using soil mechanics terminology (Fredlund and Morgenstern, 1976)

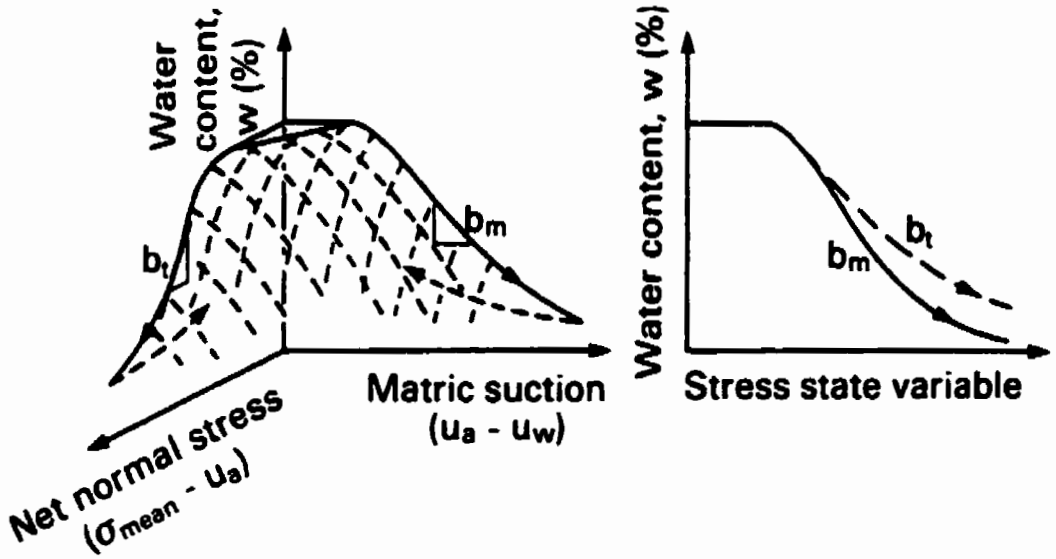

Figure 5-2 Water content constitutive surface for an unsaturated soil (Fredlund and Morgenstern, 1976)

The specific objective of this chapter is to provide a continuous mathematical function for the purpose of representing the compression curve. The formulation will take into account fundamental behavioral concepts already established in literature regarding the use and nature

of the compression curve. The equations are tested against a variety of published experimental results to ensure a satisfactory representation of compressibility.

5.2 History Regarding the Manner in Which Soil Compression has been Designated

In the 1920s, Terzaghi presented the fundamental manner for engineers to measure the compression of a soil. Laboratory testing methods were developed to allow the measured compressibility to represent the compression of soils in the field. The focus of much of this research was directed towards the prediction of settlement for soft soils. Common laboratory tests can be referred to as K_o loading in an oedometer and isotropic triaxial loading. There has also been a limited amount of anisotropic triaxial compression testing. Both oedometer and the isotropic triaxial test results will be examined in this chapter.

5.2.1 Oedometer Compression Test

The oedometer compression test remains the most common laboratory test used to define the compressibility properties of a soil. Documentation regarding the procedure for the oedometer test can be found in ASTM D4546 or Lambe (1951). The soil is compressed at a rate such that the water pressure in the soil is allowed to dissipate at each stress level allowing the void ratio of the soil to be plotted versus the effective stress level. Figure 5-3 shows typical results for a sample of San Francisco Bay Mud from a depth of 7.3 m. Plotting of the oedometer compression tests results is generally done in terms of void ratio as illustrated by Taylor (1948). The slope of the oedometer compression curve when plotted on an arithmetic scale is represented by the variable, a_v, defined as the coefficient of compressibility. Terzaghi (1925) recognized that the 'virgin compression branch' of a compression curve plotted essentially as a straight line when the same data was plotted on a logarithmic scale. The same data presented in Figure 5-3 is plotted on a logarithmic scale in Figure 5-4. The logarithmic slope of the compression curve when plotted on a logarithmic scale is represented as the compression index, C_c. Casagrande (1936) also noted that the virgin compression branch of the compression curve could be represented by a straight line on a logarithmic scale.

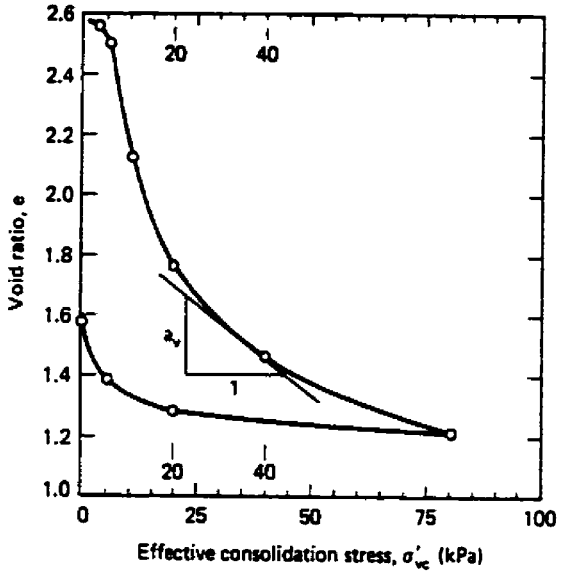

Figure 5-3 Results of oedometer compression test plotted on an arithmetic scale (from Holtz & Kovacs, 1981)

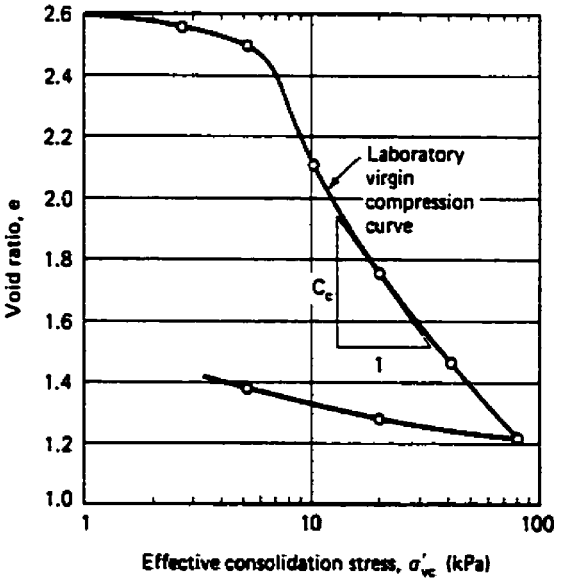

Figure 5-4 Results of oedometer compression test plotted on a logarithmic scale (from Holtz & Kovacs, 1981)

The virgin compression curve is generally represented by Equation 5-1.

$$e_f = e_o - C_c \log\left(\frac{\sigma_f}{\sigma_p}\right)$$

Equation 5-1

where: e_f = final void ratio,

e_o = initial void ratio,

C_c = compression index,

σ_f = final effective stress state,

σ_p = preconsolidation pressure.

Calculations are then performed based on the starting and ending stress states. This representation causes difficulties in the modeling of the compression curve due to the discontinuous nature of Equation 5-1.

Another variable used in the description of the compressibility of a soil is the coefficient of volume change, m_v. The relationships between the compression characteristics is as follows.

$$m_v = \frac{a_v}{1+e}$$

Equation 5-2

Where the coefficient of compressibility, a_v, can be written as,

$$a_v = \frac{0.435\,C_c}{\sigma_{avg}}$$

Equation 5-3

where: σ_{avg} = average effective stress between stress increments.

5.2.2 Data

Oedometer experimental results are abundant in the literature for soils with a wide variety of stress histories. Kaufman and Sherman (1964) presented the results of heavily overconsolidated clays. MacDonald and Sauer (1970) presented compression curves for precompressed glacial tills from Canada. Quigley and Thompson (1966) presented the oedometer results for a sensitive marine clay called the Laurentian or Leda clay. Rutledge (1944) presented the highly compressible Mexico City clay. The distinctive shapes of each of the different soils is interesting to study. In contrast to the more common compression curves mentioned above, is the compression of a windblown silt (loess). The compression curves for various loess soils were presented by Clevenger (1958). Various compression curves from research literature, as well as other laboratory data, was used to verify the results of the proposed equations presented in this chapter. Some of the experimental oedometer data can be seen in Figure 5-5.

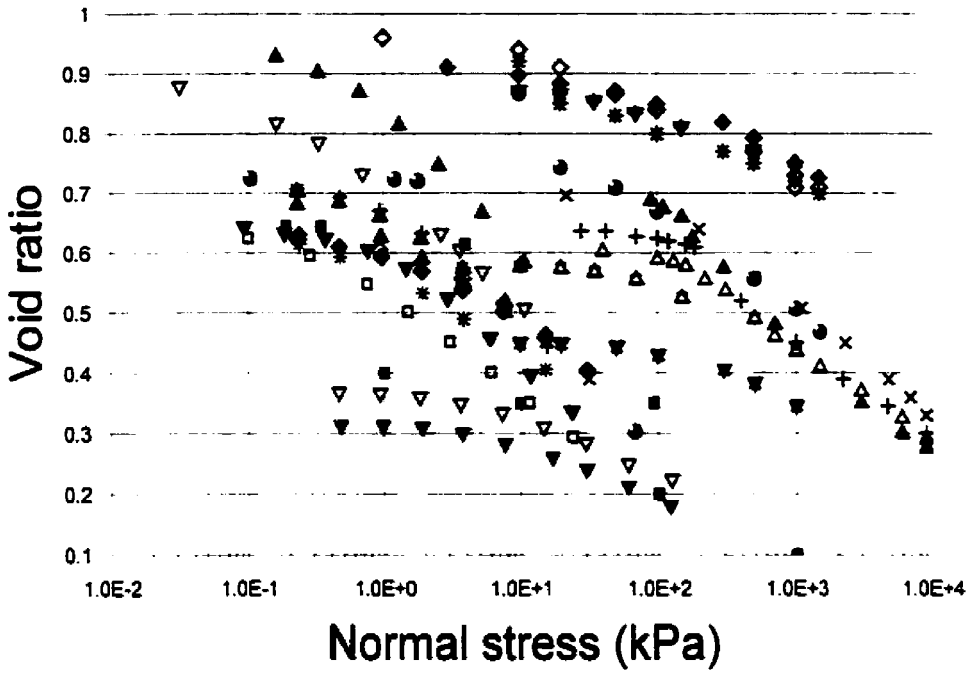

Figure 5-5 Summary of some of the experimental oedometer data used to verify the equations presented in this chapter.

5.2.3 Isotropic Triaxial Compression Test

Another model for defining the deformation characteristics of a soil is Critical State Soil Mechanics (CSSM). The Critical State model has its roots in work done by Terzaghi, Casagrande, and Hvorslev. They recognised the importance of void ratio (or specific volume, 1+e) on soil behavior and the fact that compression along the normal compression line is essentially irreversible, whereas deformations are essentially reversible along the swelling and recompression lines (Leroueil, 1997). The model was established in the late fifties and sixties in England (Roscoe et al., 1958; Roscoe and Burland, 1968; Schofield and Wroth, 1968) on the basis of tests performed on reconstituted and isotropically consolidated samples of clay.

The Critical State Model is based on the isotropic triaxial compression of a soil. Deformations are classified as elastic or plastic and follow the resulting normal compression line (ncl) or

unloading-reloading line (url) on the compression plot as shown in Figure 5-6. Specific volume, v, is typically plotted versus mean effective stress p'.

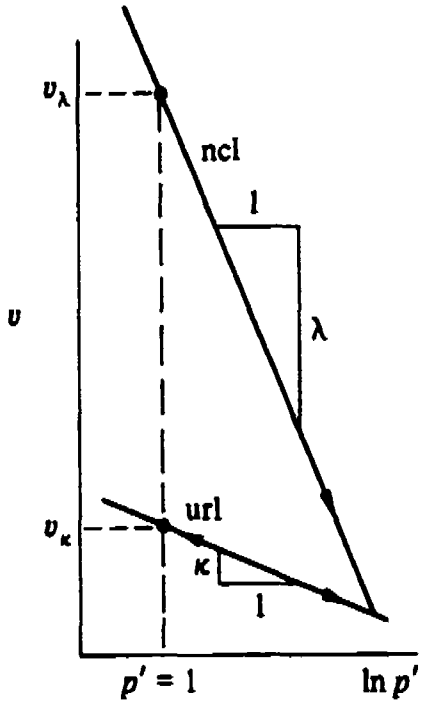

Figure 5-6 Normal compression line (ncl) and unloading-reloading line (url) in the compresison plane (Wood, 1992)

Also present in the Critical State Model is the idea of a preconsolidation pressure at which the soil moves from elastic to plastic strains. This point is illustrated in Figure 5-6 as the soil moves from the *url* line to the *ncl* line.

It was later noticed that this preconsolidation pressure or yield locus may be reached via a number of different stress paths. A multitude of triaxial tests were performed on a St. Louis clay by Tavenas, et al. (1979). The location of the yield locus for a St. Louis clay was established as shown in Figure 5-7. Graham, et al. (1983) later established the yield curves for four different clays. It was found by Graham (1983) that the different yield curves could be normalized with respect to preconsolidation pressure as seen in Figure 5-8.

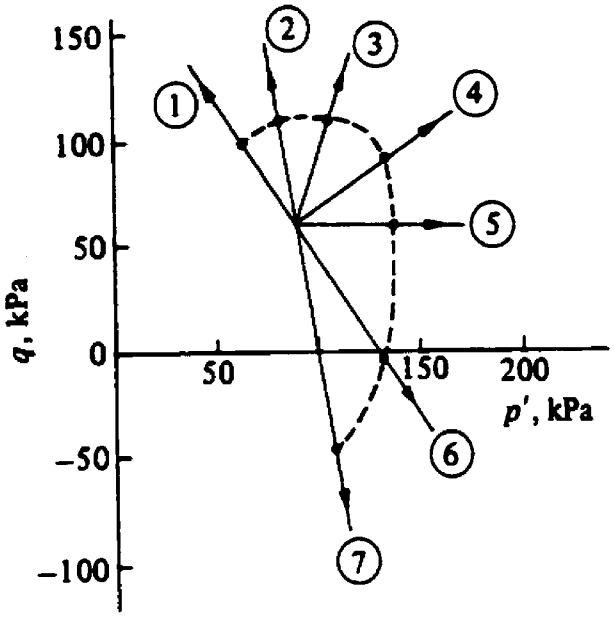

Figure 5-7 Yield curve deduced from triaxial tests on undisturbed St. Louis clay (after Tavenas, des Rosiers, Leroueil, LaRochelle, and Roy, 1979)

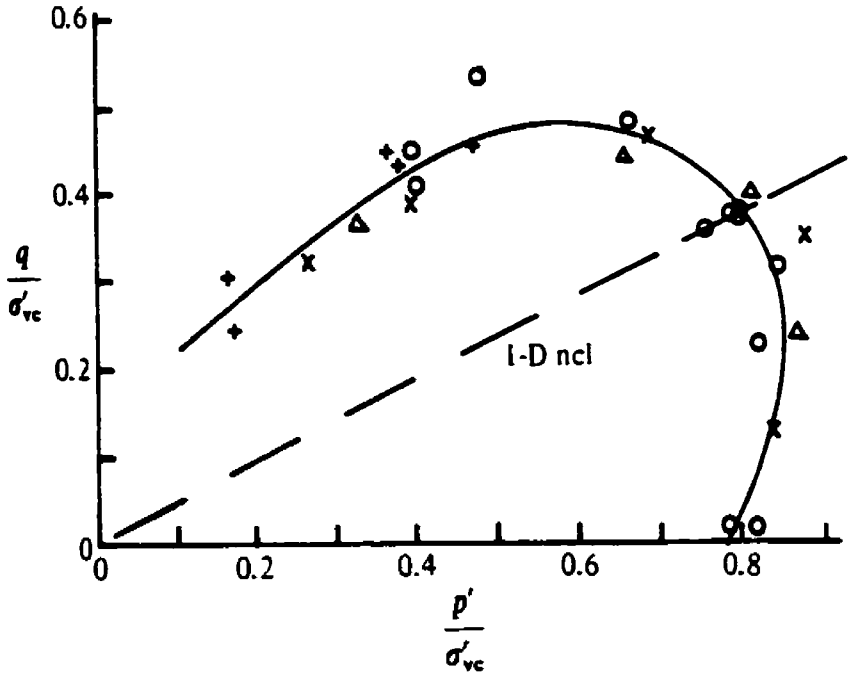

Figure 5-8 Yield curves normalized with preconsolidation pressure (Graham et al., 1983)

The yielding of sands may be handled in a like manner by the Critical State model. A major series of triaxial tests investigating the yielding of sand is reported by Tatsuoka (1972) and summarized by Tatsuoka and Ishihara (1974).Poorooshasb, Holubec, and Sherbourne (1967) also studied the yielding of Ottawa sand.

The equations used to represent the *ncl* and *url* lines in the Critical State compression plane are typically represented by the equations presented below. It can be noted that the form of the equations is similar to the form of equations which have been used to fit the results of the one-dimensional oedometer test. The equations later presented in this chapter are ideally suited to model compression curves measured in either the oedometer or the isotropic triaxial test.

Equation for the normal compression line (ncl):

$$v = v_{\lambda} - \lambda \ln p'$$

Equation 5-4

Equation for the unloading-reloading line (url):

$$v = v_{\kappa} - \kappa \ln p'$$

Equation 5-5

An exponential equation to represent the experimental data from an isotropic compression test was presented by Juarez-Badillo (1981). Equation 5-6 is similar to the Brooks and Corey (1964) equation to represent the soil-water characteristic curve and is continuous after the yield point.

$$\frac{V}{V_o} = \left(\frac{\sigma}{\sigma_o}\right)^{-\gamma}$$

Equation 5-6

where: V = volume,

V_o = initial volume,

σ = current stress level,

σ_o = initial stress,

γ = variable.

The current state of technology has provided two standard approaches for describing the volume change of soils. The intent of the equations presented in this chapter is to enhance both models for representing volume change.

5.3 Proposed Four-Parameter Equation for Compression (and Recompression)

It would appear that an optimal equation to define the compressibility of a soil should follow the same form as that shown in Equation 5-1. Familiarity with Equation 5-1would then allow for adaptation to the new form of the compression curve. A new equation, called the four-parameter equation, is presented here to remedy continuity problems and retain the basic form of the classic compression equation shown above. The four-parameter equation has the parameters C_c, C_r, σ_p, and σ_{ov} as variables in the fit providing a fit with commonly used and understood parameters. The four-parameter equation is written as follows:

$$e(\sigma) = \left[e_o - \frac{C_r}{2} \ln\left[1 + \left(\frac{\sigma}{\sigma_s} \right)^2 \right] - \frac{C_c - C_r}{2} \ln\left[1 + \left(\frac{\sigma}{\sigma_p} \right)^2 \right] \right]$$

Equation 5-7

where e_o = initial or starting void ratio,

C_r = recompression index,

C_c = compression index,

σ_s = swelling pressure (kPa),

σ_p = preconsolidation pressure (kPa).

Equation 5-7 provides a means for moving from a flat portion of the compression curve onto the recompression branch of the curve and finally onto the virgin compression branch. The equation may then be used to represent overconsolidated soils that contain both a

recompression curve and a virgin compression branch to the curve. If the soil is normally consolidated, the recompression index, C_r, will be zero. For this case, Equation 5-7 may be simplified as shown below. The simplified equation is closely related to the classic compression equation.

$$e(\sigma) = \left[e_o - \frac{C_c}{2} \ln \left[1 + \left(\frac{\sigma}{\sigma_p} \right)^2 \right] \right]$$

Equation 5-8

5.3.1.1 The Preconsolidation Pressure of Soils

Casagrande (1932) noted that the stress and other changes that have occurred during the history of a soil are preserved in the soil structure. Whenever a soil is subjected to a stress greater than the stress previously 'experienced' by the soil, the soil will experience plastic deformation. The zone where plastic yielding commences is known as the start of the virgin compression branch of the compression curve. Casagrande (1936) developed an empirical construction method of determining the stress level at which a soil begins to yield. The stress level at which the soil begins to yield is known as the preconsolidation pressure. It is assumed that the compression of a soil is generally elastic up until the preconsolidation pressure.

Inherent in the four-parameter equation presented in this chapter is its own definition of the preconsolidation pressure. The preconsolidation pressure defined by the fitting of the four-parameter equation will vary slightly from the preconsolidation pressure as defined by Casagrande (1936). The difference between the two pressures is not significant for most cases. Schmertmann (1955) also presented a graphical correction for the determination of the compression index, C_c and a field compression curve. The Schmertmann (1955) construction of the field compression curve is accounted for in this chapter. Various causes of sampling disturbance are summarized by Leonards (1976), Brumund, Jonas, and Ladd (1976) and Schmertmann (1955).

5.3.2 Parametric Study Illustrating the Four-Parameter Equation

The physical significance for each of the four parameters in Equation 5-7 can be seen in the following figures. The continuity of the four-parameter model is maintained while relating current model parameters to well-known compression variables. Modeling of the compression curves of normally and over-consolidated soils can be accomplished by the use of the four-parameter equation. The effect of varying each of the four parameters can be seen in Figure 5-9, Figure 5-10, Figure 5-11 and Figure 5-12.

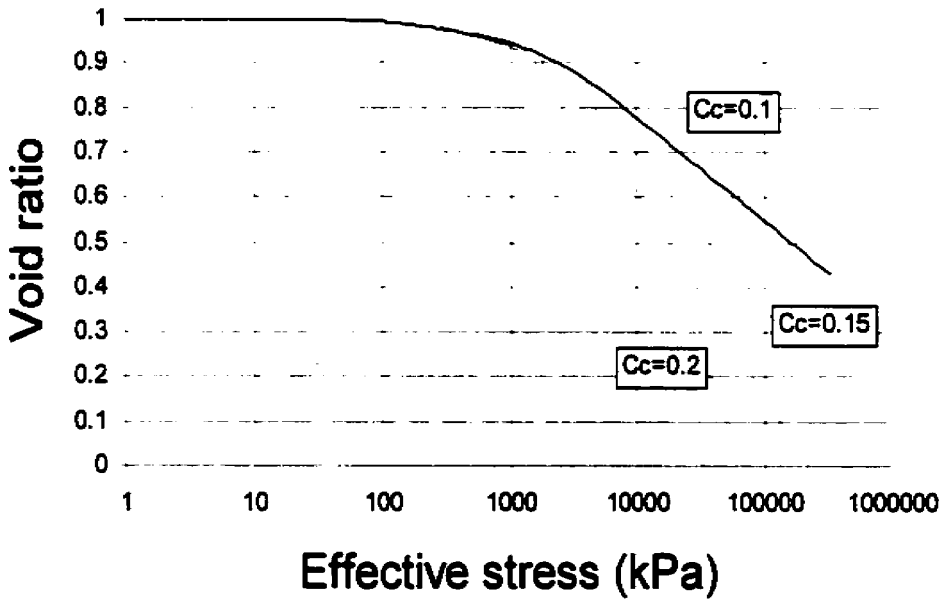

Figure 5-9 Effect of varying Cc on the four-parameter model

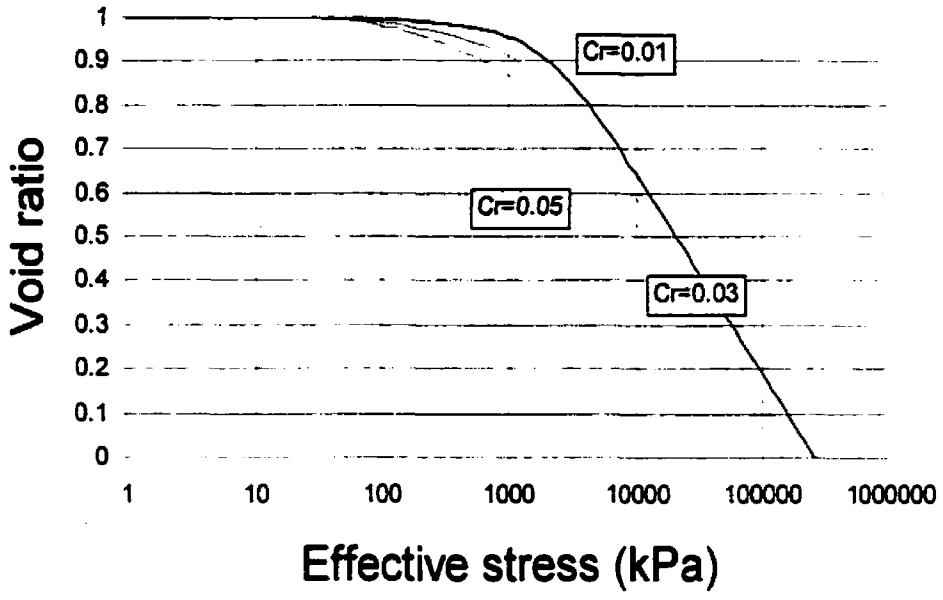

Figure 5-10 Effect of varying Cr on the four-parameter model

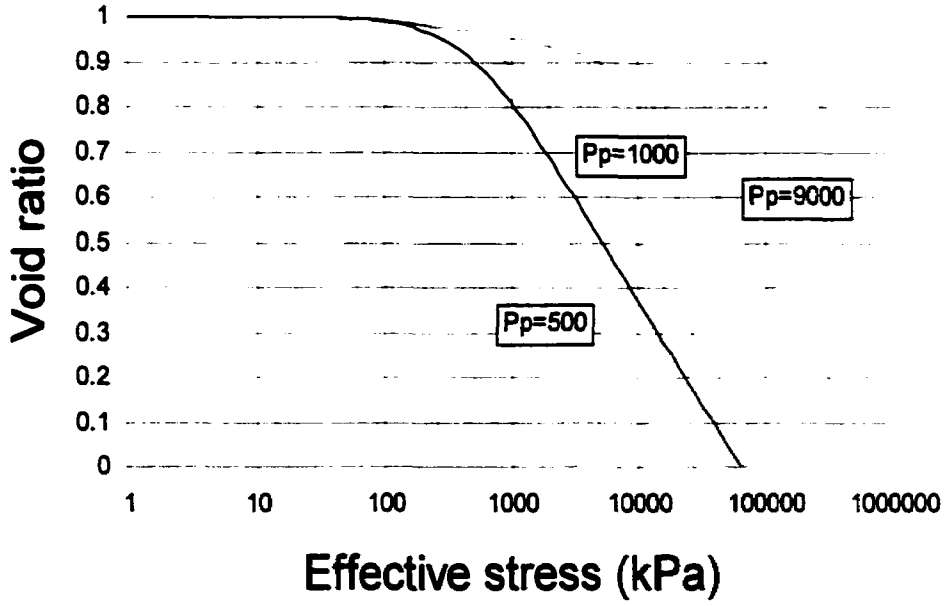

Figure 5-11 Effect of varying the preconsolidation pressure on the four-parameter model

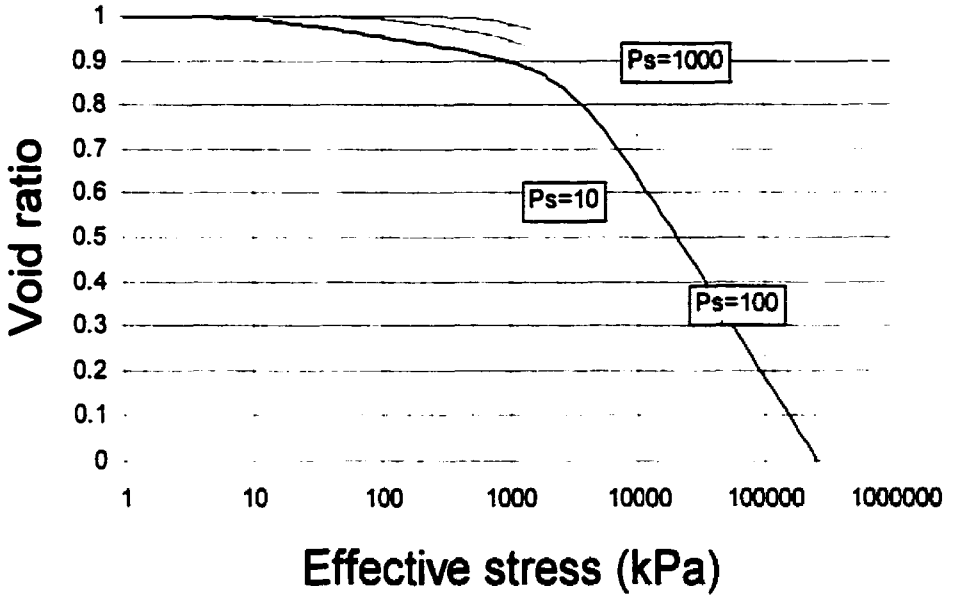

Figure 5-12 Effect of varying the swelling pressure on the four-parameter model

5.3.3 Examples Showing the Best-Fit of the Four-Parameter Equation

An example of typical fits of the compression curve by the four-parameter equation can be seen in the following figures. Fits of normally consolidated soil samples are presented in Figure 5-13, Figure 5-14, and Figure 5-15. The fit of an overconsolidated soil by the four-parameter equation can be seen in Figure 5-16. Figure 5-16 also presents the four-parameter equation adjusted to model the field compression curve as proposed by Schmertmann (1955).

The experimentally measured compression curve can be divided into elastic and plastic regions. The location of the transition from elastic to plastic depends upon the stress history of the soil. As such, it is possible to develop a family of compression curves based on the results of a single compression test. The four-parameter equation was used to generate such a family of curves for an Albany Clay as first presented by Schmertmann (1953). The generated curves along with experimental data outlining the original curve can be seen in Figure 5-17. Modeling

of the compression curve at various initial void ratios is therefore possible with the four-parameter equation.

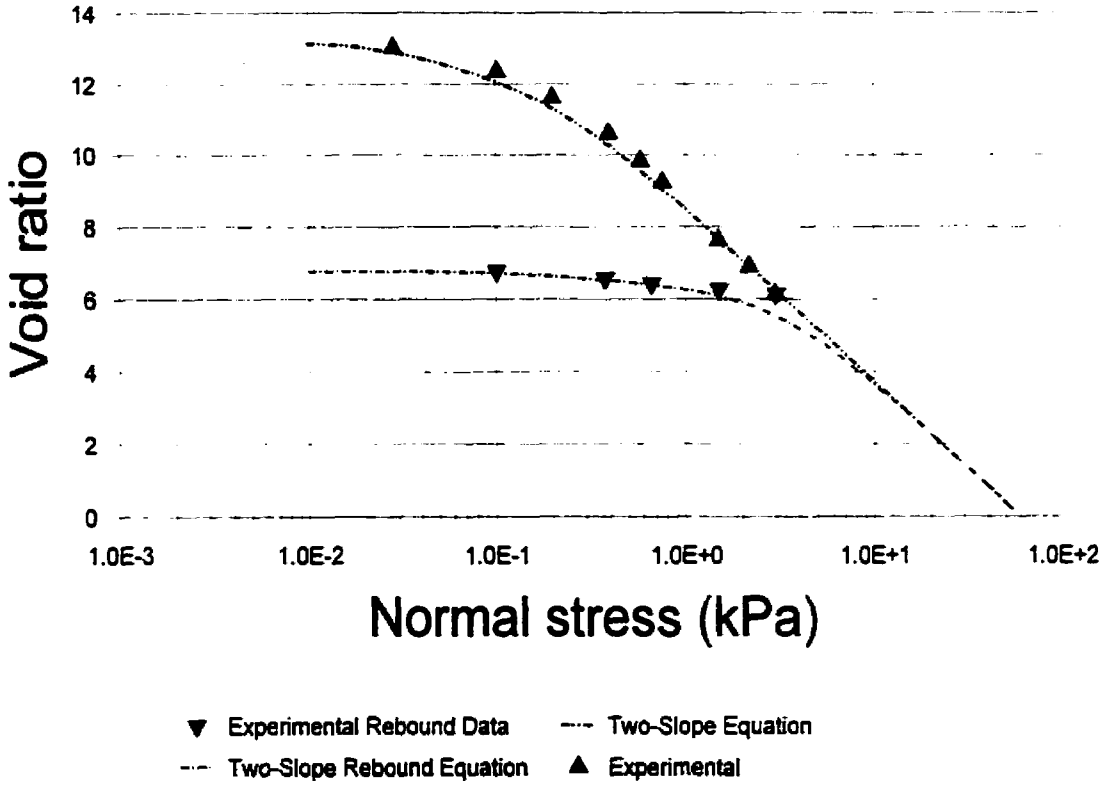

Figure 5-13 Example fit of compression data of a Mexico City clay published by Rutledge (1942) using the four-parameter equation, R^2=0.990 (12345)

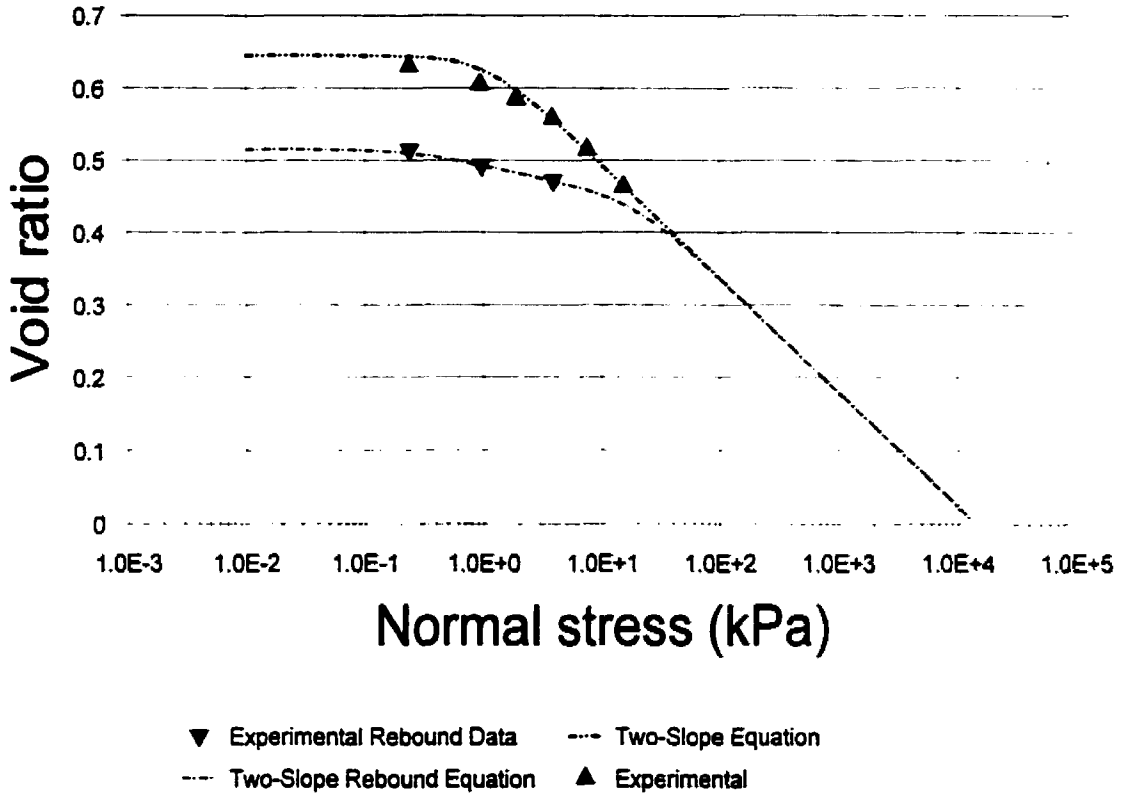

Figure 5-14 Example fit of compression data for a St. Clair clay till published by Soderman (1970) using the four-parameter equation, R^2=0.963 (12350)

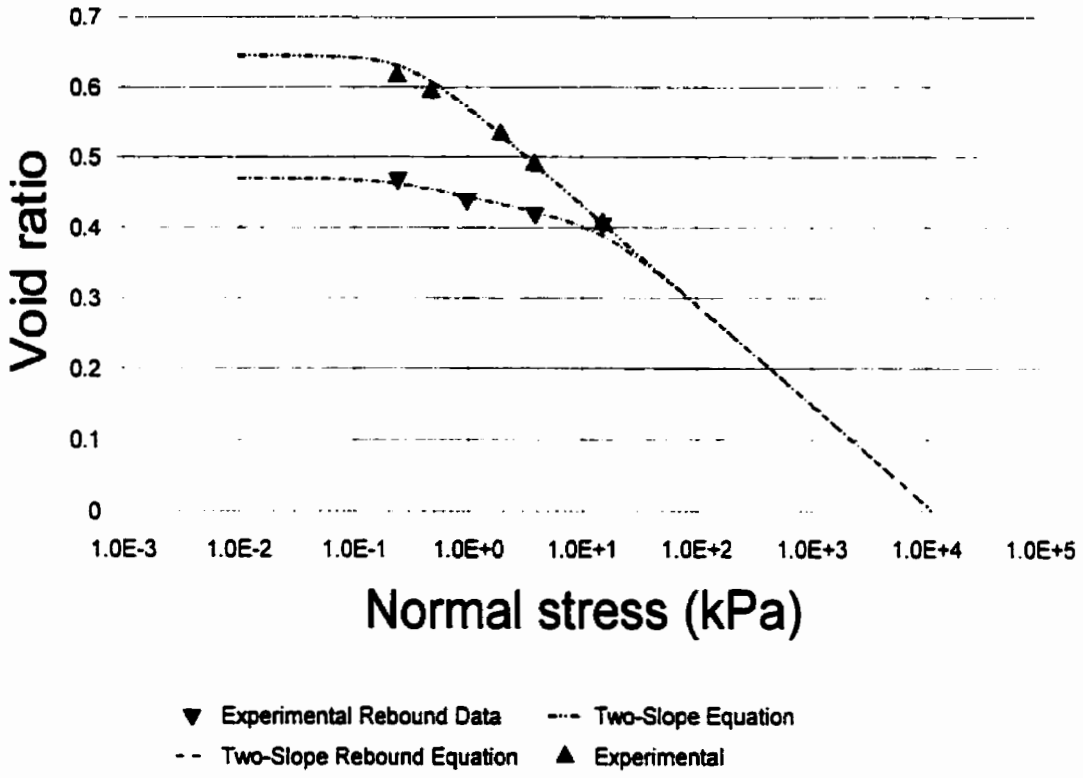

Figure 5-15 Example fit of compression data of a remoulded St. Clair clay till published by Soderman (1970) using the four-parameter equation, R^2=0.984 (12352)

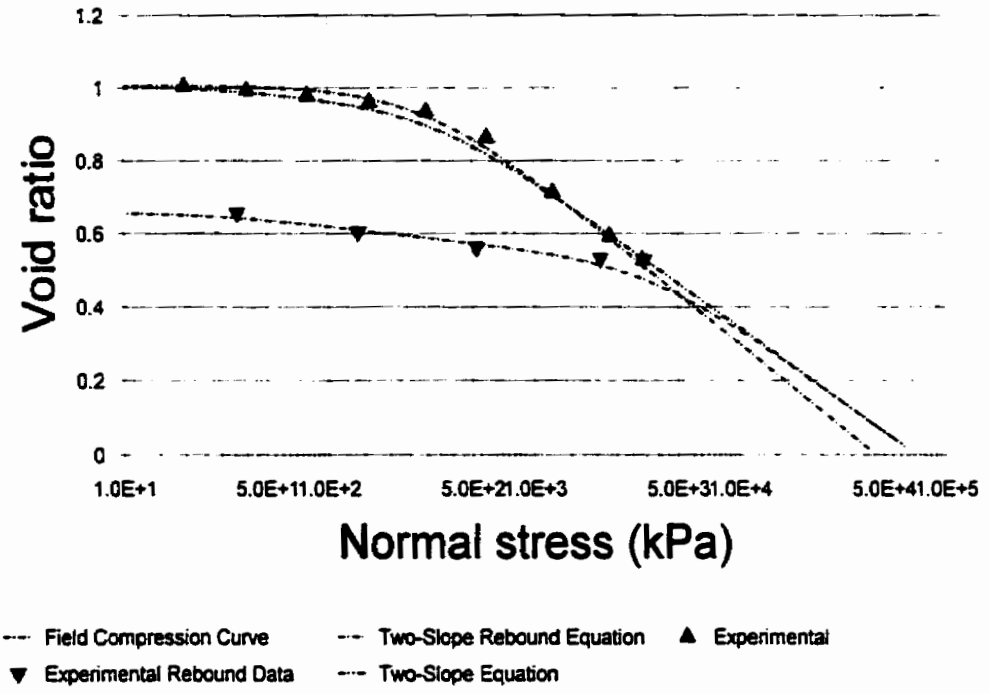

Figure 5-16 Example of field compression curve and fit of compression data of a Brazil organic silty claypublished by Schmertmann (1953) using the four-parameter equation, R^2=0.983 (12533)

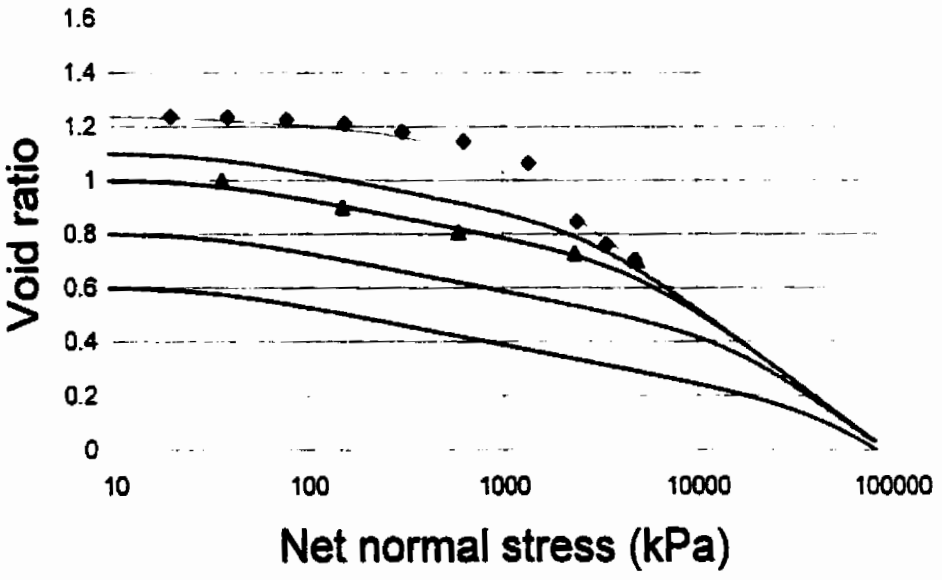

Figure 5-17 Representation of a family of compression curves generated with the four-parameter equation based on an Albany Clay published by Schmertmann (1953) (12530)

5.3.4 Assessment of the Four-Parameter Equation

The purpose of the four-parameter equation is to allow for the representation of the compression and recompression curves for a wide variety of soils. The four-parameter equation was tested using a dataset of compression data. The results of the squared differences between the equation and experimental data indicate a good fit was obtained for most soils as indicated by Figure 5-18.

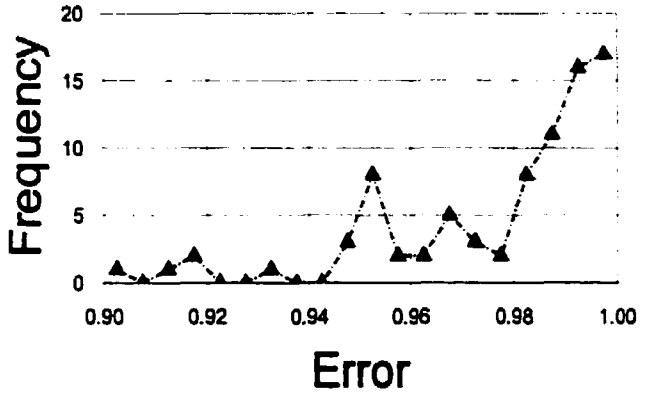

Figure 5-18 R^2 distribution of 90 soils fit with the four-parameter equation (1.0 represents a perfect fit)

The four-parameter equation allowed representation of the soil in a way that is consistent with historical soil mechanics. The swelling pressure, preconsolidation pressure, compression index, and recompression index are all parameters in the equation. The selection of these parameters in the equation provides for equation parameters which are physically realistic. The curve parameters may also be adjusted to generate a physically realistic family of compression curves for a soil on compression/recompression cycles.

A comparison of the squared differences between the three-parameter model and the four-parameter model can be seen in Figure 5-19. It can be seen that the three-parameter model provides a closer fit to experimental data the majority of the time. The reason for this seems to be the superposition fitting method used for the four-parameter equation. It was concluded, however, that the benefits of the four-parameter model outweighed the loss in fit accuracy. The

primary benefit of the four-parameter equation is its consistency with the compression index, C_c, and the swelling index, C_s, already in use in the practice of geotechnical engineering. Another benefit was that the four-parameter equation provides a straight line on a semilog scale when representing either the elastic or plastic regions of the compression function.

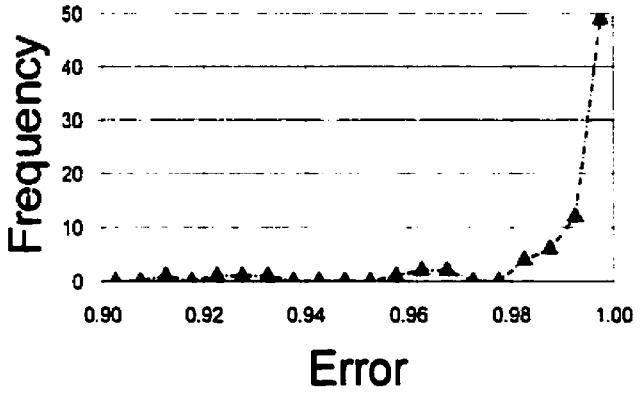

Figure 5-19 R^2 distribution of 90 soils fit with the three-parameter equation

The four-parameter equation provides a continuous and smooth model for the representation of the compression curve. A continuous and smooth model minimizes convergence problems and numerical instability when used in conjunction with a finite-element modeling package. The final result is a model which represents physical soil behavior with greater detail.

5.4 Proposed Three-Parameter Equation for Compression (and Recompression)

Fredlund and Xing (1994) proposed a three-parameter equation capable of fitting the soil-water characteristic curve. The equation differed from van Genuchten (1980) equation in several ways. The primary difference between the van Genuchten (1980) equation and the Fredlund and Xing (1994) equation was that the Fredlund and Xing (1994) equation was modified to approach zero volumetric water content at a suction of 1,000,000 kPa. The original Fredlund and Xing (1994) equation is shown as follows.

$$w(\psi) = w_s \left[1 - \frac{\ln\left(1+\frac{\psi}{h_r}\right)}{\ln\left(1+\frac{10^6}{h_r}\right)} \right] \left[\frac{1}{\left[\ln\left[\exp(1) + \left(\frac{\psi}{a_f}\right)^{n_f} \right] \right]^{m_f}} \right]$$

Equation 5-9

where: w_s = Saturated volumetric water content,

a_f = Fitting parameter closely related to the air entry value for the soil,

n_f = Fitting parameter related to the maximum slope of the curve,

m_f = Fitting parameter related to the curvature of the slope,

h_r = Constant parameter used to adjust lower portion of curve.

In the present study, it was noticed that the shape of the compression curve remains similar to the shape of the soil-water characteristic curve. The Fredlund and Xing (1994) equation was then modified to provide mathematical representation of the compression curve. The correction factor of the Fredlund and Xing (1994) equation was modified so that the equation is forced to a zero void ratio at a net normal stress of 3,500,000 kPa. This is in keeping with works presented by Ho (1988).

The modified three-parameter equation is written as follows.

$$e(\sigma_n) = e_o \left[1 - \frac{\ln\left(1+\frac{\sigma_n}{h_{rco}}\right)}{\ln\left(1+\frac{3500000}{h_{rco}}\right)} \right] \left[\frac{1}{\ln\left(\exp(1) + \left(\frac{\sigma_n}{a_{co}}\right)^{n_{co}} \right)} \right]^{m_{co}}$$

Equation 5-10

where: e_o = initial void ratio,

a_{co} = fitting parameter related to the preconsolidation pressure of the soil,

n_{co} = fitting parameter related to the maximum slope of the compression curve,

m_{co} = fitting parameter related to the shape of the curve,

h_{rco} = static fitting parameter, and

σ_n = net normal stress (kPa).

5.4.1 Parametric Study Illustrating the Three-Parameter Equation

Optimal fits of the three-parameter equation were found with the help of a least-squares regression algorithm. Variations of the equation are shown in the following figures by varying one parameter while holding the other two variables constant.

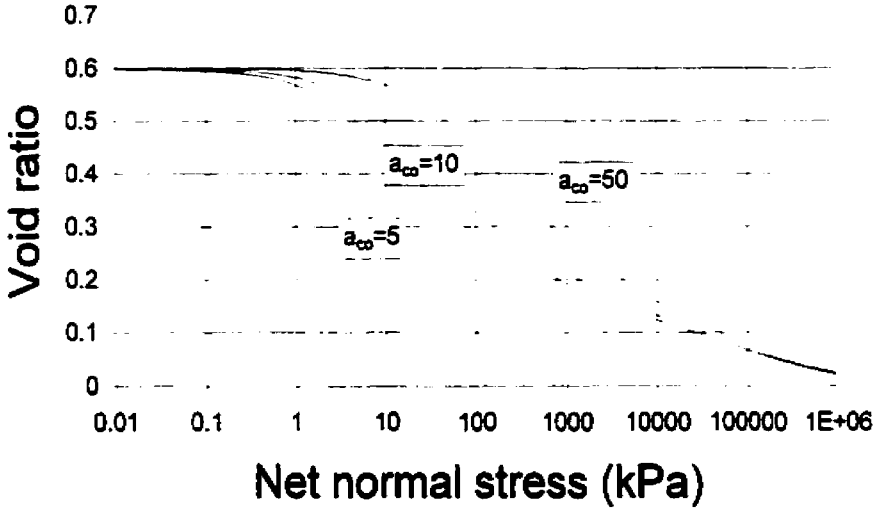

Figure 5-20 Example of varying the a_{co} parameter of the three-parameter compression equation

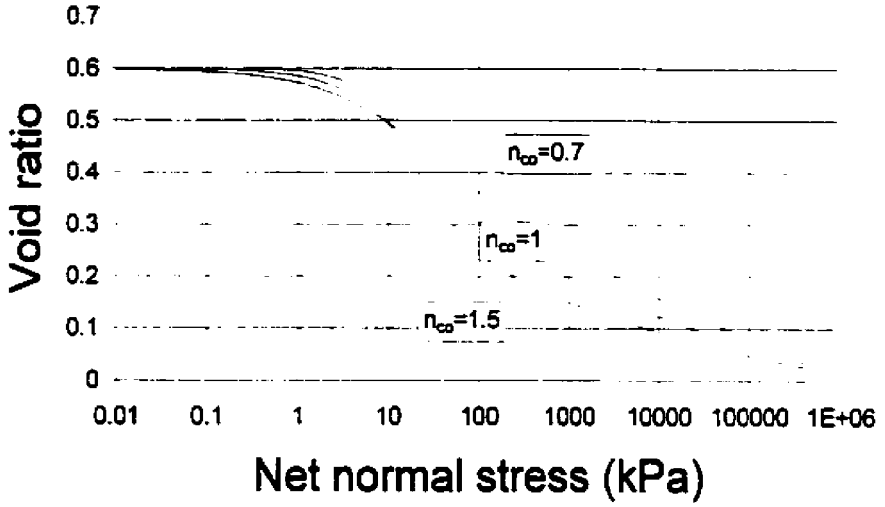

Figure 5-21 Example of varying the n_{co} parameter of the three-parameter compression equation

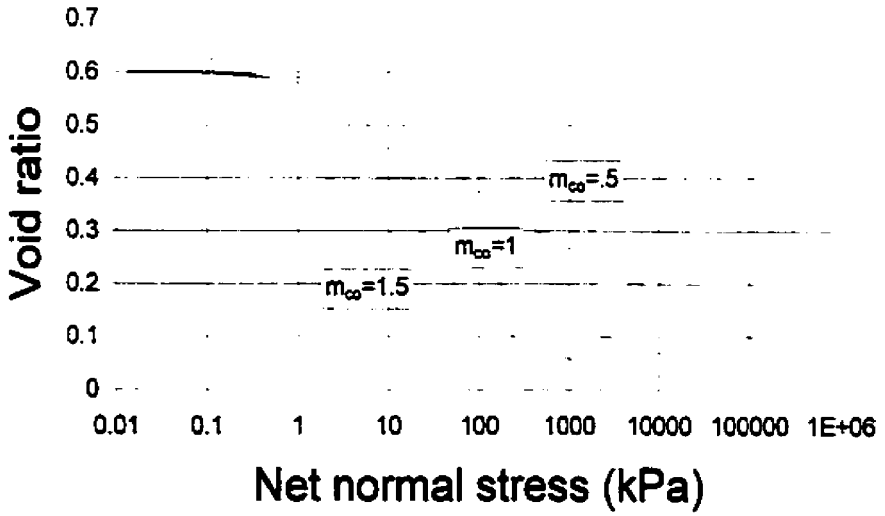

Figure 5-22 Example of varying the m_{co} parameter of the three-parameter compression equation

It can be seen from Figure 5-20 that the three-parameter compression equation behaves in a manner similar to the Fredlund & Xing (1994) equation from which it was derived. The a_{co} equation parameter primarily affects the breaking point of the compression curve and is therefore most closely related to the preconsolidation pressure of a soil. The n_{co} equation

parameter provides primarily a measure of the maximum slope of the equation as can be seen in Figure 5-21. The m_{co} equation parameter can be seen to affect the shape of the compression curve in Figure 5-22.

5.4.2 Examples Showing the Best-Fit of the Three-Parameter Equation

A number of experimentally measured compression curves were selected from literature to test the ability of the three-parameter equation to fit compression curves. The fits of the selected compression curves can be seen in Figure 5-23, Figure 5-24, Figure 5-25, and Figure 5-26.

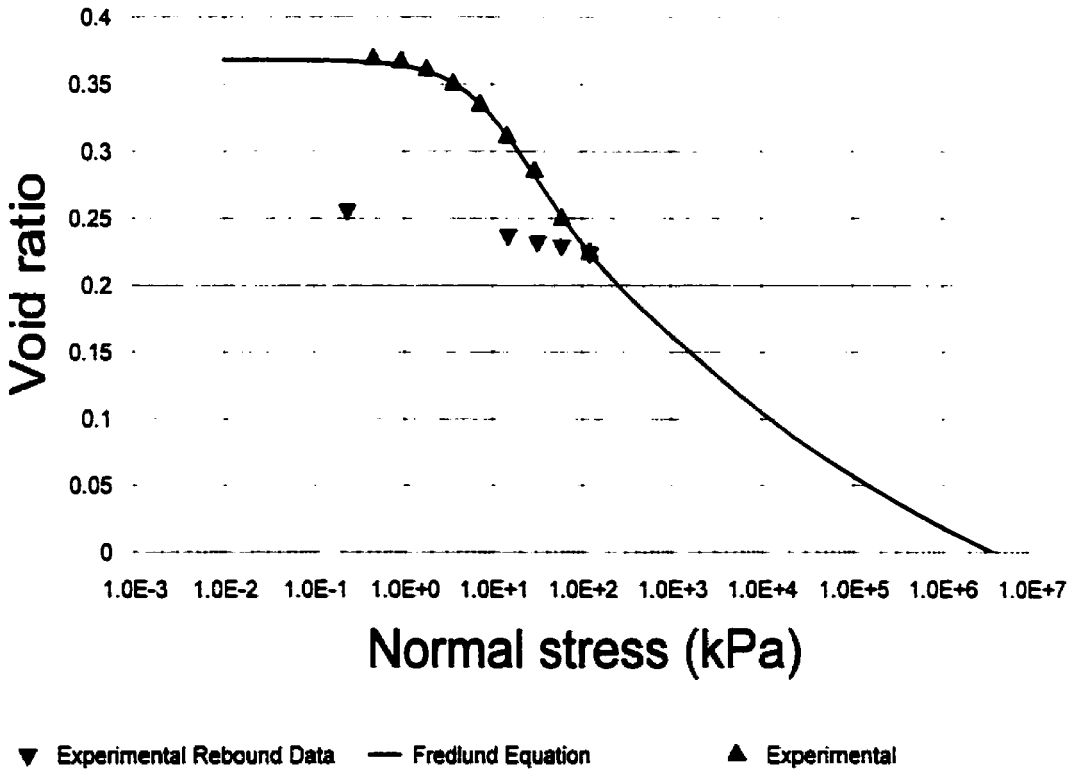

Figure 5-23 Example fit of the compression curve for a Loam published by MacDonald and Sauer (1970) using the three-parameter equation, R^2=0.990 (12385)

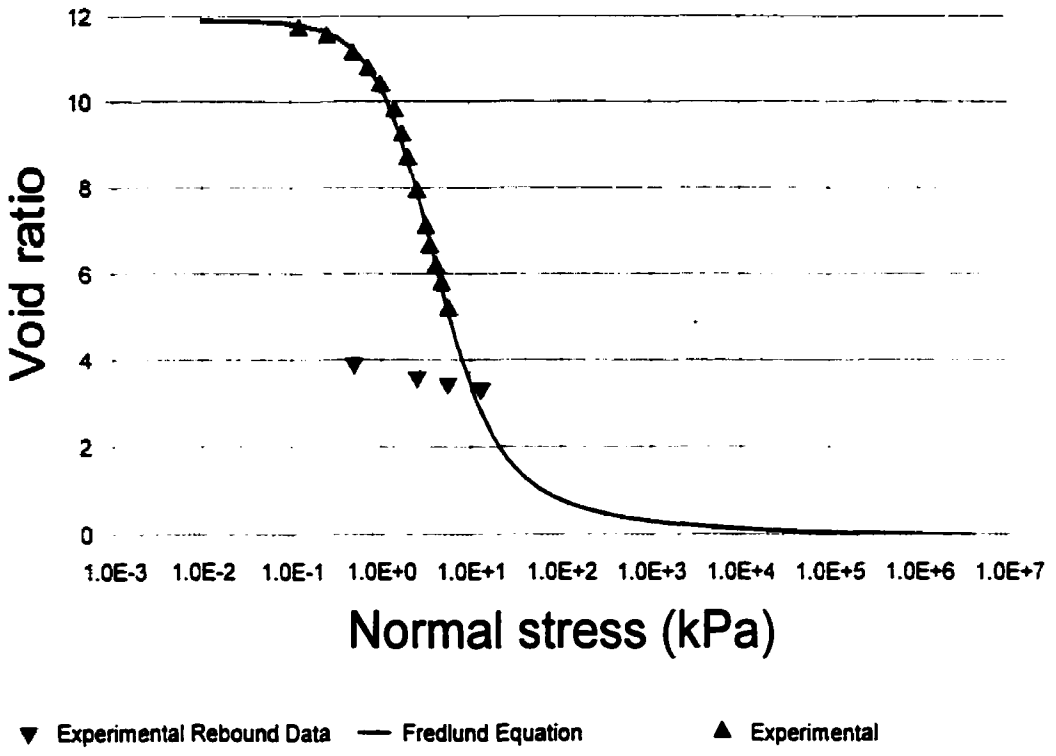

Figure 5-24 Example fit of the compression curve published by Rutledge (1942) using the three-parameter equation, R^2=0.999 (12343)

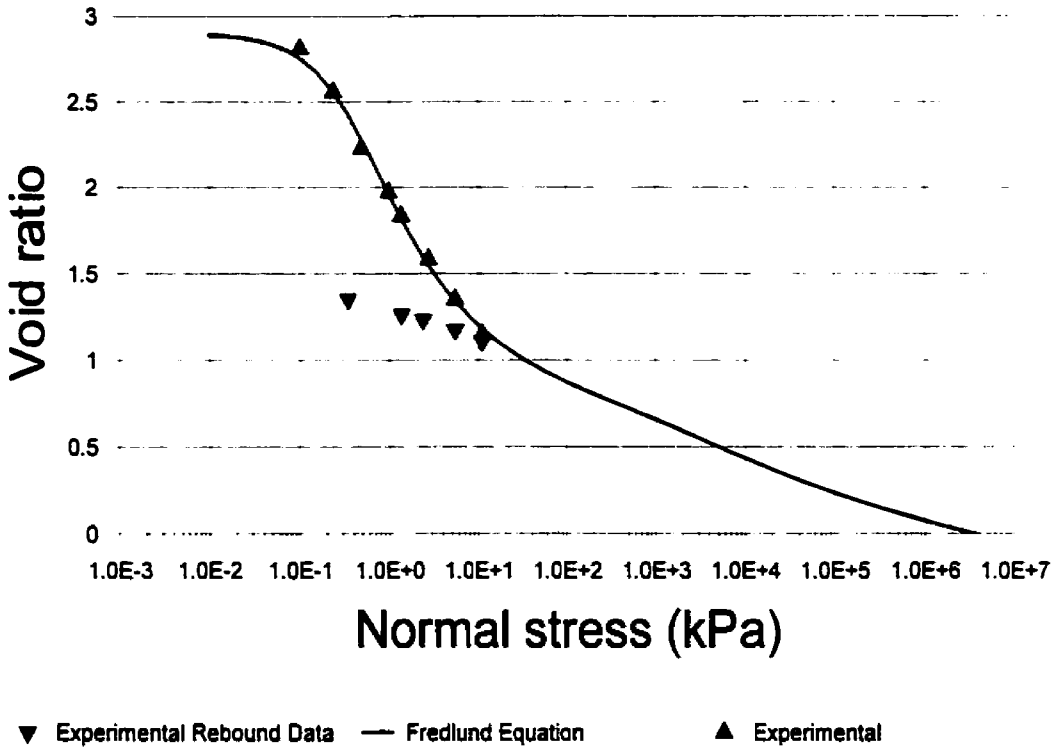

Figure 5-25 Example fit of the compression curve published by Rutledge (1942) using the three-parameter equation, R^2=0.999 (12347)

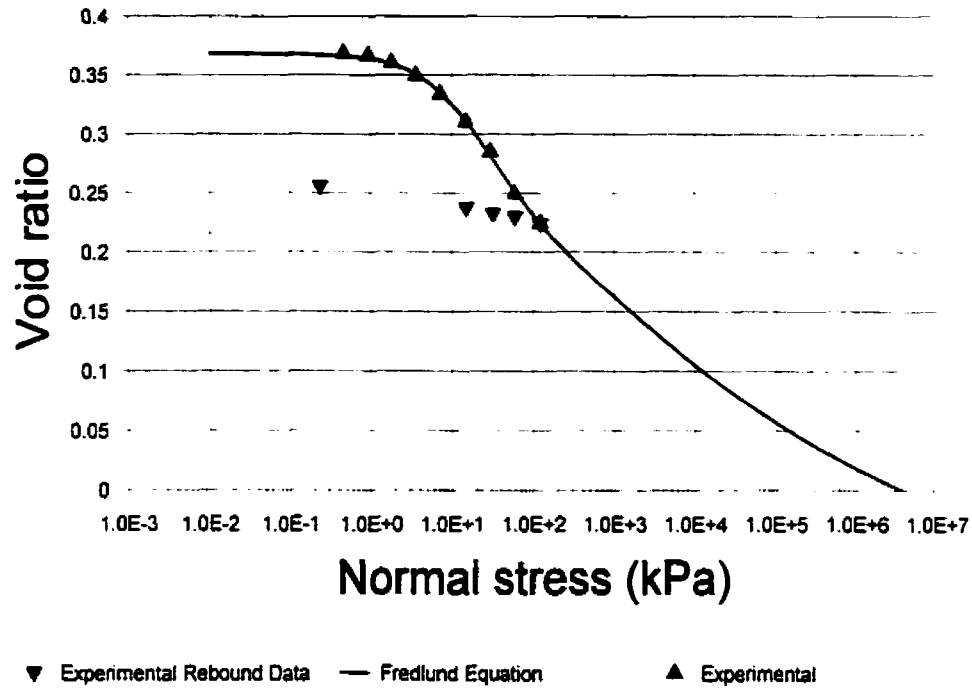

Figure 5-26 Example fit of the compression curve of a Loam published by MacDonald and Sauer (1970) using the three-parameter equation, R^2=0.990 (12385)

Performance of the three-parameter equation was good. Adequate fits were noted for most soils. The fit was found to provide optimal fits for normally consolidated soils.

5.4.3 Assessment of the Three-Parameter Equation

Performance evaluated according to the sum of squared residuals between the equation and experimental results indicated good modeling of the compression curve as indicated by Figure 5-19. The equation was used successfully for fitting of a variety of soils including remoulded or undisturbed samples. The modeling of undisturbed, highly-sensitive clays with a characteristic sharp drop-off is possible. The equation was found to be uniquely capable of modeling highly sensitive clays in a way in which the four-parameter equation was somewhat limited.

Several limitations were noticed with the three-parameter equation. The limitations were:

1. The slope of the three-parameter curve on the virgin compression portion of the curve was not constant on a semilog plot as shown in experimental data.
2. There was no relationship between the curve-fitting parameters a_c, n_c and m_c and typical values used to represent the compression curve such as the compression index, C_c, the rebound index, C_r, the preconsolidation pressure, σ_p, and the overburden pressure, σ_{ov}.

Shortcomings in the three-parameter equation can be summarized as follows. The characteristic shape of the equation is somewhat different than the experimentally determined shape of most curves. Characteristic of the analysis of compression curves (Schmertmann, 1953) is a virgin compression slope that is approximately linear when plotted on a semilog graph. The three-parameter equation virgin compression branch may or may not be linear on a semilog graph as may be seen in Figure 5-25.

Difficulties were encountered when fitting the model to soil samples exhibiting overconsolidated behavior. The shape of the model required to fit overconsolidated samples requires the existence of two separate compression branches; a recompression branch where the behavior of the soil is essentially elastic, and the virgin compression branch where both elastic and plastic deformations occur. The elastic portion of the compression curve is not adequately represented with the three-parameter model. Modeling of the compression characteristics of an overconsolidated soil requires an equation which may model two separate break points (i.e., overburden pressure and preconsolidation pressure). The three-parameter equation inherently allows only one break point.

As shown in Figure 5-17, the state of a soil is determined by its stress history. It is, therefore, useful to be able to follow the branches of various compression/rebound curves for a single soil should it be subjected to loading and unloading. The three parameter model was found to be adequate only for the representation of the compression portion of the curve. Once the compression laboratory data is fit, it is difficult to generate related compression curves beginning at varying stress states as is possible with the four-parameter model.

5.5 Conversion of the Proposed Four-Parameter Compression Curve Equations to the Coefficient of Compressibility and the Coefficient of Volume Change

Typical saturated soil mechanics has represented the compression curve using the constants C_c or C_r depending on the branch of the compression curve. Finite element programs also typically require one of these two constants to represent volume change of the soil. A problem arises in that a soil state may transfer between two branches of the compression curve when moving from one stress state to another. The finite element program then faces the problem of how to move between these two straight-line portions in a smooth and physically realistic way. The four-parameter equation provides a smooth function that can be differentiated to provide a smooth and continuous function for the slope of the compression equation. The differentiated equations for the four-parameter equation are given as follows.

$$a_v(\sigma) \quad C_r \cdot \frac{\sigma}{\sigma_s^2 \cdot \left(1 - \frac{\sigma^2}{\sigma_s^2}\right) \cdot \ln(10)} \quad \frac{2 \cdot \frac{1}{2} \cdot C_c \quad \frac{1}{2} \cdot C_r \cdot \sigma}{\sigma_p^2 \cdot \left(1 - \frac{\sigma^2}{\sigma_p^2}\right) \cdot \ln(10)}$$

Equation 5-11

The differentiated equation represents a continuous function for the coefficient of compressibility, a_v. The slope of the compression curve has also been typically represented as the coefficient of volume change, m_v. The m_v slope of the compression curve is defined by the following equation.

$$m_v = a_v \frac{\sigma}{1 + e_o}$$

Equation 5-12

where: m_v = coefficient of volume change,

a_v = arithmetic slope of the compression curve,

σ = effective stress,

eo = initial void ratio.

Equation 5-11 may then be divided by $(1+e_0)$ to give functions of m_v. The slope of the compression curve has also been referenced as the compression index, Cc. The compression index represents the slope of the compression curve on a semilog scale. The compression index equation for the four-parameter equation is shown below.

$$Cc(\sigma) := -C_r \cdot \frac{10^{\sigma^2}}{\left[\sigma_s^2 \cdot \left[1+\frac{10^{\sigma^2}}{\sigma_s^2}\right]\right]} - 2\cdot\frac{1}{2}\cdot C_c - \frac{1}{2}\cdot C_r \cdot \frac{10^{\sigma^2}}{\left[\sigma_p^2 \cdot \left[1+\frac{10^{\sigma^2}}{\sigma_p^2}\right]\right]}$$

Equation 5-13

Two soils were selected from literature to illustrate the slope of typical compression curves. A Brazil organic silty clay and a Battleford till are shown in Figure 5-27, and Figure 5-28.

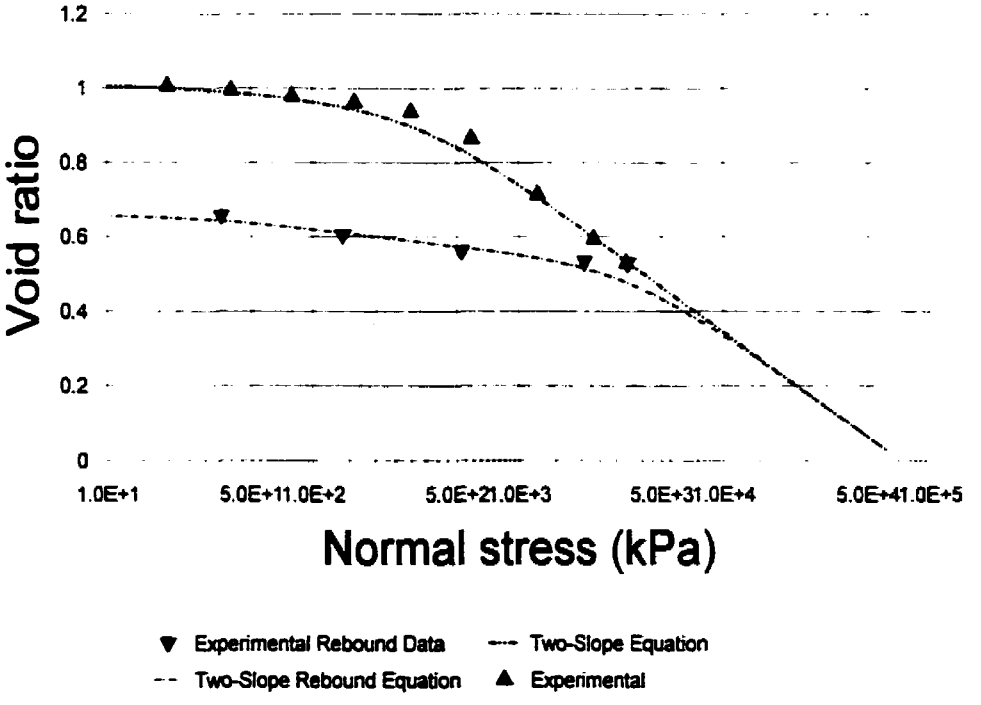

Figure 5-27 Compression curve for a Brazil organic silty clay published by Schmertmann (1953) fit with the four-parameterequation, R^2=0.983 (12533)

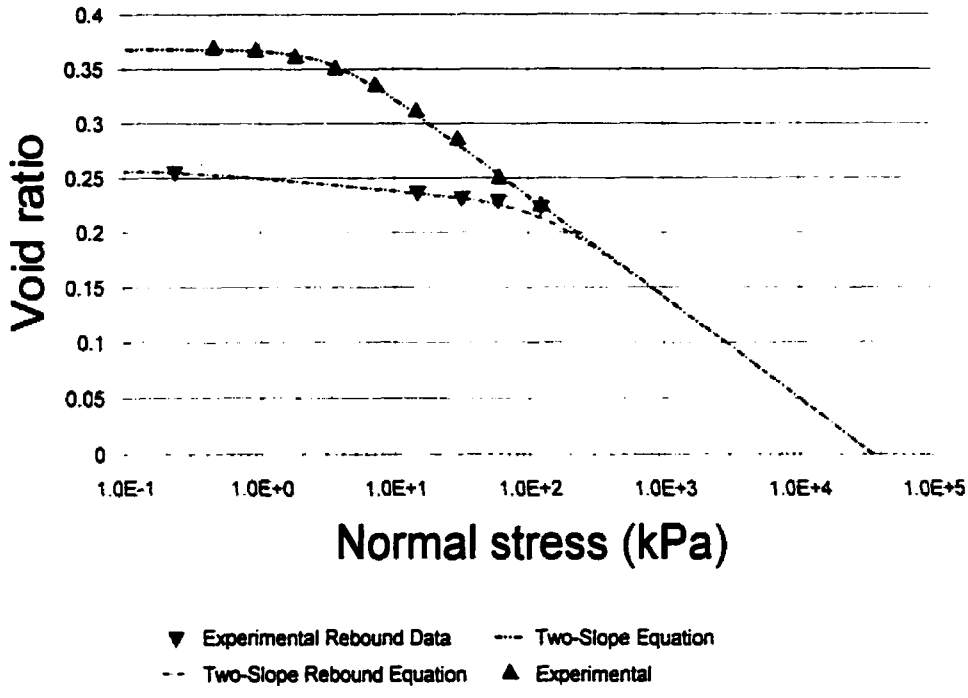

Figure 5-28 Compression curve for a Battleford Till published by MacDonald and Sauer (1970) fit with the four-parameterequation, R^2=0.998 (12385)

The Brazilian organic silty clay and the Battleford Till are shown fitted with the four-parameter equation. It can be seen from Figure 5-25 and Figure 5-26 that the four-parameter equation provides a good fit of the experimental data. The four-parameter equation was then differentiated and the continuous slope of the equation (Figure 5-29) is represented as the compression index, C_c. The equation for C_c may be seen in Equation 5-13. A group of Cc curves were plotted together and may be seen in Figure 5-31.

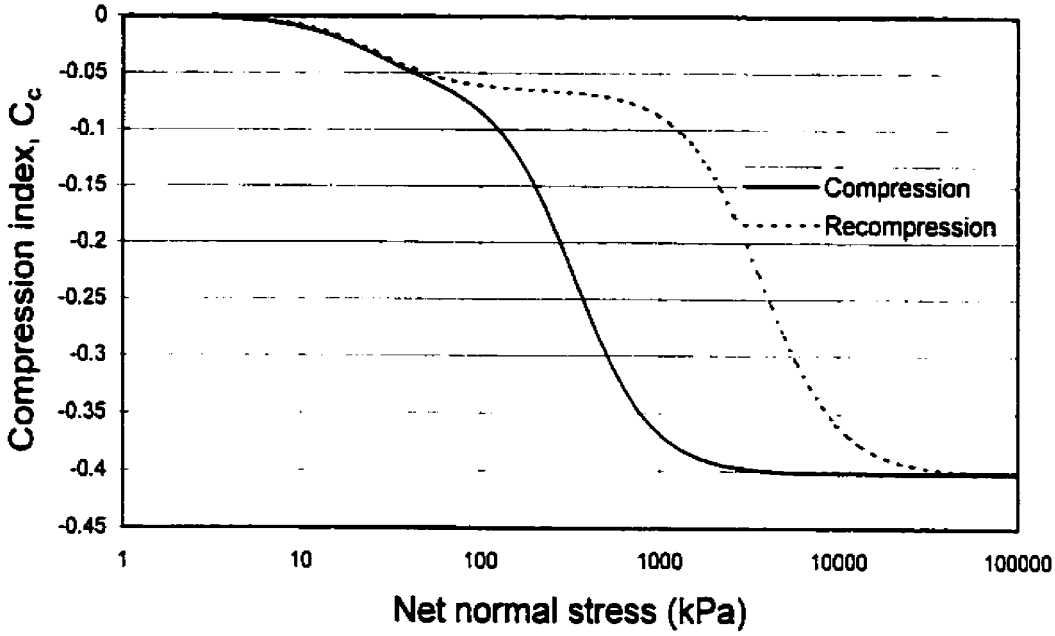

Figure 5-29 Compression index as a function of normal stress for Brazil organic silty clay (12533)

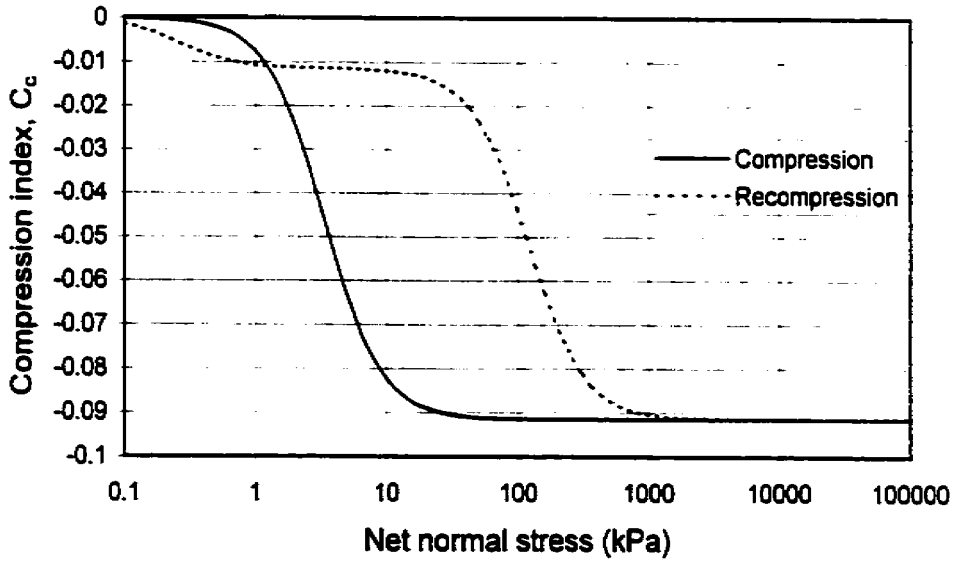

Figure 5-30 Compression index for Battleford Till (12385)

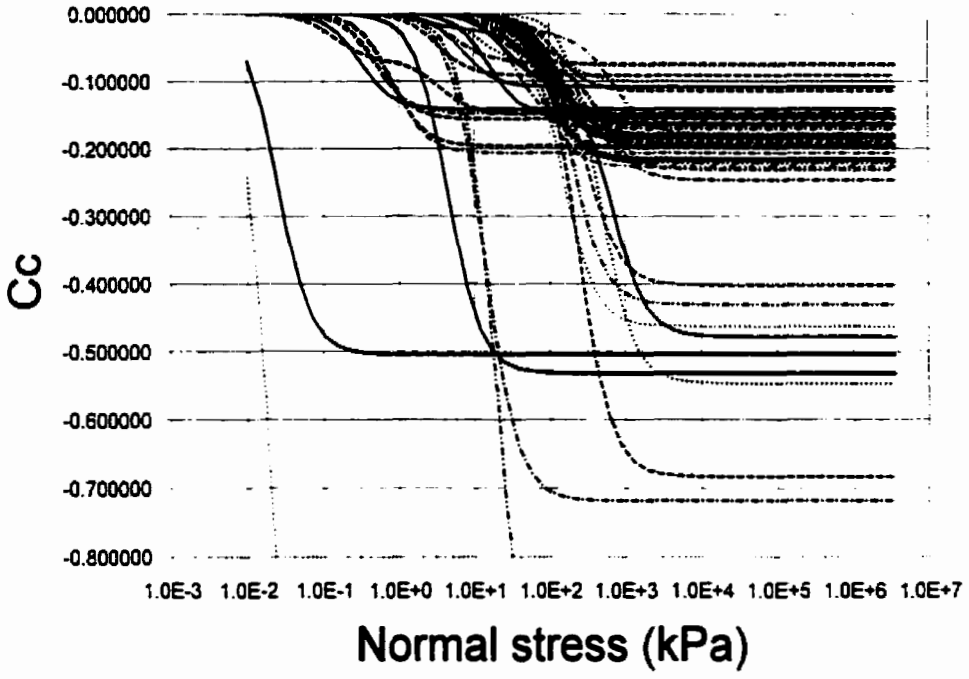

Figure 5-31 Four-parameter functions from a variety of soils illustrating the variance of the compression index, C_c, with normal stress.

5.6 Conversion of the Proposed Three-Parameter Compression Curve Equations to the Coefficient of Compressibility and the Coefficient of Volume Change

As with the four-parameter equation, the three parameter equation may also be differentiated to determine a continuous function for the coefficient of compressibility, a_v. The differentiated function for the three-parameter equation is more complex than that of the four-parameter equation and is presented in Equation 5-14. The coefficient of volume change, m_v, may be determined by dividing Equation 5-14 by $(1+e_o)$. Similarly, the compressibility index, C_c, is represented by a continuous equation presented in Equation 5-15.

$$a_v \sigma_n = \frac{e_o}{h_r \cdot \left(1 - \frac{\sigma_n(j)}{h_r}\right) \cdot \ln\left(1 - \frac{3500000}{h_r}\right)} \cdot \frac{1}{\ln\left(e^{-\left(\frac{\sigma_n(j)}{a}\right)^n}\right)^m} - e_o \cdot \left(1 - \frac{\ln\left(1 - \frac{\sigma_n(j)}{h_r}\right)}{\ln\left(1 - \frac{3500000}{h_r}\right)}\right) \cdot \frac{1}{\ln\left(e^{-\left(\frac{\sigma_n(j)}{a}\right)^n}\right)^m} \cdot \frac{m}{\ln\left(e^{-\left(\frac{\sigma_n(j)}{a}\right)^n}\right)} \cdot \frac{\left(\frac{\sigma_n(j)}{a}\right)^n}{\sigma_n(j) \cdot e^{-\left(\frac{\sigma_n(j)}{a}\right)^n}}$$

Equation 5-14

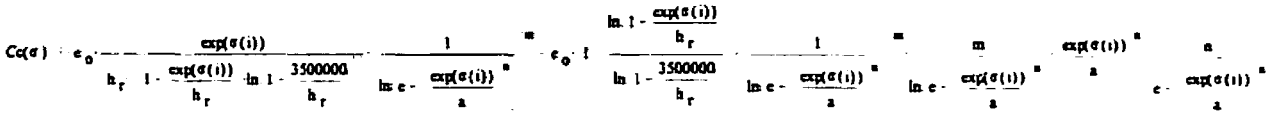

Equation 5-15

5.7 Conversion of the Compressibility Functions to Nonlinear Elastic Parameter Functions

A requirement for the modeling of volume change in soils is Young's Modulus, E. Young's Modulus is defined as $\Delta\sigma/\Delta\varepsilon$. Typical modeling practice has accepted Young's Modulus as a constant. Theoretical development of unsaturated soil mechanics carried out by Fredlund (1964) has shown Young's Modulus to be a function of net normal stress. Theoretically, Young's Modulus is not a constant.

Poisson's Ratio and the slope of the compression curve, m_v, are required for the determination of Young's Modulus. Young's Modulus becomes a function of net normal stress since it is dependent of m_v. The calculation of Young's Modulus is also dependent upon the test method used to determine the compression curve. Relations of Young's Modulus for varying loading conditions can be seen in Table 5-1.

Table 5-1 Coefficients of volume change for various loading conditions

Loading	*Deformation State Variable*	m_i^s
Three-dimensional (General)	$d\varepsilon_v$	$3\left(\frac{1-2\mu}{E}\right)$
Isotropic	$d\varepsilon_v$	$3\left(\frac{1-2\mu}{E}\right)$
Uniaxial	$d\varepsilon_v$	$3\left(\frac{1-2\mu}{E}\right)$

Triaxial (General Case)	$d\varepsilon_v$	$3\left(\frac{1-2\mu}{E}\right)$
Ko-loading (One-dimensional)	$d\varepsilon_v$	$\frac{(1+\mu)(1-2\mu)}{E(1-\mu)}$
Plane Strain (Two-dimensional)	$d\varepsilon_v$	$\frac{2(1+\mu)(1-2\mu)}{E}$
Plane Stress (Two-dimensional)	$d\varepsilon_v$	$2\left(\frac{1-2\mu}{E}\right)$

Other combinations of elasticity variables are possible. For example, Lame's constants may be used (Chou et al., 1967). These constants and their relation to Young's Modulus and Poisson's Ratio are shown in Equation 5-16 and Equation 5-17.

$$G = \frac{E}{2(1+\mu)}$$

Equation 5-16

where: G = modulus of rigidity,

E = Young's modulus,

μ = Poisson's ratio.

$$\lambda = \frac{\mu E}{(1+\mu)(1-2\mu)}$$

Equation 5-17

Both soils selected for analysis in this chapter were tested in an oedometer (K_o). Therefore, the K_o loading condition is used in the calculation of Young's Modulus. A Poisson's Ratio of 0.4 was assumed for the analysis presented here. The Young's Modulus presented as a function of net normal stress for the Brazil organic silty clay and Battleford Till are presented in Figure

5-27 and Figure 5-28 is shown in Figure 5-32. The four-parameter equation was used as the basis for the calculation of Young's Modulus.

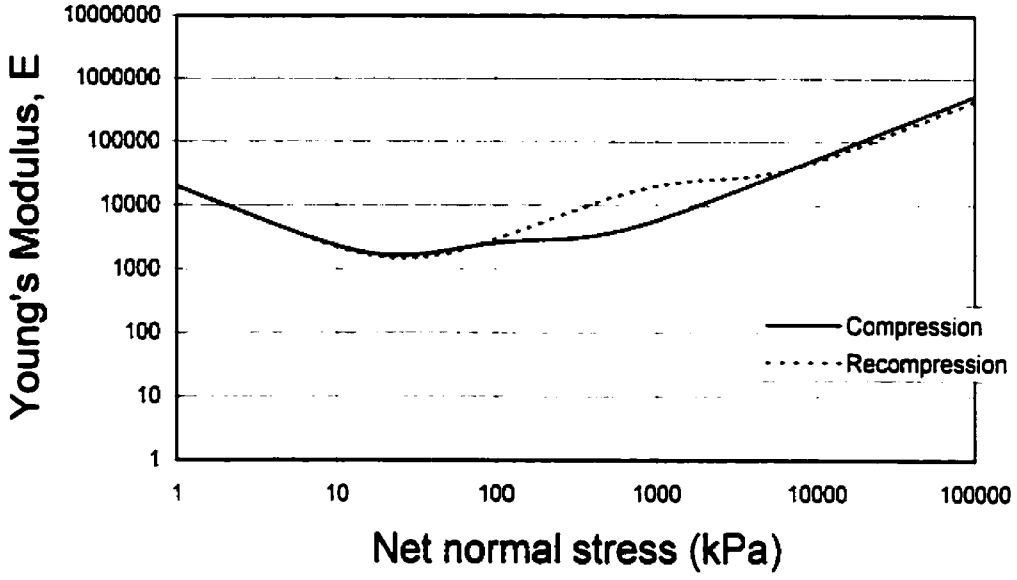

Figure 5-32 E modulus for compression and recompression of Brazil organic silty clay (12533)

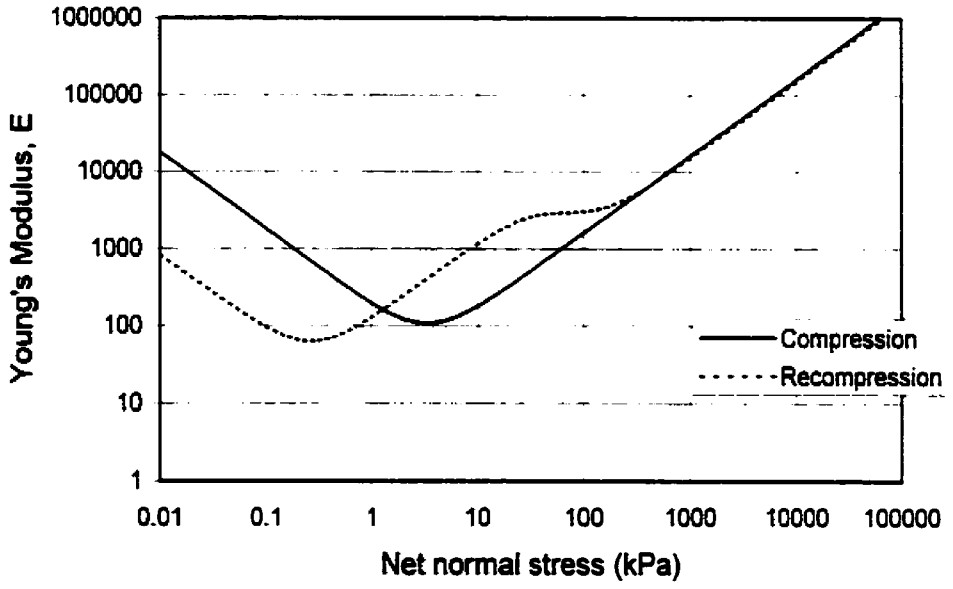

Figure 5-33 E modulus for compression and recompression curve of Battleford Till (12385)

The method presented in Figure 5-32 and Figure 5-33 shows the Young's Modulus to be a continuous smooth equation consistent with the physical laws of soil mechanics (Fredlund, 1993).

5.8 Conclusions

The compression curve has formed the basis for volume-change calculations for saturated soils for many years. A continuous mathematical representation of the compression curve has not been presented in research literature. This chapter presents two continuous mathematical equations capable of fitting the compression curve. The three-parameter equation was found to work satisfactory for the fitting of normal and over-consolidated soils. However, it was noted that the shape of the three-parameter equation did not conform to typical shapes of the compression curve as presented by Terzaghi (1923). The parameters of the three-parameter equation could not be related to physical soil characteristics. The four-parameter equation provided good fits for normally and overconsolidated soils. Once the compression curve is fit with a continuous mathematical representation, a number of transformations are possible. The relationships of coefficient of compressibility, a_v, coefficient of volume change, m_v, and compression index, C_c as well as Young's Modulus, E, may all be represented as a function of net normal stress. The representation of the slope of the compression curve and the Young's Modulus as a function of net normal stress provides an excellent basis for the modeling of volume change of saturated and unsaturated soils.

5.9 References

Brooks R.H. and A.T. Corey,, 1964, Hydraulic Properties of Porous Media, Colorado State Univ. Hydrol. Paper, No. 3,, 27

Brumund, W.F., E. Jonal, and C.C. Ladd, 1976, Estimating in situ maximum past preconsolidation pressure of saturated clays from results of laboratory consolidometer tests, Special Report 163, Transportation Research Board, 4-12

Casagrande A., 1936, The Determination of the Preconsolidation Load and Its Practical Significance, Discussion D-34, Proc. 1st Int. Conf. Soil Mech. Found. Eng., Cambridge, MA, USA, 3, 60-64

Casagrande, A., 1932, The structure of clay and its importance in foundation engineering, Journal of the Boston Society of civil engineers, April, reprinted in Contributions to Soil Mechanics 1925-1940, BSCE, 72-113

Chakrabarti, Sukomal, and Robert G. Horvath, 1986, Conventional Consolidation Tests on Two Soils, ASTM STP 892, Philadelphia, PA, 451-464

Chou P.C., and Pagano N.J., 1967, Elasticity, D. van Nostand Inc., Princeton, N.J.

Clevenger, W.A., 1958, Experiences with loess as a foundation material, Transactions, ASCI, 123, 151-169

El-Sohby, M.A., Deformation of sands under constant stress ratios, Int. Conf. On Soil Mechs and Foundation Eng., Mexico, (Mexico City: Sociedad Mexicana de Mecanica de Suelos), vol. 1, 111-119

Fredlund D.G. H.Rahardjo, 1996, Unsaturated Soil Consolidation Theory and Laboratory Experimental Data, Consolidation of Soils: Testing and Evaluation ASTM STP 892, R.N. Yong and F.C. Townsends, Eds., ASTM, Philadephia, PA, Philadelphia, PA, USA, 154-169

Fredlund, D.G., and Rahardjo, H., 1993, Soil mechanics for unsaturated soils, John Wiley & Sons, Inc., New York, pp. 346-365

Graham, J., M.L. Noonan, and K.V. Lew, 1983, Yield states and stress-strain relationships in a natural plastic clay, Canadian Geotechnical Journal, 20(3), 502-516

Holtz, Robert D. and Kovacs, William D., 1981, An introduction to geotechnical engineering, Prentice-Hall, Inc., Englewood Cliffs, New Jersey

Hough, B.K., 1969, Basic Soils Engineering - Second Edition, The Ronald Press Company, New York

Juarez-Badillo, E., 1981, General compressibility equation for soils, Tenth International Conference on Soil Mechanics and Foundation Engineering, Stockholm, Sweden, pp. 171-178

Juarez-Badillo, Eulalio, 1986, General Theory of Consolidation for Clays, ASTM STP 892, Philadelphia, PA, 137-153

Kaufman, R.I., and W.C. Sherman Jr., 1964, Engineering Measurements for Port Allen Lock, Journal of the Soil Mechanics and Foundations Division, ASCE, Vol. 90, No. SM5, 221-247

Ladd, C.C., Settlement analysis for cohesive soils, Research Report R71-2, Soils Publication 272,, Department of Civil Engineering, Massachusetts Institute of Technology, 107 pp.

Lambe, William T., 1951, Soil Testing, John Wiley & Sons, Inc., New York

Leonards, G.A., Estimating consolidation settlements of shallow foundations, Special Report 163, Transportation Research Board, 13-16

MacDonald A.B. and E. Karl Sauer, 1970, The engineering significance of Pleistocene stratigraphy in the Saskatoon area, Saskatchewan, Canada, Canadian Geotechnical Journal, Vol. 7, No. 116, 116-126

Parry, R.H.G., 1958, Correspondence: On the yielding of soils, Geotechnique, 8(4), 183-186

Poorooshasb, H.B., I. Holubec, and A.N. Sherbourne, 1967, Yielding and flow of sand in triaxial compression: Parts II and III, Canadian Geotechnical Journal, 4(4), 376-397

Roscoe, K.H., A.N. Schofield, and C.P. Wroth, 1958, On the yielding of soils, Geotechnique, 8(1), 22-52

Schmertmann, J.H., 1955, The undisturbed consolidation behavior of Clay, Transactions, ASCI, 120, 1201-1233

Tatsuoka, F., and K. Ishihara, 1974, Yielding of sand in triaxial compression, Soils and Foundations, 14(2), 63-76

Tavenas, F. G. Blanchette, S. Leroueil, M. Roy, and P. La Rochelle, 1975, Difficulties in the in situ measurement of Ko in soft sensitive clays, Proc. Conf. On In Situ Measurement of Soil Properties, North Carolina State Univ., Raleigh, 1, 450-476

Tavenas, F., J-P des Rosiers, S. Leroueil, P. LaRochelle, and M. Roy, 1979, The user of strain energy as a yield and creep criterion for lightly overconsolidated clays, Geotechnique, 29(3), 285-303

Taylor, D.W., 1948, Fundamentals of Soil Mechanics, John Wiley & Sons, Inc., New York, 700 pp.

Terzaghi, Karl, Ralph B. Peck, and Gholamreza Mesri, 1996, Soil Mechanics in Engineering Practice - Third Edition, John Wiley & Sons, New York

von Fay, Kurt F., Jack G. Byers, and Betsy A. Kunzer, 1986, Desktop Computer Application for Consolidation Testing and Analysis, ASTM STP 892, Philadelphia, PA, 217-235

Wood, David Muir, 1990, Soil Behaviour and Critical State Soil Mechanics, Cambridge University Press, New York

Yong, R.N., and F.C. Townsend, 1985, Consolidation of Soils: Testing and Evaluation, ASTM Special Technical Publication, Philadelphia, PA

CHAPTER 6.0 The Constitutive Meaning and the Representation of the Shrinkage Curve

6.1 Introduction

The consequences of shrinkage of soils on the performance of structures and earth structures is significant. Shrinkage under highway embankments and subgrades results in soil cracking and potential loss of stability. Expansive soils sometimes shrink causing more damage than the swelling of the soil. Analysis of the shrinkage of a soil is related to the modeling of volume change of soils. Numerical modeling requires that there be a mathematical description of the shrinkage behavior of a soil. This chapter presents methods for representing and estimating the shrinkage curve. As well as, an explanation is presented on the meaning of the shrinkage curve as it relates to the volume change behavior of a soil.

An analysis of the shrinkage processes in clays is also significant because of the impact that shrinkage cracks and surface subsidence have on physical and chemical processes in clay soils. (Bronswijk, 1990). An example is water and solute transport. The movement of water and solutes in clay soils is determined largely by shrinkage cracks and other macropores. Buildings and pavements on clay soils can be seriously damaged by vertical ground movements.

Shrinkage also has an application in the area of soil science. Applications include the estimation of the water content profile which is relevant to irrigation scheduling (Mitchell, 1992). Field surface shrinking and swelling under rainfall, as well as the effects of plant root systems on shrinkage, are also areas involving the application of the shrinkage curve.

Many disciplines in engineering, such as road design and construction, are primarily concerned with the soil above the water table where pore-water pressures are generally negative with respect to atmospheric pressure (Croney, 1961). Such a zone is commonly referred to as the "vadose zone" where the soils remain unsaturated. The general physical behavior of soils, including moisture and heat transfer, shear strength, deformation, and volume change, are

highly dependent upon the degree of saturation of a soil (Sibley, 1993). An example is the thermal conductivity of soils which is directly related to the amount of air in the soil pores (Salmone and Kovacs, 1984).

Many mathematical equations have been presented for the representation of the soil-water characteristic curve and their relative performance has been analyzed by Sillers (1996). The soil-water characteristic curve has also been shown to be related to other soil functions (Fredlund, 1993). Methods for estimating the soil-water characteristic curve has also been reviewed (Fredlund, 1998). This chapter presents calculations using the soil-water characteristic curve to compute the volume change function and the soil-water characteristic curve as a function in terms of volumetric water content.

This chapter emphasizes the theoretical character of the shrinkage curve and its relationship to other unsaturated soil property functions. A mathematical equation describing the shrinkage curve, as well as a theoretical method for estimating the shrinkage curve, is presented. The subsequent development of volume-mass constitutive relations from the shrinkage curve is also presented.

6.2 Literature Review

Tempany, (1917) investigated the character of shrinkage as it relates to the drying of soils. Haines (1923) delineated different shrinkage phases as a soil dries. Others such as, Keen, (1931), Stirk (1954), and Bronswijk (1991) also assisted in defining the following shrinkage process of soils,

1. **Structural shrinkage**: when a saturated soil began to dry, large water-filled pores may began to empty without any accompanying volume change
2. **Normal shrinkage**: occurs when volume decrease of soil aggregates is equal to the loss of water. The soil aggregates remain fully saturated.

3. **Residual shrinkage**: occur in the drying process when the volume of soil aggregates decreases and water loss exceeds volume decrease. Air enters the pores of the soil aggregates at this stage.
4. **Zero shrinkage**: occur when the soil particles have reached their densest configuration. The water loss is equal to the increase of the air volume in the soil aggregates and the aggregate volumes do not decrease any further.

Extensive laboratory testing has been performed to determine the relationship between water content and void ratio for clay pastes, soil aggregates, soil clods, and soil cores of various sizes. Field experiments of shrinkage behavior, however, are scarce. It is known that shrinkage involves the a process of densifying soil under capillary pressures (or increasing soil suction). During shrinking, volume change occurs as long as the capillary forces are larger than the internal resistance to volume change (Subba Rao, 1985). The suction pressures which can be obtained within a drying soil can reach a total suction level of 1,000,000 kPa (Fredlund, 1993; Wilson, 1990).

The amount of shrinkage a soil experiences depends on a numerous factors such as the percentage of clay in the soil, the type of clay mineral, the mode of geological deposition, the particle arrangement or structure, the overburden pressure, the degree of weathering, the exchangeable cations, the orientation of soil fabric, and the initial water content (Yong et al. 1966, Seed et al. 1960, Dejong et al 1965, Lambe 1958).

The effect of each of the above factors on shrinkage has been documented to various degrees over the years. Haines (1923) appears to have been the first to present a complete interpretation of the shrinkage curve. The interpretation of the shrinkage curve made use of two straight lines such as shown in Figure 6-1. Haines (1923) defined portion C-B of the shrinkage curve as **normal shrinkage** where the volume of water evaporated was equal to the reduction in the total volume of the specimen. Portion B-A of the shrinkage curve represented residual shrinkage where part of the water lost was replaced by air.

The phenomenon of shrinkage was first examined from an engineering point of view by

Terzaghi (1925). The similarity between shrinkage of a soil and its compression were identified. The primary difference between the compression of a soil and the shrinkage of a soil is that compression could be carried out indefinitely while shrinkage of the soil eventually halted upon complete desaturation.

A comprehensive study of the shrinkage phenomenon was carried out by Stirk (1953). The influence of structure and texture upon shrinkage was assessed. Residual shrinkage was assumed to commence at suction levels drier than the wilting point of plants (1500 kPa). It was observed that there was a relatively unique relationship between soil suction at the end of shrinkage and the percent clay (Figure 6-2). Stirk (1953) also studied the influence of structure on the various types of shrinkage.

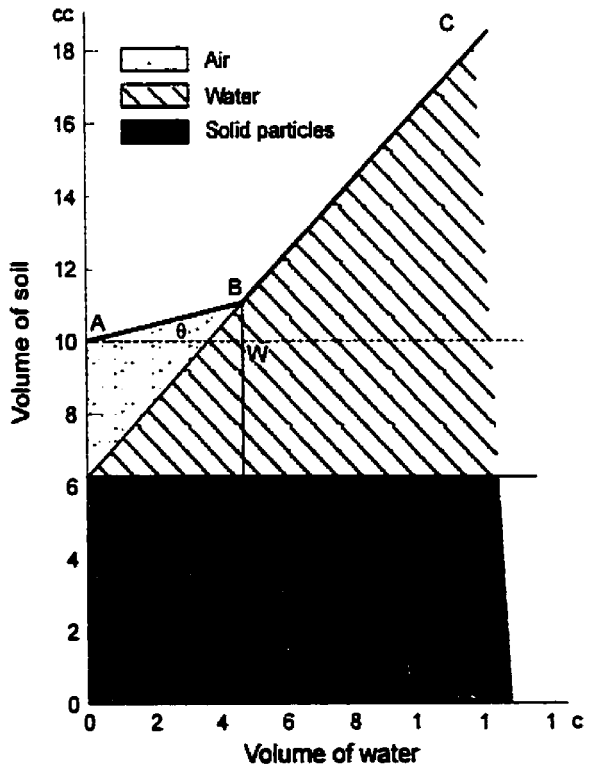

Figure 6-1 The shrinkage curve as defined by Haines (1923).

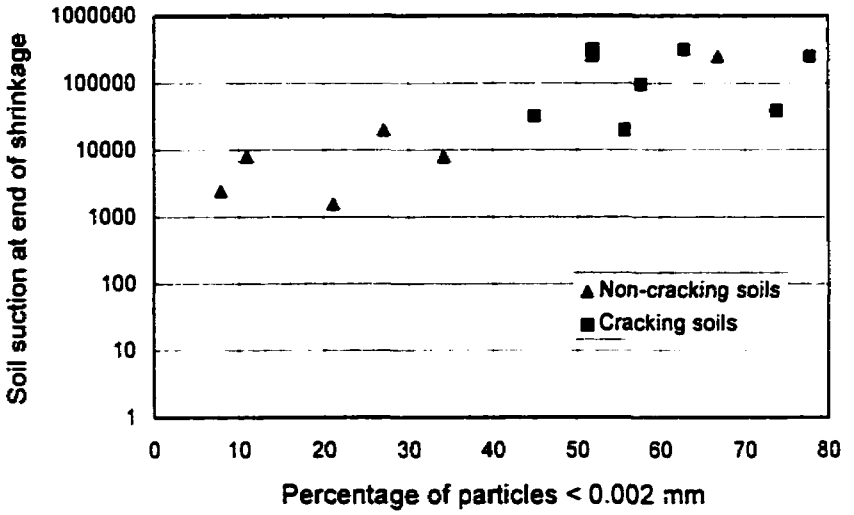

Figure 6-2 Influence of percent clay on soil suction at shrinkage limit (Stirk, 1953)

Croney (1961) summarized methods of measuring soil suction that had been developed at the Road Research Laboratory. Changes in suction were related to the volume change behavior of soils. The application of soil suction in soil mechanics was documented. The influence of texture and clay content on shrinkage was studied by De Jong (1965). Soil specimens were prepared in the laboratory with varying proportions of Leda clay and glass beads. The total shrinkage per unit weight of clay in the mixtures increased with decreasing clay content. It was observed that the clay in parallel orientation around glass beads had a higher water content than the remainder of the clay. An almost linear relationship was found between the water content at the shrinkage limit and the percent clay.

Sridharan (1971) discussed the physical mechanism involved in the process of shrinkage in a clay soil. The effective stress concept was modified in an attempt to explain shrinkage behavior. Sridharan (1971) came to the following conclusions: (1) shrinkage void ratio increases as the effective stress increases and vice versa, (2) shrinkage void ratio decreases as the dielectric constant of the pore medium increases, (3) a relatively oriented soil fabric has a higher electrical repulsive potential and hence a lesser effective stress, thereby yielding larger shrinkage, and (4) an externally applied load induces larger shrinkage than shrinkage with no load applied.

Interest in the movement of clays undergoing heave or shrinkage under foundations or pavements has resulted in significant research efforts. Lytton (1970) produced methods of estimating soil properties and modeling the movement of shrink or swell in soils using finite element. Coupled unsaturated moisture flow and elasticity finite element allowed the modeling of soil suctions at various sites around the state of Texas. It was also demonstrated by Lytton (1995) that interest remains high in the modeling of moisture flow under pavements.

The character of the shrinkage curve has been established for a wide range of soils. This chapter attempts to extend the knowledge on the shrinkage curves by providing a mathematical representation of the shrinkage curve. The physical meanings of each of the curve parameters assists in the quantification of soil shrinkage parameters. An estimation method is also presented that allows for a suitable estimation of the shrinkage curve to be obtained where experimental data is limited.

Little research has been done regarding the application of the shrinkage curve towards the formulation of unsaturated soil constitutive relationships. The fairly complete analysis of the shrinkage curve functions has been carried out by Marinho (1994). This chapter extends the work of Marinho (1994), using the mathematical representation of the shrinkage curve and illustrating its application to unsaturated soil constitutive relationships.

6.3 Shrinkage Theory for Soils

Shrinkage is usually represented as either the inverse of dry density of a soil (i.e., volume per 100 grams of dry soil) versus water content, or void ratio versus water content. A plot showing typical representations of the shrinkage curve can be seen in Figure 6-3. The three basic types of shrinkage behavior that an initially saturated specimen can exhibit are shown in Figure 6-4 as curves A, B, and C. The particle size distribution and the stress history of the soil are the primary factors controlling shrinkage behavior.

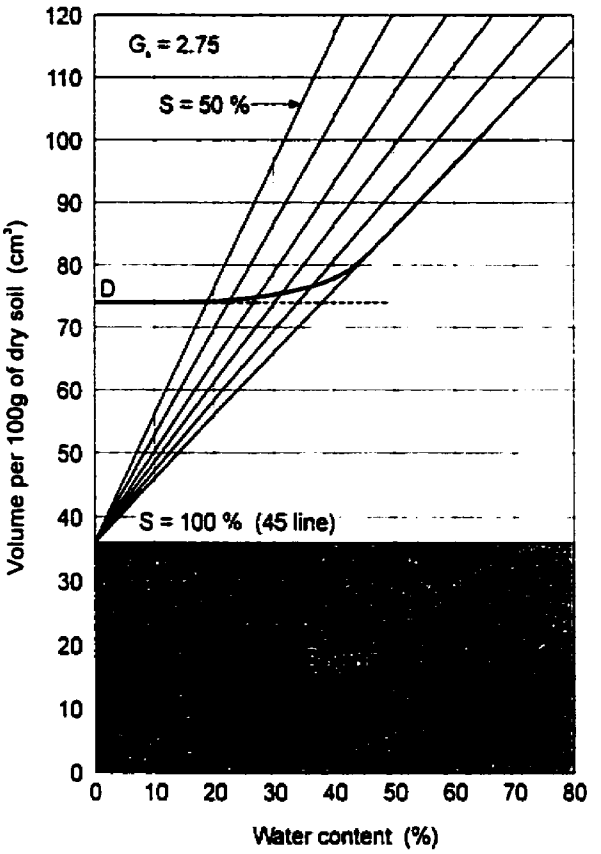

Figure 6-3 Drying phenomenon with theoretical lines for a constant degree of saturation (Marinho, 1994).

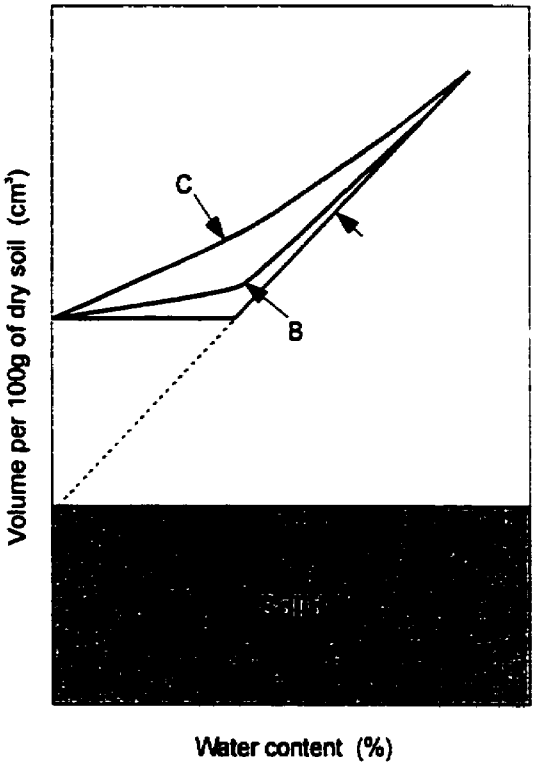

Figure 6-4 Three basic characteristics of shrinkage curves (Marinho, 1994).

The data collected for analysis in this chapter represent three different initial states. Soils were found to be either i) *undisturbed samples from the field*, ii) *compacted specimens*, or iii) *slurred/remolded specimens at the liquid limit*. The analysis presented in this chapter represents the findings using data from each of these three initial states.

The typical behavior of the drying of a slurred soil can be seen in Figure 6-5. The soil sample is fully saturated at the beginning of the test. The sample follows the saturation line until air begins to enter the soil voids. This point is termed the General Air Entry (GAE) point. As the soil continues to dry, it reaches the minimum void ratio at which there is no further volume change. The water content at the intersection between the minimum void ratio and the saturation line is called the Shrinkage Limit. The pattern of behavior observed in soils that are dried from degrees of saturation less than 100% is shown in Figure 6-6.

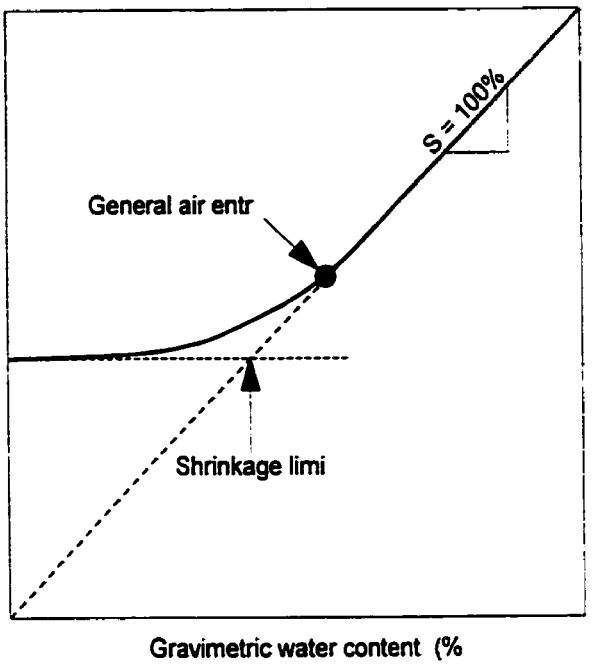

Figure 6-5 Volume-mass relationships for the drying curve of an initially slurried soil specimen..

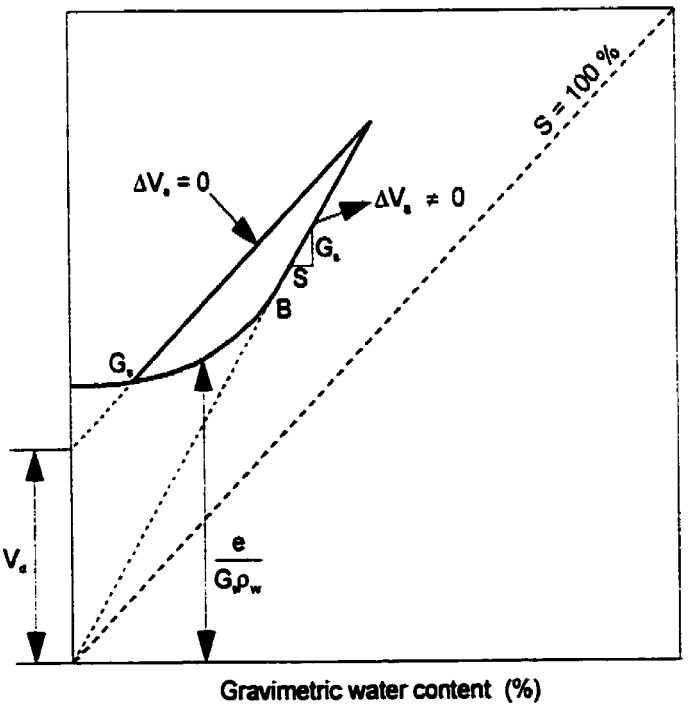

Figure 6-6 Volume-mass shrinkage relationship for an unsaturated soil specimen. G_s=specific gravity, S=saturation, e=void ratio, V_a=volume of air.

6.4 Development of the Shrinkage Equation

A database of soil shrinkage curves was assembled from research literature to characterize a variety of possible shrinkage curves. Soils were organized according to the soil state at the beginning of the shrinkage test. Because of the influence of structure on the test results, soils were organized and grouped as i) *undisturbed*, ii) *compacted*, or iii) *slurried near the liquid limit*. Figure 6-7 shows a group of soils from the dataset used in the analysis.

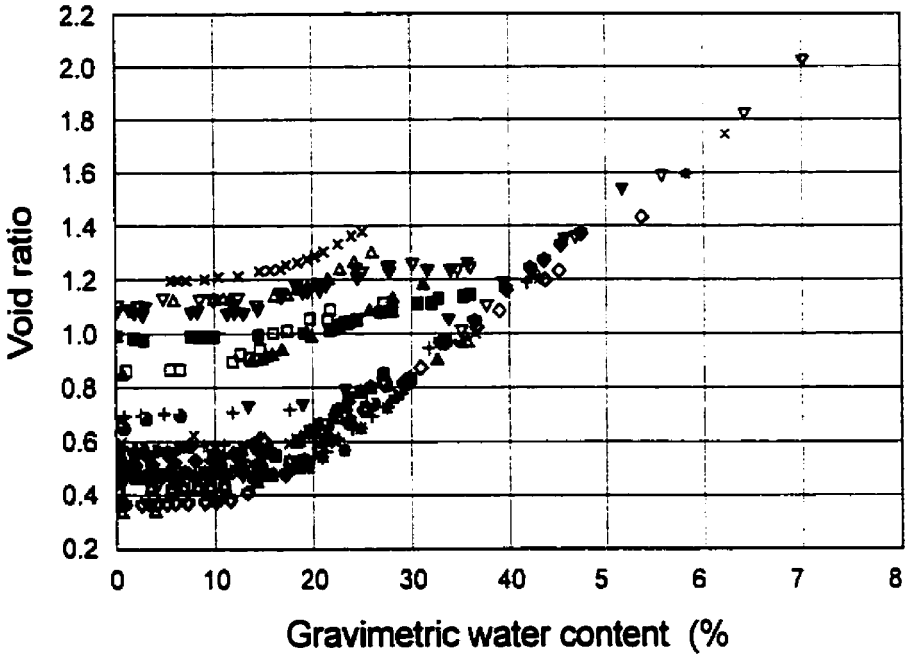

Figure 6-7 Subset of dataset used to characterize soil shrinkage behavior.

A reasonable assumption for the shape of the shrindkage curve is hyperbolic. The hyperbolic equation was, therefore, adapted to represent the character of the curves. The desire was to develop an equation having parameters with physical meaning. The equation utilized is as follows:

$$e(w) = a_{sh}\left[\frac{w^{c_{sh}}}{b_{sh}{}^{c_{sh}}} + 1\right]^{\left(\frac{1}{c_{sh}}\right)}$$

Equation 6-1

where: a_{sh} = the minimum void ratio, e_{min},

b_{sh} = slope of the line of tangency,

c_{sh} = curvature of the shrinkage curve,

and $\frac{a_{sh}}{b_{sh}} = \frac{G_s}{S}$ = constant for a specific soil.

A non-linear, least-squares fitting algorithm was used to fit the equation to various data sets. The results of a typical fit can be seen in Figure 6-8. Soils with varying initial saturation levels can also be represented with the above equation as seen in Figure 6-9.

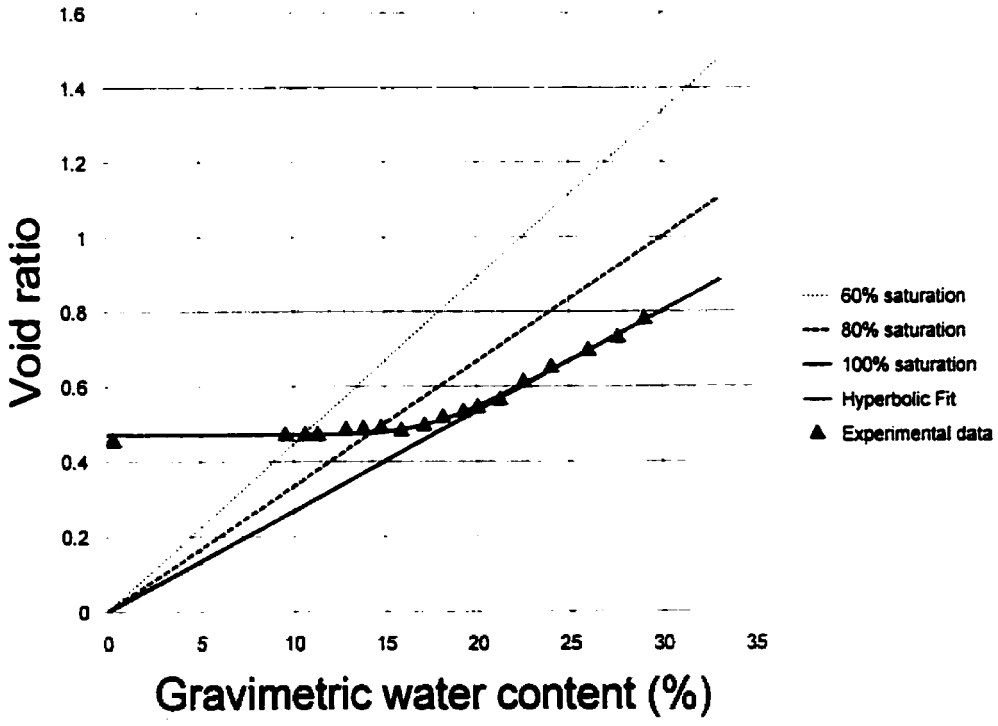

Figure 6-8 Fit of London Clay from Croney and Coleman (1954) using the proposed shrinkage equation with parameters; a_{sh} = 0.47, b_{sh} = 0.176, c_{sh} = 10.56, R^2=0.994 (12398)

6.5 Study of the Parameters Associated with the Shrinkage Equation.

The shrinkage curve equation appears to be general enough to fit a variety of shrinkage curves. The effects of soil structure and initial degree of saturation can be accommodated with the proposed equation. It is also noted that the soil parameters have physical meaning.

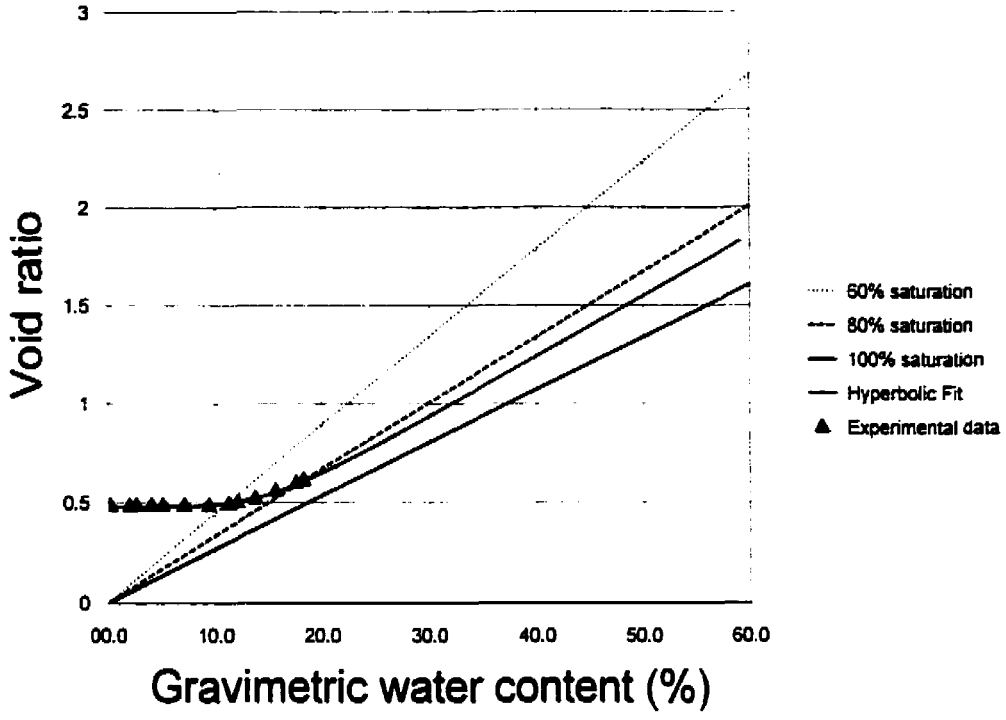

Figure 6-9 Fit of Silty Clay from Russam (1958) at an initial degree of saturation less than 100% with parameters; $a_{sh} = 0.477$, $b_{sh} = 0.154$, $c_{sh} = 5.03$, $R^2=0.992$ (12427).

The a_{sh} parameter represents the minimum void ratio possible from the shrinkage of the soil. It can be seen from Equation 6-2 that if degree of saturation, S, is held constant, the relationship between void ratio and gravimetric water content will be linear. It is also related to the initial volume-mass properties of the soil sample as shown in Equation 6-3. Equation 6-3 is developed based on the definition of a hyperbola. The slope of the tangent line must be equal to a_{sh}/b_{sh}. The effect of varying the a_{sh} parameter can be seen in Figure 6-10.

$$wG_s = Se$$
$$e = w\frac{G_s}{S}$$

Equation 6-2

$$\frac{a_{sh}}{b_{sh}} = \frac{G_s}{S}$$

Equation 6-3

The influence of the b_{sh} parameter can be seen in Figure 6-11. The b_{sh} parameter is taken to be equal to the slope of the degree of saturation line on the shrinkage plot. Equation 6-3 dictates that once the minimum void ratio of a soil is known, the b_{sh} parameter can be calculated. The b_{sh} parameter is then considered a fixed parameter when fitting the equation to experimental data by a least-squares analysis.

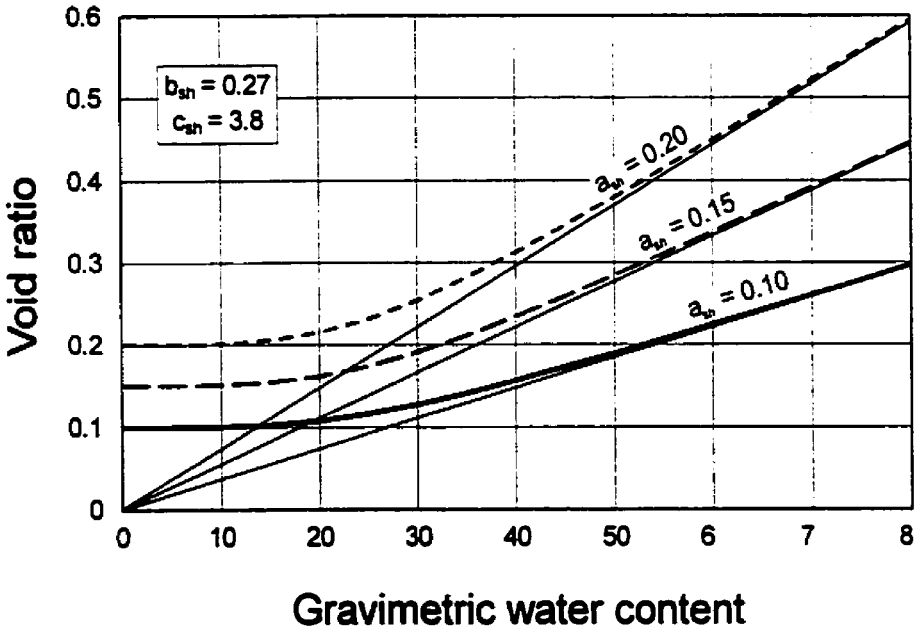

Figure 6-10 Effect of varying the a_{sh} parameter on the shrinkage equation.

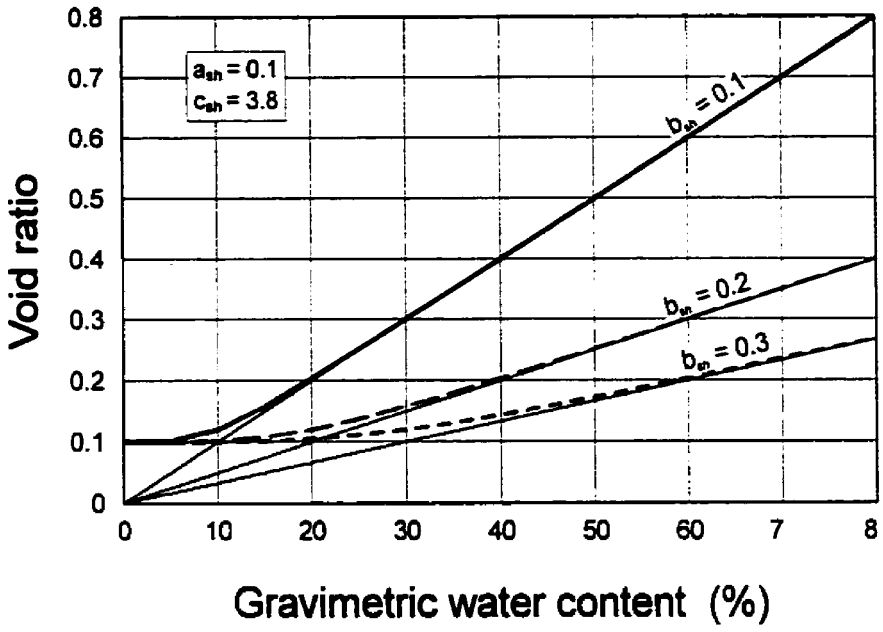

Figure 6-11 Effect of varying the b_{sh} parameter on the shrinkage equation.

The c_{sh} equation parameter controls the rate of curvature of the shrinkage curve as the soil begins to desaturate. The variance of the c_{sh} parameter allows for the fitting of the three basic types of drying behavior described by Marinho (1994) in Figure 6-4. The effect of varying the c_{sh} parameter can be seen in Figure 6-12.

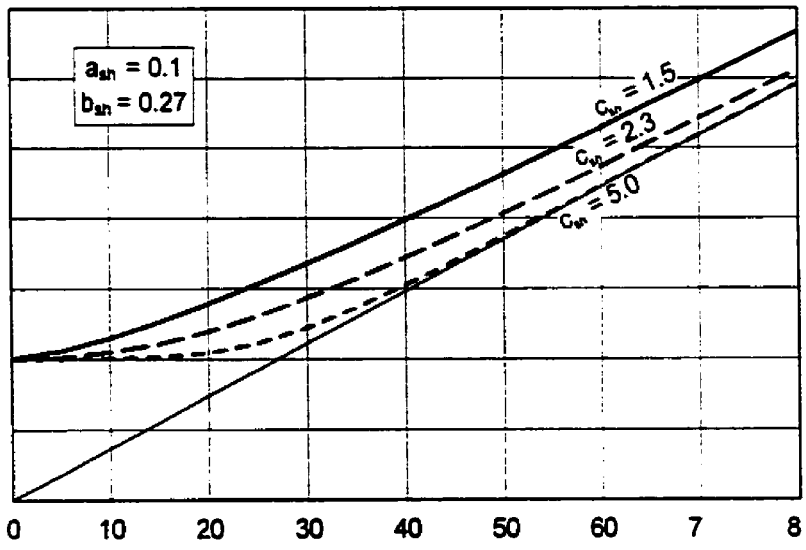

Figure 6-12 Effect of varying the c_{sh} parameter on the shrinkage equation.

6.6 Estimation of the Shrinkage Curve

The volume change in a soil specimen is generally not measured when performing a laboratory test for the soil-water characteristic curve. The experimental data associated with the soil-water characteristic curve is generally the gravimetric water content versus soil suction. Since volume change is generally not undertaken, the shrinkage curve can be used to estimate the void ratio versus soil suction relationship. This section presents a method whereby the shrinkage curve can be used to determine the void ratio versus soil suction relationship.

The amount of shrinkage a soil will experience depends on many factors such as the percentage of clay, the type of clay mineral, the mode of geological deposition, the particle arrangement or soil structure, the overburden pressure, the degree of weathering, the exchangeable cations, the orientation of soil fabric, and the initial water content. The estimation technique presented in this chapter primarily takes into account the effects of soil structure and plasticity.

A dataset of shrinkage curves published in journal papers were selected and best-fit with the proposed equation for the shrinkage curve. Since the ratio between the a_{sh} and b_{sh} equation parameters is fixed by the degree of saturation, S, and specific gravity, G_s, the two parameters that are allowed to vary are a_{sh} and c_{sh}. When the shrinkage curves were grouped according to their initial states (i.e., undisturbed or slurried), a consistency in the c_{sh} parameter was noted. The average value of the c_{sh} parameter for undisturbed soil specimens was 9.57 with a standard deviation of ±9.33. The average value of the c_{sh} parameter for initially slurried soil specimens was 25.31 with a standard deviation of ±25.41. Finally, the average value for the c_{sh} parameter for compacted soil specimens was 8.47 with a standard deviation of ±3.56.

The minimum void ratio or a_{sh} equation parameter can be estimated from data presented by Holtz and Kovacs (1981) as shown in Figure 6-13. The shrinkage limit is a valuable soil parameter that may be used to estimate residual water content as well as the minimum void ratio (Biwei et al., 1998). A correlation is presented that allows for the estimation of the shrinkage limit once the plastic limit of the soil has been measured. The dataset presented in

this chapter was plotted along with the data as presented by Holtz and Kovacs (1981) and can be seen in Figure 6-14. Linear regression was performed on the two datasets provided by Holtz and Kovacs (1981) and on the compacted soil data. The linear regression models were then used as estimators for the a_{sh} curve parameter. Linear representation of the shrinkage limit versus plastic limit allowed for higher R^2 values than similar logarithmic straight line representation with a power series equation.

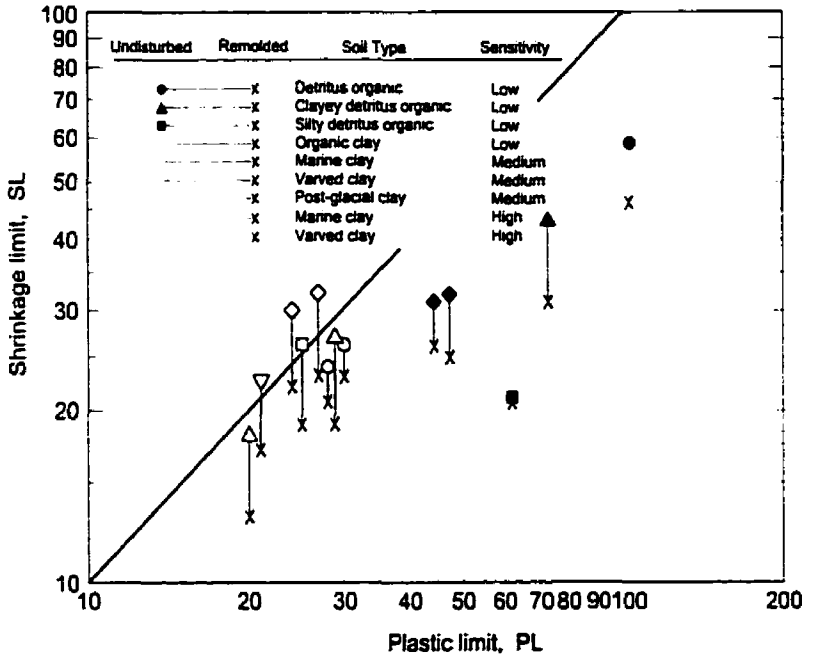

Figure 6-13 Relationship between the shrinkage limit and the plastic limit for various soils (Holtz and Kovacs, 1981).

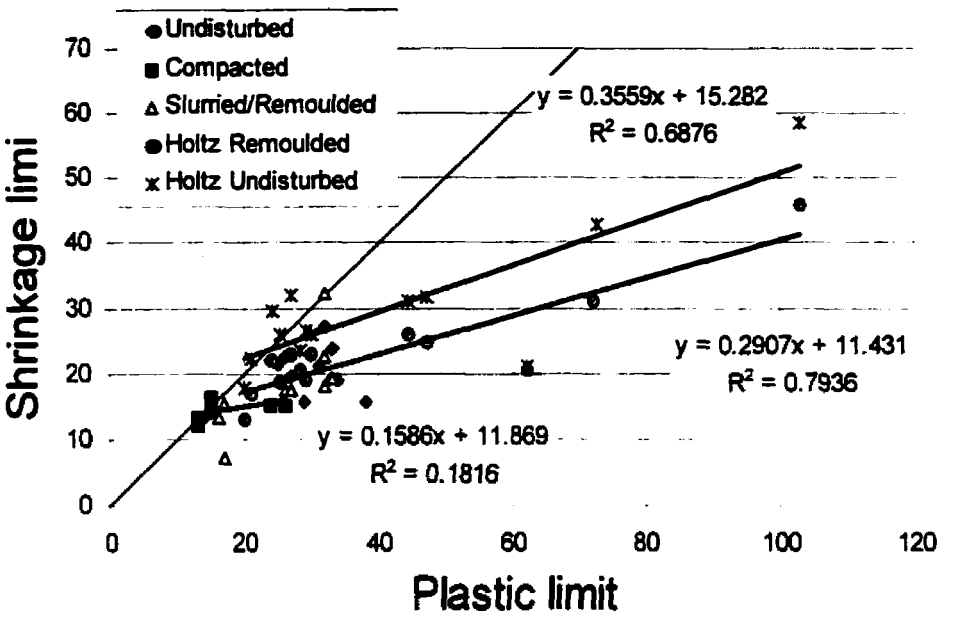

Figure 6-14 Relationship between the shrinkage limit and the plastic limit for soils in the current dataset and soils from Holtz and Kovacs (1981).

The results of the above estimation technique were applied to a randomly selected group of the soils in the dataset. The results of the estimation can be seen in Figure 6-15, Figure 6-16, Figure 6-17, and Figure 6-18. In summary, the estimation techniques worked well to estimate the shape of the shrinkage curve but worked poorly to estimate the minimum void ratio for most soils. The most critical parameter in the estimation of the shrinkage curve is the minimum void ratio, a_{sh}. It is recommended that the minimum void ratio be experimentally measured for the soil being studied. The c_{sh} provides the shape of the shrinkage curve. The physical difference in the shrinkage properties produced by varying the c_{sh} parameter was found to be minimal. As such, the estimation of the c_{sh} parameter was considered reasonable. A more complete dataset would allow for an extended analysis of the estimation technique.

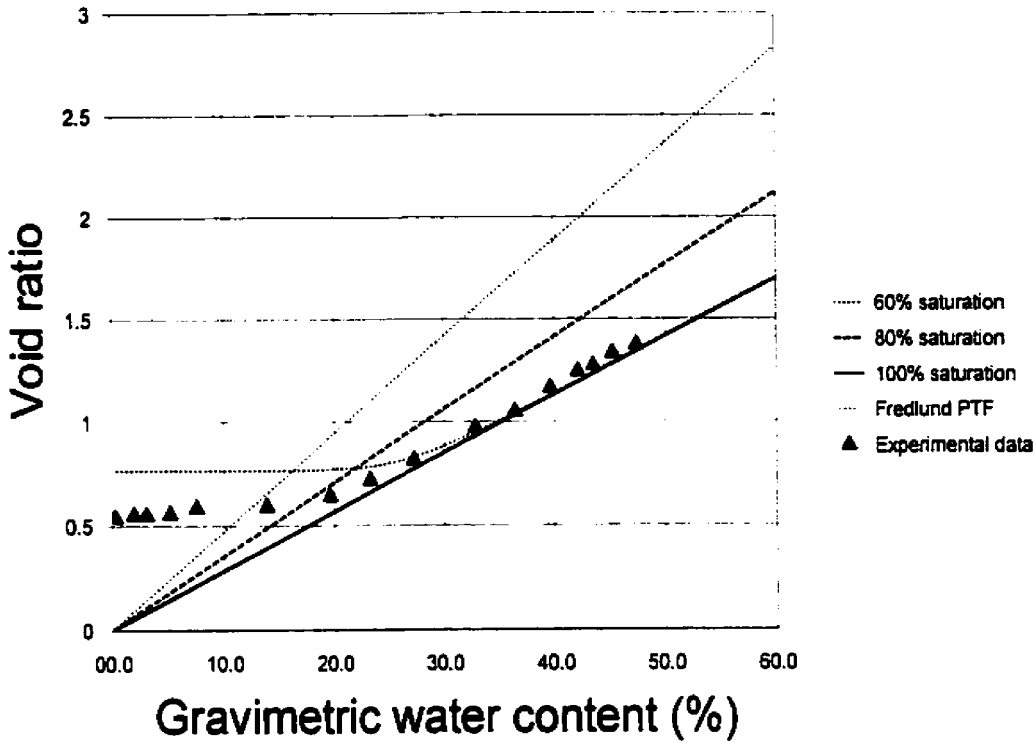

Figure 6-15 Results of shrinkage pedo-transfer function for a heavy clay originally published by Russam, 1958, a_{sh}=0.765, b_{sh}=0.27, c_{sh}=9.57, R^2=0.818 (12431)

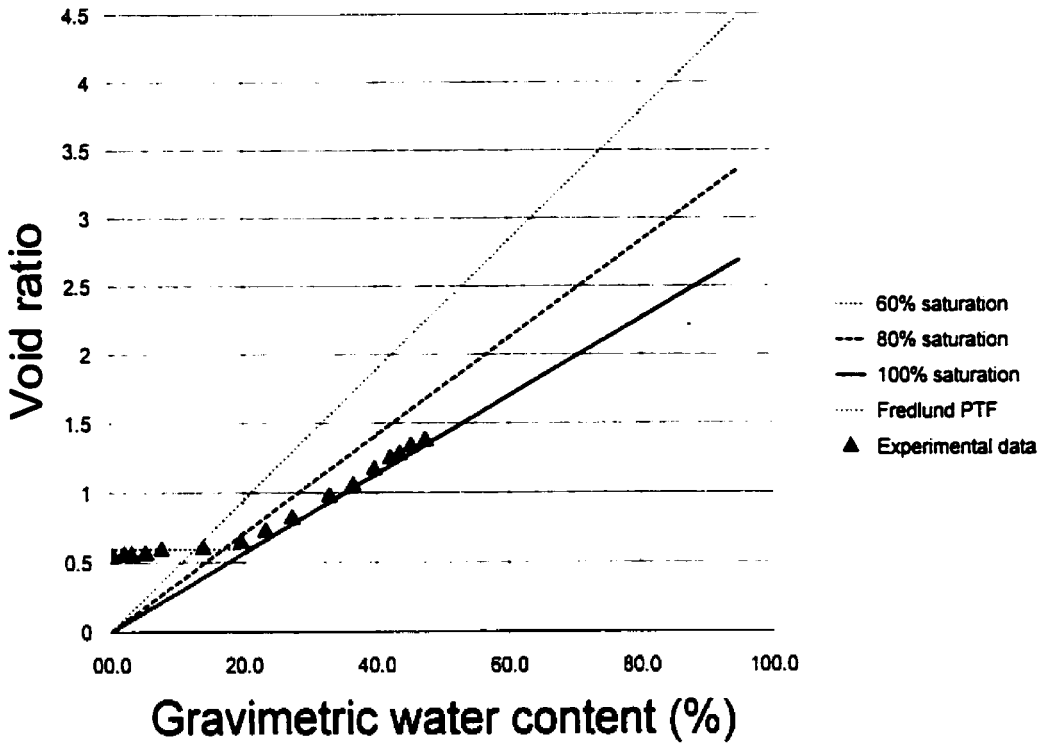

Figure 6-16 Results of shrinkage pedo-transfer function for a heavy clay originally published by Russam, 1958, a_{sh}=0.595, b_{sh}=0.21, c_{sh}=25.31, R^2=0.983 (12435)

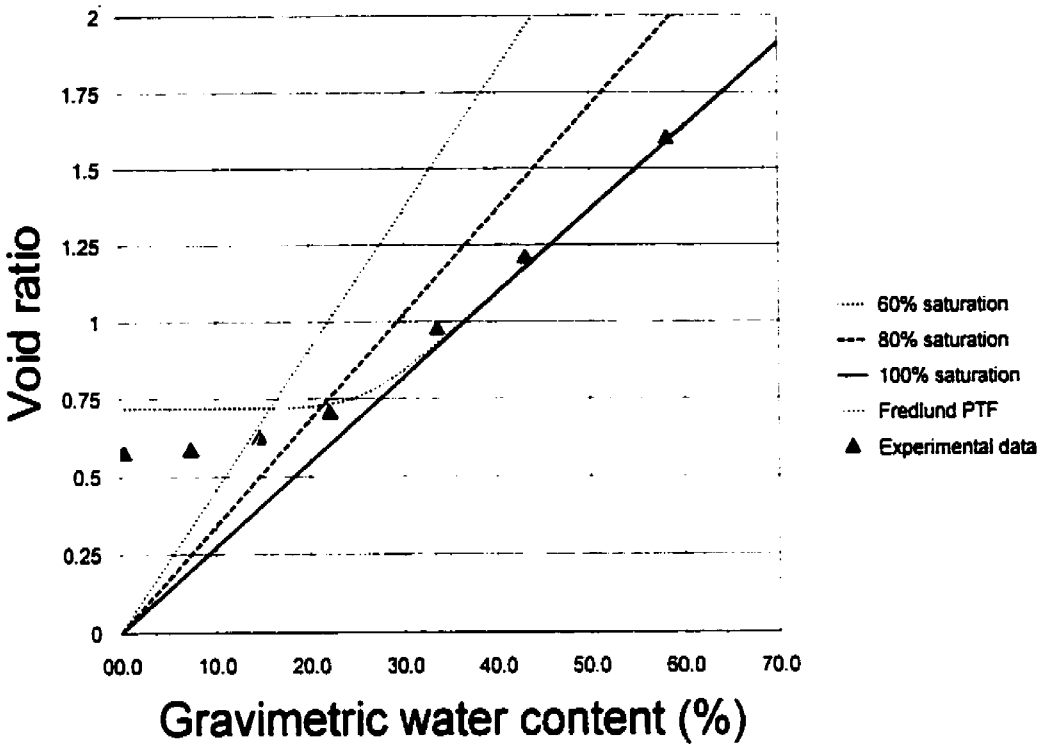

Figure 6-17 Results of shrinkage pedo-transfer function for a oligocenic clay originally published by Nascimento, 1961, a_{sh}=0.718, b_{sh}=0.26, c_{sh}=9.57, R^2=0.941 (12436)

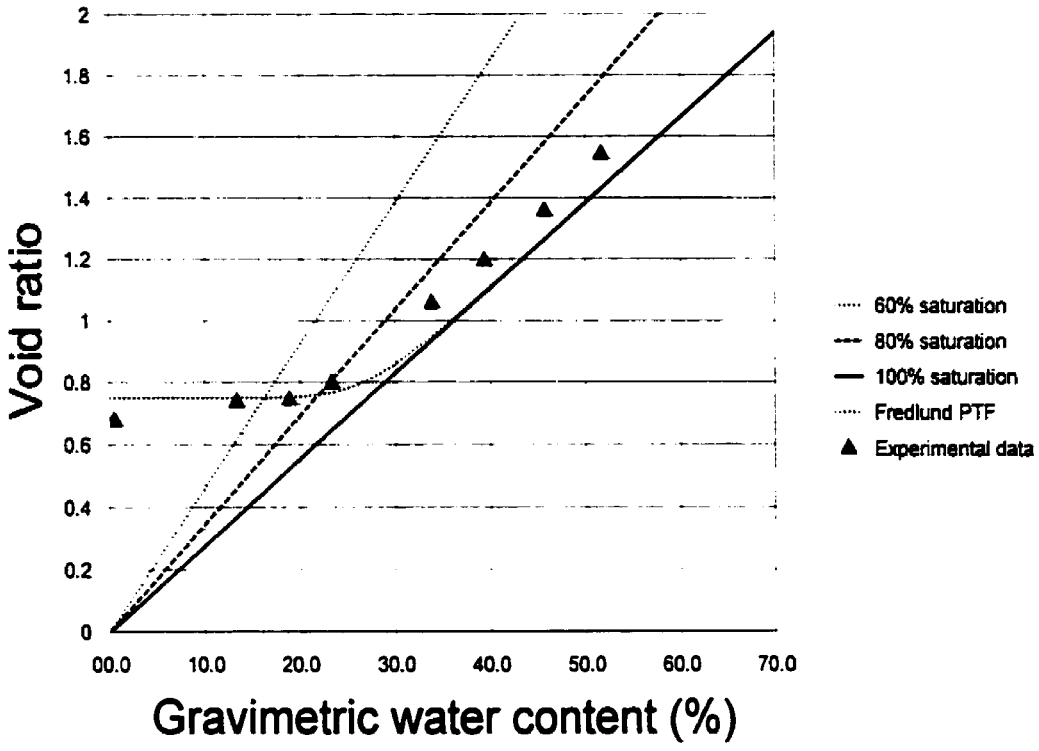

Figure 6-18 Results of shrinkage pedo-transfer function for a alluvial clay originally published by Nascimento, 1961, a_{sh}=0.749, b_{sh}=0.27, c_{sh}=9.57, R^2=0.933 (12443)

6.7 Calculation of Void Ratio Versus Soil Suction

The soil-water characteristic curve describes the relationship between the water content of a soil and soil suction. Unsaturated soil mechanics has used this soil function as the basis for the estimation of others property functions.

Measurement of the soil-water characteristic drying curve is typically performed by measuring the mass of water which leaves a soil sample during drying. It should be noted that volume changes occurring when drying a plastic soil should be measured for later representation of the shrinkage curve. An example of soil-water characteristic data can be seen in Figure 6-19.

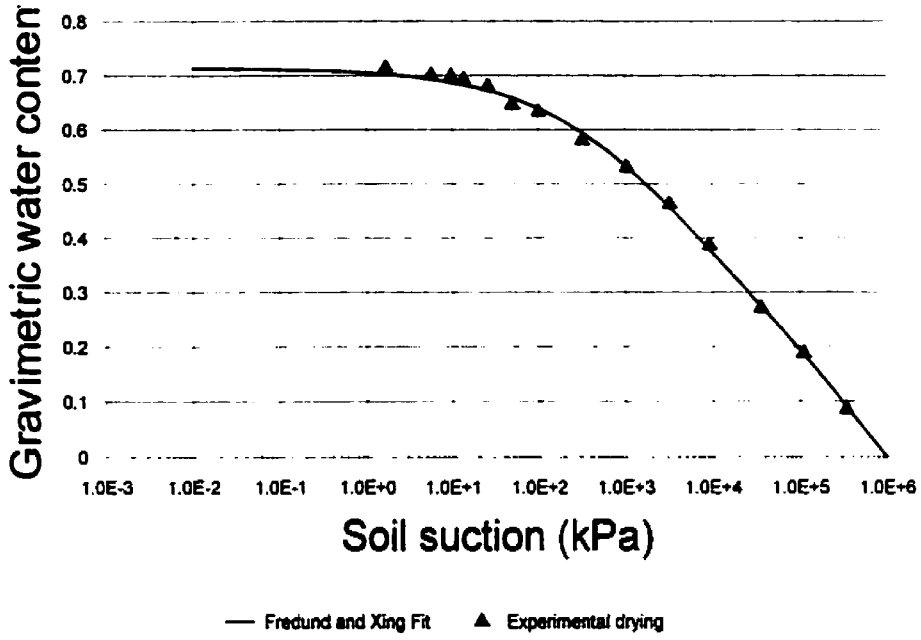

Figure 6-19 Experimental data for a Black Clay originally presented by Dagg et al., 1966 (12422).

If the change in volume is measured during the drying process, it is possible to determine the void ratio and plot the shrinkage curve. The shrinkage curve for the soil presented in Figure 6-19 is presented in Figure 6-20. The data presented below represents the shrinkage of an initially slurried soil specimen in which the soil structure has been disturbed or remolded.

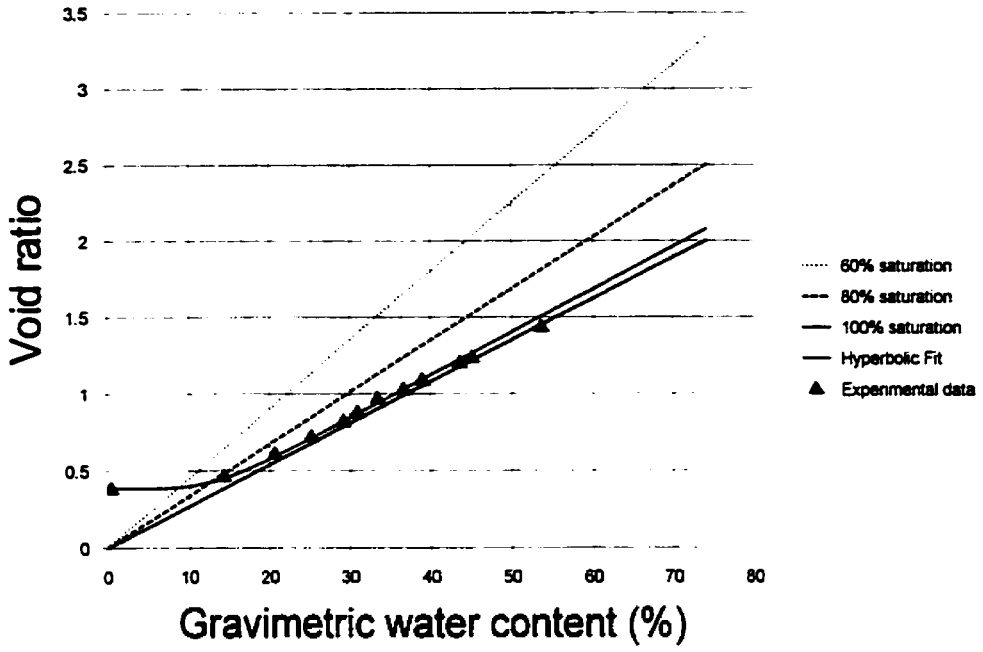

Figure 6-20 Experimental shrinkage data for a Black Clay originally presented by Dagg et al., 1966, a_{sh}=0.386, b_{sh}=0.14, c_{sh}=5.04, R^2=0.993 (12422).

The shrinkage curve represents the volume change in an unsaturated soil due to a change in soil suction. Typical measurements for the shrinkage curve of a soil are performed at a net normal stress of zero (ASTM Test Method for Shrinkage Factors of Soils [D 427]). The shrinkage curve therefore represents the measurement of state along the limiting boundary of the constitutive surface. The shrinkage curve can then be used to calculate the relationship between void ratio and soil suction as shown in Figure 6-22. The curve was calculated by substituting the gravimetric water content represented by the soil-water characteristic curve Fredlund & Xing equation (Equation 6-4) into Equation 6-5. The relationship between void ratio and soil suction as represents the limiting boundary condition of the void ratio constitutive surface as shown in Figure 6-21.

$$w_w(\psi) = w_s \left[1 - \frac{\ln\left(1+\frac{\psi}{h_r}\right)}{\ln\left(1+\frac{10^6}{h_r}\right)} \right] \left[\frac{1}{\left[\ln\left[\exp(1) + \left(\frac{\psi}{a_f}\right)^{n_f} \right] \right]^{m_f}} \right]$$

Equation 6-4

$$e(w) = a_{sh} \left[\frac{w^{c_{sh}}}{b_{sh}^{\ c_{sh}}} + 1 \right]^{\left(\frac{1}{c_{sh}}\right)}$$

Equation 6-5

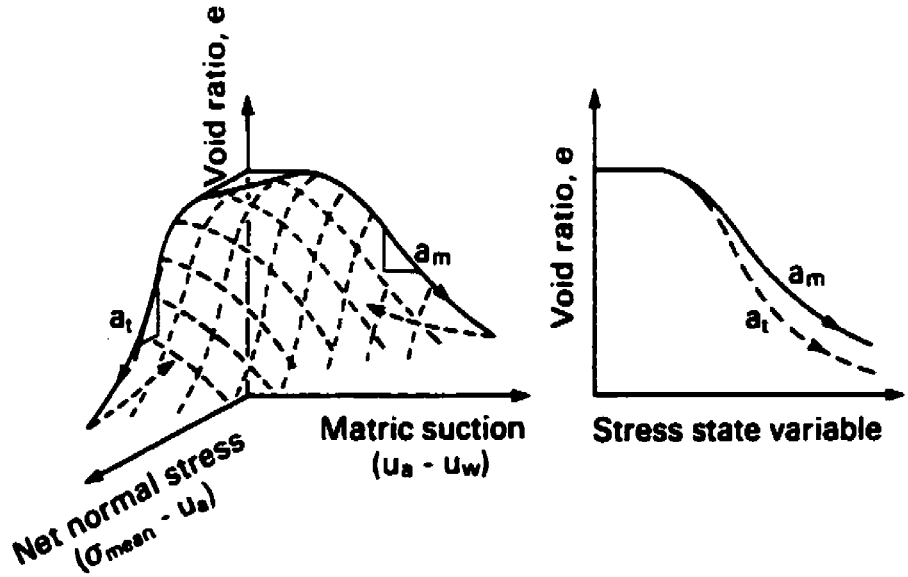

Figure 6-21 Void ratio constitutive surfaces for an unsaturated soil expressed using soil mechanics terminology (Fredlund and Morgenstern, 1976)

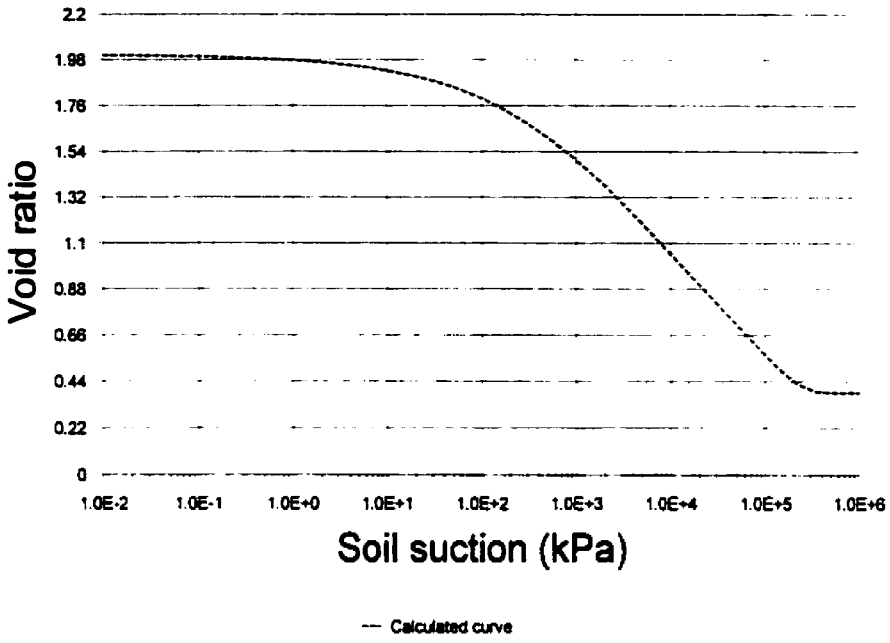

Figure 6-22 Calculated volume change curve for a Black Clay originally presented by Dagg et al., 1966 (12422).

6.8 A More Precise Representation of the Soil-Water Characteristic Curve

It has become general practice in geotechnical engineering and soil science to represent the soil-water characteristic curve as a plot of volumetric water content (V_w/V_t) versus soil suction. Measurements of the volumetric water content are calculated based on the volume of water leaving the soil specimen as it dries. The total volume of the soil specimen is generally only measured at the start of the test. This laboratory method yields reasonable experimental data if the volume change of the soil specimen during drying is minimal (i.e., sands). This test method becomes increasingly inaccurate for soils with a reasonable clay content in which volume change is significant during the test.

Inaccuracies in the experimental results can occur if the experimental data for the soil-water characteristic curve for a swelling soil is uncorrected for changes in volume (Figure 6-23). The air entry value of a soil is important in determining unsaturated soil property function, such as permeability and shear strength. Measurements of the soil-water characteristic curve

uncorrected for volume change can affect the interpretation of air entry and other parameters from experimental data. Measurements of volume change of a highly plastic soil are important when measuring the soil-water characteristic curve.

Figure 6-23 shows the correct soil-water characteristic curve based on the measured shrinkage curve for a Black clay. The experimental points on the uncorrected curve consist of measurement of saturated volumetric water content in the laboratory. Subsequent volumetric water contents are then calculated assuming no volume change in the soil sample. The true volumetric water content is calculated as follows.

Firstly, measurements of gravimetric water content and void ratio would be performed in the laboratory as the soil sample dried and soil suction increased. This would provide the relationship between gravimetric water content and soil suction, $w(\psi)$, and the shrinkage curve, $e(w)$. Correct volumetric water content could then be calculated according to Equation 6-6.

$$\theta_w(\psi) = \frac{w(\psi)G_s}{1 + e(w(\psi))}$$

Equation 6-6

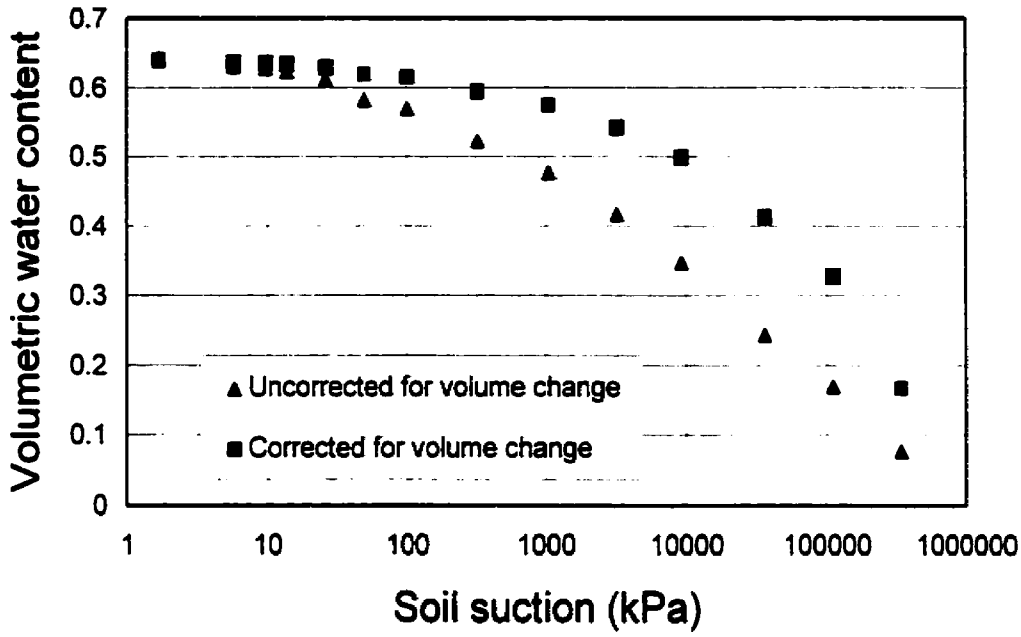

Figure 6-23 Comparison between experimental soil-water characteristic data corrected and uncorrected on a Black Clay originally presented by Dagg et al., 1966 (12422).

The shrinkage curve provides a measure of the true air entry value for a soil. The deviation of the shrinkage curve from the line of saturation marks the true point at which the soil begins to desaturate. Typically the air entry value has been determined from the soil-water characteristic curve. The calculation of the air entry value from the soil-water characteristic curve is inaccurate for clays and silts which undergo volume change when drying. The difference between the air entry value determined from the soil-water characteristic curve (i.e., 20 kPa) and the true air entry value determined from the shrinkage curve (i.e., 1000 kPa) may be seen in Figure 6-24. Many subsequent soil calculations depend upon a correct air entry value. Correction for the effect of volume change when measuring the soil-water characteristic curve of clays is of importance.

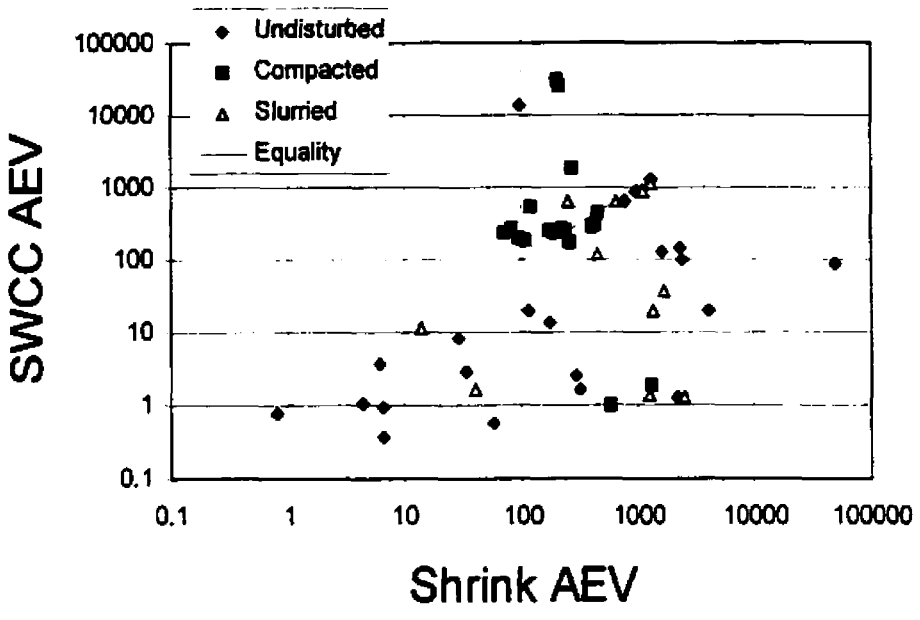

Figure 6-24 Comparison between the air-entry value (AEV) as determined from the soil-water characteristic curve and the shrinkage curve

6.9 Summary

The shrinkage characteristics of a large number of soils have been established in the literature. Soils information was drawn from the literature and used to develop a mathematical relationship to model the shrinkage behavior of slurried, compacted, and undisturbed soils. The shrinkage equation was shown to fit a wide variety of soils with a minimal error.

The shrinkage curve can be used in conjunction with the soil-water characteristic curve for the calculation of the void ratio versus soil suction relationship. The void ratio relationship forms the boundary of the void ratio constitutive surface.

An estimation method was also proposed for the estimation of the shrinkage curve based on the soil-water characteristic curve air-entry value, volume-mass properties and the initial state of the soil. The importance of the measurement of volume changes (or their estimation) of a soil during shrinkage was also presented.

The analysis of the shrinkage behavior of a soil requires a proper soil property function to describe behavior. This chapter provides mathematical fitting and estimation methods for modeling the shrinkage (i.e., volume decrease) behavior of highly plastic soils as well as low plasticity soils.

6.10References

Biwei Gong, Yanhua Liu, and Liantong Zhan, 1998, The relationship between residual water content and shrinkage limit for expansive soils, Proceedings of the 2nd Int. Conf. On Unsaturated Soils, Beijing, Vol. 2, pp. 202-207

Bronswijk J. J. B., 1989, Prediction of actual cracking and subsidence in clay soils, Soil Science, 148 2, pp. 87-93

Bronswijk J. J. B., 1991, Relation between vertical soil movement and water-content changes in cracking clays, Soil Scl.Soc. Am. Journal, 55 Sept.-Oct., pp. 1220-1226

Bronswijk J. J. B., 1990, Shrinkage geometry of a heavy clay soil at various stresses, Soil Sci. Soc. Am. J., 54 Sept.-Oct., pp. 1500-1502

Bronswijk J.J. B., 1991, Drying, cracking, and subsidence of a clay soil in a lysimeter, Soil science, 152 1, pp. 92-99

Chandler R.J., Crilly M.S., Montgomery-Smith G., 1992, A low-cost method of assessing clay desiccation for low-rise buildings, Proc. Instn Civ. Engrs., 92 May, pp. 82-89

Clarke Christopher R., Nevels Jr. James B., Shrinkage and suction properties of Pledger-Roebuck alluvial clay, Transportation Research Record, 1546, pp. 162-173

Croney D., Coleman J. D., 1953, Soil Moisture Suction Properties and their bearing on the moisture distribution in soils, Proceedings of the Third International Conference on Soil Mechanics and Foundation Engineering, 1 S. 1-4, pp. 13-18

Dasog G. S., Action D. F., Mermut A. R., De Jong E., 1988, Shrink-swell potential and cracking in clay soils of Saskatchewan, Canadian Journal of Soil Science, 68, pp. 251-260

De Jong E. , Warkentin B. P., 1965, Shrinkage of soil samples with varing clay concentration, Canadian Geotechnical Journal, 11 1, pp. 16-22

Gens A., Alonso E. E., 1992, A framework for the behaviour of unsaturated expanive clays, Canadian Geotechnical Journal, 29, pp. 1013-1031

Haines William B., 1923, The volume-changes associated with variations of water content in soil, Journal of Agriculture Science, 13, pp. 296-310

Henkel D. J., 1960, The Relationships between the effective stresses and water content in saturated clays, Geotechnique, 10, pp. 41-54

Henkel D. J., 1959, The relationships between the strength, pore-water pressure, and volume-change characteristics of saturated clays, Geotechnique, 9, pp. 119-135

Kingery W. D., Francl J., 1954, Fundamental study of clay: XIII, drying behaviour and plastic properties, journal of American Ceram Society, 37, pp. 596-602

Krizek Raymond J., Corotis Ross B., El-Moursi Houssam H., 1976, Probabilistic analysis of predicted and meseared settlements, Canadian Geotechnical Journal, 14, pp. 17-33

Lauritzen C. W., 1948, Apparent specific volume and shrinkage characteristics of soil materials, Soil Science, 65, pp. 155-179

Lytton R.L., 1995, Foundations and pavements on unsaturated soils, 1st International Conference on Unsaturated Soils, Paris

Lytton R.L., and Kher R.K., 1970, Prediction of moisture movement in expansive clays, Research Report 118-3, Center for Highway Research, University of Texas at Austin, Austin, May

Mitchell Alan R., van Genuchten M. Th., 1992, Shrinkage of bare and cultivated soil, Soil Sci. Soc. Am. J., 56, pp. 1036-1042

Rao R. Rama, Rahardjo Harianto, Fredlund Delwyn G., 1988, Closed-form heave solutions for expansive soils, Journal of Geotechnical Engineering, 114 5, pp. 573-588

Sibley John Walter , Williams David John, 1989, A procedure for determining volumetric shrinkage of an unsaturated soil, Geotechnical Testing Journal, ASTM, 12 3, pp. 181-187

Silvestri Vincent, 1994, Water content relationships of a sensitive clay subjected to cycles of capillary pressures, Geotechnical Testing Journal, 17 1, pp. 57-64

Sridharan A., Venkatappa Rao G., 1971, Effective stress thory of shrinkage phenomena, Canadian Geotechnical Journal, 8 4, pp. 503-513

Stirk G. B., 1954, Some aspects of soil shrinkage and the effect of cracking upon water entry into soil, Australian Journal of Agriculture, 5, pp. 279-290

Subba Rao Kanakapura S., Satyadas Gifferd C., 1985, Measurement of volumetric and linear shrinkage on black cotton soil, Geotechnical Testing Journal, ASTM, 8 2, pp. 66-70

Tempany H. A., 1917, The shrinkage of soils, J. Agr. Sci., 8, pp. 312-330

Warkentin B. P., Bozozuk M., 1961, Shrinking and swelling properties of two Canadian clays, Proceedings, 5th international congress in Soil Mechanics and Foundation Engineering, 3A, pp. 851-855

Zhujiang Shen, Advances in numerical modelling of deformation behaviours of unsaturated soils, 2nd International Conference on Unsaturated soils, 1, pp. 1_14

CHAPTER 7.0 Mathematical Representation of Volume-Mass Constitutive Surfaces

7.1 Introduction

It has been known for a number of years that the volume change behavior of a soil may be linked to two stress state variables, $(\sigma-u_a)$ and (u_a-u_w). This constitutive formulation forms the basis for modeling the volume change of a saturated/unsaturated soil. Modeling of such soil processes as stress/deformation, shrink/heave, and consolidation require an adequate description of the constitutive volume-change behavior of a soil. This chapter presents the mathematical formulation of the volume-change constitutive surfaces for a saturated/unsaturated soil.

The formulation of the constitutive surfaces is based on common laboratory compression, shrinkage and soil-water characteristic curve tests. A series of assumptions are presented to form a guide in the formulation of the constitutive surfaces.

7.2 Literature Review

The complexity related to the development of unsaturated constitutive surfaces appears to have resulted in a minimal amount of previous research. The following section summarizes some of the key developments in the area of unsaturated soil constitutive relations in the 20^{th} century.

Biot (1941) presented constitutive relations for a soil as part of his three-dimensional consolidation theory model. This model assumed that the soil was isotropic and behaved in a linear elastic manner. Two constitutive relationships were proposed to describe the deformation of an unsaturated soil. One constitutive relationship was for the soil structure and the other constitutive relationship was for the water phase relationship. Biot (1941) used two independent stress state variables and four volumetric deformation coefficients to link stress

and deformation states. The consolidation theory was derived only for the case of occluded air bubbles in the water phase.

There have been previous attempts to link the behavior of unsaturated soils to a single-valued effective stress equation (Bishop, 1959). These attempts have resulted in limited success (Jennings and Burland, 1962). The results of numerous oedometer and triaxial compression tests have indicated that there does not exist a unique relationship between volume change and effective stress for most soils. This is particularly true for a soil that is not fully saturated.

Coleman (1962) suggested the use of independent stress state variability for the water phase and the soil structure. The proposed volume change constitutive relation associated with the soil structure was as follows:

$$-\frac{dV}{V} = -C_{21}(du_w - du_a) + C_{22}(d\sigma_m - du_a) + C_{23}(d\sigma_1 - d\sigma_3)$$

Equation 7-1

where: dV = overall volume change of a soil element,

V = current overall volume of the soil element,

u_a = pore-air pressure,

u_w = pore-water pressure,

σ_1 = total axial normal stress (i.e., major principle stress),

σ_3 = total confining pressure (i.e., minor principal stress),

σ_m = mean total normal stress (i.e., $1/3(\sigma_1+2\sigma_3)$), and

C_{21}, C_{22}, C_{23} = soil parameters associated with the soil structure volume change.

Coleman (1962) proposed a similar constitutive relationship for the water phase. It should also be noted that the effects of the mean stress and the deviator stress were independently assumed to produce volume change.

Bishop and Blight (1963) proposed that volume change data be plotted against the $(\sigma-u_a)$ and (u_a-u_w) stress variables in a three-dimensional form. Burland (1965) later restated that

deformation in unsaturated soils should be independently related to the $(\sigma-u_a)$ and (u_a-u_w) stress state variables. Aitchison (1967) also proposed that volume changes be related to independent stress state variables.

Matyas and Radhakrishna (1968) introduced the concept of state parameters for an unsaturated soil. The three state parameters proposed were the mean stress, σ_m, equal to $\sigma_m=(\sigma_1+2\sigma_3)/3-u_a$, $(\sigma_1-\sigma_3)$, and (u_a-u_w). These three parameters reduced to (σ_3-u_a) and (u_a-u_w) for isotropic compression. Three-dimensional state surfaces were formed with void ratio and degree of saturation plotted against the independent state parameters, $(\sigma-u_a)$ and (u_a-u_w). Matyas and Radhakrishna (1968) also experimentally tested the uniqueness of the proposed constitutive surfaces. The soil used in the testing program turned out to have a metastable soil structure (i.e., collapsible soil). However, the laboratory results confirmed the uniqueness of the constitutive surface for the soil structure. The degree of saturation constitutive surface appeared to deviate from a unique surface. Stress paths that followed wetting/drying cycles were found to be non-unique. This behavior was attributed to the hysteretic phenomenon of unsaturated soils. The results of laboratory testing program remain as the most complete laboratory results on unsaturated soil constitutive surfaces to the present time. The results can be seen in Figure 7-1.

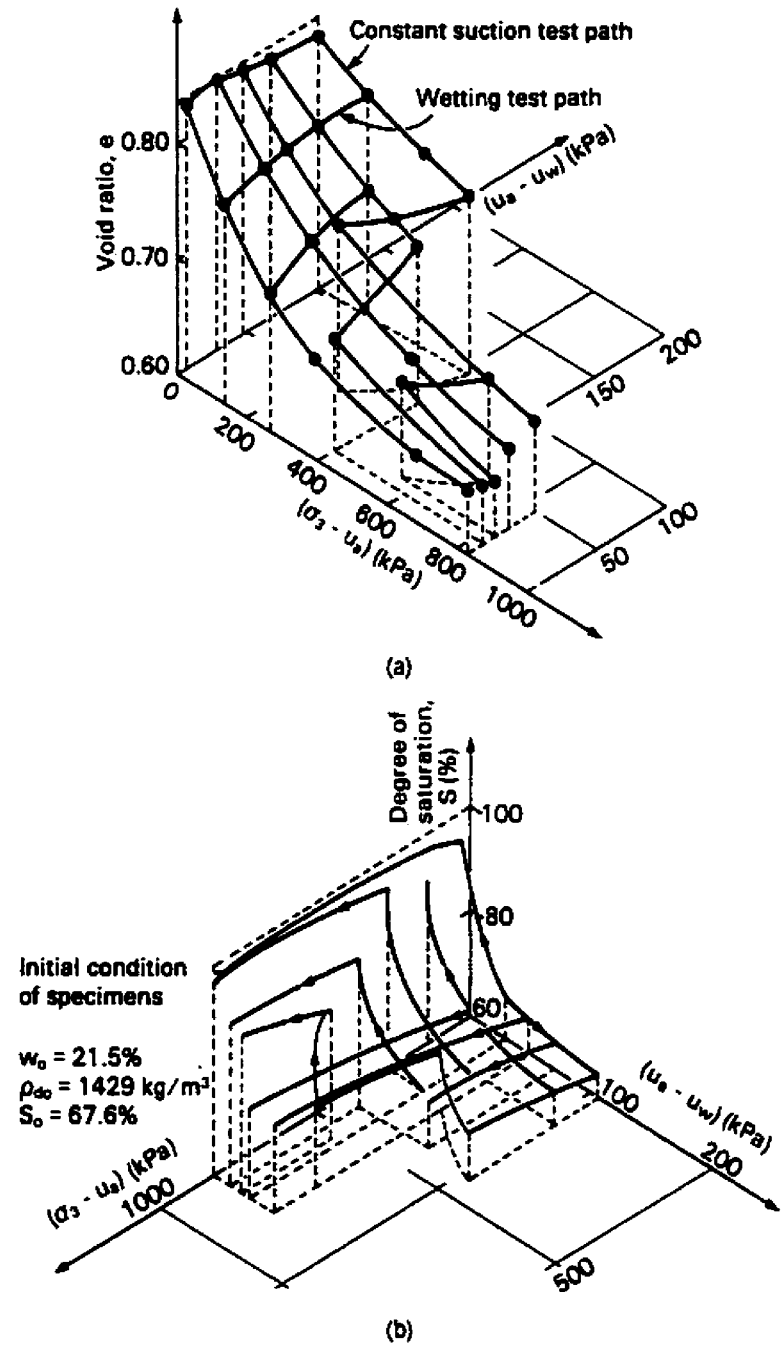

Figure 7-1 Void ratio and degree of saturation constitutive surfaces for a mixture of flint and kaolin under isotropic loading conditions. (a) Void ratio constitutive surface, (b) degree of saturation constitutive surface (from Matyas and Radhakrishna, 1968).

Barden (1969) studied the volume change characteristics of unsaturated soils under K_o-loading conditions. The results of the testing indicated the volume change was stress-path dependent when wetting/drying cycles were introduced. It was also concluded that the volume change

behavior of an unsaturated soil was best analyzed in terms of separate components of stress, $(\sigma-u_a)$ and (u_a-u_w).

Subsequent research has confirmed the validity of representing the constitutive behavior of soil with the two stress variables $(\sigma-u_a)$ and (u_a-u_w) (Aitchison and Woodburn, 1969; Brackley, 1971; Aitchison and Martin, 1973; Fredlund, 1974; and Fredlund and Morgenstern, 1977). Fredlund and Morgenstern (1977) demonstrated that a stress analysis based on multiphase continuum mechanics showed that any two of three independent stress variables [i.e., $(\sigma-u_a)$, (u_a-u_w), and $(\sigma-u_w)$] could be used to describe the stress state in an unsaturated soil.

In 1977, Fredlund and Morgenstern proposed semi-empirical constitutive relations for an unsaturated soil using any two of the three independent stress state variables. The proposed form for the soil structure and water phase constitutive relationships are shown in Figure 7-2.

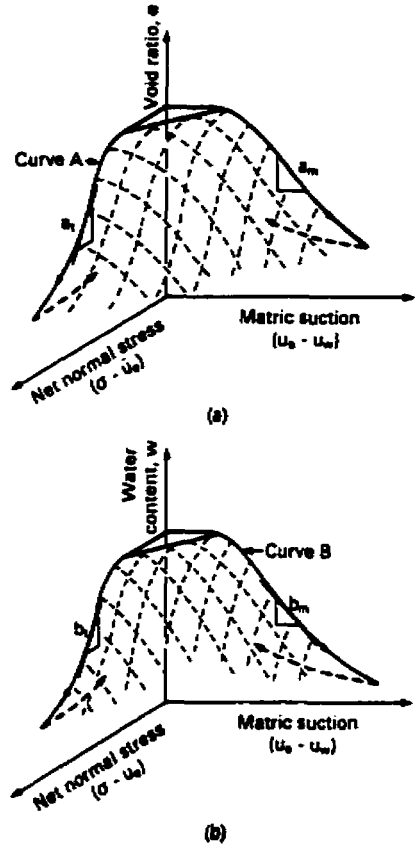

Figure 7-2 Three-dimensional void ratio and water content constitutive surfaces for an unsaturated soil. (a) Void ratio constitutive surface; (b) water content constitutive surface. (Fredlund, 1993)

Alonso and Lloret (1982) conducted an analytical study on the behavior of an unsaturated soil under drained loading conditions. Two equations were developed for the purpose of predicting the changes associated with the overall volume and degree of saturation.

Ho, (1988) developed the limiting (or boundary) conditions of the constitutive surfaces by testing a Battleford Till and a uniform silt in the laboratory. The boundary conditions for the two soils [i.e., $(u_a-u_w) = 0$ or $(\sigma-u_a) = 0$] were presented and indications of the probable behavior of soils under the influence of both suction and normal stress were suggested.

The research presented in this chapter extends current knowledge by presenting mathematical representations of each boundary function used in the development of the constitutive surfaces for unsaturated soils. Smooth, nonlinear functions allow for a mathematical approximation of

the physical behavior of a wide variety of soils. Each mathematical function can be differentiated to provide the volume change indices necessary for the modeling of the volume change of a soil (e.g., a finite element numerical model). A method of combining these mathematical boundary conditions to represent the three-dimensional behavior of an unsaturated soil is presented.

7.3 Application – Consolidation of Mining Tailings

Examples of stress paths that follow constitutive can be found in waste management problems for mine tailings. In practice, however, these stress paths are often reduced to two-dimensional stress paths to reduce the complexity of the problem. This section illustrates a typical stress path followed during the consolidation of the tailings at the McClean Lake mine site in northern Saskatchewan, Canada

The McClean Lake site is a uranium mine operated by Cogema Corporation. The Jeb Pit at McClean Lake was constructed in October, 1999. The pit will provide storage for 6.8 million m^3 of mine tailings. The depth of the Jeb pit is 105m and the in-pit disposal system was designed with under drainage to allow the mine tailings to consolidate under self-weight. A diagram illustrating the Jeb Pit can be seen in Figure 7-3.

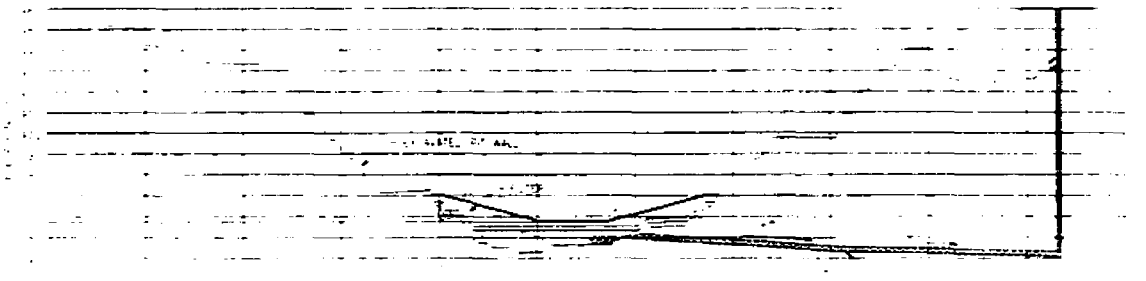

Figure 7-3 Cross section of Jeb pit at McClean Lake

A local consulting firm was contracted to provide estimates of the most probable amount and rate of consolidation. The key issue to be addressed was to determine if the final volume of mine tailings could be accommodated within the pit. A large strain consolidation model was implemented using a finite difference solution to predict the large volume change that would occur during filling of the pit.

The mine tailings at the Jeb Pit are discharged as a slurry and allowed to consolidate under their own self weight. The effective stress in the soil will therefore increase with time, depth of tailings, and drainage. As the deposition of tailings slows, the tailings near the ground surface will be subject to drying as a result of high evaporative fluxes during summer months. The soil suction stress state will increase and the stress path will move along the constitutve surface as shown in Figure 7-4. Understanding the volume change behavior of the near surface tailings is a critical issue in the design of cover systems for long term closure and reclamation. This process is difficult to model without a mathematical representation of the constitutive surface of a soil

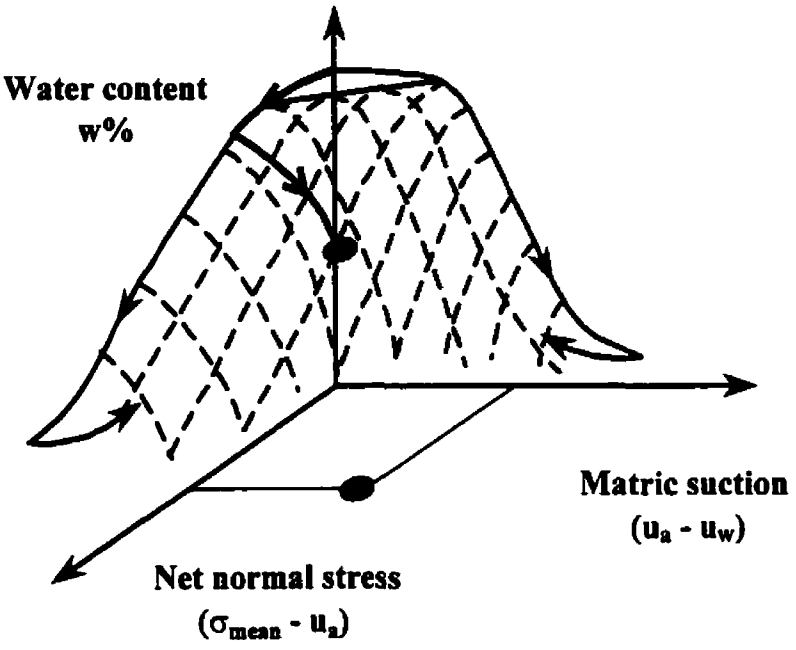

Figure 7-4 Example of stress page followed by mine tailings

This thesis provides methods for the development of such constitutive surface for a problem such as in-pit disposal of mine tailings. The volume-mass constitutive surface is predicted on the basis of the compression (consolidation) curve and the soil-water characteristic curve.

7.4 Theory Related to the Prediction or Estimation of the Volume-Mass Constitutive Surface

Two constitutive surfaces must be defined for an unsaturated soil in order that the volume-mass properties can be defined under any stress state conditions. The first constitutive surface selected is related to overall volume change and can be defined in terms of void ratio, e, or specific volume, υ, (i.e., 1+e). The void ratio is used herein to define the first constitutive surface. The second constitutive surface selected defines the amount of water in the soil and is called the water content (gravimetric), w, constitutive surface.

A series of "postulates" are proposed for the prediction of the volume-mass constitutive relations. The postulates establish a series of priorities that must be adhered to when attempting

to estimate the volume-mass relationships. Certain information has become well established in the research literature and this information forms a series of hierarchical priorities when predicting the constitutive surfaces.

7.4.1 Soil Structure (or Overall Volume Change) Constitutive Surface

The soil structure constitutive surface can be defined as the relationship between two independent stress state variables and a deformation state variable. The independent stress state variables are:

$(\sigma-u_a)$	net normal (isotropic) confining pressure, and
(ψ)	soil suction.

The deformation state can be defined in terms of void ratio, e.

The proposed "postulates" for the soil structure (i.e. void ratio) constitutive surface are as follows for the case of an increase in both of the stress state variables (i.e., a monotonic decrease in volume). In addition, it is assumed that the testing of the soil starts with the specimen being in a saturated state. There are a number of loading stress paths as well as wetting and drying paths that could be analyzed; however, it is important to start by developing constitutive surfaces for the conditions on which the most information is available.

7.4.1.1Postulate 1

The primary reference condition for the volume change (overall) constitutive relationship is determined by applying a net (isotropic) total stress loading of the soil with the pore-water and pore-air pressures maintained at zero, while measuring the change in void ratio.

This relationship is commonly referred to as the drained, effective stress loading path for a saturated specimen (Figure 7-5). The term "isotropic" is placed in brackets to suggest that isotropic loading is the preferred stress path. However, it is also possible for K_o or other stress

paths to be considered. Isotropic stress loading is preferable because: a) the stress path is the same as that used for critical state (or elasto-plastic) models, and, b) the matric suction stress state variable is also isotropic in character.

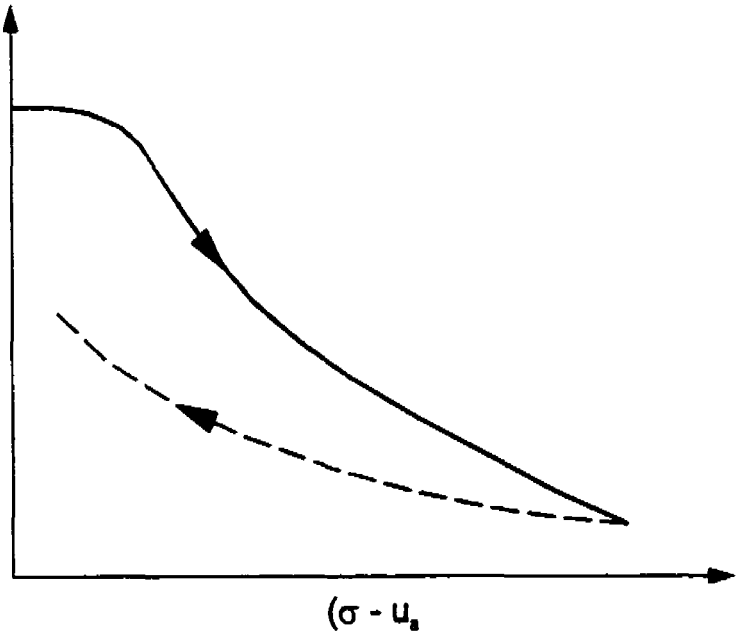

Figure 7-5 Typical loading and unloading curves of void ratio versus the applied load.

7.4.1.2Postulate 2

The secondary reference condition for the volume change (overall) constitutive relationship is determined by applying various soil suctions to the soil with the net isotropic applied stress equal to zero, while measuring the change in void ratio (Figure 7-6).

There is a practical difficulty associated with directly measuring the volume change versus soil suction relationship. The difficulty is related to measuring volume change in three directions while changing soil suction. As a result of the above difficulty, "Postulate 2a" suggests an alternative means to indirectly provide the necessary secondary reference condition. The alternative procedure makes use of a combination of data from a shrinkage test and a soil-water characteristic curve test described in Chapter 6.

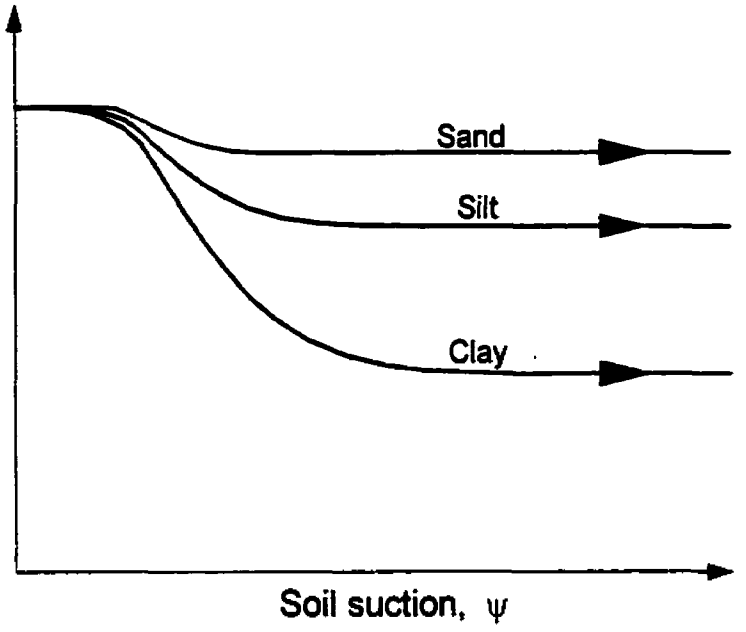

Figure 7-6 Typical void ratio versus soil suction plot for three soils (suction increase)

7.4.1.3Postulate 2a

The void ratio versus soil suction relationship can also be computed using the soil-water characteristic curve for the soil along with the shrinkage curve, both sets of data are measured under condition of zero net isotropic stress.

Figure 7-7a) shows three typical soil-water characteristic curves under drying conditions (or conditions of an increase in suction. Figure 7-7b) shows a typical shrinkage curve associated with the drying of a clay soil.

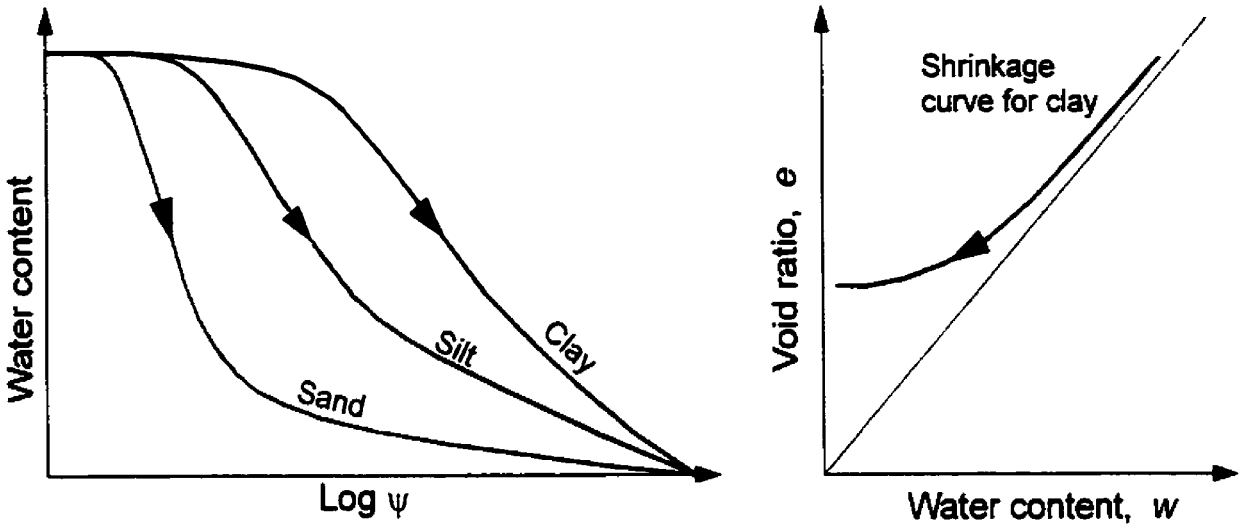

Figure 7-7 a) Typical soil-water characteristic curves for three soil types. b) Typical shrinkage curve for a clay soil.

It is possible to combine the results of a pressure plate test (i.e., soil-water characteristic curve data) and a shrinkage test to obtain a void ratio versus suction plot. The shrinkage test defines a curve that gives the ratio of change in volume of water to overall volume, for a change in soil suction. Mathematically, the slope of the shrinkage curve can be written as follows.

$$\frac{de}{dw} = \frac{de/d\psi}{dw/d\psi} = \frac{a_m}{b_m}$$

Combining the two sets of information makes it possible to compute the void ratio versus soil suction relationship. This forms the second reference (or limiting) condition for the soil structure constitutive surface.

7.4.1.4Postulate 3

There is a unique volume change constitutive surface defined for conditions of monotonic deformation.

The surface for a decrease in volume under an increase in stresses is considered herein and shown in Figure 7-8.

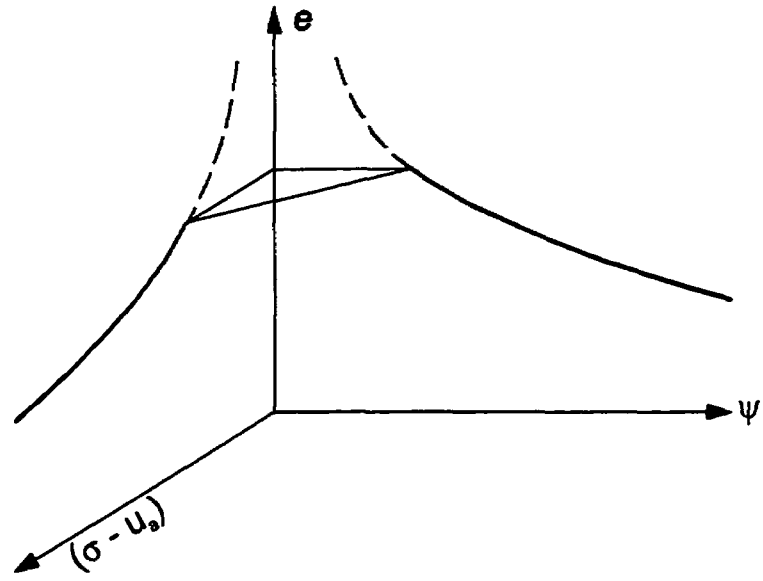

Figure 7-8 Three-dimensional plot showing the primary and secondary reference conditions for the void ratio constitutive surface.

The limiting (or reference) conditions associated with the void ratio constitutive surface have now been defined. The next step is to define the character of the constitutive surface between the limiting reference conditions. The remaining postulates pertain to establishing intermediate stress state conditions on the constitutive surface.

7.4.1.5Postulate 4

The slope along any constant net total stress plane on the volume change constitutive surface is a function of the void ratio, as defined on the zero soil suction plane.

This postulate comes about as a result of postulate 1 where it is stated that the void ratio versus net total stress is the primary and most fundamental relationship between void ratio and the stress state. As a consequence of postulate 4, the slope of any line emanating from the soil suction versus void ratio curve, in a constant suction plane, must be equal to the compressibility defined on the primary reference curve at a corresponding void ratio. Appropriate slopes for the constitutive surface can be determined by constructing a triangle in the horizontal plane, between the reference conditions.

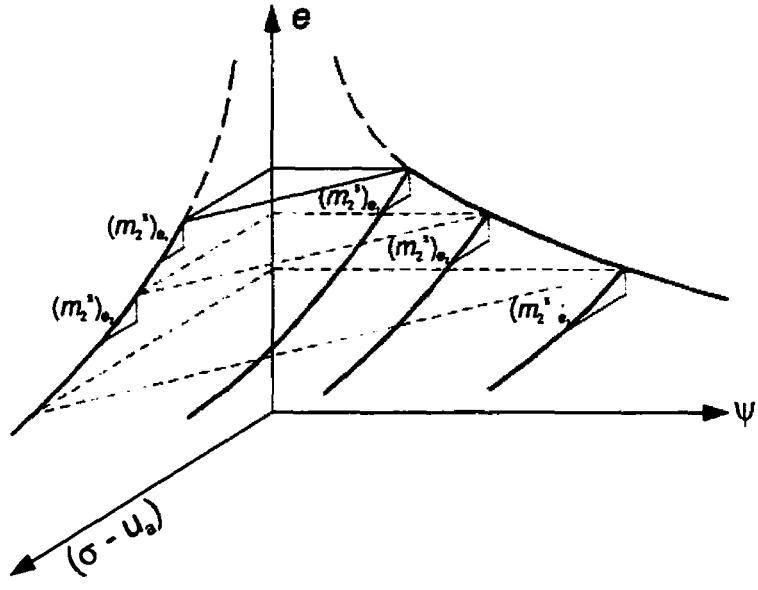

Figure 7-9 Illustration of the definition of the void ratio constitutive surface based on the slopes of the primary reference curve.

7.4.1.6Postulate 5

A change in net normal stress has the same effect on volume change or void ratio as does a change in soil suction when soil suction is less than the air-entry value. (Figure 7-10).

This mean that a 45 degree relationship will be defined between the two stress state variables when the void ratio constitutive surface is viewed along the void ratio axis.

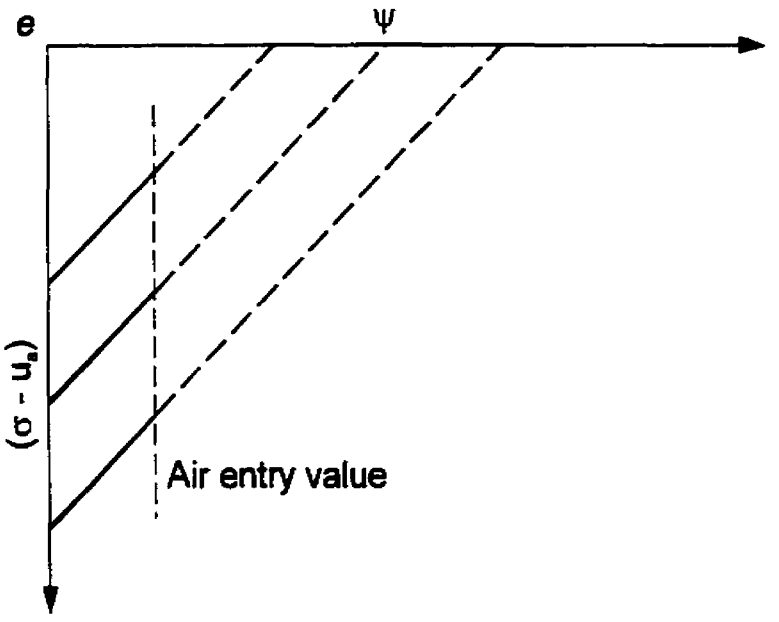

Figure 7-10 Variation of constant void ratio contours when the surface is viewed along the void ratio axis.

The straight line contour across the constitutive surface should be theoretically correct as long as the soil is saturated. This is in accordance with the effective stress concept for a saturated soil. It should be noted that the dashed lines drawn in Figure 7-10 may not intersect the secondary reference condition along the plane of net total stress equal to zero. It is necessary to comment further on the air entry value of the soil before suggesting a further refinement on void ratio contours.

7.4.1.7Postulate 5a

As a first approximation, the air entry value of the soil can be assumed to be a constant, but for greater refinement, the air entry value may need to be defined as a function of void ratio or the net isotropic stress (Figure 7-11).

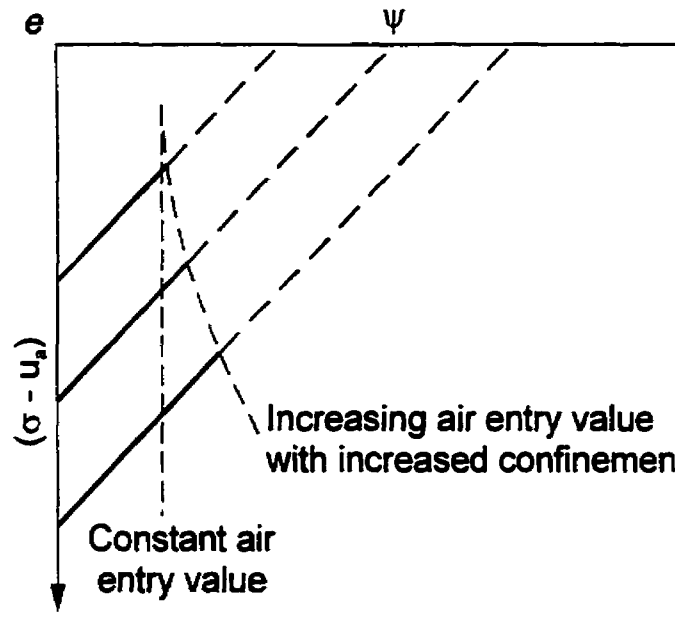

Figure 7-11 Effect of a variation in the air entry value on the void ratio contours.

The air entry value would be anticipated to increase with a decrease in void ratio. This means that the 45 degree contour would be adhered to for a greater distance from the net total stress reference plane. No attempt is made at this time to define the air entry value of the soil as a function of void ratio (or stress state).

7.4.1.8Postulate 6

A gradual curve forms from the air entry value to the secondary reference condition, corresponding to a particular void ratio on the soil structure constitutive surface (Figure 7-12).

The curve must be tangent at the air entry value and increase in curvature as the secondary reference condition is approached. This means that it should always be possible to join the secondary reference curve provided it is positioned further from void ratio than is the primary reference curve. In other words, at a particular void ratio, the soil suction value should exceed the net total stress value.

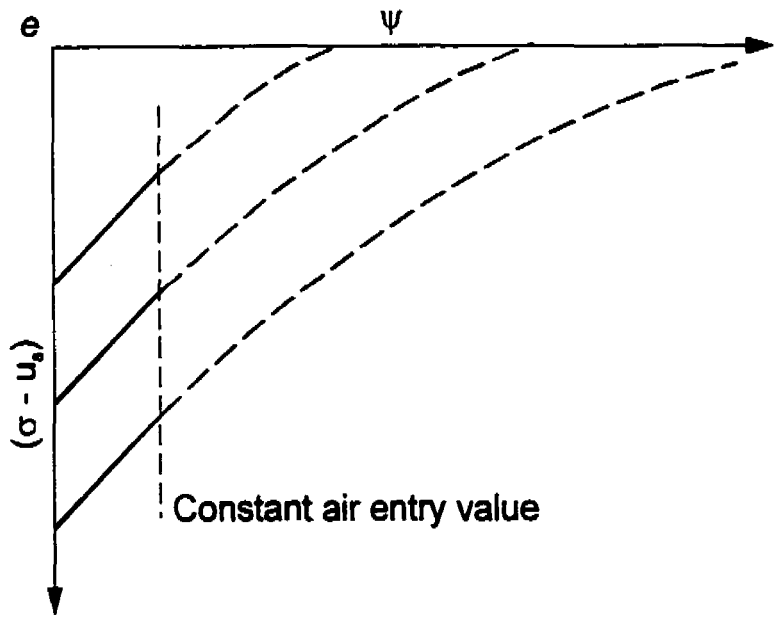

Figure 7-12 Variation in the constant void ratio contours as the soil becomes increasingly desaturated.

The curves should always bend in the direction of the soil suction axis for a clayey, stable-structured soil. For a sandy soil, the curves will bend even more rapidly and may never reach the reference soil suction axis.

The loading portion of the void ratio constitutive surface can be approximated using the steps outlined above. The general character of the void ratio constitutive surface should apply for sands, silts and clays. The greatest difficulty should be observed in defining the constitutive surface near to initial conditions. This is due to the fact that not all of the tests are started from precisely the same stress state and volume-mass state. As well, different tests may follow different stress paths particularly near the start of the test. It is therefore necessary to take into consideration the initial state of the soil. For example, the soil could be initially slurried, compacted or be in an undisturbed state. This item will be discussed further in section 7.5.3.

The above postulates do not cover all aspects of defining the void ratio constitutive surface. The postulates pertain to the loading only (by net total stress or soil suction) constitutive surface of an initially saturated soil. Other postulates will be required to define the unloading void ratio constitutive surface. Still other postulates are required for the case where one state

variable is increased while the other one may be decreased. The scope of this thesis is limited to monotonic loading of an initially saturated soil.

7.4.2 Water Content Constitutive Surface

The water content constitutive surface can be defined as the relationship between two independent stress state variables and a deformation state variable. The water content constitutive surface is defined for loading conditions with a corresponding, monotonic decrease in water content.

The independent stress state variables are:

$(\sigma-u_a)$ = Net normal (isotropic) confining pressure, and

(ψ) = Soil suction.

The deformation state can be defined in terms of gravimetric water content, w.

The proposed "postulates" for the establishing the water content constitutive surface are as follows. The constitutive surface related to an increase in each of the stress state variables is defined. The soil is assumed to start from a saturated condition.

7.4.2.1Postulate 7

The primary reference condition for the water content constitutive relationship is determined by applying a suction to the soil with the net isotropic stress maintained at zero, while measuring the change in water content.

This relationship is known as the soil-water characteristic curve and is usually plotted with soil suction on a log scale. An example, along with the definition of the air entry value and residual conditions, is shown in Figure 7-13.

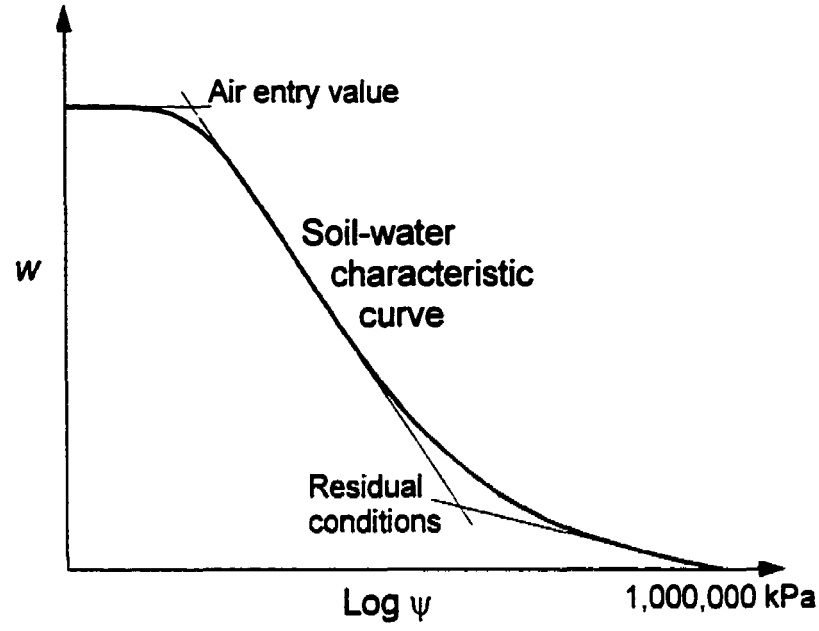

Figure 7-13 The water content versus soil suction relationship forms the primary reference condition for the water content versus soil suction constitutive relationship.

7.4.2.2Postulate 8

The secondary reference condition for the water content change constitutive relationship is computed from the void ratio constitutive surface for the condition of zero soil suction where the void ratio is multiplied by the specific gravity of the soil (i.e., $w = e/G_s$).

The water content versus net normal stress has the same character as the compression curve as shown in Figure 7-14.

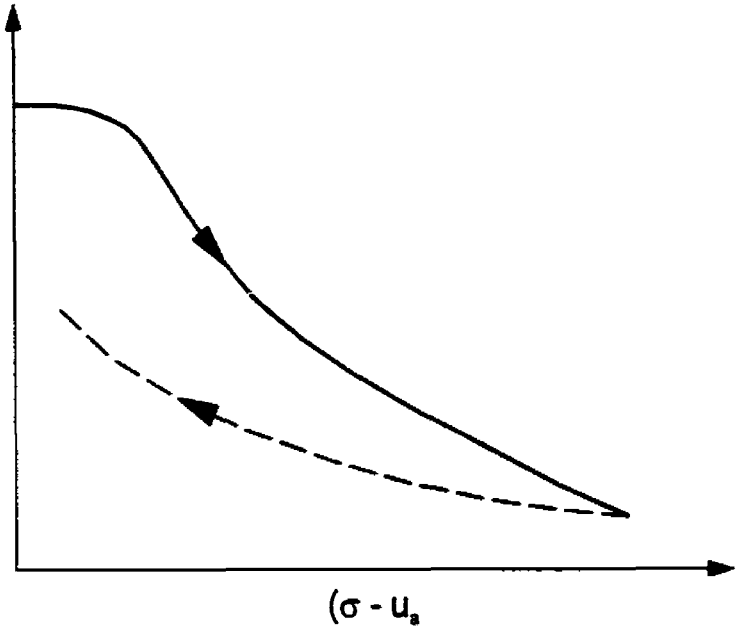

Figure 7-14 The secondary reference condition for the water content constitutive surface is equal to the primary reference condition for the void ratio constitutive surface divided by the specific gravity of the soil, G_s.

The water content versus net loading curve is secondary in its role in defining the intermediate conditions of the water content constitutive surface.

7.4.2.3Postulate 9

There is a unique water content constitutive surface defined for conditions of monotonic water volume change.

The surface for a decrease in water volume under an increase in stress is shown in Figure 7-15.

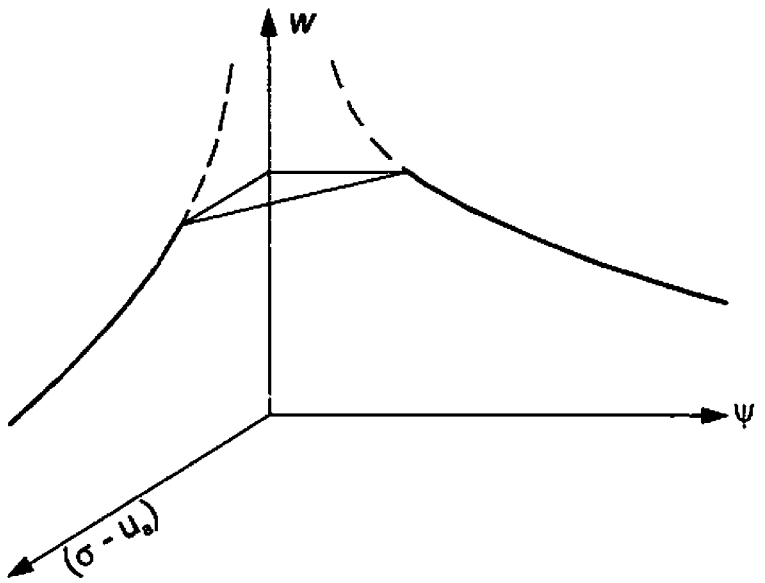

Figure 7-15 Three-dimensional plot showing the primary and secondary reference conditions for the water content constitutive surface.

7.4.2.4Postulate 10

The slope along any constant soil suction plane on the water content constitutive surface is a function of the water content, as defined on the zero net total stress plane.

Figure 7-16 illustrates how the water content constitutive surface is strongly influenced by the soil-water characteristic curve.

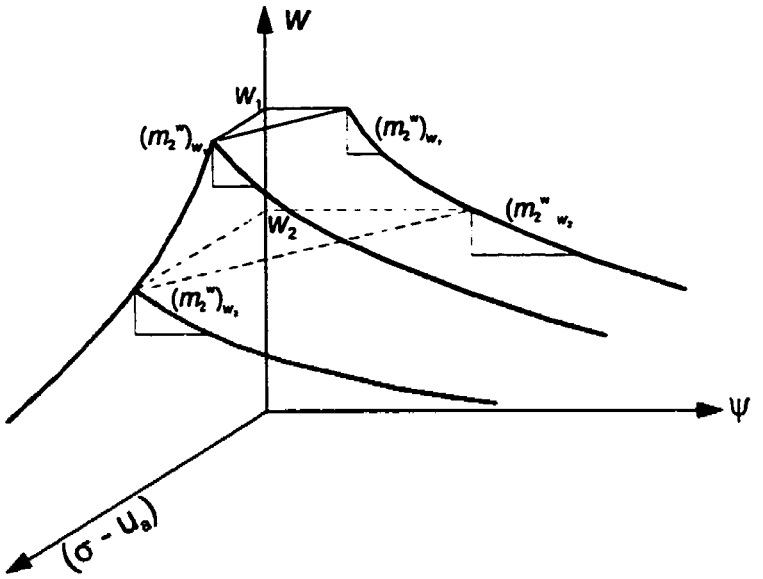

Figure 7-16 Illustration of the definition of the water content constitutive surface based on the slopes of the primary reference curve.

7.4.2.5Postulate 11

There is a one-to-one relationship between the effects of a change in net total stress and a change in soil suction, when the soil suction is less than the air entry value of the soil.

This means that a 45 degree relationship occurs between the two stress state variables when the water content constitutive surface is viewed along the water content axis as shown in Figure 7-17. Once again the air entry value can be made a function of the water content (or stress state) as described for Postulate 5 of the void ratio constitutive surface.

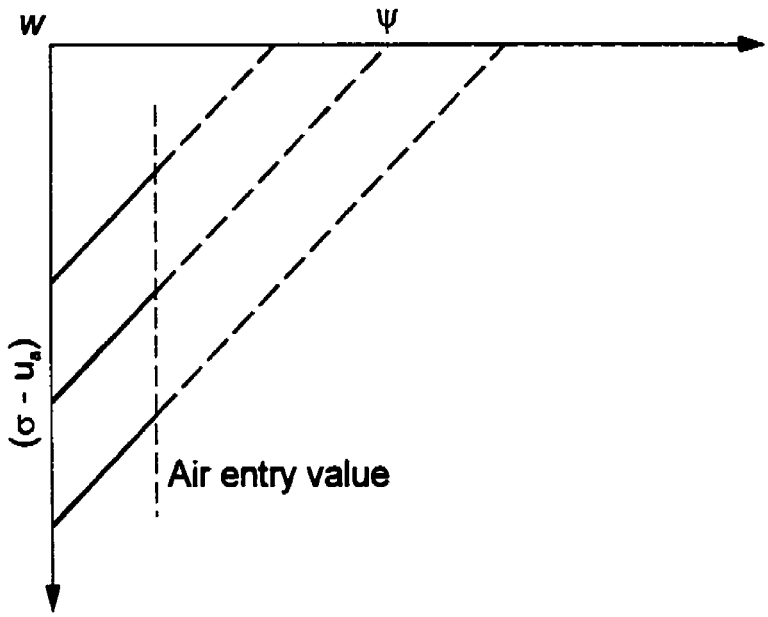

Figure 7-17 Variation of the constant water content contours when the constitutive surface is viewed along the water content axis.

7.4.2.6Postulate 12

A gradual curve forms from the air entry value to the primary water content reference condition, corresponding to a particular water content on the water content constitutive surface.

The curve must be tangent at the air entry value and increase in curvature as the primary reference condition is approached as shown in Figure 7-18. In other words, the character of the water content constitutive surface is different from that of the void ratio constitutive surface, as the soil becomes unsaturated.

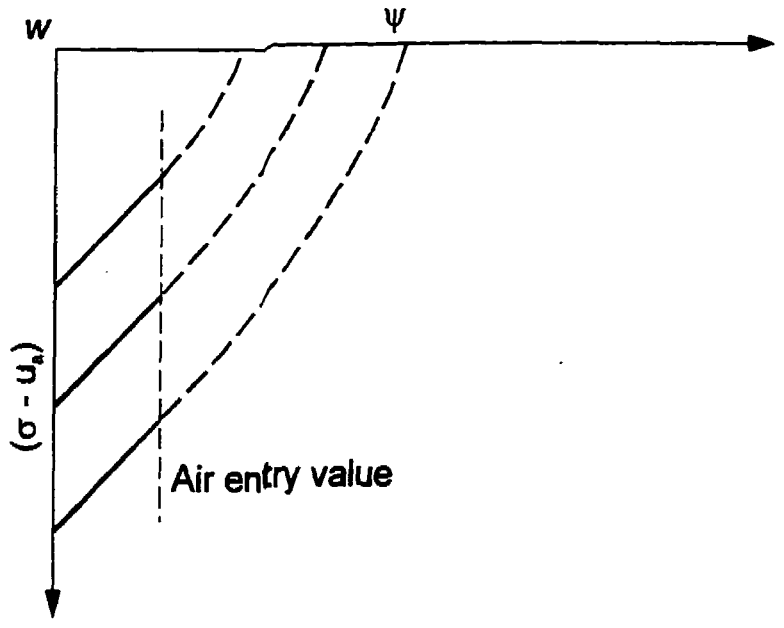

Figure 7-18 Variation in the constant water content contours as the soil becomes increasingly desaturated.

It is possible that the air entry value of the soil will change with decreasing initial water contents. However, there does not appear to have been sufficient experimental evidence to confirm this variation in air entry value at this point.

The proposed character of the water content constitutive surface should apply for sands, silts and clays. It is necessary to take into consideration the initial state of the soil. For example, the soil could be initially slurried, compacted or be in an undisturbed state.

7.5 Typical Experimental Laboratory Procedures

The uniqueness of the volume-mass constitutive surfaces has been established for stress variations from a point on the constitutive surface in previous research (Fredlund, 1973). The entire void ratio constitutive surface has been tested and found to essentially satisfy conditions of uniqueness by Matyas and Radhakrishna (1968) and Barden, Madador and Sides (1961). The experimental results for the water content constitutive surface are not quite as conclusive as those for the void ratio constitutive surface.

Until now a method for developing the entire constitutive surfaces from standard laboratory tests has not been established. To establish the relationships between conventional laboratory testing and constitutive surfaces, a review of current laboratory methods is presented. The procedure with which tests are performed influences the form of the constitutive surfaces.

7.5.1.1Compression

Current laboratory tests form the extremities of the constitutive surfaces. The compression (or consolidation) test forms boundary A in Figure 7-2. While an isotropically loaded test is superior from the standpoint of developing a theoretical context, most available test data is for K_o or one-dimensional oedometer tests. The compression test provides information on the void ratio and water content with respect to net normal stress. Two types of tests are commonly performed to obtain compression data in the oedometer. These two tests are referred to as "free-swell" or "constant volume" test results.

During a "free-swell" test, the soil specimen is placed in the consolidometer, submerged in water, and allowed to swell with a small load placed on the specimen. The "constant-volume" compression test is similar with the exception that load is constantly applied while the specimen is exposed to water so that the initial volume of the sample remains constant. The stress-paths followed by the oedometer test are shown as curve (a) in Figure 7-19. It should be noted that it is the initial conditions that vary between the two types of Ko tests. This is of interest since there are a variety of ways in which specimens are conditioned before the testing of the soil takes place. This creates a special difficulty when data from several types of tests are being combined to form the constitutive surfaces.

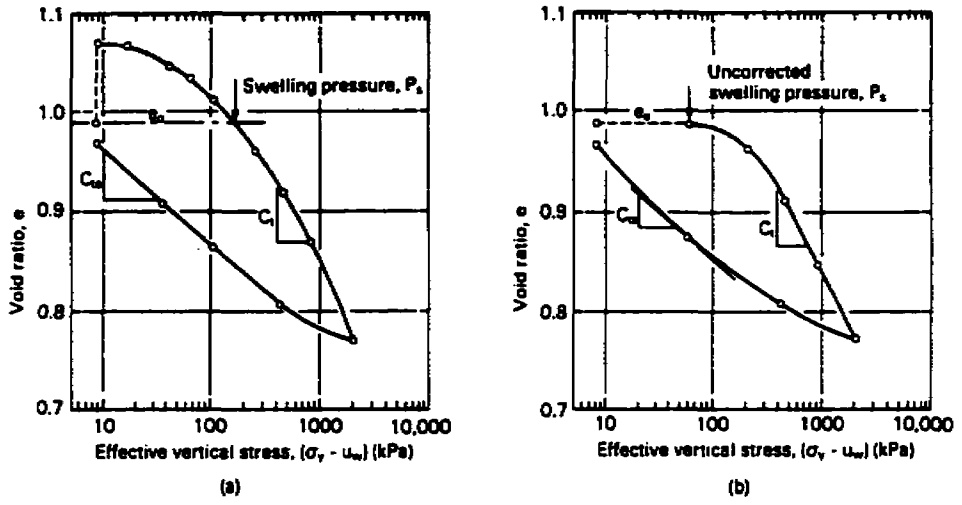

Figure 7-19 Typical "free-swell" and "constant volume" one-dimensional oedometer test results. (a) "Free-swell" test procedure; (b) "constant volume" test procedure. (Fredlund, 1993)

The "constant-volume" and "free-swell" tests follow different stress paths at the beginning of the compression test. The three-dimensional representation of each of these tests may be seen in Figure 7-20 and Figure 7-21. It can be seen from Figure 7-20 that the initial stress path for either test actually proceeds across the constitutive surface. The significance of this is that the compression test results are not totally representative of constitutive surface boundary conditions until the swelling pressure, P_s, has been reached. Therefore, the development of the constitutive surfaces presented in this paper utilize the data from the virgin compression branch.

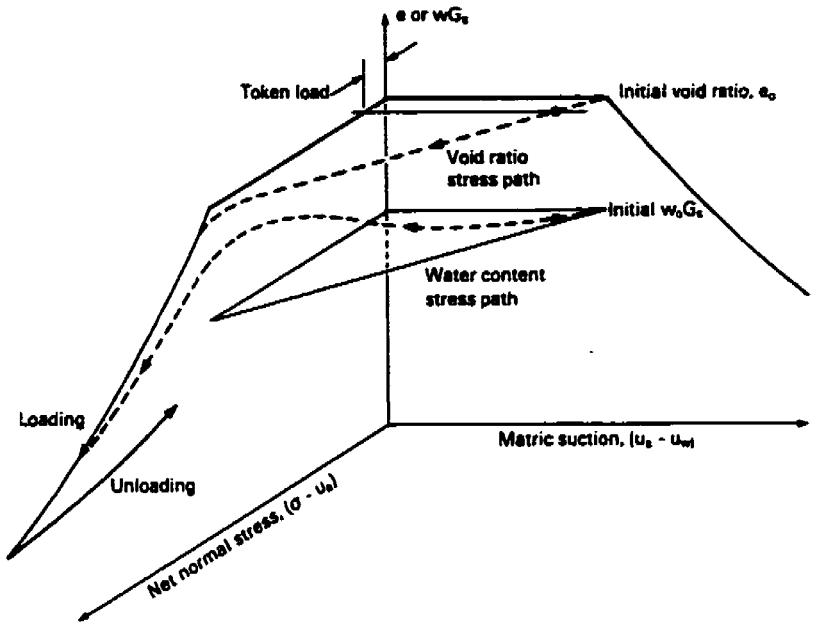

Figure 7-20 "Ideal" stress path representation for a "constant volume" oedometer test. (Fredlund, 1993)

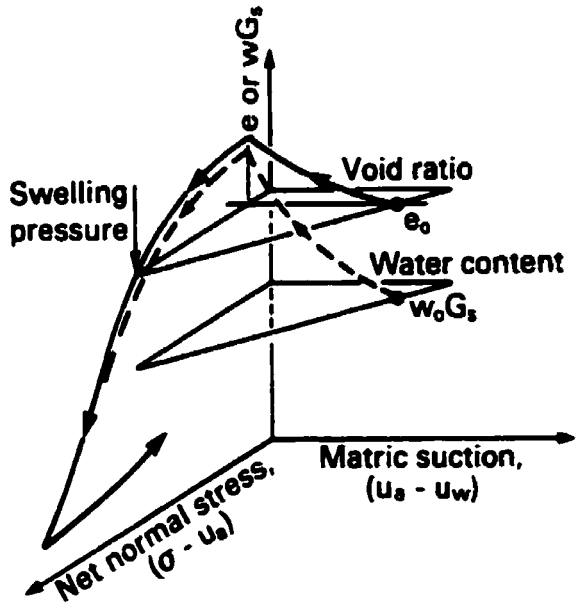

Figure 7-21 "Ideal" stress path representation for the "free-swell" oedometer test. (Fredlund, 1993)

7.5.1.2Soil-water characteristic curve

A variety of apparatuses exist for the measurement of the soil-water characteristic curve in the laboratory. The Tempe cell or pressure plate is the most commonly used apparatus to determine

the relationship between gravimetric water content and soil suction. The most commonly used laboratory procedure for obtaining the soil-water characteristic curve appears to be as follows:

1. place a specimen in a Tempe cell and expose it to water to allow saturation,
2. increase the pore-air pressure in the chamber surrounding the specimen to simulate an increase in soil suction, (u_a-u_w), and
3. measure the decrease in gravimetric water content of the soil specimen.

The stress state followed by the procedure described above can be seen in Figure 7-22. It should be noted that the standard laboratory procedure initially follows a scanning curve onto the adsorption portion of the hysteresis loop. While the effect of hysteresis may be significant in certain analysis, it is generally ignored in the calculations presented in this chapter. When determining the constitutive surfaces presented in this chapter, it is assumed that the soil-water characteristic curve is determined by bringing the soil to an initially saturated condition and drying the specimen to achieve subsequent gravimetric water contents.

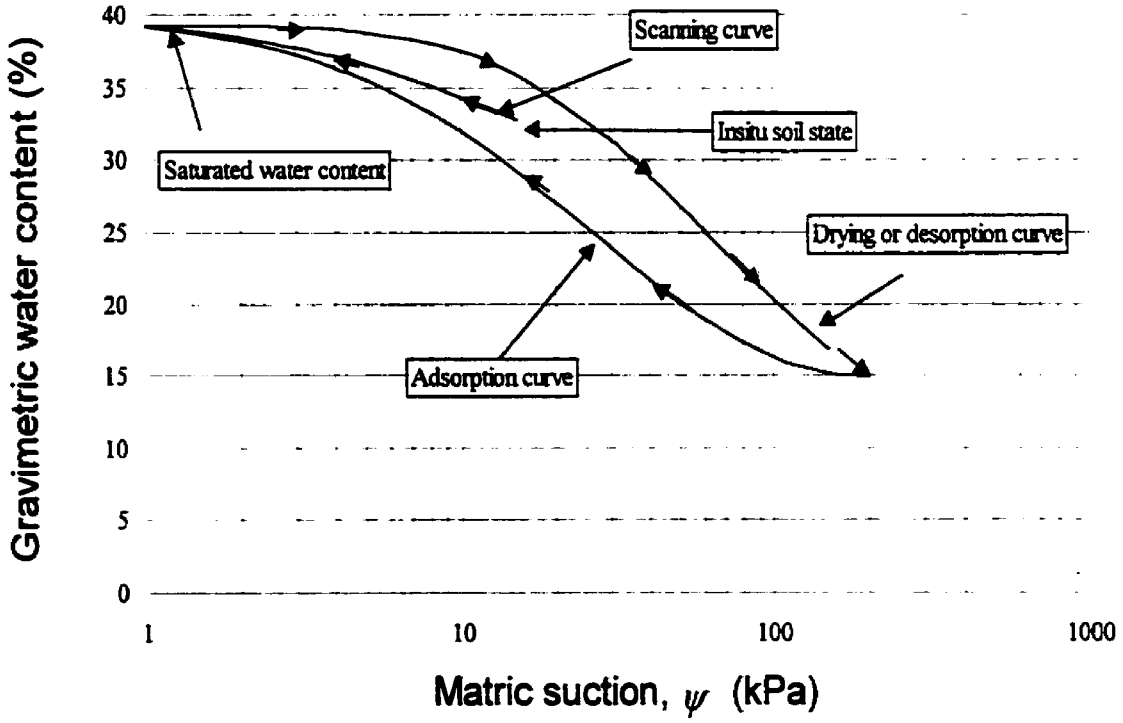

Figure 7-22 Typical laboratory hysteresis loop for Tempe cell test

7.5.2 Laboratory Data

A literature review was performed to obtain laboratory data in which a consolidation test (compression curve), and a Tempe cell test (soil-water characteristic curve and shrinkage curve) were obtained. Results of such laboratory tests have been presented by Nascimento, 1961, Ridely, 1993, and Ho, 1990. The soil types include a uniform silt (optimum, and dry of optimum), a glacial till (optimum, and, dry of optimum), an oligocenic clay, a fine sand, silt, a miocenic clay, an argillaceous coarse sand, a coarse sand, a basaltic clay, an alluvial clay, and a speswhite kaolinite (virgin-dried, overconsolidated-dried, 80% kaolin - 20% silt, compacted-dried, 50% kaolin - 25% sand - 25% silt, swelled-dried). The laboratory results of thirty different soil samples were used in the study of the void ratio and water content constitutive relationships.

7.5.3 Initial States of Compression, Shrinkage, and Soil-Water Characteristic Laboratory Tests

The selection of initial soil states forms the basis for the proper calculation of the constitutive surfaces. Four separate initial soil states were identified based on the laboratory data collected for analysis. The initial soil states are summarized below.

Laboratory Test	Soil State	
Soil-water characteristic curve	Saturated condition (maximum swell allowed)	initially slurried undisturbed compacted
Shrinkage test	Saturated condition (maximum swell allowed)	initially slurried undisturbed compacted
Consolidation (compression) test	Free-swell	undisturbed compacted
	Constant-volume	initially slurried undisturbed compacted

Generation of constitutive relations requires the selection of specimens where similar initial soil states were used for all tests. It was determined that the saturated condition obtained at the start of the soil-water characteristic curve is the most common starting condition and, that will be

used in this study. Additionally, the soils used in this study vary between being initially slurried, undisturbed, and compacted.

Calculation of the void ratio versus soil suction curve requires the use of a soil-water characteristic curve and a shrinkage curve. It is also necessary that the initial states and initial stress paths be the same for both tests. Complicating this matter are the shrinkage tests in which the soil is initially unsaturated (or as-compacted). Such soils required the re-calculation of the shrinkage curve such that the saturated condition is approximated. It was, therefore, a requirement that experimental data used to generate the constitutive surface have a saturated initial condition.

The re-calculation of the shrinkage curve is possible when the shrinkage data is fit with the shrinkage equation as presented in Chapter 4. The equation used to model the shrinkage curve is seen below.

$$e(w) = a_{sh}\left[\frac{w^{c_{sh}}}{b_{sh}^{\,c_{sh}}} + 1\right]^{\left(\frac{1}{c_{sh}}\right)}$$

Equation 7-2

where: a_{sh} = the minimum void ratio, e_{min},

b_{sh} = slope of the line of tangency,

c_{sh} = curvature of the shrinkage curve,

and $\frac{a_{sh}}{b_{sh}} = \frac{G_s}{S}$ = constant for specific soil.

Re-calculating a shrinkage curve at saturation involves changing the ratio between the a_{sh} and b_{sh} parameters. The c_{sh} parameter controls the curvature of the curve and is assumed to be unchanged. The a_{sh} parameter is equal to the minimum void ratio and is also assumed to be unchanged. The fit curve can, therefore, be adjusted to saturation by re-calculating the b_{sh} according to the relationship presented above. An example of such a calculation can be seen in Figure 7-23.

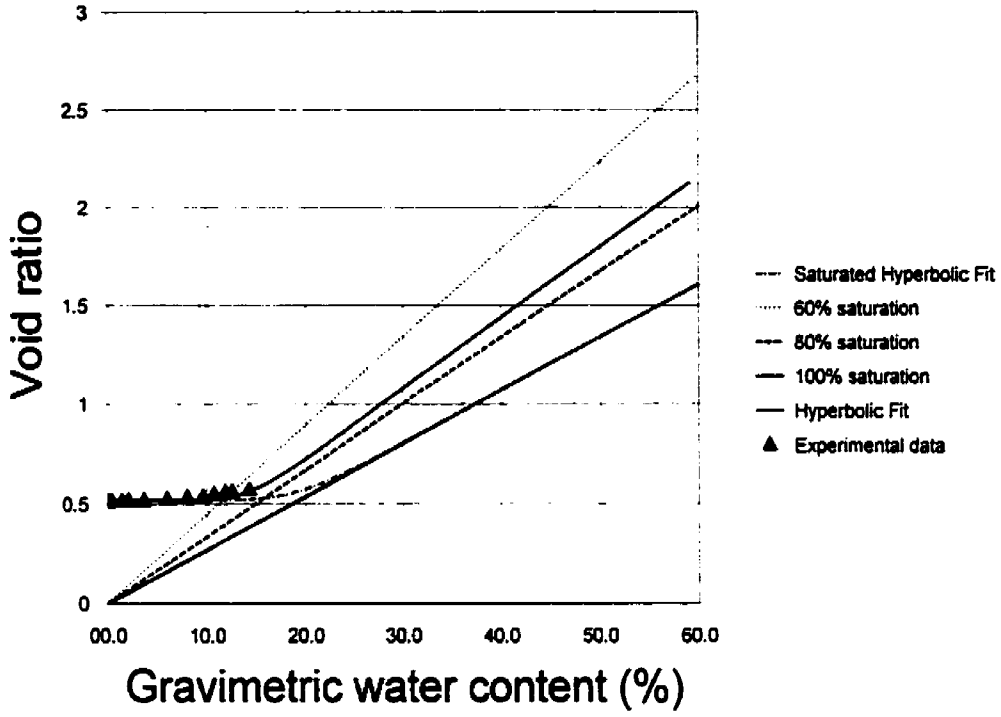

Figure 7-23 Shrinkage curve for a silty sand from partly saturated conditions (Russam, 1958) index #12423

Re-calculation of the compression equation is required when the initial conditions for the experimentally measured compression equation are different from the initial conditions of the soil-water characteristic curve. The compression curve was first fit with Equation 7-3. Re-calculation of the compression curve, therefore, involves the calculation of a new swelling pressure, σ_s, and preconsolidation pressure, σ_p. The rebound index, C_r, and compression index, C_c, of a particular soil remain constant. The modification of a typical compression test to account for varying initial conditions is shown in Figure 7-24.

$$e(\sigma) = \left[e_o - \frac{C_r}{2} \ln\left[1 + \left(\frac{\sigma}{\sigma_s}\right)^2\right] - \frac{C_c - C_r}{2} \ln\left[1 + \left(\frac{\sigma}{\sigma_p}\right)^2\right]\right]$$

Equation 7-3

where e_o = initial or starting void ratio,

C_r = recompression index,

C_c = compression index,

σ_s = swelling pressure (kPa),

σ_p = preconsolidation pressure (kPa).

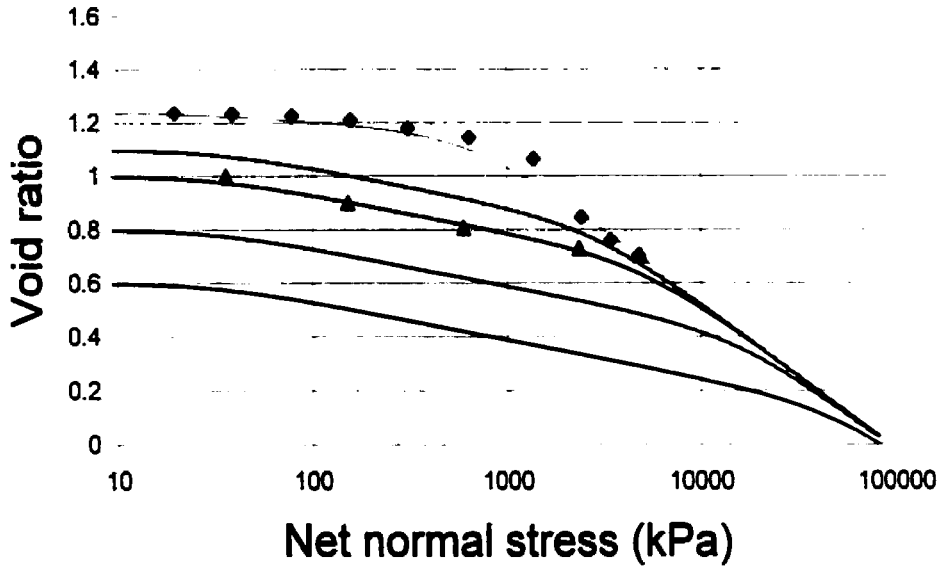

Figure 7-24 Representation of a family of compression curves generated with the four-parameter equation based on an Albany Clay published by Schmertmann (1953) (12530)

The calculation of the swelling pressure, σ_s, and the preconsolidation pressure, σ_p, is required for the generation of a series of curves for Figure 7-24. σ_s may be taken as the minimum net normal stress on the rebound curve. If rebound data is not present, σ_s may be calculated from the compression branch of the curve. σ_s would then be equal to σ_p if the soil is normally consolidated or mathematically determined from the fitting algorithm is the soil is overconsolidated.

The preconsolidation pressure, σ_p, may be determined by the following method. Firstly, a straight line on a semilog plot is used to represent the virgin compression branch of the curve. Another straight line is used to represent the rebound portion of the curve. The rebound line is

assumed to pass through the initial void ratio of the current soil state and the swelling pressure, σ_s. The intersection of these two straight lines will yield σ_p.

7.6 Calculation of Volume-Mass Constitutive Surfaces

The following sections describe the mathematical steps necessary for the generation of a mathematical description of the void ratio and water content constitutive surfaces.

7.6.1 Void Ratio Constitutive Surface

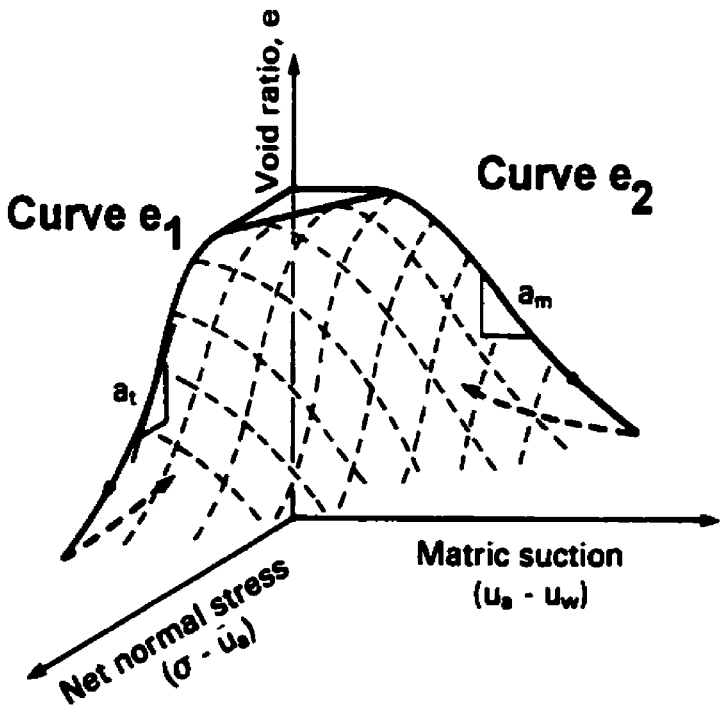

Figure 7-25 Generalization of the void ratio constitutive surface

The void ratio constitutive surface is developed to describe the volume-change aspects of soil behavior in keeping with previous developments of constitutive surfaces. The void ratio constitutive surface describes the relationship between void ratio, net normal stress, and soil suction. Methods for obtaining the boundaries of this constitutive surface and calculations across the surface are presented.

7.6.1.1 Void ratio versus net normal stress

The void ratio versus net normal stress boundary constitutive relation may be formulated either from an oedometer test or an isotropic triaxial compression test. The formulations presented in this paper apply to oedometer and triaxial compression test results. Accommodation of the type of test performed must be done during the calculation of Young's Modulus. The calculation of Young's Modulus may be seen in Chapter 4.

Oedometer data is more common in the literature than isotropic triaxial data. The results presented in this chapter, therefore, are calculated primarily with the use of oedometer data. The two-slope equation presented in Equation 7-3 will be used to mathematically represent the experimental oedometer data.

7.6.1.2 Void ratio versus soil suction

The relationship between void ratio and soil suction can be experimentally determined. Volume change and soil suction measurements during the drying process will yield both a soil-water characteristic curve and a shrinkage curve. The void ratio versus soil suction boundary constitutive relationship can be calculated using a continuous mathematical relationship to represent the soil-water characteristic curve and the shrinkage curve. The Fredlund and Xing (1994) equation can be used to fit experimental soil-water characteristic curve data using a least-squares algorithm. The shrinkage relationship between void ratio and gravimetric water content can be represented using the hyperbolic equation as presented in Equation 7-2. Calculations may proceed in the following manner once mathematical representation of the soil-water characteristic curve and the shrinkage curve is achieved.

The soil-water characteristic curve is represented by the Fredlund and Xing (1994) equation (Equation 7-4).

$$w_w(\psi) = w_s\left[1 - \frac{\ln\left(1+\frac{\psi}{h_r}\right)}{\ln\left(1+\frac{10^6}{h_r}\right)}\right]\left[\frac{1}{\left[\ln\left[\exp(1)+\left(\frac{\psi}{a_f}\right)^{n_f}\right]\right]^{m_f}}\right]$$

Equation 7-4

where:

w_s = saturated gravimetric water content,

ψ = soil suction,

a_f = fitting parameter closely related to the air entry value for the soil,

n_f = fitting parameter related to the maximum slope of the curve,

m_f = fitting parameter related to the curvature of the slope,

h_r = constant parameter used to adjust lower portion of curve.

The shrinkage of a soil can be represented by a hyperbolic equation as presented in Equation 7-2. The substitution of Equation 7-2 into Equation 7-4 gives the relationship between gravimetric water content and soil suction. The boundary of the consitutive surface describing the relationship between void ratio and soil suction may then be described as follows.

$$e(\psi) = e(w(\psi))$$

or

$$e(\psi) = a_{sh}\left[\frac{\left[\left[w_s\left[1-\frac{\ln\left(1+\frac{\psi}{h_r}\right)}{\ln\left(1+\frac{10^6}{h_r}\right)}\right]\right]\left[\frac{1}{\left[\ln\left[\exp(1)+\left(\frac{\psi}{a_f}\right)^{n_f}\right]\right]^{m_f}}\right]\right]^{c_m}}{b_{sh}^{\ c_m}}+1\right]^{\left(\frac{1}{c_m}\right)}$$

Equation 7-5

7.6.1.3 Calculated Void ratio surface

It was considered important to formulate a complete mathematical representation of the void ratio constitutive surface. To allow mathematical representation, and considering Postulate 4, it was necessary to restrict Equation 7-3 to a soil undergoing normal compression only. This restriction allows Equation 7-3 to be simplified to Equation 7-6. The inverse of Equation 7-6 may then be determined as Equation 7-7. Equation 7-7 represents the translation between the void ratio produced by suction and the equivalent net normal stress. Substitution of Equation 7-5 into Equation 7-7 allows for the translation of suction to net normal stress. Therefore, the void ratio at any point on the constitutive surface may be represented by adding the net normal stress to an equivalent, suction induced, net normal stress represented by Equation 7-7. Equation 7-8 then represents the equation of the void ratio constitutive surface.

$$e(\sigma) = \left[e_o - \frac{C_c}{2}\ln\left[1+\left(\frac{\sigma}{\sigma_p}\right)^2\right]\right]$$

Equation 7-6

$$\sigma(e) = \sqrt{\left[\exp\left(-2\ln(10)\frac{(e(\psi)-e_o)}{C_c}\right)-1\right]}\sigma_p$$

Equation 7-7

$$e(\sigma) = \left[e_o - \frac{C_c}{2}\ln\left[1+\left(\frac{\sigma+\sigma(e)}{\sigma_p}\right)^2\right]\right]$$

Equation 7-8

The void ratio constitutive surface for a number of different soils may be seen in Figure 7-26 and Figure 7-27.

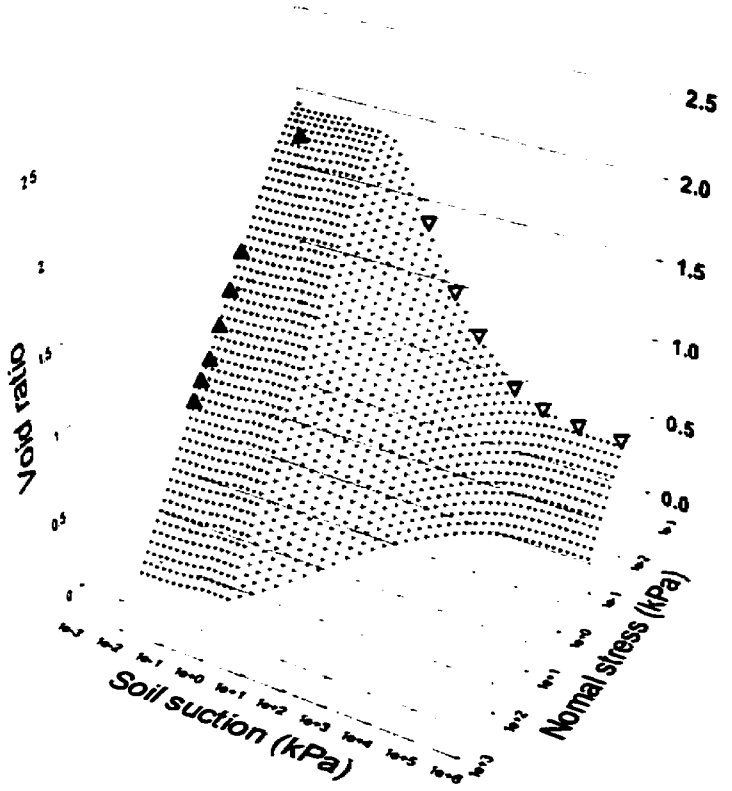

Figure 7-26 Void ratio constitutive surface for a oligocenic clay published by Nascimento, 1961 (12436)

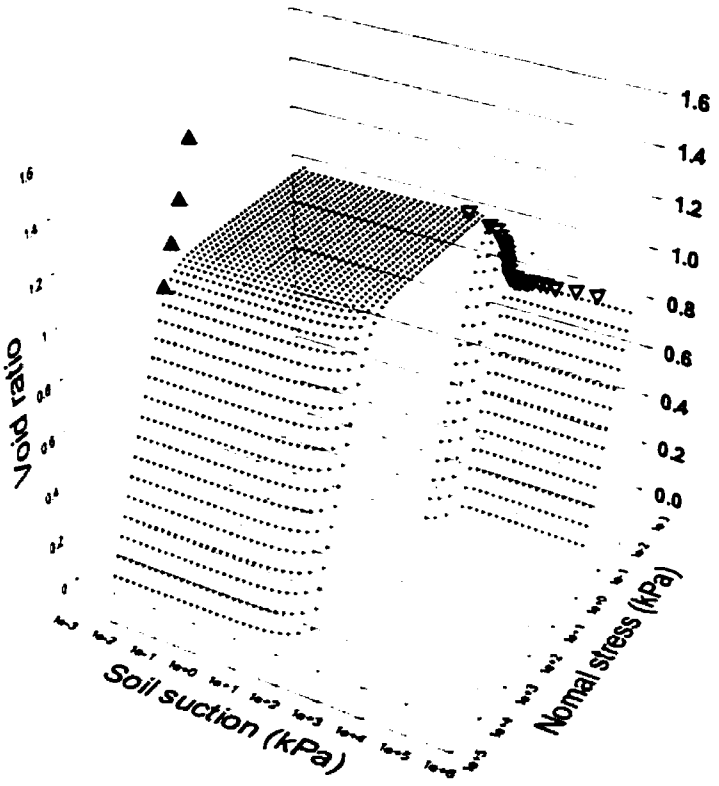

Figure 7-27 Void ratio constitutive surface for an overconsolidated-dried Speswhite Kaolinite published by Ridley, 1993 (12445)

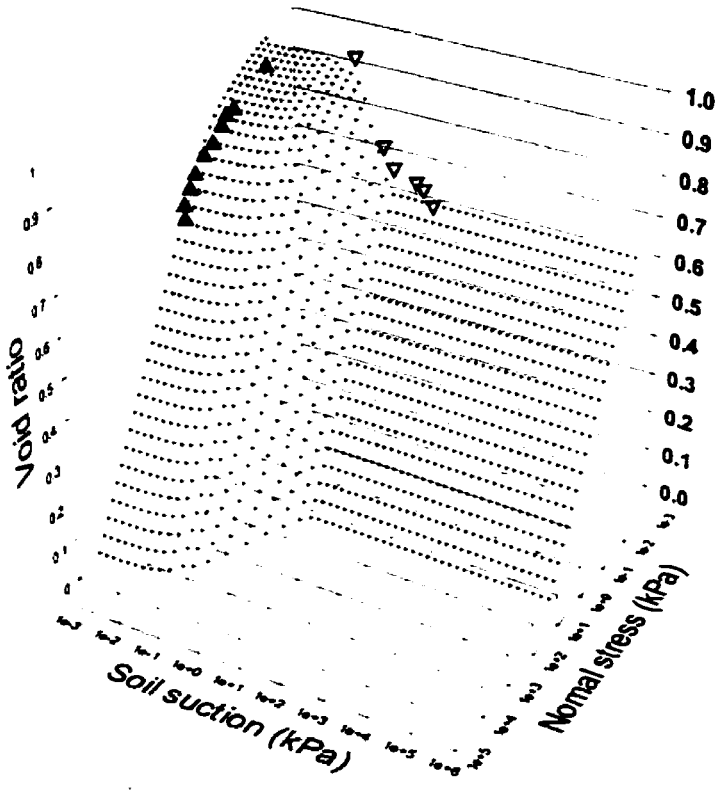

Figure 7-28 Void ratio constitutive surface for a fine sand published by Nascimento, 1961 (12437)

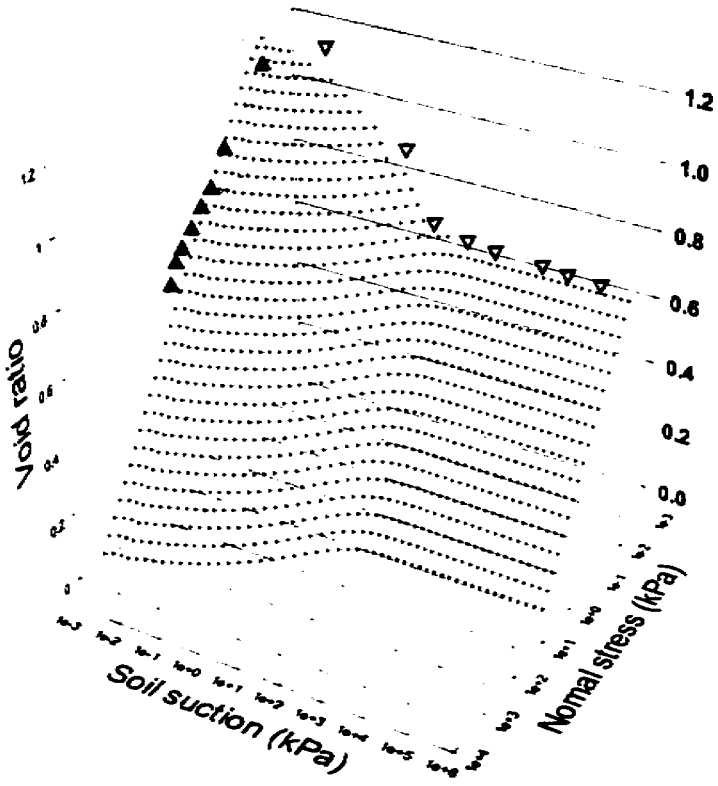

Figure 7-29 Void ratio constitutive surface for a silt published by Nascimento, 1961 (12438)

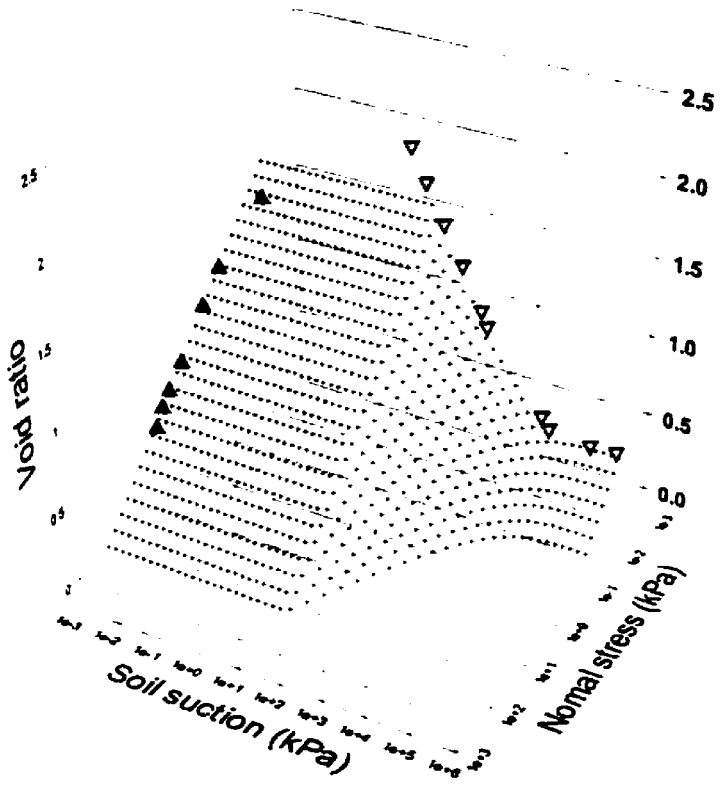

Figure 7-30 Void ratio constitutive surface for a basaltic clay published by Nascimento, 1961 (12442)

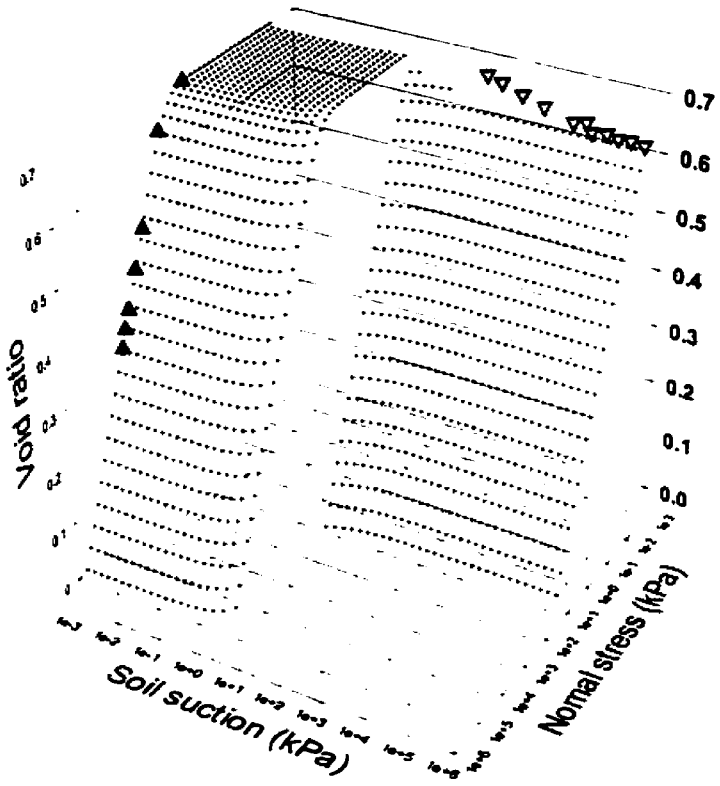

Figure 7-31 Void ratio constitutive surface for a compacted Uniform Silt from Ho (1988) (18681)

7.6.2 Water Content Constitutive Surface

The water content constitutive surface is developed to describe the water content of the soil in keeping with previous developments of constitutive surfaces. The water content constitutive surface describes the relationship between water content, net normal stress, and soil suction. Methods for obtaining the boundaries of this constitutive surface and calculations across the surface are presented.

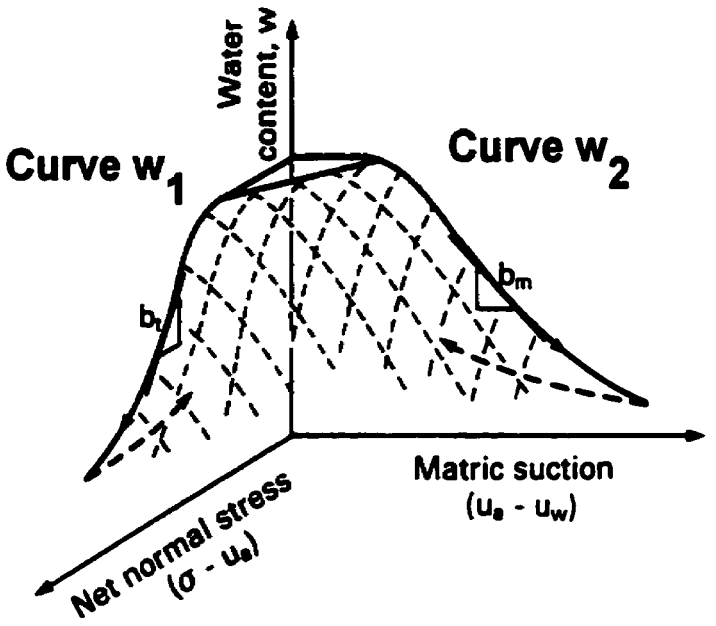

Figure 7-32 Generalization of the water content constitutive surface

7.6.2.1 *Water content versus soil suction*

Curve w_2 (shown in Figure 7-32) boundary of the water content constitutive surface can be represented by the soil-water characteristic curve. Experimental data is fit with a nonlinear least squares regression algorithm to mathematically represent laboratory results. The Fredlund and Xing (1994) equation is used to represent the soil-water characteristic curve due to its ability to model the high suction range. The Fredlund and Xing (1994) equation may be seen in Equation 7-4. Since the soil-water characteristic curve is typically measured as water content versus soil suction, no mathematical conversion is necessary to allow representation of the w_2 boundary.

A correction is introduced to the soil-water characteristic curve to allow the air entry value of the Fredlund and Xing (1994) equation to increase as compression increases. The effect of various compression levels on the air entry value has been examined by Vanapalli (1994). Vanapalli (1994) suggested that the air entry value of a soil followed a line drawn through the steepest slope of the soil-water characteristic curve for soils compacted at optimum and dry of optimum. A straight line of slightly different slope was followed for soils compacted wet of optimum. A modification to the Fredlund and Xing (1994) equation is therefore presented to

account for changes in the air entry value as the level of compression increases. As a first approximation, the air entry value is assumed to increase linearly on a semilog plot at a rate equal to the steepest point of the soil-water characteristic curve.

Modification of the air entry value for the Fredlund and Xing (1994) equation is achieved by making the a_f parameter a function of net normal stress. The a_f parameter has been shown to be related to the air entry value, therefore, this is considered a reasonable relation. Firstly, a straight line is drawn through the steepest point on the soil-water characteristic curve. The line is then shifted so that the soil-water characteristic curve is unmodified when the net normal stress is at a minimum. The construction may be seen in Figure 4-26. The final equation for the modified Fredlund and Xing (1994) equation may be seen in Equation 4-14.

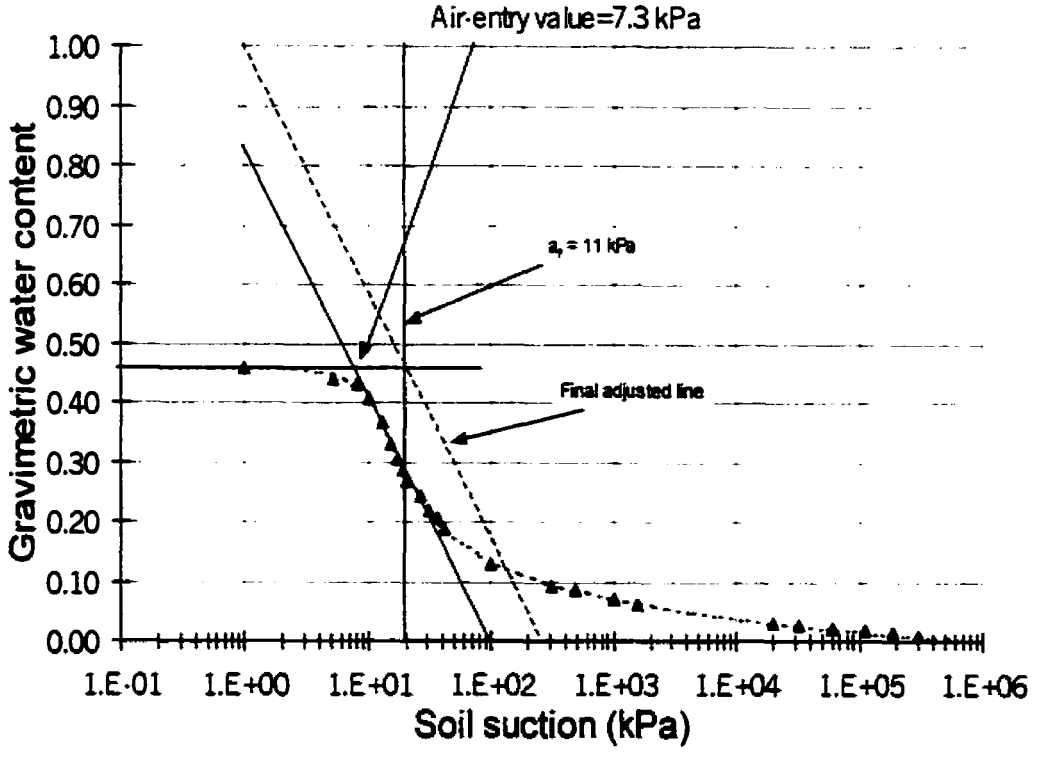

Figure 7-33 Calculation of modification for air-entry value for a Loam using the Fredlund and Xing (1994) equation, a_f=11.1, n_f=3.56, m_f=0.54, h_r=48.4 (91)

The straight line on a semilog plot may be represented by Equation 4-12.

$$w = m \log(a_f) - b$$

Equation 7-9

where: a_f = Fredlund and Xing (1994) parameter related to the air entry value of the soil,

w = initial water content of the soil sample,

m = slope of the line on a semilog plot,

b = y axis intercept at a value of 1.0.

Calculation of the a_f parameter, therefore, requires that Equation 4-12 be solved in terms of a_f.

$$a_f = 10^{\frac{(b-w)}{m}}$$

Substituted into the Fredlund and Xing (1994) equation this correction now becomes:

$$w_w(\psi) = w_s \left[1 - \frac{\ln\left(1+\frac{\psi}{h_r}\right)}{\ln\left(1+\frac{10^6}{h_r}\right)} \right] \left[\frac{1}{\left[\ln\left[\exp(1) + \left(\frac{\psi}{10^{\frac{(b-w_s)}{m}}} \right)^{n_f} \right] \right]^{m_f}} \right]$$

Equation 7-10

Which yields an equation for the soil-water characteristic curve in terms of soil suction and initial water content.

7.6.2.2 *Water content versus net normal stress*

The boundary curve w_1 (Figure 7-32) of the water content constitutive surface may be experimentally determined with a compression test. Experimental data is then fit with the four-parameter model seen in Equation 7-3. It is not a requirement that the initial condition for the compression test match the initial condition for the measurement of the soil-water characteristic curve. The reason for this is that once the slope of the recompression and the virgin compression branch have been determined, a representative compression curve may be generated based on any initial void ratio. The procedure for this may be seen in section 7.5.3.

The relationship Se=wGs is used to convert void ratio to water content for the w_1 boundary of the water content constitutive surface. Saturation will be 100% for all compression tests in accordance with ASTM D4546. Therefore the method for representing curve w1 can be expressed as:

$$w = \frac{e}{G_s}$$

The above relationship may then be expressed as a function since void ratio is a function of net normal stress.

$$w(\sigma) = \frac{\left[e_o - \frac{C_r}{2} \ln\left[1 + \left(\frac{\sigma}{\sigma_s} \right)^2 \right] - \frac{C_c - C_r}{2} \ln\left[1 + \left(\frac{\sigma}{\sigma_p} \right)^2 \right] \right]}{G_s}$$

Equation 7-11

Equation 7-11 may then be used to represent curve w_1 (Figure 7-32) once the equation parameters have been determined by least squares regression.

7.6.2.3 Calculated water content surface

In the preceding sections the boundary conditions of the water content constitutive surfaces are developed. A method of mathematically representing the interior of the constitutive surface is now presented. The compression curve is first used to represent initial water content conditions along the saturated boundary. The soil-water characteristic curve is then calculated at varying initial conditions and various air entry values in accordance with Postulate 4 and Equation 4-14. Equation 7-11 is substituted in place of w_s in Equation 4-14 to yield the equation for the entire constitutive surface. The combination of Equation 4-14 and Equation 7-11 allows for complete mathematical representation of the water content constitutive surface. The water content constitutive surface for a number of different soils may be seen in Figure 7-26 and Figure 7-27.

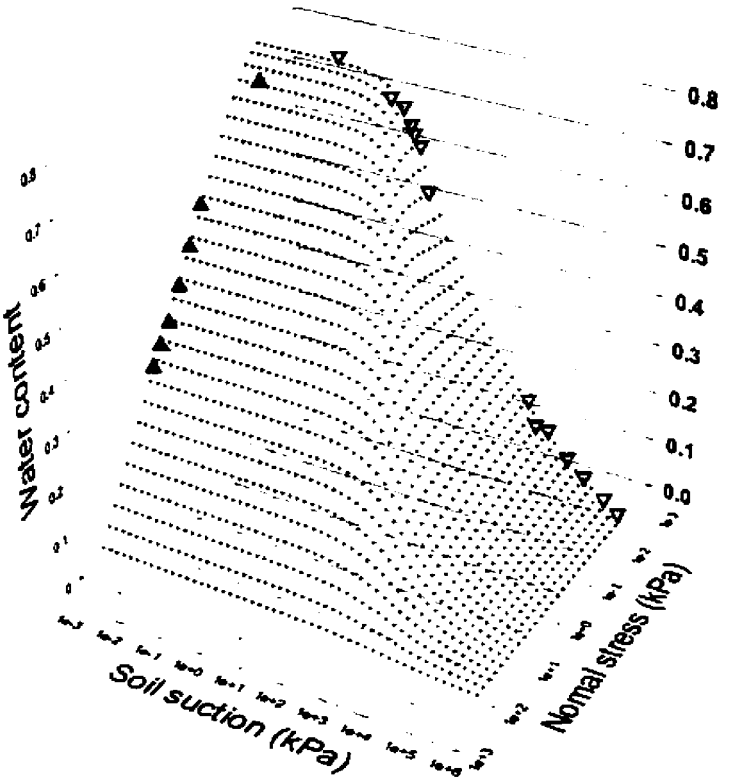

Figure 7-34 Water content constitutive surface for an undisturbed oligocenic clay published by Nascimento, 1961 (12436)

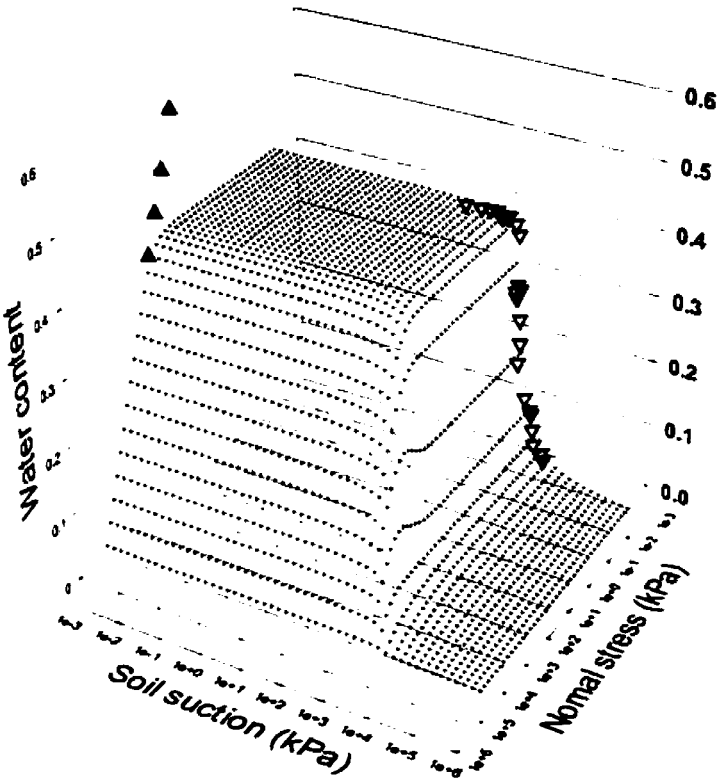

Figure 7-35 Water content constitutive surface for a slurried overconsolidated-dried Speswhite Kaolinite published by Ridley, 1993 (12445)

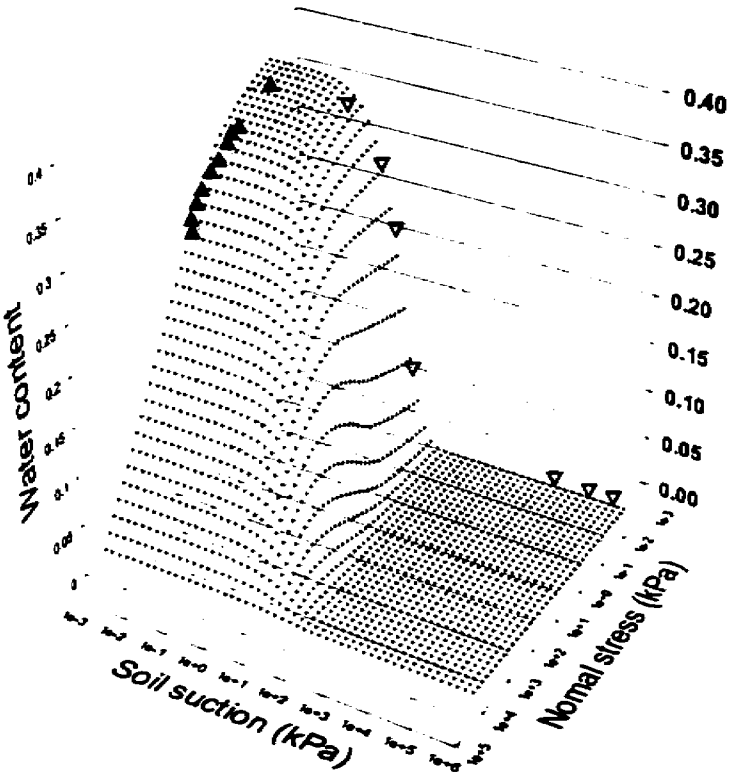

Figure 7-36 Water content constitutive surface for an undisturbed fine sand published by Nascimento, 1961 (12437)

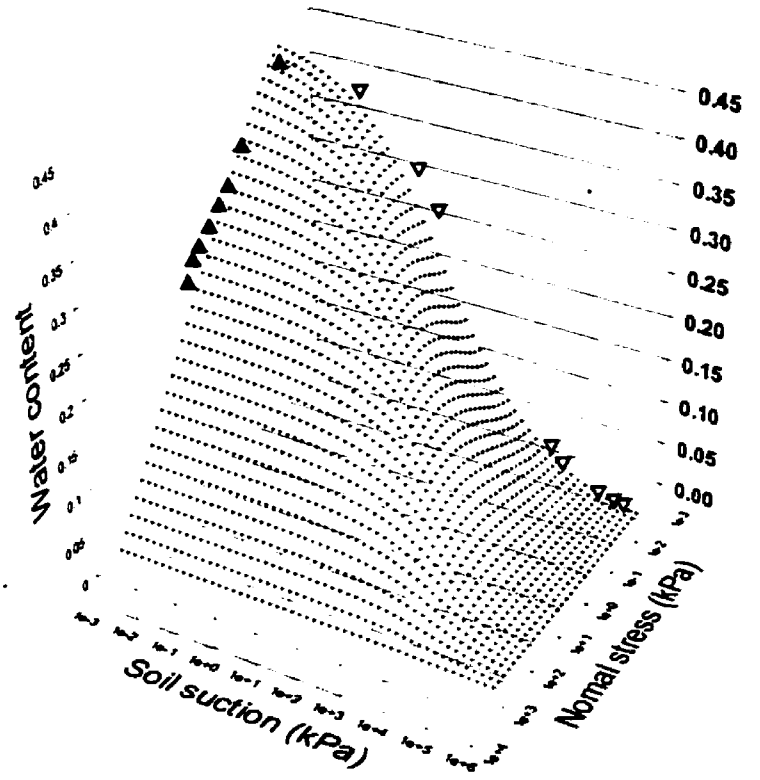

Figure 7-37 Water content constitutive surface for an undisturbed silt published by Nascimento, 1961 (12438)

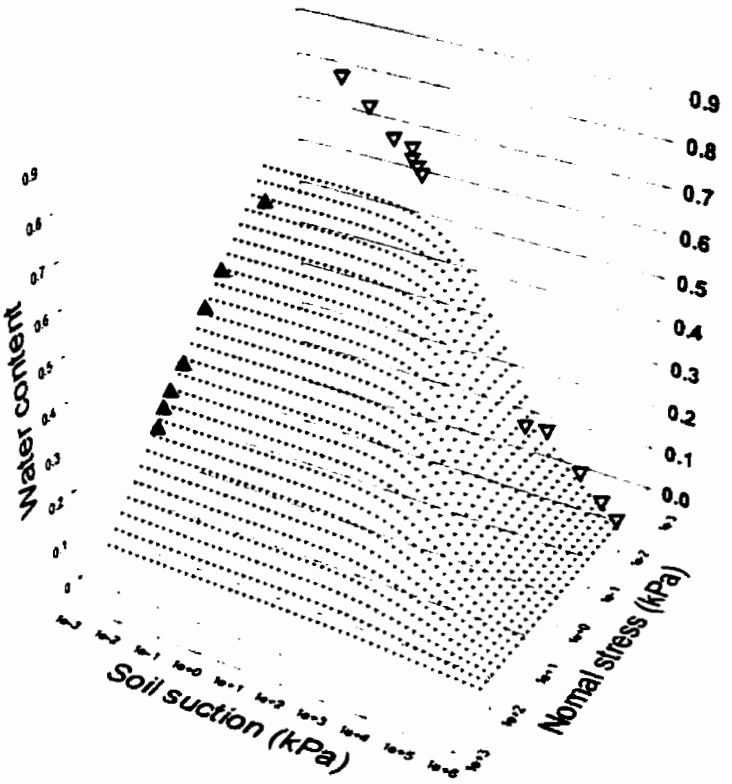

Figure 7-38 Water content constitutive surface for an undisturbed basaltic clay published by Nascimento, 1961 (12442)

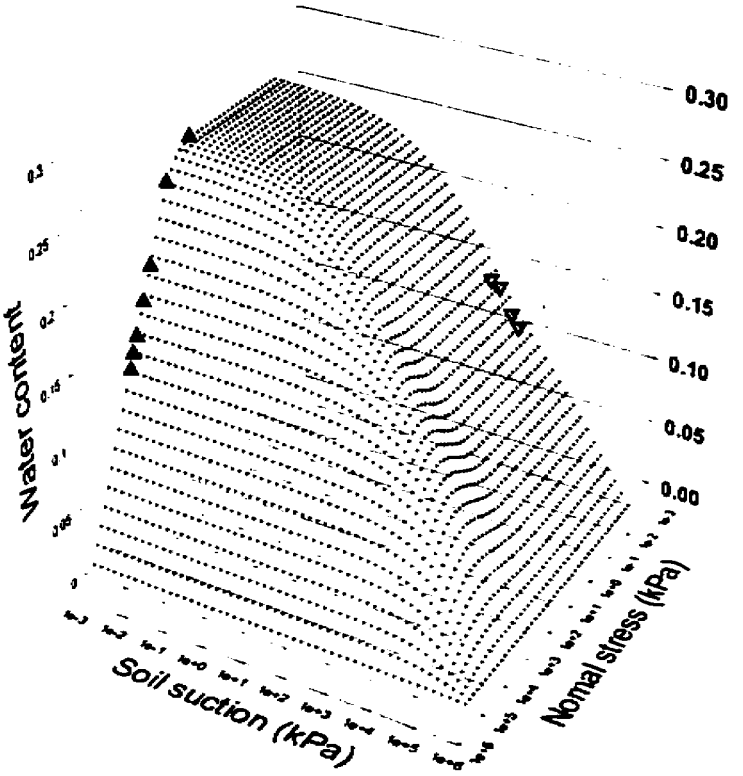

Figure 7-39 Water content constitutive surface for a compacted Uniform Silt from Ho (1988) (18681)

7.7 Conclusions

Based on analysis of the data collected for this chapter, it can be concluded that it is possible to mathematically represent the void ratio and water content constitutive surfaces. It has previously been shown that the void ratio and water content constitutive surface for monotonic deformation are unique. A series of postulates were developed based on observed soil behavior. These postulates were then used as a basis to extend laboratory testing of boundary conditions to a representation of the entire constitutive surface. Mathematical representation of the constitutive surface also allows significant flexibility in the application of the mathematical model to finite element solution methods.

7.8 References

Aitchison G.D., 1967, Separate Roles of Site Investigation, Quantification of Soil Properties, and Selection of Operational Environment in the Determination of Foundation Design on Expansive Soils, in Proc.3rd Asian Reg. Conf. Soil Mech. Found. Eng., Haifa, Israel, 3, 72-77

Aitchison G.D. J.A. Woodburn, 1969, Soil Suction in Foundation Design, in Proc. 7th Int. Conf Soil Mech. Found. Eng., Mexico, 2, 1-8

Aitchison G.D. R. Martin, 1973, A Membrane Oedometer for Complex Stress-Path Studies in Expansive Clays, in Proc. 3d Int Conf. Expansive Soils, Haifa, Israel, 2, 83-88

Alonson E.E. A. Lloret, 1982, Behaviour of Partially Saturated Soil in Undrained Loading and Step by Step Embankment Construction, in Proc. IUTAM Conf. Deformation and Failure of Granular Mater, Delft, The Netherlands, 173-180

Barden L. A.O. Madedor and G.R. Sides, 1969, The Flow of Air and Water in Partly Saturated Clay Soil, presented at the Int. Symp. fundamentals of Transport Phenomena in Flow Through Porous Media, Haifa, Israel

Barden L. A.O. Madedor and G.R. Sides, 1969, Volume Chage Characteristics of Unsaturated Clay, ASCE J. Soil Mech. Found. Div., SM1, 95, 33-52

Biot M.A., 1941, General Theory of Three-Dimensional Consolidation, J. Appl. Phys., 12, no. 2, 155-164

Bishop A.W., 1959, The Principal of Effective Stress, lecture delivered in Oslo, Norway; published in Teknisk Ukeblad, Oslo, Norway, 106, no39, 859-863

Bishop A.W. G.E. Blight, 1963, Some Aspects of the Effective Stress in Saturated and Unsaturated Soils, Geotechnique, 13, no.3, 177-197

Brackley I.J.A., 1971, Partial Collapse in Unsaturated Expansive Clay, in Proc. 5th Reg. Conf. Soil Mech. Found. Eng., South Africa, 23-30

Burland J.B., 1965, Some Aspects of the Mechanical Behavior of Partly Saturated Soils, Moisture Equilibria and Moisture Changes in the Soils Beneath Covered Areas A Symp. in print, G.D. Aitchison, Ed., Australia: Butterworths, 270-278

Coleman J.D., 1962, Stress/Strain Relations for Partly Saturated Soils, Geotechnique (Correspondence), 12 no. 4, 348-350

Fredlund D.G., 1974, Engineering Approach to Soil Continua, in Proc 2nd Symp. Application of Solid Mech., Hamilton, Ontario, Canada, 46-59

Fredlund D.G. N.R. Morgenstern, 1973, Pressure Response Below High Air Entry Discs, in Proc. 3rd Int. Conf. Expansive Soils Jerusalem Academic Press, Haifa, Israel, 1, 97-108

Fredlund D.G. N.R. Morgenstern, 1977, Stress State Variables for Unsaturated Soils (1), ASCE J. Geotech. Eng. Div. GT5, 103, 447-466

Fredlund, D.G., and Xing, A., 1994, Equations for the soil-water characteristic curve, Canadian Geotechnical Journal, Vol. 31, No. 3, pp. 521-532.

Fredlund, D. G., 1964, Comparison of Soil Suction and One-Dimensional Consolidation Characteristics of a Highly Plastic Clay, M. Sc. Thesis, University of Alberta, 26 pp.

Fredlund, D.G., 1973, Volume change behavior of unsaturated soils, Ph.D. dissertation, University of Alberta, Edmonton, AB, Canada, 490 pp.

Fredlund, D.G., and Rahardjo, H., 1993, Soil mechanics for unsaturated soils, John Wiley & Sons, Inc., New York, pp. 346-365

Ho, D. Y., 1988, The Relationship Between the Volumeteric Deformation Moduli of Unsaturated Soils, Ph. D. Thesis, University of Saskatchewan, 1-379

Jennings J.E. and Burland J.B., 1962, Limitations to the Use of Effective Stresses in Partly Saturated Soils, Geotechnique, vol. 12, no. 2, pp.125-144

Matyas E.L. and Radhakrishna H.S., 1968, Volume Change Characteristics of Partially Saturated Soils, Geotechnique, nol. 18, no. 4, pp. 432-448

Nascimento U., 1961, Contribution on the physical interpretation of Soil Properties

Ridley Andrew M., 1993, The measurement of soil moisture suction, University of London, London

Vanapalli, S.K., 1994, Simple test procedures and their interpretation in the evaluation of the shear strength of an unsaturated soil,, Ph.D. thesis,, University of Saskatchewan, Saskatoon, Canada,, pp. 350.

CHAPTER 8.0 Conclusions and Recommendations

8.1 Introduction

The thesis consists of a series of articulated research studies that come together to form an approach to assist in the implementation of unsaturated soil mechanics into geotechnical engineering practice. The conclusions and recommendations are presented for each of the chapters of the thesis.

8.2 Conclusions

The conclusions for each of the chapters can be summarized as follows:

Chapter 1 sets the stage for the chapters to follow as well as establishing the need for a new approach to the implementation of unsaturated soil mechanics.

1. A new philosophical approach is required for the application of unsaturated soil mechanics. The classical approach used in saturated soil mechanics has become too costly to implement for unsaturated soil mechanics, primarily because of the costs associated with the assessment of unsaturated soil properties. It is suggested that there is need to move into a new paradigm (i.e., an entirely new mindset towards the problem) for the assessment of unsaturated soil properties.
2. The use of estimated non-linear, coefficient of permeability functions (or hydraulic conductivity functions) for an unsaturated soil has been successfully applied and is well-established in the area of geo-environmental engineering. The unsaturated coefficient of permeability function is estimated from the soil-water characteristic curve and the saturated coefficient of permeability for the soil. The success of using this approach for seepage problems involving unsaturated soil provides a confidence assurance that a similar approach or methodology can be used for other areas of unsaturated soil mechanics such as volume change and shear strength.

3. Finite element models make use of the latest numerical methods to assist in numerical convergence for highly non-linear boundary-value problems such as those encountered in saturated-unsaturated soils. The development of mathematical techniques to represent soil property functions is necessary for the modeling of complex unsaturated soil problems.
4. Unsaturated soil property functions are, in general, difficult and costly to obtain experimentally. Methods for the estimation of the soil-water characteristic curve, the shrinkage curve, and other constitutive soil properties need to be developed and subsequently tested and verified. This process is extensive and only the first phase of this area of study is within the scope of this thesis.

Chapter 2 provides a background summary of the current development in unsaturated soil mechanics. Future direction for research and the application of unsaturated soils technology is presented. A review of the research literature sets the stage for the establishment of needs relative to the application of unsaturated soil mechanics.

1. The soil-water characteristic curve (SWCC) has become the central relationship involved in the empirical estimation of unsaturated soil property functions for unsaturated soil mechanics.
2. The soil-water characteristic curve provides an approximate relationship for the partitioning of the air and water phases in an unsaturated soil. As such, it provides a basis for the estimation of many other unsaturated soil property functions.
3. A reasonably accurate mathematical representation of the soil-water characteristic curve is important. Equations for the soil-water characteristic curve, as well as a theoretical description of the zones of desaturation have been characterized in the literature. The mathematical models presented by Fredlund and Xing (1994), van Genuchten (1980), van Genuchten and Mualem (1980), van Genuchten and Burdine (1980), Gardner (1964), and Brooks and Corey (1964) are reviewed with respect to general characteristics of each equation.
4. The soil-water characteristic curve can be used as a foundation for calculating soil property functions for properties such as the coefficient of permeability, shear strength and volume change for an unsaturated soil. The soil-water characteristic curve forms a partial basis for

describing the engineering behavior of an unsaturated soil and provides a common (and focal) means of relating fundamental soil properties to one another.

5. A review of common soil-property functions relevant to unsaturated soil mechanics, along with their application to geotechnical engineering practice is presented.
6. A generalized procedure for the determination of unsaturated soil properties is proposed.

Chapter 3 introduces several mathematical equations for the representation of the grain-size distribution curve. Calculations based on the grain size distribution data are presented for illustration and verification purposes. Chapter 3 provides the basis for chapter 4 which utilizes the grain-size curve equation to estimate a soil-water characteristic curve.

1. The grain-size distribution curve has historically been analyzed as a manual process. There has also been some attempt to use a lognormal distribution fit consisting of one, two, or three parameters. Unimodal and bimodal equations are presented in this chapter to fit essentially any grain-size distribution dataset. The unimodal equation was found to provide an excellent fit to a wide variety of uniform and well-graded soils. The extremes of the grain-size distribution were also well-fit by using an equation that allowed independent control of the extremities.
2. Gap-graded soils were best fit using a bimodal type equation. The bimodal equation allowed for the mathematical representation of any grain-size distribution where the sample contained two distinctly different, but dominant particle size groups.
3. Mathematical representation of the grain-size distribution curve was shown to provide numerous benefits. Curves can be identified and categorized by means of the best-fit coefficients or engineering parameters back-calculated from the fit curve. Likewise, grain-size curves can be located in a data base using searching techniques. Other grain-size variables (i.e., % clay, d_{10}, d_{60}, etc.) can be mathematically determined from the best-fit equation. The unimodal and bimodal equations provide a method for fitting the three major categories of soils (i.e., well-graded soils, uniform soils, and gap-graded soils).
4. The proposed continuous mathematical function for the grain-size curve sets the stage for performing further analyses such as to estimate the soil-water characteristic curve of a soil.

Chapter 4 proposes a new method for the estimation of the soil-water characteristic curve from grain-size distribution curve. A wide range of grain size data sets are analyzed and the predicted soil-water characteristic curves are compared to laboratory measured soil-water characteristic curve datasets.

1. The estimation of soil-water characteristic curve from grain-size distribution was found to be reasonably accurate for sands, and silts. The predictions appear to be best for uniformly graded soils but the prediction technique certainly appears to have good promise for all silts and sands.
2. It is more difficult to estimate the soil-water characteristic curve for clays, tills and loams. However, the accuracy of the soil-water characteristic curve estimation algorithm was still reasonable. Results tended to be sensitive to the "packing porosity", n_p, and more research needs to be done to fully understand how to take into account the arrangement of the particles.
3. The proposed new pedo-transfer function (i.e., function to predict the soil-water characteristic curve) was compared to five other previously proposed pedo-transfer functions. The success of each pedo-transfer function was evaluated based on the R^2, air-entry value, and the maximum slope. The proposed new pedo-transfer function showed an improved accuracy with respect to the R^2 error distribution.
4. The proposed new pedo-transfer function showed reasonable accuracy when compared to the maximum slope as determined from the experimental dataset. The best performance was obtained when using the Vereecken (1989) method. There was some uncertainty as to whether the Rawls (1985) method was properly implemented in the calculations for this chapter.
5. Comparisons between the measured and estimated air-entry values, AEV, indicated a significant improvement when using the new pedo-transfer function as opposed to other existing methods. The new pedo-transfer function and the Arya and Paris (1981) methods showed the highest level of confidence in correctly estimating the air-entry value of a soil.

Chapter 5 introduces the fundamental soil properties and the mathematical equations necessary to characterize the volume change behavior of an unsaturated soil. Mathematical equations are proposed for the representation of the compression curve from experimental data measured in

an oedometer test, as well as data measured in an isotropic triaxial test. These functions are for a saturated soil and form the reference (or basic) soil characteristic for defining volume change.

1. The compression curve from a one-dimensional oedometer test has formed the basis for volume-change calculations since the inception of soil mechanics. This chapter presents two continuous mathematical equations capable of fitting the classical forms for compression curves for a saturated soil.
2. The three-parameter equation was found to perform well for fitting the compression curves for normally and over-consolidated soils.
3. The parameters of the three-parameter equation does not appear to be related to physical properties of the soil.
4. The four-parameter equation provided a good fit for normally and overconsolidated soils, over a wide range of loading conditions.
5. Once the compression curve is best-fit with a continuous mathematical equation, a number of practical soil mechanics functions can be computed. The relationship of coefficient of compressibility, a_v, coefficient of volume change, m_v, and compression index, C_c as well as Young's Modulus, E, may all be represented as a function of net normal stress. The mathematical representation of the slope of the compression curve in terms of Young's Modulus provides a function that can be used for the modeling of volume change of saturated and subsequently unsaturated soils.

Chapter 6 introduces an equation that can be used to best-fit the shrinkage curve. A method of estimating the shrinkage curve is also proposed and verified using experimental data from the research literature.

1. The shrinkage characteristics of a large number of soils have been established in the literature. A mathematical relationship was developed to model the shrinkage behavior of slurried, compacted, and undisturbed soils. The shrinkage equation was shown to closely fit a wide variety of soils.
2. The shrinkage curve can be used in conjunction with the soil-water characteristic curve for the calculation of the void ratio versus soil suction relationship. The void ratio relationship forms the second boundary of the void ratio constitutive surface (the first boundary being formed by the void ratio versus net normal stress).

3. An estimation method was proposed and verified for the estimation of the shrinkage curve based on the air entry value of the soil-water characteristic curve, volume-mass properties and the initial state (i.e., slurried, compacted, remoulded) of the soil. The importance of measuring of volume changes (or estimating volume changes) of a soil during shrinkage due to suction changes, was studied.
4. The analysis of the shrinkage (and swelling) behavior of an unsaturated soil requires a mathematical soil property function. A mathematical fitting and estimation method was proposed for modeling the shrinkage (i.e., volume decrease) behavior of highly plastic soils as well as low plasticity soils.

Chapter 7 applies individual soil-property functions to the development of three-dimensional constitutive surfaces for volume change (and water content change) for unsaturated soils.

1. Based on the analysis of the research data found in the literature, it was concluded that it is possible to mathematically represent the entire void ratio and water content constitutive surfaces. The limiting conditions for each of the constitutive surfaces are first mathematically defined and then the assumptions related to intermediate stress states are proposed and mathematically formulated.
2. The void ratio (and water content) constitutive surface must be defined independently for monotonic deformations. In other words, an independent formulation and set of mathematical relationships are required for the volume decrease (and water content decrease) and for volume increase (and water content increase). The limiting conditions for volume increase and decrease are independent of one another.
3. A series of postulates are developed for the definition of the overall constitutive surfaces. The postulates are based on data from various research studies on unsaturated soil behavior. These postulates form the basis for the extension of laboratory tests which define the boundary conditions of the entire constitutive surfaces.
4. Mathematical representation of the entire void ratio (and water content) constitutive surfaces allows for the mathematical representation of a Young's modulus unsaturated soil property function for the modeling of finite element problems. The same is true for an unsaturated soil property function for the water content constitutive surface.

8.3 Recommendations for Future Research Studies

Future work may be performed on various topics associated with each of the chapters. In Chapter 4 there is need for further refinement and modification of pedo-transfer function for the soil-water characteristic curve. The method outlined in this thesis assumes a constant distribution of porosity for all grain-sizes comprising the soil. This assumption should be modified to become a function of particle size and possibly other factors. This modification would allow for influences such as soil structure, as well as the effects of hysteresis, to be modeled.

In Chapter 5 there is need to extend the mathematical equations used to fit the compression curve. These mathematical equations may be further developed to represent critical state behavior of a soil.

The estimation of the shrinkage behavior of a soil presented in Chapter 6 should be improved. Further experimental testing must be performed to establish a reasonable method of estimating the shrinkage limit of a soil.

In Chapter 7, there is need for experimental verification of the theorems used in the development of the constitutive surfaces is necessary. Due to the complexity of the laboratory program involved it has not been possible to verify all the assumptions made regarding the development of the surfaces.

The soil property functions presented in this thesis form the basis for modeling volume change, water content change, and the seepage behavior of unsaturated soils in more detail than was previously possible. The application of these new models forms a large area of potential research. The accuracy accociated with this new form of of finite element modeling when using soil property functions should be studied in detail.